

Copyright
by
Zhicheng Zhang
2019

**The Dissertation Committee for Zhicheng Zhang Certifies that this is the approved
version of the following Dissertation:**

**Exploration of Structure and Chemistry in Modular Polyketide
Synthases**

Committee:

Adrian Keatinge-Clay, Supervisor

Brent Iverson

Eric Anslyn

Hungwen Liu

Emily Que

**Exploration of Structure and Chemistry in Modular Polyketide
Synthases**

by

Zhicheng Zhang

Dissertation

Presented to the Faculty of the Graduate School of

The University of Texas at Austin

in Partial Fulfillment

of the Requirements

for the Degree of

Doctor of Philosophy

The University of Texas at Austin

December 2019

Remerciements

Tout d'abord, je dois remercier Dr Keatinge-Clay pour me secourir spécialement quand j'avais un moment difficile pendant le temps j'échangeais mon laboratoire. Sauf vous, je ne pourrais pas accomplir mon étude doctorante ! Vous êtes extraordinairement intelligent et souvent je ressens que je sois absolument submergé par vous.

Deuxièmement, je suis reconnaissant à tous les professeurs, Dr Anslyn, Dr Iverson, Dr Liu et Dr Que, dans le jury parce que vous avez épargnés le temps pour lire ma dissertation ou participer à ma défense finale. Après tout, C'est difficile de rassembler tous en même temps.

Bien sûr, je remercie les membres à mon laboratoire, diplômés et non diplômés, doctorats et non doctorats. Particulièrement Dr Cole, Dr Bailey, Dr Wagner, Dr Zeng, Dr Meinke, Mlle Luna, Mlle Hirsch, M Cepeda, M Valencia, M Kumru. Vous avez m'aidés fréquemment quand je voulais. J'admets que je ne suis pas personne intelligente. Sauf vos aides je ne peux pas accomplir mon travail dans le laboratoire.

Je tiens aussi à distribuer mon remerciement aux amis privés autres à Austin, Mme et M Taylor, Dr Tobin, M Morris, Dr Whitmore et M Maus. J'ai passé du bon temps, en musique et en équitation. Je jouissais du temps où je restais avec vous tous.

Finalement, je voudrais remercier la famille de mon enseignant musical. Ils sont réellement ma mère spirituelle et mon père spirituel. Je délibérément écris cette partie en français afin que vous puissiez comprendre les mots. Désolé pour mon français maladroit et mon vocabulaire monotone. Vous êtes mon rapport mental et mon secours fort.

Je par la présente dédie ma dissertation aux vous tous ! Merci mille fois !

Acknowledgements

If you ask me what's the common point between classical music and chemistry in polyketide-synthase. It's difficult for me to give a correct answer. They are totally different! I frequently complained to my "mother" and "father" about how different is this world with that world. They just kept appeasing me, telling me the story about Russian composer Borodin, who was both chemistry master and classical music master.

When I was 4, I tried to watch television about advanced calculus that shocked my parents. They decided to let me do something more "normal". Thus, I was met with my piano teacher and his wife, my actual "father" and "mother". Since then, I was immersed with classical music for over 20 years. I spent most time of my childhood with classical music. Beethoven, Wagner, Mozart, Palestrina, Victoria, Puccini, Bizet, Couperin, Rameau... all are my favorites. My piano teacher is a conductor and a pianist, a talented musician. His wife is an opera singer, who can fluently speak 7 languages, also a talented musician. They both travelled a lot especially to Europe. I still remember the time when they showed me the beautiful landscape of each European countries. I love the blue of Mediterranean; I miss the white of Alps; I remember the green of Schwarzwald. As the other students they have, studying music, going to musical school, going to Europe and becoming a musician seemed like the right track for me. I did play piano very hard and, as I thought, very well when I was a kid. When most of other kids were playing, I could play Chopin's études and polonaises without any difficulties. I was dreaming having concerts in Europe as a successful pianist and teaching piano in musical school. I watched opera

quiet often as well. Wagner was, and for sure always is, my most favorite composer. My favorite Wagnerian piece is not *Der Ring des Nibelungen* but *Parsifal*.

However, when it was the time to decide whether to go to special conservatory preparative school (usually 13), I was seriously frustrated by my music teacher that I could not have the chance because they said I was too lazy and stupid. That heartrending moment when I had the conversation with them truly left me mourning and weeping in this valley of tears. They said, you couldn't do whatever you wanted to do. Musicians need serendipity. Otherwise you could only have a miserable life. Why not find other hobbies as your future?

Well, I had to face the reality. Except music, chemistry is another hobby for me. Then I started my chemistry journey! I was matriculated into my undergraduate college as a chemistry major without even taking entrance exam due to excellent score in high school chemistry competition. During my undergraduate studies, I chose organic chemistry as my research direction. Organic chemistry is an interesting subject. I loved those name reactions and mechanism as well. Most of these name reactions were memorized by their inventors, usually American, German and Japanese. During this time, I gradually developed the idea going to a foreign country to continue my PhD study. US, Germany and Japan are all ideal options for me. I hesitated to make the decision and finally was convinced going to US.

Everything is so coincident. The University of Texas gave me the first offer and then I showed up in Austin. And then I anchored finally in Dr. Adrian Keatinge-Clay's lab playing with polyketide-synthase. I still remember the first day walking into his office discussing polyketide with him. I must say Dr. Keatinge-Clay was indeed among the smartest person I have ever met in science field. He is not only smart but also tall and handsome. According to my arrogant opinion, it is a pity Dr. Keatinge-Clay didn't become

a movie star! Anyway, he outsmarted me almost in every aspect. Only in graduate school, I realized how hard was the PhD chemistry study: Just the same as in the music school. No weekends, few parties, little leisure time, and more smart and diligent persons! I was suffered with huge mental pressure. However, Dr. Keatinge-Clay is very nice. He allowed me to “vent” myself when I didn’t feel comfortable working in the laboratory. I used vacations taking journeys in Europe. I visited 10 countries totally, all by wheels. For sure, mental ventilation was very important: it significantly raised the working efficiency and reduced the mental pressure!

Beyond Dr. Keatinge-Clay’s academic guidance, labmates coordination is also important. In my PhD study, there were plenty of people gave me generous aids. Dr. Bailey, Dr. Cole, Dr. Zeng, Dr. Meinke, Dr. Wagner and Mr. Valencia gave me various academic guidance in my PhD study and allowed me to participate in their research. Ms. Luna, Ms. Hirsch, Mr. Cepeda, Mr. Kumru contributed a large part to my research and finish plenty of works for me. Without you all I couldn’t finish work by myself.

At the end of this chapter, I am going to answer that question in the beginning. Classical music and chemistry in polyketide-synthase do have same points! First, they are all difficult and require hard work. Second, some people study them. Third, these people are more intelligent and more diligent than me. Fourth, these people are great person. Finally, these people truly enjoy it and dedicate their lives to it. Although I cannot become another Borodin, thank you Dr. Keatinge-Clay, for your mentorship in my graduate school. Thank you also all my defense committee members, Dr. Anslyn, Dr. Iverson, Dr. Liu and Dr. Que, for guidance with my PhD study. Sometimes I still feel very strange how could I finish my PhD study in Chemistry. With joys and tears, I cannot believe most of my work is done and I am about to depart.

Abstract

Exploration of Structure and Chemistry in Modular Polyketide Synthases

Zhicheng Zhang, PhD

The University of Texas at Austin, 2019

Supervisor: Adrian Keatinge-Clay

Nowadays the development of new-generation drugs has been rendered with high urgency in pharmaceutical industry, since existing medicines are not adequate to cope with new appeared diseases. Among these medicines, anticancer and antibiotic are the most important two categories which require new drugs to meet the need of frustrated patients. More efficacy and less toxicity are the target of developing new-generation drugs in the future. However, the intrinsic complexity of these chemicals compromises the effort for organic chemists to synthesize them in an eco-friendly and efficient way. In traditional organic chemistry, complex compound always means long synthetic routine, bad total yield and usually expensive and toxic chiral catalyst.

Au contraire, biology now gives organic chemists an alternative way to mull the synthetic routine in a different view. In the natural world, plenty of useful complex potentially medicinal molecules are synthesized in an efficient and eco-friendly way with delicate stereochemistry. Room temperature, atmospheric pressure, aqueous environment,

neutral pH and recyclable catalyst all lure chemists into the world of enzymatic biocatalysis.

We study polyketide synthases to learn the mechanism how they function to produce polyketides. In our laboratory, we not only utilize enzyme to synthesize complex chiral compound but also explore the intrinsic structure of these enzymes.

We first introduce the new developed general chemo-enzymatic polyketide synthesis using ketoreductases. We successfully synthesized a library of four complex polyketides with two chiral centers involving two ketoreductases. In order to prove our result, we found a strategy to chemically synthesize the same molecule as well involving high pressure catalytic hydrogenation. We also report a seven-enzyme cascade reaction to synthesize another complex polyketide derivative in one-pot with a technique to monitor the reaction *in situ*. We studied the mechanism of pyran synthase in a *trans*-acyltransferase assembly line. By mutagenesis we determined the catalytic domain of the pyran synthase using chemically prepared analogues. We also studied the mechanism of monomethylation and dimethylation in a methyltransferase module. Finally, we conducted docking motif swapping proving the portability of docking domain in *trans*-Acyltransferase PKS modules.

With the development of our study, we not only hope to explore more structural and functional details about the PKSs but also strive to use our enzyme to create more complex pharmaceutically useful polyketide building blocks in an easier and greener way.

Table of Contents

List of Figures	xiii
Chapter 1: Introduction	1
A Brief View of Polyketides in Pharmaceutical Industry.....	1
Using Polyketide Synthases to Build Chiral Building Blocks.....	3
Past work in Our Lab	7
Chapter 2: General Chemoenzymatic Synthesis Involving Ketoreductase to Triketide Building Blocks	8
Introduction.....	8
Results and Discussions.....	12
Chemo-enzymatic Synthetic Routine to Triketide Acid.....	12
Synthesis Design.....	12
Total Synthesis.....	14
Chemical Synthetic Routine to Triketide Acid Using Metal Catalyst....	18
Synthesis Design.....	18
Total Synthesis.....	19
Characterizations	22
NMR	22
Chromatography	23
Experimental Procedures	27
Summary	56
Acknowledgements.....	57

Chapter 3: Seven-Enzymes Cascade Reaction Making Diketide	58
Introduction.....	58
Results and Discussions.....	58
Synthesis Design.....	58
Synthesis	59
Characterizations	61
Experimental Procedures	65
Summary	65
Acknowledgements.....	65
Chapter 4: Mechanism Study of Pyran Synthase Domain in trans-AT Assembly Line	66
Introduction.....	66
Results and Discussions.....	68
Structural Study of PS	68
Synthesis of Chemical Analogues	68
Enzymatic Reactions.....	70
Brief Mechanism of PS.....	73
Experimental Procedures	74
Summary	75
Acknowledgements.....	75
Chapter 5: Structural and Mechanism Study of gem-Dimethylating Methyltransferase from a trans-AT Assembly Line	76
Brief Introduction	76
Acknowledgements.....	78

Chapter 6: Structural Study of Four-Helix Bundle Docking Domain in trans-Acyltransferase Modular Polyketide Synthases.....	79
Brief Introduction	79
Acknowledgements.....	82
Conclusions and Future Directions	83
Appendix.....	84
Appendix A: Supplementary Information of Chapter 2.....	84
Appendix B: List of Publications	178
References.....	179
Vita	185

List of Figures

Figure 1.1: Sea Sponge Halichondria Okadai, Eribulin, Norhalichondrin A and Halichondrin B.....	2
Figure 1.2: the Structure of Erythromycin A.....	3
Figure 1.3: 3.2Å-resolution Structure of type I PKS of the Porcine FAS and the General Mechanism of Chain Elongation Catalyzed by KS.....	5
Figure 1.4: Modular Polyketide Synthase for Polyketide Narbonolide	6
Figure 1.5: The Structure of Two Modules from a Multimodular PKS including Dimeric KS, AT, DH, KR, ACP and ER.....	7
Figure 2.1: Chemo-enzymatic Synthesis to Chiral Building Blocks by KR from DEBS PKS.	9
Figure 2.2: Basic Mechanism of Metallic Asymmetric Catalysis.....	11
Figure 2.3: The Preparation and Structure of Ir-Spiro-PAP and Ir-Spiro-SAP.....	12
Figure 2.4: Proposed Synthesis Schedule for Triketide Acid 9'	14
Figure 2.5: Synthesis from 1 to 4	15
Figure 2.6: Synthesis from 4 to 6 and Structure of 10	17
Figure 2.7: Synthesis from 6 to 9	18
Figure 2.8: Proposed Synthesis Schedule for triketide acid 9'	19
Figure 2.9: Synthesis from 12 to 9	21
Figure 2.10: ¹³ C NMR Comparison of C-3, C-5 in <i>syn</i> -isomers and <i>anti</i> -isomers of 9	22
Figure 2.11: ¹³ C NMR Comparison of Major Peaks in <i>syn</i> -/ <i>anti</i> -isomers of 9	23
Figure 2.12: Chiral Chromatography of Chemo-enzymatically generated 8aa , 8ab , 8ba , and 8bb	25

Figure 2.13: Synthesis from 9 to 8	26
Figure 2.14: Protein Gels for MycKR6, TylKR2, and GDH.....	28
Figure 3.1: Proposed Synthesis Schedule for 3-hydroxybutyryl-NAC.....	59
Figure 3.2: Synthesis Schedule from CoA 16 to Final Product 23 and 24	60
Figure 3.2: Synthesis Schedule from CoA 16 to Final Product 23 and 24 (continue)....	61
Figure 3.3: LC/MS Analysis of 23	62
Figure 3.4: UV-HPLC Analysis of 24	63
Figure 3.5: ³¹ P NMR Analysis of 23	64
Figure 4.1: Different Patterns of PS/DH Cyclization with Different Stereochemistry.....	67
Figure 4.2: Synthesis of Chemical Analogues 30, 31, 36, 37	70
Figure 4.3: Activity Assays of SorPS9 and Point Mutants.	72
Figure 4.4: Proposed Mechanism of PS Active Site and Conformation of <i>Oxa</i> - Michael Addition	74
Figure 5.1: The Model of DisMT3 and Mutagenesis Study on LC/MS.....	76
Figure 5.2: Reaction of DisMT3 with Ketopentanoyl-SNAC.....	77
Figure 6.1: Mln Synthesis Assembly Line and The Four-Helix Docking Motifs between KS in MlnD and KR in MlnE.....	80
Figure 6.2: Polypeptide Association Mediated by DD Motifs.....	81

Chapter 1: Introduction

A BRIEF VIEW OF POLYKETIDES IN PHARMACEUTICAL INDUSTRY

To general consumers, products labeled with ‘natural’ and ‘organic’ are considered as good and healthy, but ‘chemicals’ have negative connotations as ‘unnatural’. The simplest definition of a natural product is a small molecule that is produced from a biological source. Thus, natural products and natural product mimics have become a hot topic followed by researchers in both chemistry and biology fields.¹ In pharmacy industry, researchers use natural products as lead structures to discover and develop the final drug entity. Indeed, besides synthetic drugs, natural products and their analogs (including unaltered natural product, botanical drug, natural product derivative and mimic of natural product) are important sources of new approved drugs. For example, from circa the 1940s to the end of 2014, among the 175 small molecules approved by FDA in the area of cancer, 49% are either natural products or their derivatives.² However, compared to synthetic drugs, natural products still have many disadvantages, such as controversy on intellectual property rights, slow working progress, complexity of chemistry and, most importantly, difficulties in access and supply. Until recently, many large pharmaceutical companies had reduced the proportion of natural products in drug discovery, but now there has been a re-emergence of natural products, evenly distributed as small-molecule drug candidates, in the develop pipelines.³

A preeminent prototype of the natural product limitations describe above is the series of halichondrins, antitumor polyethers first separated from the marine sponge *Halichondria okadai* in 1986 (**Figure. 1.1**). There were eight total anti B-16 melanoma cells halichondrins isolated, but the major product extract, norhalichondrin A (**Figure. 1.1**), gave only 5×10⁻⁶% yield.⁴ Among these extraordinarily sophisticated compounds, halichondrin

B (**Figure. 1.1**) demonstrates exceptional biological inhibition against cancer ($IC_{50}=0.3$ nM for L1210 murine leukemia cells).⁵ Albeit halichondrin B has such a strong potency against cancer, access and supply difficulties severely restricted future efforts for development. Thus, based on the structure of halichondrin B, its simplified analog ER-086526 (known as Eribulin) (**Figure. 1.1**), which retains the activity of halichondrin B *in vitro* and *in vivo*, has been developed synthetically to treat breast cancer, colon cancer, melanoma, and ovarian cancer.⁶ Later the FDA approved Eribulin in treating late-stage breast cancer.⁷

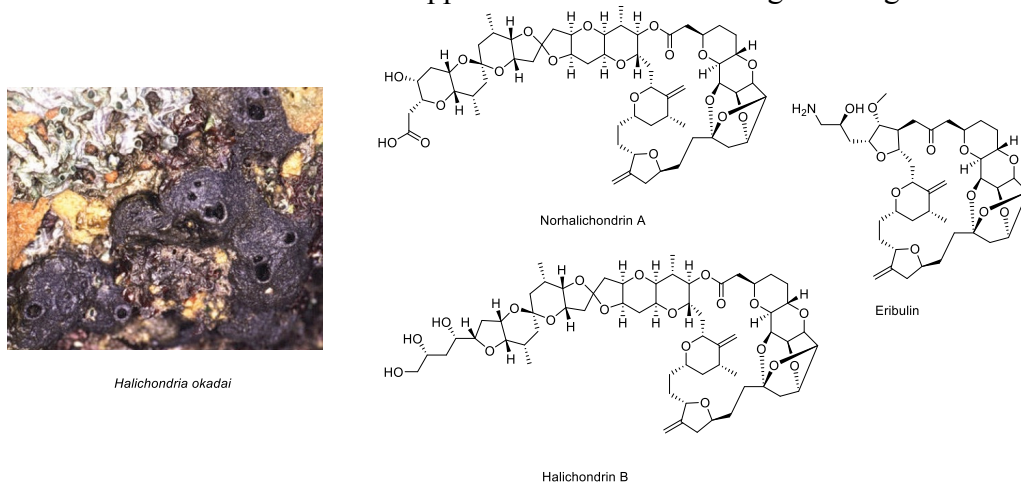
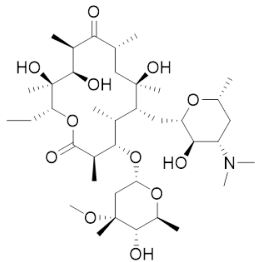


Figure 1.1. Sea Sponge Halichondria Okadai, Eribulin, Norhalichondrin A and Halichondrin B.⁹

Halichondrins belong to the polyketide family. Polyketide derivatives, among the most important microbial metabolites for human medicine, comprise a remarkable percentage (20% of the top-selling drugs) of pharmaceutically relevant natural products. In pharmacy, polyketides are utilized as antibiotics (erythromycin A, rifamycin S), anticancer drugs (doxorubicin, epothilone), cholesterol-lowering agents (lovastatin), antiparasitics (ivermectin), antifungals (amphotericin B), insecticides (spinosyn A) and immunosuppressants (rapamycin).¹⁰ The hit rate of polyketide metabolites to be chosen as commercial pharmaceuticals is 0.3%, much better than the hit rate of synthetic compound libraries using high-throughput screening (HTS), which is <0.001%.¹¹

Due to low abundance of natural products when sourced from their native environment, total synthesis becomes an alternative. Despite the complicity of some polyketides, the total synthesis of polyketides appeals to many synthetic chemists. Erythromycin A (**Figure 1.2**), generated by a strain of *Streptomyces erythreus*, is the best known of the macrolide antibiotics, a subcategory of polyketide antibiotics.



Erythromycin A

Figure 1.2. The Structure of Erythromycin A.¹²

Erythromycin A contains a 14-membered lactone ring with 10 asymmetric centers, and *L*-cladinose and *D*-desosamine residues.¹² Thus, this complex compound, citing the greatest synthetic chemist Woodward's word, "looks at the present time quite hopelessly complex, particularly in view of its plethora of asymmetric centers."¹³ Woodward himself did not witness the completion of the total synthesis of erythromycin A. His student, Kishi, finally completed this project in 1981.¹² Kishi also incredibly finished the total syntheses of other members in the halichondrins family, including halichondrin A/B/C and norhalichondrin B.¹⁴

USING POLYKETIDE SYNTHASES TO BUILD CHIRAL BUILDING BLOCKS

Although asymmetric methodologies have progressed significantly in past decades, the total syntheses of polyketides still remain difficult due to high step counts, low atom economy, and involution of expensive/toxic metal catalysts preventing wide application of chemical synthetic polyketides. One eclectic way to promote the efficacy of synthesis is using a chiron approach strategy. A "chiron" (chiral synthon) is interpreted as an

enantiopure “synthon”.¹⁵ In the chiron approach, the target molecule is synthesized from enantiomerically pure chiral building blocks “chirons”, usually prepared biocatalytically from natural sources, such as enzymes.¹⁶ Currently there are many mature affordable biocatalytic chiral building blocks involved in pharmaceutical industry synthesis.¹⁷ This semi-synthesis strategy is powerful and amenable to the preparation of structurally similar complex analogs, which can be assembled quickly from the simple building blocks with subsequent chemical processing.¹⁸ Therefore, it is exciting for us developing an enzymatic system, using polyketide synthases (PKSs), to generate polyketide building blocks.

Polyketide synthases (PKSs) are a family of complex enzyme systems responsible for stepwise biosynthesis of natural polyketides. Using simple CoA-activated extender units like acetyl/propionyl/butyryl-CoA, and malonyl/methylmalonyl/ethylmalonyl-CoA, their activated derivatives, polyketide synthases can elongate the main chain to finally reach complex final products. From an activated acyl starter unit, polyketides are elongated by repetitive decarboxylative Claisen thioester condensations with different extender units (**Fig. 1.3**).¹⁹

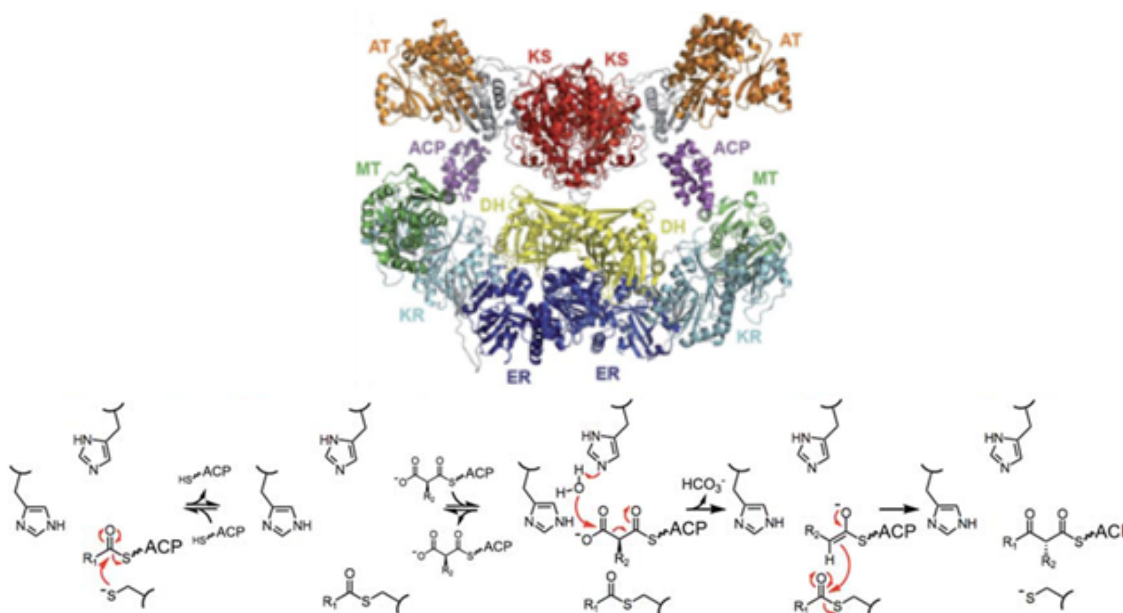


Figure 1.3. 3.2Å-resolution Structure of type I PKS of the Porcine FAS and the General Mechanism of Chain Elongation Catalyzed by KS.²⁰

A chain elongation involves a ketosynthase (KS) catalyzing the decarboxylative Claisen condensation, an acyl transferase (MAT/AT) selecting the extender unit, and a phosphopantetheinylated acyl carrier protein (ACP) tethering the growing polyketide chain to the next domain. After every elongation, the β -oxo functionality may be processed by a ketoreductase (KR) stereoselectively reducing the β -carbonyl group to a hydroxyl group by a dehydratase (DH) dehydrating β -hydroxyl group to olefin, and then an enoyl reductase (ER) reducing olefin to alkane. Finally thioesterases (TE) catalyze hydrolysis and macrocyclization of polyketide chain from the previous ACP domain to release the product. A set of KS, AT, and ACP domains, alongside other optional processing domains together compose a module, which is responsible for a single elongation cycle (**Fig. 1.4**). For Modular PKS of Type I PKS, the number of modules is related to the number of elongation cycles executed by the PKS.²¹ In the case of pikromycin, six modules of the pikromycin PKS sequentially extend and modify the polyketide intermediate for every

round of extension, and the TE finally hydrolyzed the polyketide intermediate, leading to either 10-dml from module 5 or narbonolide from module 6.²²

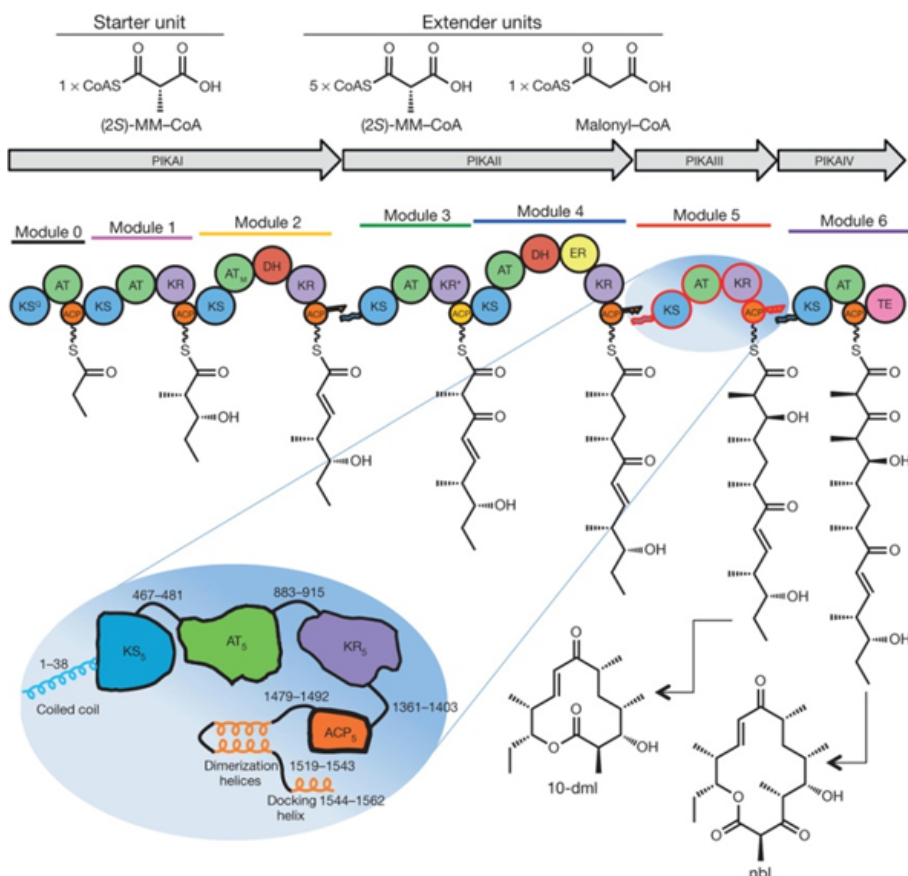


Figure 1.4. Modular Polyketide Synthase for Polyketide Narbonolide. An intermediate of pikromycin.²²

Modular PKSs are predominantly found in actinobacteria, myxobacteria, pseudomonades, and cyanobacteria. A minimal module from Modular PKS is comprised of a KS domain, an AT domain, and an ACP domain with optional KR domain, DH domain, and ER domain (**Fig. 1.5**).²³

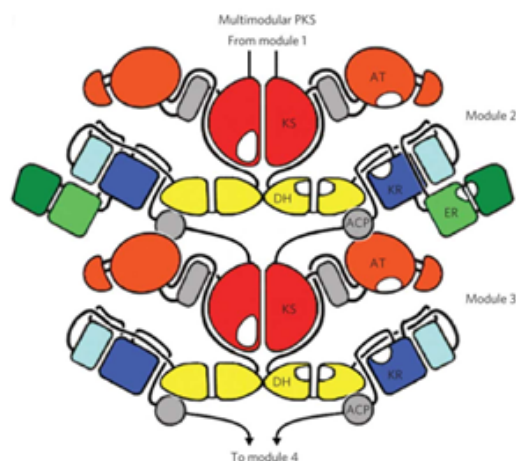


Figure 1.5. The Structure of Two Modules from a Multimodular PKS including Dimeric KS, AT, DH, KR, ACP and ER.²⁴

PAST WORK IN OUR LAB

Using PKSs, we have a mature technique to synthesize a library of diketide chiral building blocks. A scalable chemo-enzymatic reaction generating chiral diketides from α -substituted, β -ketoacyl *N*-acetylcysteamine thioesters has been well developed using isolated modular polyketide synthase (PKS) ketoreductases (KRs). The reaction is a biocatalytic reduction powered by regenerable glucose-fueled NADPH cycle.²⁵ Based on our previous work with diketides, we have also developed a methodology to generate triketide pyrones²⁶ and a versatile *in vitro* PKS platform to access six triketide lactones produced at larger scales. The terminal module and TE of the erythromycin PKS (EryMod6TE), a module that accepts non-natural substrates, is the core of this biocatalytic platform.²⁷ The extender units with truncated substrate mimics applied in the reaction can be prepared *in vivo* by malonyl CoA ligase (MatB).²⁸

Chapter 2: General Chemo-enzymatic Synthesis Involving Ketoreductase to Triketide Building Blocks

INTRODUCTION

In previous study, we discovered that the KR determines both the stereoselectivity of the hydroxyl group and the neighboring α -methyl group, producing two consecutive stereogenic centers, in one biocatalytic KR reduction.²⁹ In modular polyketide synthases, only a few certain residues control the stereospecificity of the product, and so the stereoselectivities can be deduced from conserved residues. Those KRs can also be categorized by the stereocenter created. A-type KRs generate L- β -hydroxyls and B-type KRs generates D- β -hydroxyls.³⁰ Later, this nomenclature system was polished by imposing extra denominations onto the α -methyl substituted diketides: D- α -methyl groups are counted as “1,” and L- α -methyl groups are counted as “2”. Therefore, a diketide-SNAC would produce the “2R, 3S” product if reduced by an A1-type KR, the “2S, 3S” product if reduced by an A2-type KR, the “2R, 3R” product if reduced by a B1-type KR, and the “2S, 3R” product if reduced by a B2-type KR. However, if a KR cannot reduce the carbonyl group, it is named a C-type KR (**Figure. 2.1**). We also found β -keto-SNACs were suitable enough to retain their natural stereoselectivities in the KR domain as the NAC handle mimics the acylated phosphopantetheinyl arm of the ACP domain.²⁹

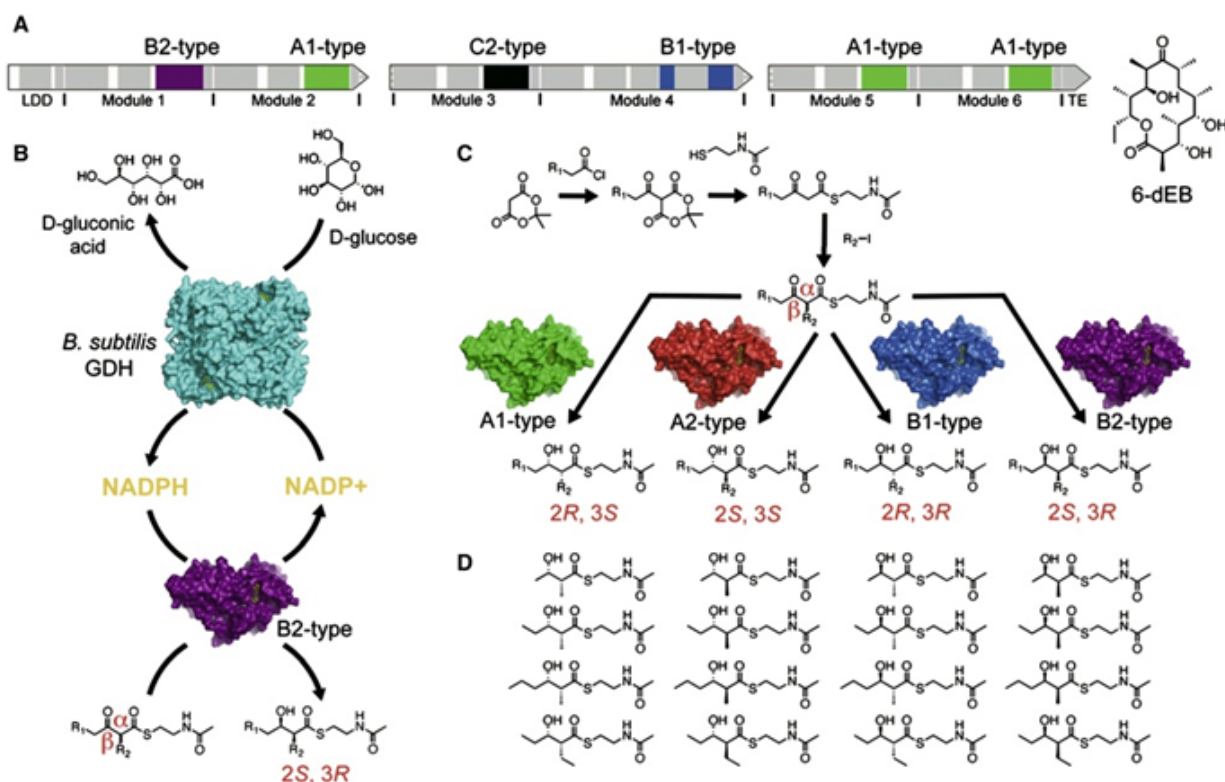


Figure 2.1. Chemo-enzymatic Synthesis to Chiral Building Blocks by KR from DEBS PKS.²⁵

(A) 6-Deoxyerythronolide B synthase (DEBS) assembly line to 6-dEB.

(B) The reduction of diketide-SNACs, with the help of GDH regenerating NADPH through the oxidation of D-glucose.

(C) A general synthesis to α -substituted, β -keto diketides.

(D) Nomenclature system of the library of diketide chiral building blocks.

Since a library of diketide building blocks was already established. It was logical to extend the diketide into more complex triketide. However, during the extension of diketides by EryMod6TE, we found a serious side-reaction, thioesterase (TE)-mediated hydrolysis decomposing the thioester substrate. A triketide without protecting group anchored on PKS tended to self-cyclize to form more stable six-membered lactone even without the existence of TE. Because the cyclization prioritized the reduction, the half-life of triketide intermediate anchored on PKS was not long enough to allow triketide to be reduced by KR. In addition, due to the stereospecificity of the diketide substrate, not all chiral triketides

were suitable to be generated via this method, because the KS could only extend the recognizable subset of these chiral diketide intermediates. Thus, we had to conceive a new strategy to build a library of triketide building blocks without KS. The major problem was the extension of polyketide intermediate. We turned to biomimetic decarboxylative Claisen condensation,³¹ the key elongation step suitable for all diastereomers of diketide substrates. For sure there were other methods available to branched chain extension.³² Fortunately, a chemical equivalent of KS decarboxylative Claisen condensation was investigated 40 years ago which could be efficient to replace the role of KS.³³ Also, the addition of protecting group on 4-hydroxyl functionality could effectively avoid untimely spontaneous cyclization thus allowed triketide stay long enough on the KR to be reduced. Beyond KR, there was an efficient but expensive way to synthesize triketide building blocks by new generation metal catalyst. Asymmetric catalysis was investigated starting from 1960's, when the example of experiment involving chiral transitional metal complex was observed. Noyori catalyst (BINAP-Ruthenium) is the most well-known metal catalyst in laboratory use. It is powerful to reduce various substrates including olefins and ketones with different functionality. The basic mechanism of such a metal complex involves three parts: molecular metal with chiral ligand, reactant (usually hydrogen gas) and substrate. The reactant and substrate first were coordinated onto the metal catalyst. The reactant and substrate reacted on the metal catalyst forming chiral product, which then left the metal catalyst(**Figure 2.2**).³⁴

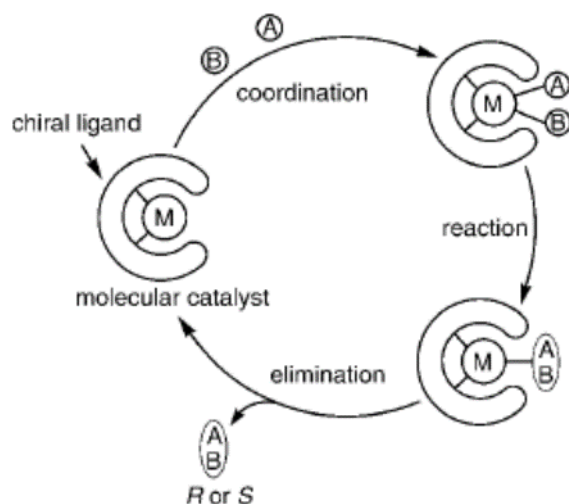


Figure 2.2. Basic Mechanism of Metallic Asymmetric Catalysis. A and B are reactant and substrate.³⁴

Not only Ruthenium, but also other transition metals are capable to catalyze hydrogenation such as Rhodium, Iridium or even Iron, due to their intrinsic similarity.³⁵ Also in recent years, new generations of commercially available catalysts with improved chiral ligands are appearing on the market. Ir-Spiro-AP series catalyst is an example with great steric hindrance leading to great chiral selectivity. Characterized by new tridentate multi-chiral centered spiro P-N-S ligands instead of traditional P-N-P ligands (Ir-Spiro-PAP), the new-designed Ir-Spiro-SAP perfectly performed asymmetric hydrogenation on β -ketoesters with high stereoselectivity, high substrate-catalyst ratio and high yield (**Figure 2.3**).³⁶

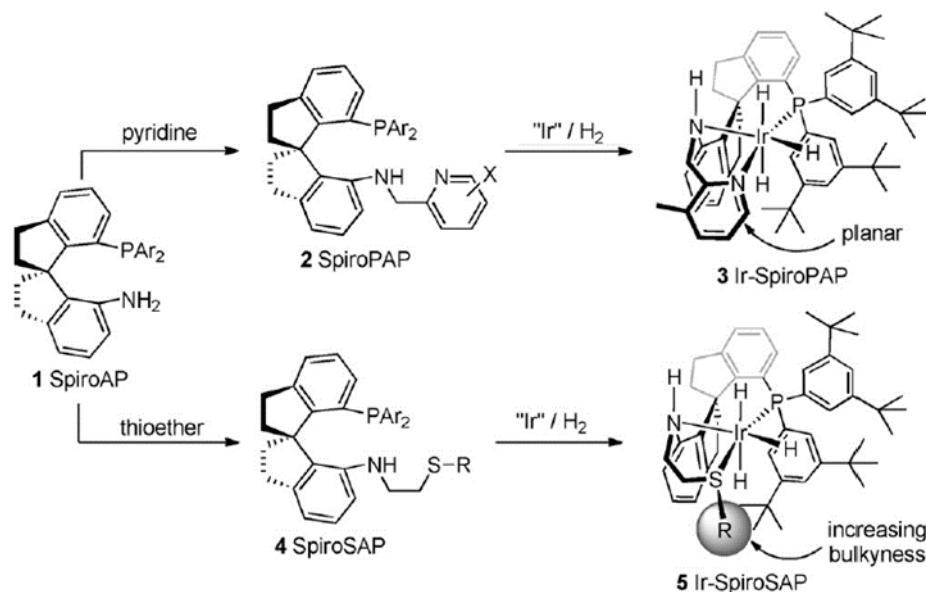


Figure 2.3. The Preparation and Structure of Ir-Spiro-PAP and Ir-Spiro-SAP.³⁶

From recent research progress, Ir-Spiro-PAP was successfully applied in complex polyketide intermediate synthesis (-)-Cynolide A and (-)-Doliculide with good chirality and conversion.³⁷ The reactions were also featured with high substrate/catalyst ratio, fast reaction time and excellent protection group tolerance. Thus, Ir-Spiro-PAP was conceived an excellent substituent of KR to reduce carbonyl in the same triketide building block synthesis.

RESULTS AND DISCUSSIONS

Chemo-enzymatic synthetic routine to Triketide Acid

Synthesis Design

Because the synthetic routine resembled the natural PKS enzyme, the starting material to begin with was propionyl-Meldrum's acid **1**, which could be easily prepared from commercially available Meldrum's acid. Propionyl-Meldrum's acid **1** could be refluxed with *N*-acetylcysteamine (NAC) in afford diketide β -keto-diketide **2**. β -keto-diketide **2**

could be easily reduced to L- or the D- β -hydroxy-diketide **3**²⁵ in aqueous solution depending on the KR enzyme chosen. MycKR6 would lead to L- β -hydroxy-diketide **3** and TylKR2 would lead to D- β -hydroxy-diketide **3** respectively. The reduction system characterized by a regeneration system involving nicotinamide adenine dinucleotide phosphate (NADPH), glucose dehydrogenase (GDH) and D-glucose, which was designed to regenerate KR *in situ*. β -hydroxy-diketide **3** was subsequently hydrolyzed to give corresponding β -hydroxy acid **4**. β -hydroxy acid **4** could be modified by protecting group to generate protected acid **5'** in order to exclude self-cyclization later in enzymatic reduction. Protected acid **5'** as polyketide chain should react with malonyl ethanethiol thioester as extender unit to afford β -keto-triketide **6'**. Thiol-thioester exchange of β -keto-triketide **6'** *in situ* with the existence of excessive NAC should give ideal compound NAC-bound β -keto-triketide **7'**. NAC-bound β -keto-triketide **7'** would afterwards be reduced to give β -hydroxy triketide **8'** by either MycKR6 or TylKR2 giving L/D configuration respectively. Subsequent hydrolysis of β -hydroxy triketide **8'** would finally give target compound triketide acid **9'** (**Figure 2.4**).

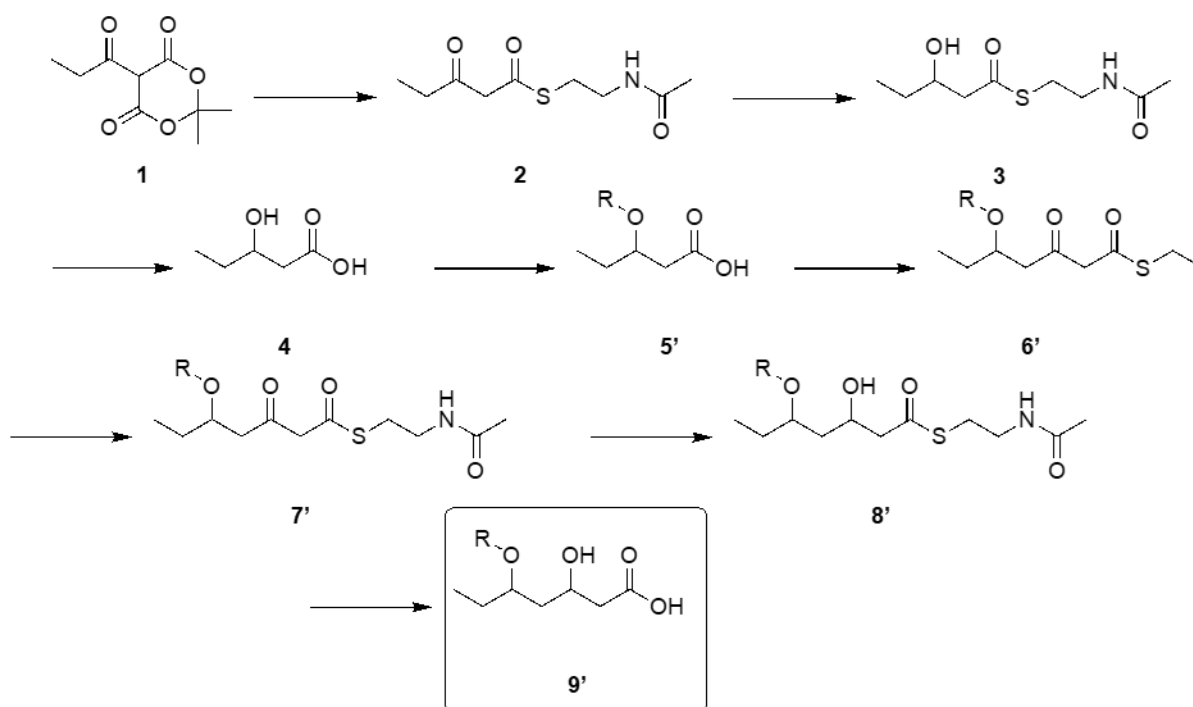


Figure 2.4. Proposed Synthesis Schedule for Triketide Acid 9'.

Total Synthesis

An improved procedure with the beginning two steps based on our previous work was utilized to synthesize large quantity starting material with a higher purity.²⁵ Pyridine and propionyl chloride were consecutively added to Meldrum's acid in cold DCM solution to give propionyl-Meldrum's acid **1** without chromatography separation in a 70% yield.³⁸ Propionyl-Meldrum's acid **1** was then refluxed at 115 °C with NAC in toluene to give β-keto-diketide **2** with 61% yield as a dark yellow solid. Flash chromatography with copper sulfate impregnated silica was employed in to remove unreacted NAC during separation. The NAC handle was necessary for KR biocatalysis as well as other similar handle like ethanethiol, because they were mimics of the natural ACP side chain to afford greater stereocontrol³⁹. Water soluble β-keto-diketide **2** was then incubated with either MycKR6 to generate β-hydroxy-diketide **3a** or TylKR2 to generate β-hydroxy-diketide until reaction was completed (usually overnight, depending on the quantity of enzyme).²⁵ Reaction of β-

keto-diketide **2** with the A-type KR MycKR6 provided β -hydroxy-diketide **3a** in 65% yield, whereas reaction with the B-type KR TylKR2 provided β -hydroxy-diketide **3b** in 58% yield. These enantiomers were sticky yellow oil with a specific odor. Stereochemistry of these enantiomers and standards were measured and compared by chiral HPLC (**Figure S3A-1/S3B-1**). Both enantiomers were afterwards hydrolyzed overnight at 80 °C by adding 5 M sodium hydroxide solution, giving the corresponding L- β -hydroxy acid **4a** and L- β -hydroxy acid **4b** in respectively 51% and 59% yields; this hydrolysis removed the contaminant NAC and its oxidized dimer generated during the reaction (**Figure 2.5**).

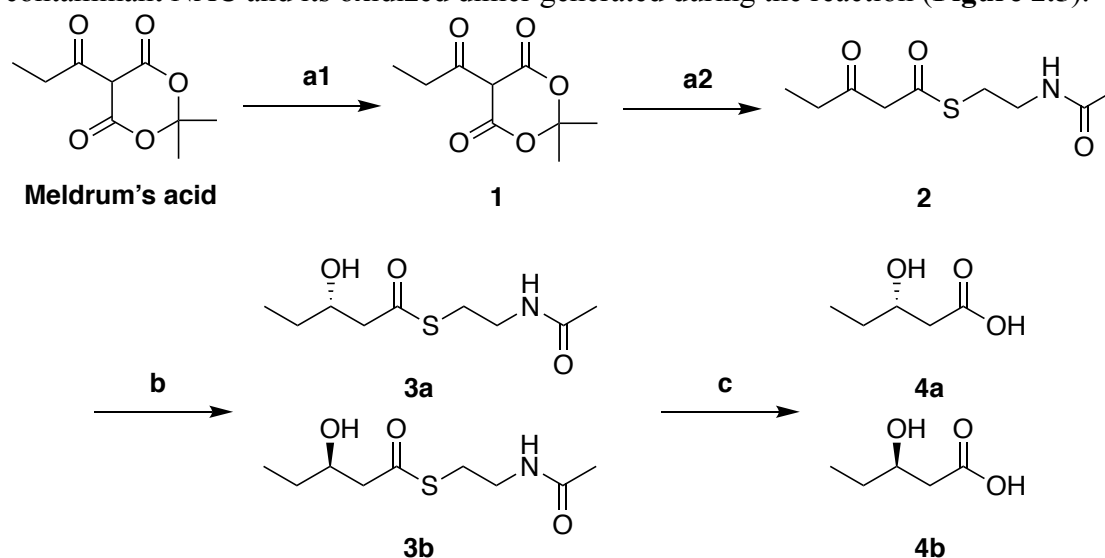


Figure 2.5. Synthesis from **1** to **4**.

Conditions: a) 1) pyridine (2.0 eq.), propionyl chloride (1.0 eq.), DCM, overnight, 0 to 22 °C (76% yield); 2) *N*-Acetylcysteamine (NAC, 0.95 eq.), toluene, 115 °C, 5 h (61% yield), b) Either MycKR6 (A-type KR) for **3a** or TylKR2 (B-type KR) for **3b**, GDH, NADP⁺, pH 7.7, overnight, 22 °C (**3a**, 65%, **3b**, 58%), c) 5 M NaOH aq., 80 °C, overnight (**4a**, 51%, **4b**, 59%).

Regarding the β -hydroxyl substituent, several protecting groups were considered, as acetyl, methyl, methoxymethyl, and even silyl groups. The acetyl protecting group was attempted first and did give desired product. However, during the second reduction of triketide, when elimination predominated over desired transformation leading to decomposition of starting

material. Therefore, methyl protecting group with high stability was chosen to protect the β -hydroxy acid **4b** since *O*-methylation was common in natural polyketides biosynthesis. *O*-methyltransferase (*O*-MT) domains existed in PKS system which often methylated β -hydroxyl substituents. Therefore, unlike those larger silyl groups, the methyl protecting group was chosen because its small steric hindrance wouldn't prevent the target polyketide from the catalytic sites of downstream enzymes (KR). The β -hydroxy acids **4a** and **4b** reacted with *n*-butyllithium in DMSO first and then were methylated by methyl iodide, giving respectively L/D- β -methoxy acids **5a** and **5b** in 73% and 78% yields as a dark yellow oil. The reaction could be easily monitored by color change since the dianion (dark brown) and monoanion (light orange) had different colors. When methyl iodide was added into the system, the color shifted from dark brown gradually to light orange. According to the original report, this reaction was intended for synthesizing dimethylated acids **10a** and **10b**. However, based on observation actually it only generated the intermediate mono-methylated compound β -hydroxy acids **4a** and **4b**,⁴⁰ which, fortunately, were the desired compounds. The removal of DMSO was not necessary but could be achieved by column chromatography. Protected β -methoxy acids **5a** and **5b** reacted with malonyl ethanethiol thioester in mono-magnesium salt form to give important intermediate β -keto-triketide **6a** and **6b** in 35% and 34% yields, respectively.³³ The product β -keto-triketide **6a** and **6b** were light fluent yellow liquid with distinct onion-like aroma. This decarboxylative Claisen condensation mimics the role of KS to extend the polyketide chain with two more carbons (Figure 2.6).

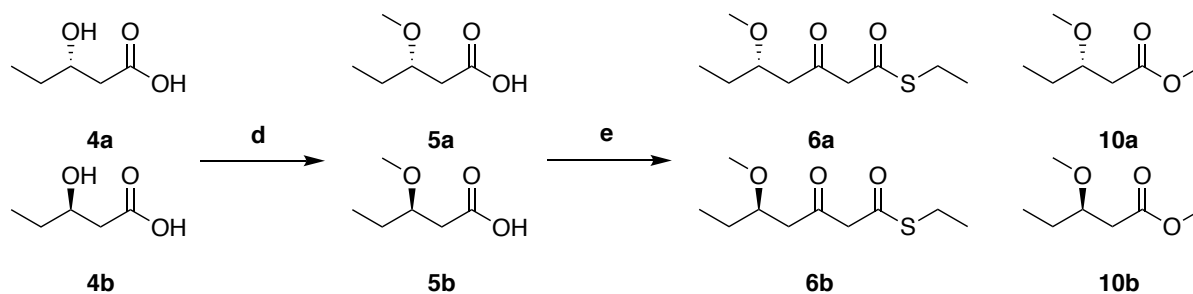


Figure 2.6. Synthesis from **4** to **6** and the Structure of **10**.

Conditions: d) 2.5 M *n*-BuLi (3.0 eq.), DMSO, MeI (2.4 eq.), under argon, 22 °C, overnight (**5a**, 73%, **5b**, 78%), e) 1,1'-Carbonyldiimidazole (CDI) (1.1 eq.), Mg(OEt)₂ (0.55 eq.), malonic acid half ethyl thioester (1.1 eq.), anhydrous THF, 22 °C, overnight (**6a**, 35%, **6b**, 34%).

As convenient thiol-thioester exchange, β -keto-triketide **6a** and **6b** were converted to NAC-bound β -keto-triketide **7a** and **7b** using 10 equivalents of NAC at room temperature *in situ*. The reaction could easily be monitored by TLC as well as the smell of volatile ethanethiol as a reaction byproduct. After installation of NAC, the pH was then turned to 7.7 and either MycKR6 or TylKR2 alongside the NADPH regeneration system were added to form reduced β -hydroxy triketide **8** with a new L-/D-orientated stereocenter. However, due to byproducts like NAC dimer, the purifications of **8aa**, **8ba**, **8ab**, and **8bb** were too difficult through flash chromatography. Different conditions were attempted but only lead to failure. This was because β -hydroxy triketide **8** and NAC dimer had similar polarities on the column. Fortunately, if β -hydroxy triketide **8** was hydrolyzed using aqueous 5 M sodium hydroxide at 70 °C, the purification of corresponding triketide acid **9** was relatively simplified. Hydrolysis could remove majority of the byproducts, including NAC dimer, from the reaction mixture, to generate final compound triketide acids **9aa**, **9ba**, **9ab**, and **9bb** respectively as a brown oil in 57%, 44% 36% and 24% yields through three steps (Figure 2.7).

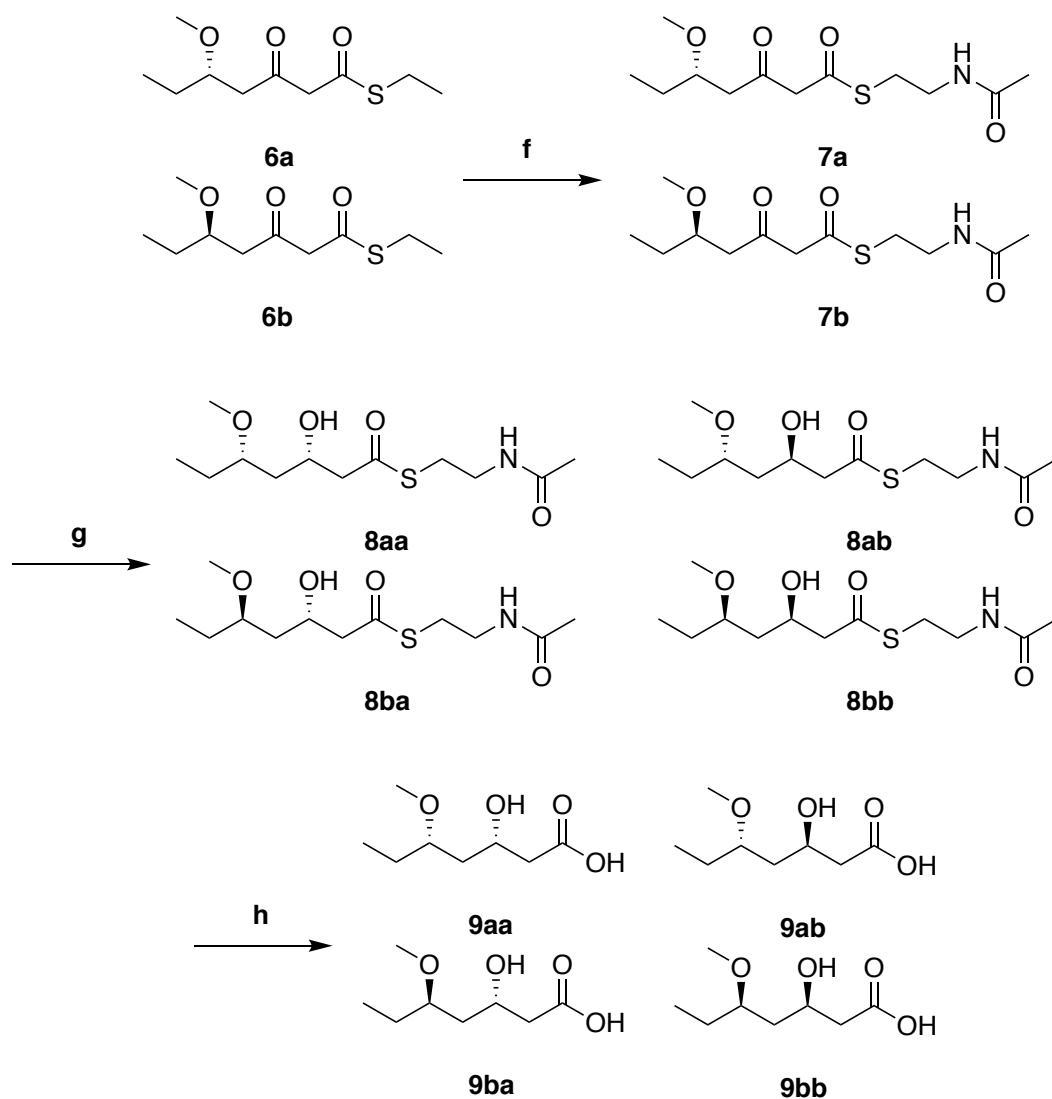


Figure 2.7. Synthesis from **6** to **9**.

Conditions: f-h) NAC, pH 8.5, 22 °C, 2 h, then either MycKR6 (A-type KR) or TylKR2 (B-type KR), GDH, NADP⁺, pH 7.7, overnight, then 5 M NaOH, 70 °C, overnight (yields: **9aa**, 57%; **9ab**, 36%; **9ba**, 44%; **9bb**, 24%).

Chemical Synthetic Routine to Triketide Acid Using Metal Catalyst

Synthesis Design

The synthesis of triketide acid **9'** using metal catalyst was similar to chemo-enzymatic synthesis. Instead of KR, Ir-spiro-SAP was utilized to reduce the carbonyl in both diketide and triketide reductions. The synthesis started with ester **12**, because ester **12** was

commercially available in bulk and also could be directly to use for reduction. Ester **12** was reduced to afford ester **13** by asymmetric catalysis via Ir-spiro-SAP. After that, ester **13** was hydrolyzed to form same hydroxyl acid **3**. From hydroxyl acid **3** to β -keto-triketide **6'**, the same synthetic routine was adopted. Instead of thiol-thiolester exchange, alcoholysis was applied to β -keto-triketide **6'** to generate oxoester **14**. Oxoester **14** was reduced by Ir-spiro-SAP and then hydrolyzed to produce target compound triketide acid **9'** (**Figure 2.8**).

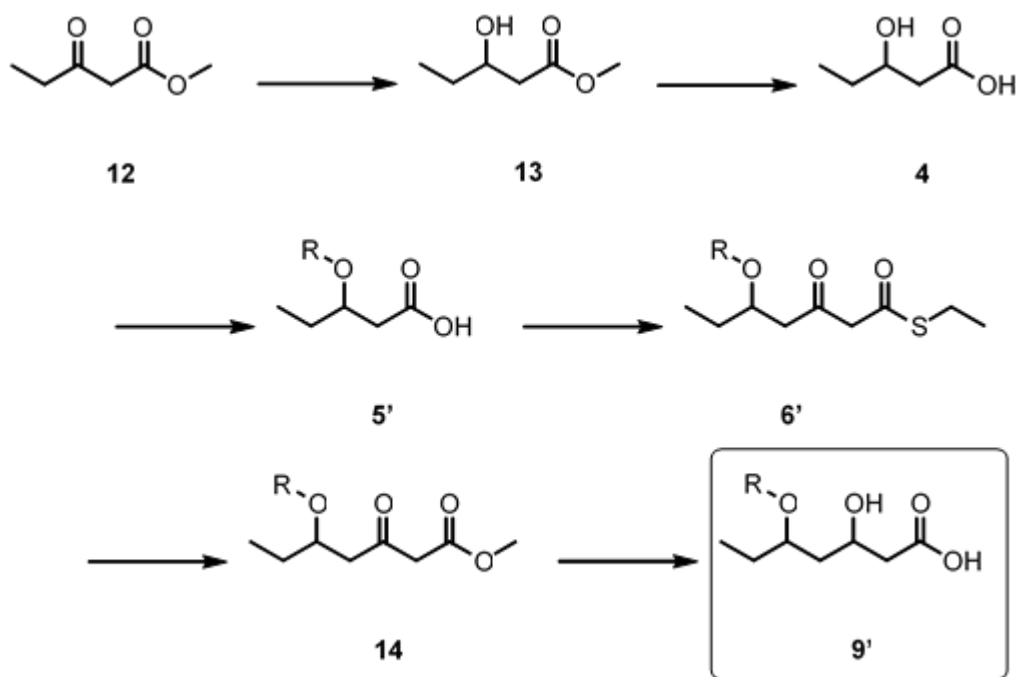


Figure 2.8. Proposed Synthesis Schedule for Triketide Acid **9'**.

Total Synthesis

Using above-mentioned Ir-spiro-SAP,³⁷ ester **12** was readily reduced under 100 atm hydrogen gas in methanol almost quantitatively to form diektide **13a** or **13b** as a light yellow liquid without separation. The chirality of reduction depended on the catalyst. (*S*)-Ir-spiro-SAP produced L-enantiomer whereas (*R*)-Ir-spiro-SAP produced D-enantiomer. **13a** and **13b** were hydrolyzed using 5 M sodium hydroxide solution overnight at 80 °C, to

form corresponding hydroxy acid **4a** and **4b** in 51% and 59% yields. Afterwards the synthesis was the same until β -keto-triketide **6a** and **6b**. During alcoholysis, excessive sodium methoxide in methanol was employed to transform β -keto-triketide **6a** and **6b** into oxoester **14a** and **14b** with moderate yields 27% and 16% as slightly aromatic yellow oil. Luckily most unreacted β -keto-triketide **6a** and **6b** could be recycled by chromatography whereas part of them was lost due to side-reaction. Oxoester **14a** and **14b** were then reduced by Ir-spiro-SAP again. Subsequent hydrolysis generated final compound triketide acid **9aa**, **9ab**, **9ba** and **9bb** as yellow oil respectively through two steps (77%, 97%, 83%, 86%). This synthetic routine allowed a larger quantity than chemo-enzymatic synthesis thus provided higher and cleaner NMR resolution (**Figure 2.9**).

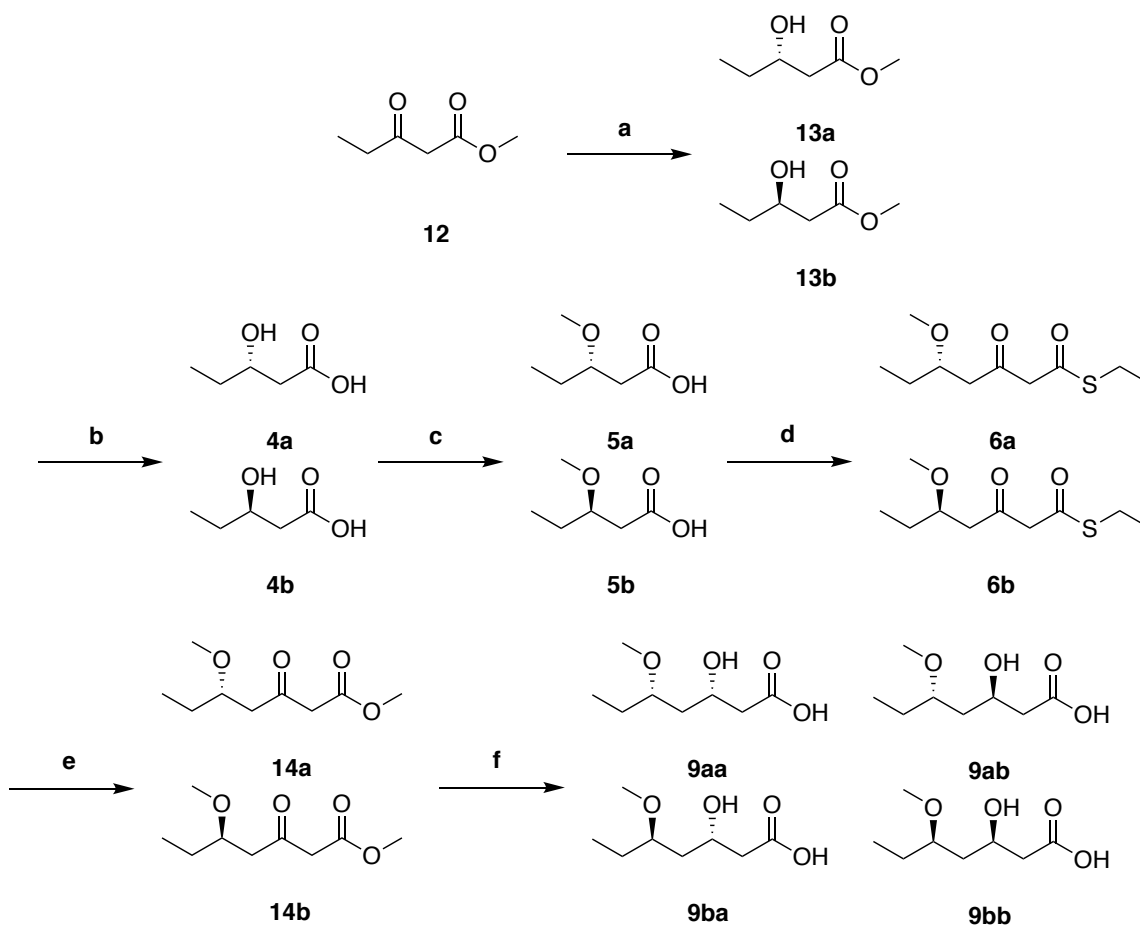


Figure 2.7. Synthesis from **12** to **9**.

Conditions: a) Either (*S*)-Ir-spiroSAP, 100 atm H₂, MeOH, 22 °C, 48 h for **11a** or (*R*)-Ir-spiro-SAP, 100 atm H₂, MeOH, 22 °C, 48 h for **11b** (both yields >99%), b) 5 M NaOH aq., 80 °C, overnight (**4a**, 51% and **4b**, 59%), c) 2.5 M *n*-BuLi (3.0 eq.), DMSO, MeI (2.4 eq.), under argon, 22 °C, overnight (**5a**, 73% and **5b**, 78%), d) 1,1'-Carbonyldiimidazole (1.1 eq.), Mg(OEt)₂ (0.55 eq.), malonyl ethanethiol thioester (1.1 eq.), anhydrous THF, 22 °C, overnight (**6a**, 35% and **6b**, 34%), e) sodium methoxide (10.0 eq), anhydrous MeOH, 22 °C, 6-9 h, (**12a**, 27% and **12b**, 16%), f) Either (*S*)-Ir-spiroSAP, 100 atm H₂, MeOH, 22 °C, 48 h then 5 M NaOH aq., 60 °C, overnight for **9aa** and **9ba** or (*R*)-Ir-spiroSAP, 100 atm H₂, MeOH, 22 °C, 48 h then 5 M NaOH aq., 60 °C, overnight for **9ab** and **9bb** (**9aa**, 77%; **9ab**, 97%; **9ba**, 83%; **9bb**, 86%).

Characterization

NMR

Although ^1H NMR did demonstrate difference between *syn*-isomer **9aa** and **9bb** from their *anti*-isomer **9ab** and **9ba**. Slight chemical shift difference on the hydroxyl proton was observed around 4.2-4.3 ppm. However, there were often impurities generated in enzymatic reduction, which appeared around this area, causing difficulty to interpret the result. Therefore, ^{13}C NMR technology was preferred over ^1H NMR to interpret the stereochemistry because it was straightforward and facile to exclude impurity interference. The interpretation of ^{13}C NMR was based on Hoffmann's empirical rule.⁴¹ The signals of C-3, C-5 of *anti*-isomers **9ab** and **9ba** were at higher field than their *syn*-isomers counterparts because due to intramolecular hydrogen bond *anti*-isomers adopted chair conformations (for sure the terms *threo*- and *erythro*- are better). Therefore, there were more stereo-hindrance in *anti*-isomers **9ab** and **9ba** because the substituents were likely to be axial instead of equatorial (Figure 2.10).

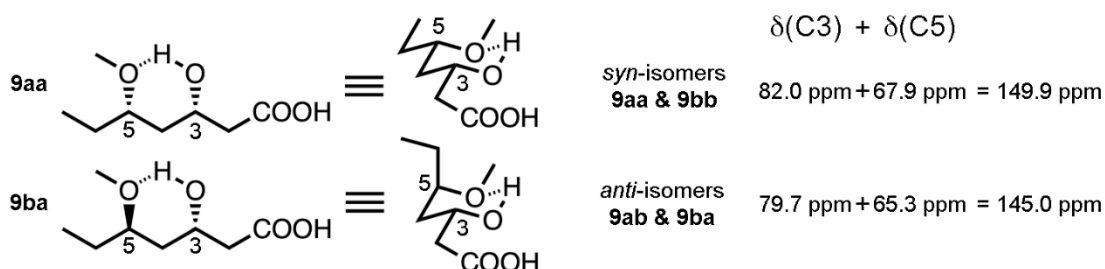


Figure 2.10. ^{13}C NMR Comparison of C-3, C-5 in *syn*-isomers and *anti*-isomers of **9**. The triketide stereoisomers stereochemistry could be assigned using Hoffmann's rule by adding the ^{13}C NMR shifts of the C3 and C5 signals together: the *anti*-isomers (e.g., **9ba**) would give a smaller $\delta(\text{C3})+\delta(\text{C5})$ value than *syn*-isomers (e.g., **9aa**) because of axial substituents on the chair conformation.

Regarding **9aa** and **9ba**, the conformation seemed to adopt C-3 as axial substituent since in **9ba** there was more difference observed in chemical shift of C-3 than that of C-5. In ^{13}C

NMR, the chemical shift difference was obvious (~ 3 ppm for C-3, ~ 2 ppm for C-5) so that there was no chance to confuse *syn*-isomer with *anti*-isomer. Also, there were difference of other carbon atoms (C-1, C-2 and C-7) in chemical shift, which excluded interference of impurities and demonstrated high credibility using ^{13}C NMR to determine the stereochemistry (**Figure 2.11**). On both ^1H NMR and ^{13}C NMR, all stereoisomers from chemically synthesized **9** were congruent with those from chemo-enzymatically synthesized **9**.

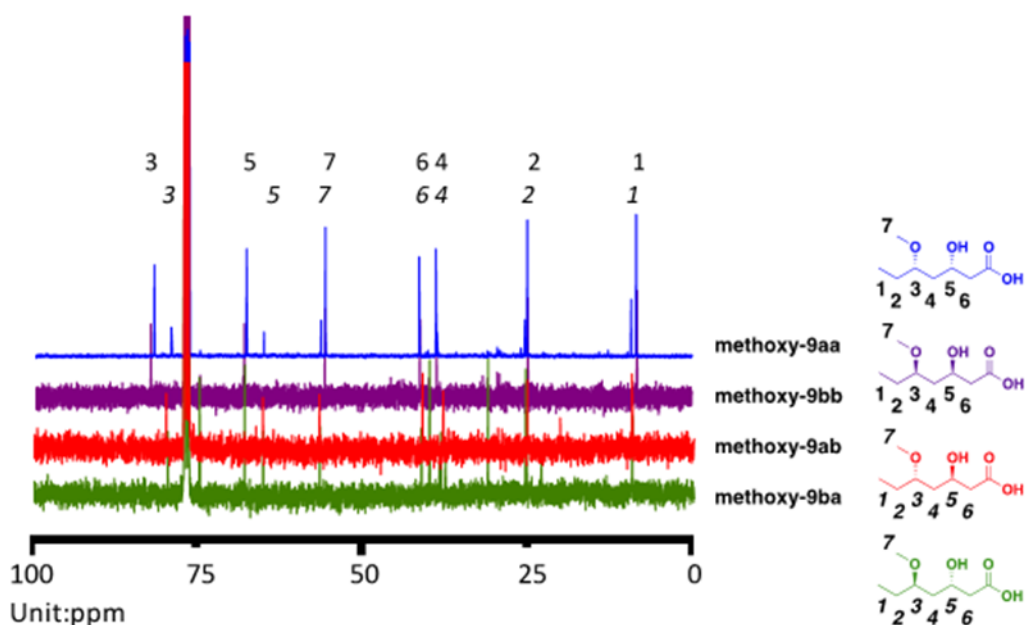


Figure 2.11. ^{13}C NMR Comparison of Major Peaks in *syn*-/*anti*-isomers of **9**. *Syn*-isomers have the same chemical shift pattern different from *anti*-isomers.

Chromatography

Two complementary, chiral chromatography systems were used to determine which stereoisomers were generated in the chemo-enzymatic synthesis of triketides **8aa**, **8ab**, **8ba**, and **8bb** - an OC-H column (normal phase) coupled with a UV detector and an IF3

column (reversed phase) coupled with a time-of-flight (TOF) mass spectrometer (**Figure 5**). The peaks of *anti*-products, **8ab** & **8ba**, were always observed before those of the *syn*-products, **8aa** & **8bb**, in both chromatography. Albeit the *anti*-products could not be separated from each other on the OC-H column, they could be separated on the IF3 column fortunately. Similarly, the *syn*-products could not be separated from each another on the IF3 column, but they could be separated on the OC-H column. In all of the cases, the targeted stereoisomer was the majority (at least 90%) of all stereoisomers. Therefore, it was concluded the A-type KR MycKR6 and the B-type KR TylKR2, which were robust towards diketide NAC thioesters⁹ stereoselectively, were robust also towards triketide NAC thioesters stereoselectively (**Figure 2.12**).

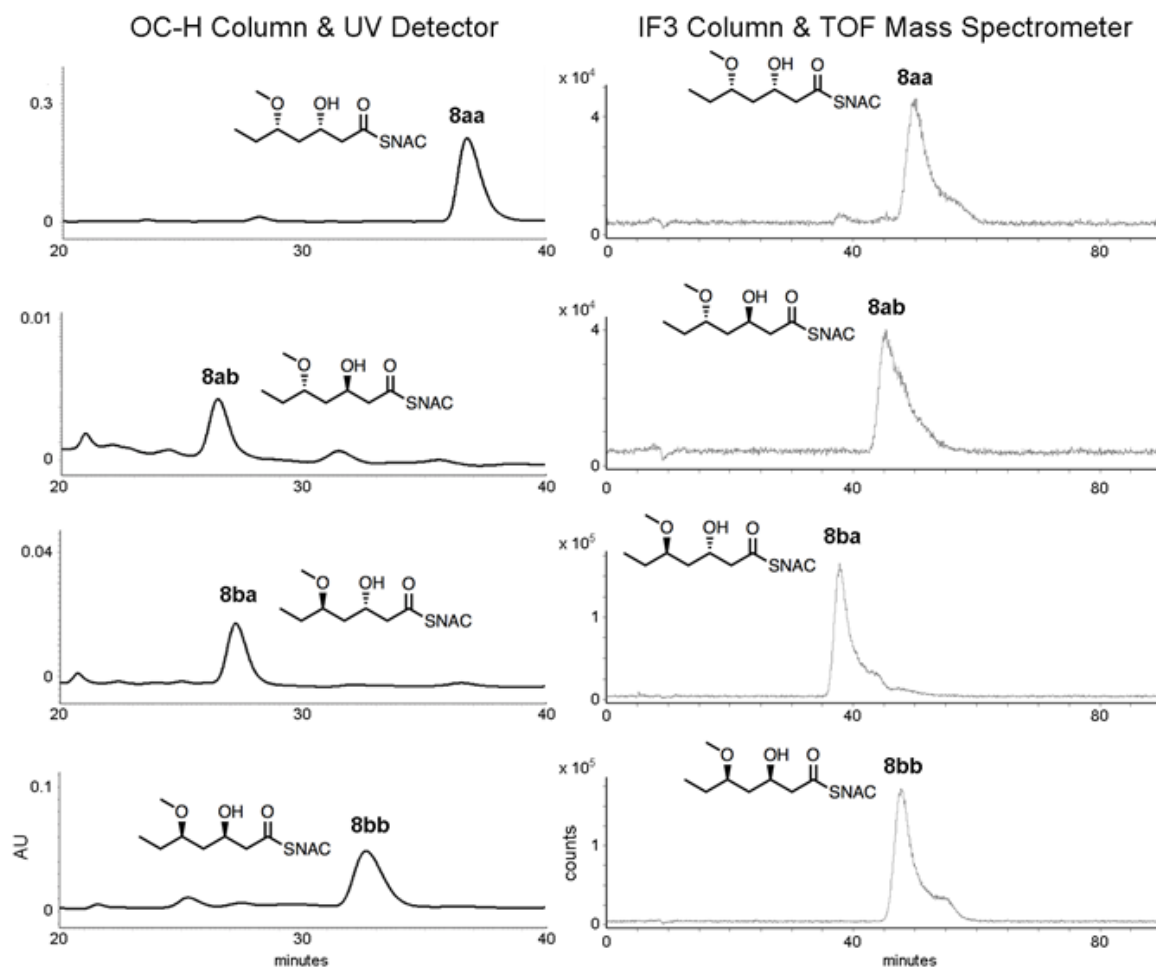


Figure 2.12. Chiral Chromatography of Chemo-enzymatically Generated **8aa**, **8ab**, **8ba**, and **8bb**. by two systems: an OC-H column with a UV detector (left) and an IF3 column with a time-of-flight mass spectrometer (right). The OC-H column was capable to resolve the *syn*-products, whereas the IF3 column was capable to resolve the *anti*-products. Retention times matched those of standards (Table S1). For each target species, the desired triketide stereoisomer comprises at least 90% of all four possible stereoisomer products.

Chemical Standard Comparison

In order to compare products from both synthetic routine, chemically synthesized **9** was transformed to **8** inspired by previous work (Figure 2.13).⁴² Surprisingly but expected, the products from metallic reductions showed exactly the same stereoselectivity as predicted from reactions with β -ketoesters, with (*S*)-Ir-spiro-SAP yielding an (*S*)- β -hydroxyl group

and (*R*)-Ir-spiro-SAP yielding an (*R*)- β -hydroxyl group. In a word, the chemically synthesized **8aa**, **8ab**, **8ba**, and **8bb** had the same characteristics on HPLC and LC/MS with enzymatically synthesized **8aa**, **8ab**, **8ba**, and **8bb**. Thus based on the analysis that the research results were trustworthy.

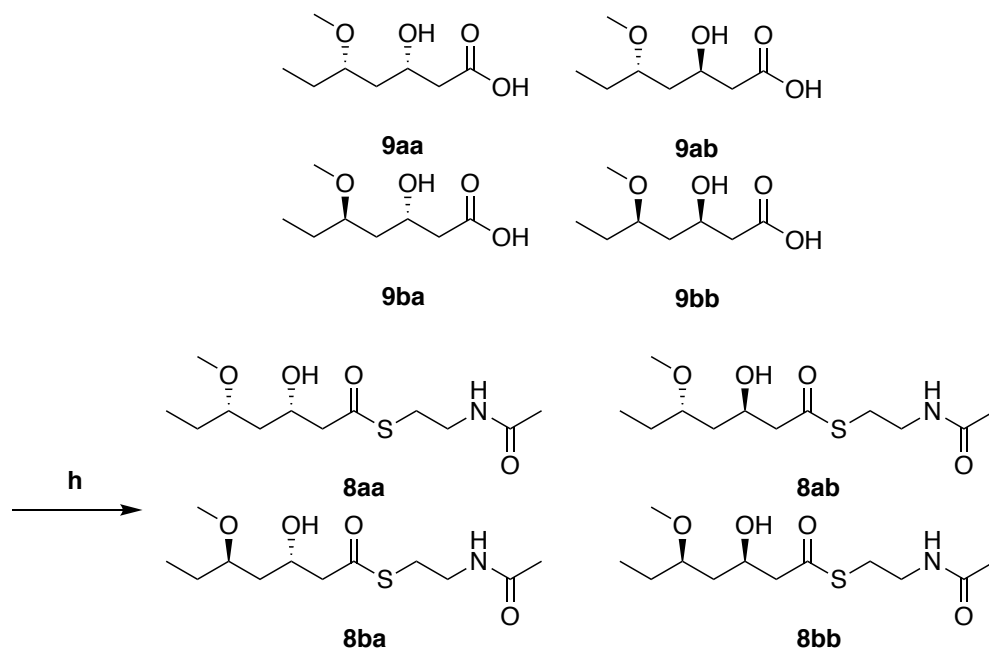


Figure 2.13. Synthesis from **9** to **8**.

Conditions: h) THF, DMAP (0.5 eq.), EDC-HCl (2.3 eq.), NAC (5.0 eq.), 22 °C, overnight.

EXPERIMENTAL PROCEDURES

Equipment and Settings for Characterization

NMR: NMR 400 MHz Agilent and NMR VNMRS 600 MHz Agilent

HPLC condition (normal-phase, chiral): Daicel Chiralcel OC-H dp 5 μm 4.6 mmx25 cm, Beckman Coulter HPLC system with a 20 μl loop, UV 230 nm.

Condition: 7% ethanol 93 % hexane 0.8 ml/min.

LC/MS analysis (for all pure compounds)

Agilent Technologies 6530 Accurate-Mass Q-TOF, Direct Inject, Jet Stream Ion Source ESI, in positive/negative mode.

LC/MS analysis (reverse-phase, chiral, for triketide reaction reactant)

Agilent 1260 Infinity II HPLC with an Agilent 6230 TOF ESI instrument, in positive mode; CHIRALPAK[®] IF-3 column, 4.6 mm \times 250 mm, 3 μm ; column temperature of 30°C.

Condition: 88% water 12 % acetonitrile 0.8 ml/min.

Protein preparation

The expression plasmids for MycKR6, TylKR2, and GDH as well as the purification of GDH have been previously described²⁵. To harvest large quantities of KR for the biocatalytic reactions, ammonium sulfate precipitations were performed. After growing 6 L of transformed *E. coli* BL21(DE3) in LB supplemented with 50 mg/L kanamycin to $OD_{600}=0.6$, cells were harvested through centrifugation (4000 x g, 10 min). They were then resuspended in 75 mL lysis buffer [30 mM HEPES, 500 mM NaCl, 5% (v/v) glycerol, pH 7.0], sonicated, and centrifuged (30,000 x g, 30 min) to obtain the cell lysate. Ammonium sulfate was slowly added to the lysate while stirring at 4 °C until the solution was 65% saturated. The mixture was centrifuged (30,000 x g for 30 min) to yield protein pellets that were stored at -80 °C.

Precipitate is from lysate (**Figure 2.14**).

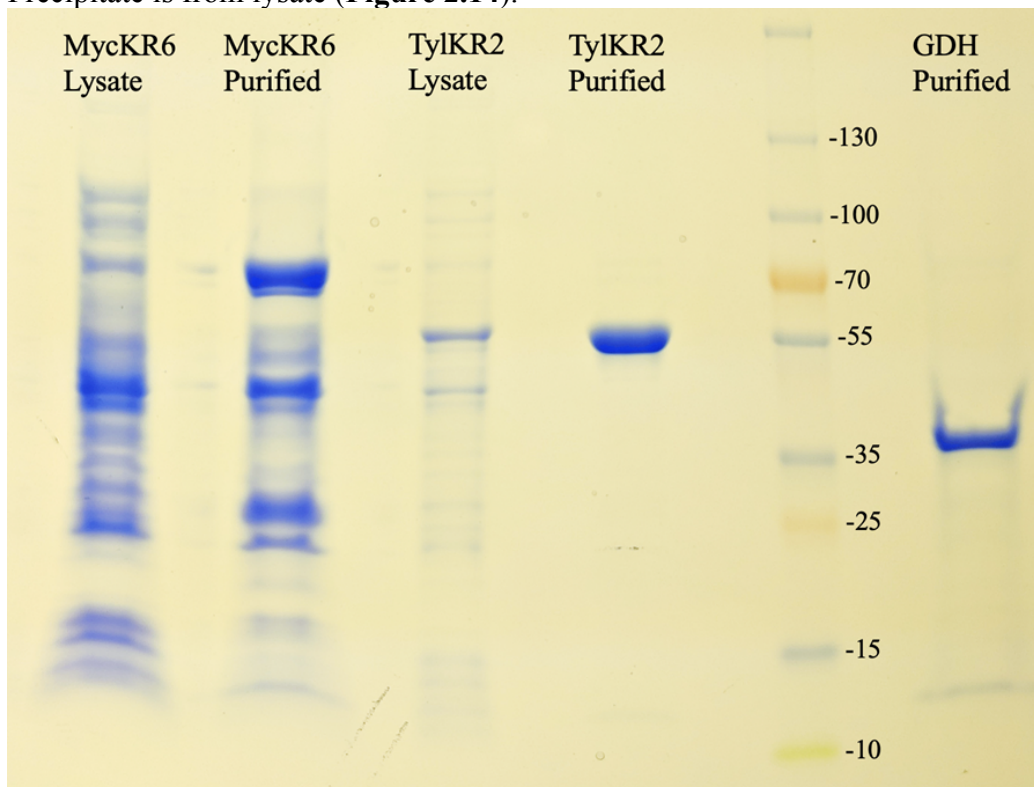
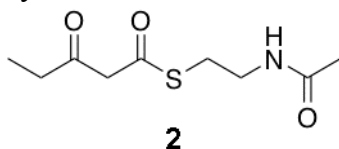


Figure 2.14. Protein Gels for MycKR6, TylKR2, and GDH.

Synthesis and Characterization

Synthesis of **2**



Meldrum's acid (7.2 g, 50.0 mmol) was dissolved in 80 mL dry DCM at 0 °C, and pyridine (8 mL, 100 mmol) was added to the solution. Propionyl chloride (4.35 mL, 50 mmol) was then supplied dropwise over 15 min. The color of the system gradually turned dark orange. The reaction was allowed to warm to 22 °C (r.t.) and stirred overnight. After that, the reaction was washed with 6 x 50 mL 0.1 M HCl to remove pyridine. The organic layer was dried over Na₂SO₄ and concentrated under reduced pressure. Crude **1** (7.6 g, 76.0%) was obtained as dark orange crystals and used directly in the next step.

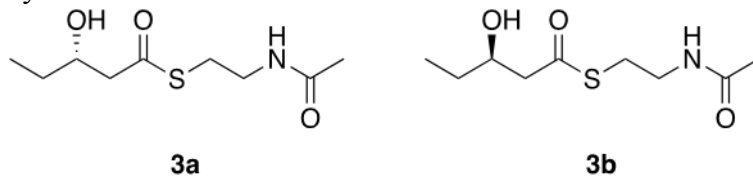
1 (16.8 g, 200 mmol) was dissolved in 150 mL dry toluene, and *N*-acetylcysteamine (NAC, 9.5 g, 119 mmol) was added. The reaction was refluxed at 115 °C for 5 h. The reaction was then cooled down to 22 °C, and the solvent was removed through reduced pressure. Purification of the residue through CuSO₄-impregnated silica gel gave **2** (11.1 g, 61%) as a light yellow to dark brown solid. Column conditions used for half of the crude product: 6 x 11 cm; 600 mL (2:1 hexane: EtOAc), 600 mL (1:1 hexane: EtOAc), followed by pure EtOAc until all of the product was eluted.

¹H NMR (400 MHz, chloroform-*d*) δ 5.97 (s, 1H), 3.69 (s, 2H), 3.45 (m, 2H), 3.08 (t, *J* = 6.0 Hz, 2H), 2.56 (q, *J* = 7.3 Hz, 2H), 1.96 (s, 3H), 1.10 (t, *J* = 7.2 Hz, 3H).

¹³C NMR of **2** (101 MHz, chloroform-*d*) δ 202.61, 192.40, 170.45, 56.91, 39.17, 36.73, 29.20, 23.19, 7.48.

HRESIMS of **2** *m/z* 218.0850 [M+H]⁺ (218.085091 calculated for C₉H₁₆NO₃S).

Syntheses of **3a** and **3b**



Syntheses of **3a**

2 (4.0 g, 18.4 mmol) was combined with 120 mL water, 144 mL 1 M HEPES (pH 7.7), 9.6 mL 5 M NaCl solution, 80 mL 2 M d-glucose, 320 μ L 150 mM NADP⁺, 240 μ L 20 mg/mL GDH, and 80 mL MycKR6 lysate (around 3 mg/ml). The reaction was stirred at 22 °C overnight or until judged complete by LC/MS. To prevent emulsification, heat was applied, and denatured enzyme was separated by centrifugation. After that, the reaction was extracted with 2 L EtOAc, which was dried over Na₂SO₄. Solvent was removed by reduced pressure to give crude **3a** (2.6 g, 65%) as an odorless, yellow oil without further separation.

¹H NMR (400 MHz, chloroform-*d*) δ 6.49 (s, 1H), 3.95 (m, 1H), 3.41 – 3.30 (m, 2H), 3.05 – 2.93 (m, 2H), 2.75 – 2.54 (m, 2H), 1.92 (s, 3H), 1.52 – 1.42 (m, 2H), 0.90 (t, *J* = 7.4 Hz, 3H).

¹³C NMR (101 MHz, chloroform-*d*) δ 199.12, 170.76, 69.92, 50.66, 39.04, 29.59, 28.62, 22.98, 9.69.

HRESIMS of **3a** *m/z* 242.0819 [M+Na]⁺ (242.082686 calculated for C₉H₁₇O₃NSNa).

Syntheses of **3b**

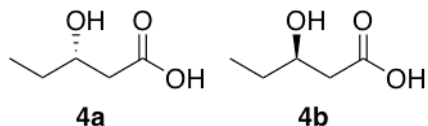
2 (4.0 g, 18.4 mmol) was combined with 120 mL water, 144 mL 1M HEPES (pH 7.7), 9.6 mL 5 M NaCl solution, 80 mL 2 M d-glucose, 320 μ L 150 mM NADP⁺, 240 μ L 20 mg/ml GDH, and 80 mL TylKR2 lysate (around 3 mg/ml). The reaction was stirred at 22 °C overnight or until judged complete by LC/MS. To prevent emulsification, heat was applied, and denatured enzyme was separated by centrifugation. After that, the reaction was extracted with 2 L EtOAc, which was dried over Na₂SO₄. Solvent was removed by reduced pressure to give crude **3b** (2.3 g, 58%) as an odorless, yellow oil without further separation.

¹H NMR of **3b** (400 MHz, chloroform-*d*) δ 6.55 (s, 1H), 3.93 (m, 1H), 3.38 – 3.32 (m, 2H), 2.97 (m, 2H), 2.68 – 2.57 (m, 2H), 1.91 (s, 3H), 1.52 – 1.42 (m, 2H), 0.94 – 0.85 (t, 3H).

¹³C NMR of **3b** (101 MHz, chloroform-*d*) δ 199.03, 170.80, 69.90, 50.67, 39.01, 29.58, 28.59, 22.96, 9.68.

HRESIMS of **3b** m/z 242.0820 [M+Na]⁺ (242.0827 calculated for C₉H₁₇O₃NSNa).

Syntheses of **4a** and **4b**



Syntheses of **4a**

3a (2.5 g, 11.4 mmol) was dissolved in 60 mL 5.0 M sodium hydroxide and stirred at 80 °C overnight. The solution was adjusted to ~pH 9 and washed with 3 x 50 mL EtOAc. Next, it was acidified to pH 1 with concentrated HCl and extracted with 5 x 100 mL EtOAc. The organic phase was dried over Na₂SO₄, and the solvent was twice co-evaporated with 20 mL toluene through reduced pressure to give crude **4a** (630 mg, 51%) as a dark oil without further purification.

¹H NMR of (400 MHz, chloroform-*d*) δ 3.97 (m, 1H), 2.59 (dd, *J* = 16.0, 3.1 Hz, 1H), 2.48 (dd, *J* = 16.3, 8.9 Hz, 1H), 1.67 – 1.45 (m, 2H), 0.97 (t, *J* = 7.5 Hz, 3H).

¹³C NMR of **4a** (101 MHz, chloroform-*d*) δ 177.60, 69.32, 40.62, 29.43, 9.78.

HRESIMS of **4a** *m/z* 117.0557 [M-H][−] (117.055170 calculated for C₅H₉O₃).

Synthesis of **4b**

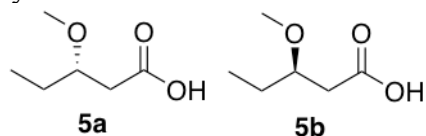
3b (2.6 g, 11.6 mmol) was dissolved in 60 mL of 5 M sodium hydroxide and stirred at 80 °C overnight. The solution was adjusted to pH 9 and washed with 3 x 50 mL EtOAc. Next, it was adjusted to pH 1 with concentrated HCl and extracted with 5 x 100 mL EtOAc. The organic phase was dried over Na₂SO₄, and the solvent was twice co-evaporated with 20 mL toluene under reduced pressure to give crude **4b** (820 mg, 59%) as a dark oil without further purification.

¹H NMR (400 MHz, chloroform-*d*) δ 3.97 (m, 1H), 2.58 (dd, *J* = 16.7, 3.1 Hz, 1H), 2.41 (dd, *J* = 16.7, 8.9 Hz, 2H), 1.63 – 1.45 (m, 2H), 0.97 (t, *J* = 7.4 Hz, 3H).

¹³C NMR of **4b** (101 MHz, chloroform-*d*) δ 177.60, 69.34, 40.60, 29.38, 9.76.

HRESIMS of **4b** *m/z* 117.0556 [M-H][−] (117.055170 calculated for C₅H₉O₃).

Syntheses of **5a** and **5b**



This procedure is a modification of a published protocol.⁴⁰

Synthesis of **5a**

5.8 mL 2.5 M *n*-butyllithium in hexanes (14.5 mmol) was carefully dripped into 7.0 mL dry DMSO under argon. The reaction was stirred for 40 min to form DMSO lithium base. **4a** (567 mg, 4.80 mmol) was dissolved in 4.0 mL DMSO, and this solution was slowly added to the reaction and stirred for 2 h. 0.71 mL MeI (1.67 g, 11.34 mmol) was then added, and the reaction was stirred at 22 °C overnight. Then 15 mL water was added to quench the reaction, and the mixture was washed with 4 x 50 mL diethyl ether. The solution was adjusted to pH 1 and extracted with 6 x 50 mL diethyl ether, which was dried over Na₂SO₄. The solvent was passed through CuSO₄-packed silica gel and removed under reduced pressure to give crude **5a** (462 mg, 73%) as a dark oil without further purification.

¹H NMR (400 MHz, chloroform-*d*) δ 3.59 (m, 1H), 3.39 (s, 3H), 2.55 (dd, *J* = 15.4, 7.3 Hz, 1H), 2.49 (dd, *J* = 15.4, 5.1 Hz, 1H), 1.69 – 1.53 (m, 2H), 0.93 (t, *J* = 7.5 Hz, 3H).

¹³C NMR of **5a** (101 MHz, chloroform-*d*) δ 174.88, 78.56, 56.64, 38.64, 26.09, 9.02.

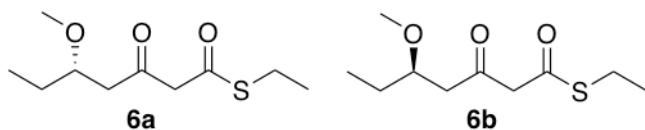
HRESIMS of **5a** *m/z* 131.0717 [M-H]⁻ (131.070820 calculated for C₆H₁₁O₃).

Synthesis of **5b**

7.8 mL 2.5 M *n*-butyllithium in hexanes (19.5 mmol) was carefully dripped into 10.0 mL dry DMSO under argon. The reaction was stirred for 40 min to form DMSO lithium base. **4b** (850 mg, 7.19 mmol) was dissolved in 6.0 mL DMSO, and this solution was slowly added to the reaction and stirred for 2 h. 1.1 mL MeI (1.67 g, 17.26 mmol) was then added, and the reaction was stirred at 22 °C overnight. After that, 20 mL water was added to quench the reaction. The mixture was washed with 4 x 50 mL diethyl ether, adjusted to pH 1, and extracted with 5 x 50 mL diethyl ether. The organic layer was dried over Na₂SO₄. The solvent was passed through CuSO₄-packed silica gel and then removed by reduced pressure to give crude **5b** (740 mg, 78%) as a dark oil without further purification. While not necessary, traces of DMSO can be removed from **5a** and **5b** through flash chromatography. Column conditions: 3 x 5 cm; 300 mL 10:1 hexane: EtOAc and then 5:1 hexane: EtOAc until all the product elutes.

¹H NMR of **5b** (400 MHz, Chloroform-*d*) δ 3.59 (m, 1H), 3.38 (s, 3H), 2.54 (dd, *J* = 15.4, 7.3 Hz, 1H), 2.47 (dd, *J* = 15.4, 5.2 Hz, 1H), 1.61 (m, 2H), 0.92 (t, *J* = 7.4 Hz, 3H).
¹³C NMR of **5b** (101 MHz, chloroform-*d*) δ 174.54, 78.36, 56.35, 38.43, 25.87, 8.79.
HRESIMS *m/z* 131.0712 [M-H]⁻ (131.070820 calculated for C₆H₁₁O₃).

Syntheses of **6a** and **6b**



Synthesis of **6a**

This protocol is modified from a reported procedure³³. Portion A: 1,1'-

Carbonyldiimidazole (CDI) (1.16 g, 7.18 mmol) and **5a** (863 mg, 6.53) were carefully dissolved in 30 mL anhydrous THF. The reaction was stirred for 6 h at 22 °C. Portion B: Mg(OEt)₂ (411 mg, 3.59 mmol) and malonic acid half ethyl thioester (1.06 g, 7.17 mmol) were dissolved in 15 mL anhydrous THF, and the reaction was kept stirring for 3 h at 22 °C. Portions A and B were then combined and stirred overnight at 22 °C. The reaction was quenched with 100 mL 0.5 M HCl and the aqueous layer was extracted with 3 x 100 mL diethyl ether. The organic layer was washed with saturated NaHCO₃ and dried over Na₂SO₄. The solvent was carefully removed through reduced pressure without heat.

Purification of the residue by column chromatography gave **6a** (633 mg, 35%) as a reddish liquid. Column condition: 3x12 cm. Eluant: 300 mL (50:1 hexane: EtOAc), 200 mL (40:1 hexane: EtOAc) and then around 200 mL (20:1 hexane: EtOAc). When product is pure, column chromatography is not required.

¹H NMR (400 MHz, chloroform-*d*) δ 3.70 (s, 2H), 3.63 (m, 1H), 3.32 (s, 3H), 2.93 (q, *J* = 7.5 Hz, 2H), 2.75 (dd, *J* = 16.5, 7.6 Hz, 2H), 2.58 (dd, *J* = 15.6, 4.6 Hz, 2H), 1.54 (m, 2H), 1.27 (t, *J* = 7.5 Hz, 3H), 0.89 (t, *J* = 7.5 Hz, 3H).

¹³C NMR of **6a** (101 MHz, chloroform-*d*) δ 201.24, 192.06, 78.09, 58.43, 56.93, 47.15, 26.17, 23.95, 14.45, 9.10.

HRESIMS of **6a** *m/z* 241.0874 [M+Na]⁺ (241.087437 calculated for C₁₀H₁₈O₃SNa).

Synthesis of **6b**

Portion A: 1,1'-Carbonyldiimidazole (CDI) (597 mg, 3.68 mmol) and **5b** (442 mg, 3.34 mmol) were carefully dissolved in anhydrous 15 mL THF. The reaction was kept stirring for 5 h at 22 °C. Portion B: Mg(OEt)₂ (221 mg, 1.84 mmol) and malonic acid half ethyl thioester (545 mg, 3.68 mmol) were dissolved in 7 mL anhydrous THF, the reaction was kept stirring for 3 h at 22 °C. Portion A and Portion B were combined and kept stirring overnight at 22 °C.

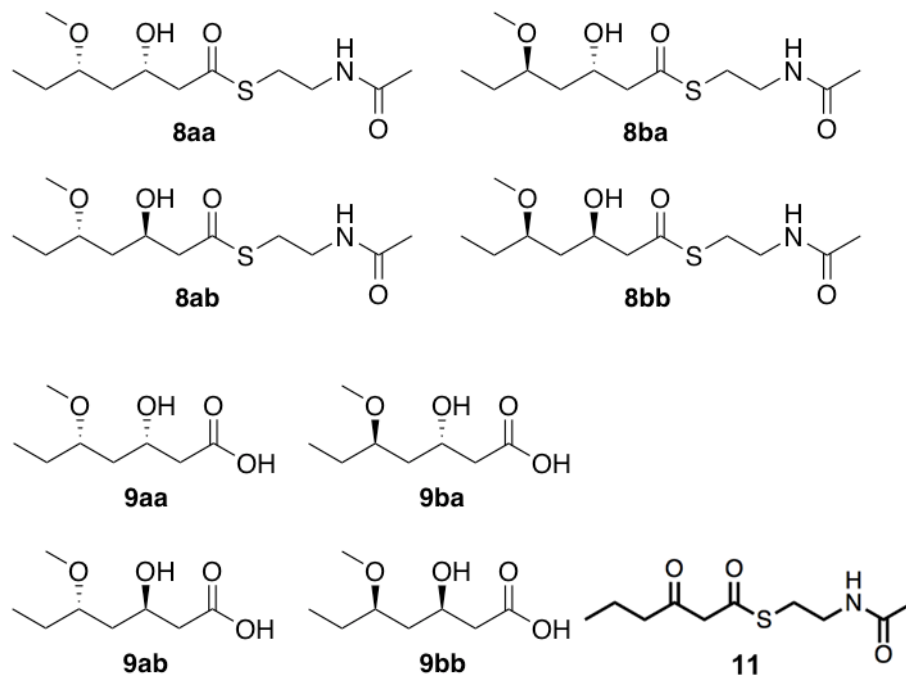
After that, the reaction was quenched with 50 mL 0.5 M HCl and partitioned by 50 mL diethyl ether. The aqueous layer was extracted by diethyl ether 50 mL twice and 25 mL once. The organic layer was washed with saturated NaHCO₃ and dried over Na₂SO₄. The solvent was carefully removed by reduced pressure without heat. Purification of the residue via column chromatography gave **6b** (251 mg, 34%) as a reddish liquid. Column condition: 1x12 cm. Eluant: 50:1 hexane: EtOAc until all coming out. When product is pure, column chromatography is not required.

¹H NMR (400 MHz, chloroform-*d*) δ 3.70 (s, 2H), 3.63 (m, 1H), 3.33 (s, 3H), 2.93 (q, *J* = 7.5 Hz, 2H), 2.75 (dd, *J* = 15.5, 7.7 Hz, 1H), 2.58 (dd, *J* = 15.9, 4.7 Hz, 1H), 1.54 (m, 2H), 1.27 (t, *J* = 7.6 Hz, 3H), 0.89 (t, *J* = 7.4 Hz, 3H).

¹³C NMR of **6b** (101 MHz, chloroform-*d*) δ 201.27, 192.08, 78.07, 58.44, 56.94, 47.16, 26.16, 23.96, 14.46, 9.11.

HRESIMS of **6b** *m/z* 241.0872 [M+Na]⁺ (241.087437 calculated for C₁₀H₁₈O₃SN_a).

Syntheses of **8aa** & **9aa**, **8ab** & **9ab**, **8ba** & **9ba**, and **8bb** & **9bb** with KRs



Two-stereocenter triketides were synthesized from **6a** and **6b** both through metallic asymmetric reduction⁴ and through KR reduction.

Two complementary, chiral chromatography systems were used to determine which stereoisomers were generated in the chemoenzymatic syntheses of triketides **8aa**, **8ab**, **8ba**, and **8bb** - an OC-H column (normal phase) coupled with a UV detector and an IF3 column (reversed phase) coupled with a time-of-flight (TOF) mass spectrometer. The *trans*-products, **8ab** & **8ba**, eluted before the *cis*-products, **8aa** & **8bb**, in both chromatographies. While the *trans*-products could not be resolved from one another on the OC-H column, they could be on the IF3 column, and while the *cis*-products could not be resolved from one another on the IF3 column, they could be on the OC-H column. For all LC/MS-TOF studies, *S*-(2-acetamidoethyl) 3-oxohexanethioate, **11**, was supplied as an internal standard (synthesized the same as **2**, except with the use of butyryl chloride). Extracted ion chromatograms of triketide targets (pp. 25-26) and internal standard **11** (p. 27) are presented.

Reduction of β -keto triketide through KRs

Using Lysate (30 ml lysate good for 100 mg starting material)

Synthesis of **8aa** & **9aa**

6a (110 mg, 0.389 mmol) was added to a solution containing 500 μ L NAC (around 10 eq.) 10 mL water, and 12 mL of 1 M HEPES (pH 8.5). The thiol-thioester exchange was performed over 2 h at 22 °C, and then the pH was adjusted to 7.7 with concentrated HCl. 800 μ L of 5 M NaCl, 6 mL of 2.0 M d-glucose, 160 μ L of 0.15 M NADP⁺, 180 μ L of GDH (15 mg/mL), and 30 mL of MycKR6 lysate (around 3 mg/ml). were then consecutively added to the reaction. The reaction was kept stirring at 22 °C overnight or until it was done monitored by LC/MS. Heat was applied by microwave, and the aggregated enzyme was separated by centrifugation. After that, the reaction was extracted by 450 mL EtOAc. The extract was dried over Na₂SO₄, and the solvent was removed by reduced pressure. Formation of **8aa** and its stereoisomers could be analyzed by chiral chromatography. 10 mL of 5 M NaOH was added to the residue, and the reaction was heated to 80 °C overnight. After that, the reaction was cooled down and washed with 2 x 50 mL EtOAc. The pH was then adjusted to 1, and the reaction was extracted with 3 x 50 mL EtOAc. The extract was dried over Na₂SO₄. The solvent was passed through a plug of CuSO₄-impregnated silica gel and co-evaporated with toluene under reduced pressure to give crude **9aa** (50 mg, 57%) as a dark oil.

HRESIMS of **8aa** m/z 300.1247 $[M+Na]^+$ (300.124551 calculated for $C_{12}H_{23}NO_4SNa$).

Stereoisomer distribution determined through complementary chiral chromatographies (see p. 26): >90% **8aa**

1H NMR (400 MHz, chloroform-*d*) δ 4.24 (m, 1H), 3.44 (m, 1H), 3.34 (s, 3H), 2.52 (m, 2H), 1.62 (m, 4H), 0.86 (t, $J = 7.6$ Hz, 3H).

^{13}C NMR of **9aa** (101 MHz, chloroform-*d*) δ 176.01, 82.06, 67.96, 55.91, 41.56, 39.04, 25.07, 8.44.

HRESIMS of **9aa** m/z 175.0977 $[M-H]^-$ (175.097035 calculated for $C_8H_{15}O_4$).

Synthesis of **8ab** & **9ab**

6a (55 mg, 0.195 mmol) was added to a solution containing 250 μ L NAC (around 10 eq.), 5 mL water and 6 mL of 1 M HEPES (pH 8.5). The thiol-thioester exchange was performed over 2 h at 22 $^{\circ}$ C, and then the pH was adjusted to 7.7 with concentrated HCl. 800 μ L of 5 M NaCl, 6 mL of 2.0 M d-glucose, 160 μ L of 0.15 M NADP⁺, 180 μ L of GDH (15 mg/ml), and 30 mL of TylKR2 lysate (around 3 mg/ml). were then consecutively added to the reaction. The reaction was kept stirring at 22 $^{\circ}$ C for 2 d or until it was done monitored by LC/MS. Heat was applied by microwave, and the aggregated enzyme was separated by centrifugation. After that, the reaction was extracted by 450 mL EtOAc. The extract was dried over Na₂SO₄, and the solvent was removed by reduced pressure. Formation of **8ab** and its stereoisomers could be analyzed by chiral chromatography. 10 mL of 5 M NaOH was added to the residue, and the reaction was heated to 80 $^{\circ}$ C overnight. After that, the reaction was cooled down and washed with 2 x 50 mL EtOAc. The pH was then adjusted to 1, and the reaction was extracted with 3 x 50 mL EtOAc. The extract was dried over Na₂SO₄. The solvent was passed through a plug of CuSO₄-impregnated silica gel and co-evaporated with toluene under reduced pressure to give crude **9ab** (16 mg, 36%) as a dark oil.

HRESIMS of **8ab** m/z 300.1245 $[M+Na]^+$ (300.124551 calculated for $C_{12}H_{23}NO_4SNa$).

Stereoisomer distribution determined through complementary chiral chromatographies (see p. 26): >96% **8ab**

1H NMR (400 MHz, chloroform-*d*) δ 4.32 (m, 1H), 3.45 (m, 1H), 3.39 (s, 3H), 2.55 (m, 2H), 1.65 (m, 4H), 0.91 (t, $J = 7.5$ Hz, 3H).

^{13}C NMR of **9ab** (101 MHz, chloroform-*d*) δ 175.71, 79.92, 65.37, 56.78, 41.31, 38.27, 25.33, 9.34.

HRESIMS of **9ab** m/z 175.0980 $[M-H]^-$ (175.097035 calculated for $C_8H_{15}O_4$).

Using Precipitate (100 mg precipitate good for 100 mg starting material)

Synthesis of **8ba** & **9ba**

6b (20 mg, 0.092 mmol) was added to a solution containing 91 μ L NAC (around 10 eq.), 1.82 mL water, and 2.2 mL of 1 M HEPES (pH 8.5). The thiol-thioester exchange was performed over 2 h at 22 $^{\circ}$ C, and then the pH was adjusted to 7.7 with concentrated HCl. 291 μ L of 5 M NaCl, 2.2 mL of 2.0 M d-glucose, 58 μ L of 0.15 M NADP⁺, 110 μ L of GDH (15 mg/mL), and 20 mg MycKR6 precipitate were then consecutively added to the reaction. The reaction was kept stirring at 22 $^{\circ}$ C overnight or until it was done monitored by LC/MS. Intermediate **8ba** could be characterized by HPLC if directly extracted by EtOAc (see HPLC before). Heat was applied by microwave, and the aggregated enzyme was separated by centrifugation. After that, the reaction was extracted by 450 mL EtOAc. The extract was dried over Na₂SO₄, and the solvent was removed by reduced pressure. Formation of **8ba** and its stereoisomers could be analyzed by chiral chromatography. 10 mL of 5 M NaOH was added to the residue, and the reaction was heated to 80 $^{\circ}$ C overnight. After that, the reaction was cooled down and washed with 2 x 50 mL EtOAc. The pH was then adjusted to 1, and the reaction was extracted with 3 x 50 mL EtOAc. The solvent was passed through a plug of CuSO₄-impregnated silica gel and co-evaporated with toluene under reduced pressure to give crude **9ba** (7 mg, 44%) as a dark oil.

HRESIMS of **8ba** m/z 300.1228 $[M+Na]^+$ (300.124551 calculated for $C_{12}H_{23}NO_4SNa$).

Stereoisomer distribution determined through complementary chiral chromatographies (see p. 26): >89% **8ba**

1H NMR (400 MHz, chloroform-*d*) δ 4.33 (s, 1H), 3.47 (s, 1H), 3.39 (s, 3H), 2.54 (m, 2H), 1.65 (m, 4H), 0.91 (t, $J = 7.6$ Hz, 3H).

^{13}C NMR of **9ba** (101 MHz, chloroform-*d*) δ 175.21, 79.84, 65.35, 56.78, 41.36, 38.42, 25.38, 9.32.

HRESIMS of **9ba** m/z 175.0974 $[M-H]^-$ (175.097035 calculated for $C_8H_{15}O_4$).

Synthesis of **8bb** & **9bb**

6b (106 mg, 0.486 mmol) was added to a solution containing 500 μ L NAC (around 10 eq.), 10 mL water, and 12 mL of 1 M HEPES (pH 8.5). The thiol-thioester exchange was performed over 2 h at 22 $^{\circ}$ C, and then the pH was adjusted to 7.7 with concentrated HCl. 800 μ L of 5 M NaCl, 6 mL of 2.0 M d-glucose, 160 μ L of 0.15 M NADP⁺, 180 μ L GDH (15 mg/mL), and 1.0 g of TylKR2 precipitate were then consecutively added to the reaction. The reaction was kept stirring at 22 $^{\circ}$ C overnight or until it was done monitored by LC/MS. Heat was applied by microwave, and the aggregated enzyme was separated by centrifugation. After that, the reaction was extracted by 450 mL EtOAc. The extract was dried over Na₂SO₄, and the solvent was removed by reduced pressure. Formation of **8bb** and its stereoisomers could be analyzed by chiral chromatography. 10 mL of 5 M NaOH solution was added to the residue, and the reaction was heated to 80 $^{\circ}$ C overnight. After that, the reaction was cooled down and washed with 2 x 50 mL EtOAc. The pH was then adjusted to 1, and the reaction was extracted with 3 x 50 mL EtOAc. The extract was dried over Na₂SO₄. The solvent was passed through a plug of CuSO₄-impregnated silica gel and co-evaporated with toluene under reduced pressure to give crude **9bb** (22 mg, 24%) as a dark oil.

HRESIMS of **8bb** m/z 300.1242 $[M+Na]^+$ (300.124551 calculated for $C_{12}H_{23}NO_4SNa$).

Stereoisomer distribution determined through complementary chiral chromatographies (see p. 26): >96% **8bb**

1H NMR (400 MHz, chloroform- d) δ 4.24 (m, 1H), 3.48 (m, 1H), 3.38 (s, 3H), 2.55 (m, 2H), 1.65 (m, 4H), 0.88 (t, $J = 7.5$ Hz, 3H).

^{13}C NMR of **9bb** (101 MHz, chloroform- d) δ 175.01, 82.52, 68.25, 55.97, 41.48, 38.95, 25.02, 8.38.

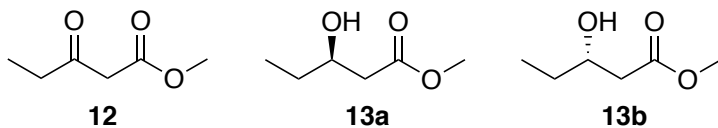
HRESIMS of **9bb** m/z 175.0970 $[M-H]^-$ (175.097035 calculated for $C_8H_{15}O_4$).

Notice:

For the final reaction, the purity of final compounds often depends on the reaction conditions. Generally speaking, purer enzyme, less reaction time and lower ambient temperature will minimize the byproduct. The byproducts have some peaks similar to those of final products on NMR, but they are not the isomers of the final products. That's why for chiral analysis, LC/MS is preferred. If removal of byproducts is desired, silica gel chromatography (eluent: 3:1 hexane: EtOAc) is preferred.

Synthesis of Chemical Standard by catalytic reduction

High-Pressure Hydrogenation using technology from Parr® Series 4760 Pressure Vessel

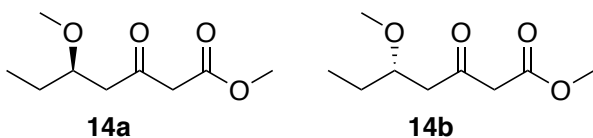


12 is commercially available

13a 13b were synthesized according to the following reference with almost full conversion³⁷.

Synthesis of **4a 4b** from **13a 13b** adopted same procedure as from **3a 3b** to **4a 4b**.

Synthesis from **4a 4b** to **6a 6b** were the same as described above.



Synthesis of **14a**

800 mg **6a** (366 mmol) was dissolved in 40 ml anhydrous methanol, 2.0 g sodium methoxide (3700 mmol) was then added portion by portion into the system. The solution should have turned into yellowish color. After that, the reaction was monitored by TLC (usually 6-9 hours). Methanol was removed when the reaction was done and the residue was turned to neutral pH by hydrochloric acid. The aqueous solution was extracted by EtOAc 50 ml thrice and dried over Na₂SO₄. The organic solvent was then removed and purification of the residue via column chromatography gave **14a** (186 mg, 27 %) as a yellowish liquid. Column condition: 3x13 cm. Eluant: 50:1 hexane: EtOAc, 40:1 hexane: EtOAc, 30:1 hexane: EtOAc, 10:1 hexane: EtOAc and then 1:1 hexane: EtOAc until all product coming out.

¹H NMR of **14a** (500 MHz, Chloroform-*d*) δ 3.74 (s, 3H), 3.62 (m, 1H), 3.51 (s, 2H), 3.32 (s, 3H), 2.74 (dd, *J* = 14.1, 7.8 Hz, 1H), 2.58 (dd, *J* = 15.9, 4.5 Hz, 1H), 1.56 (m, 2H), 0.90 (t, *J* = 7.4 Hz, 3H).

¹³C NMR of **14a** (126 MHz, Chloroform-*d*) δ 201.86, 167.58, 78.18, 56.95, 52.31, 50.02, 47.06, 26.14, 9.09.

HRESIMS of **14a** *m/z* 211.09359 [M+Na]⁺ (211.09408 calculated for C₉H₁₆O₄Na).

Synthesis of **14b**

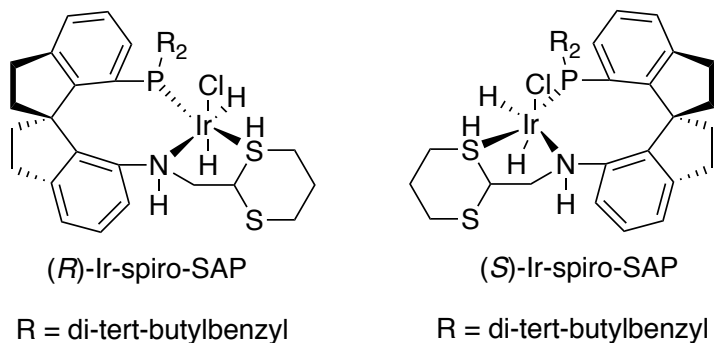
292 mg **6b** (134 mmol) was dissolved in 20 ml anhydrous methanol, 756 mg sodium methoxide (1400 mmol) was then added portion by portion into the system. The solution should have turned into yellowish color. After that, the reaction was monitored by TLC (usually 6-9 hours). Methanol was removed when the reaction was done and the residue was turned to neutral pH by hydrochloric acid. The aqueous solution was extracted by EtOAc 50 ml thrice and dried over Na₂SO₄. The organic solvent was then removed and purification of the residue via column chromatography gave **14b** (41 mg, 16 %) as a yellowish liquid. Column condition: 1x10 cm. Eluant: 50:1 hexane: EtOAc, 40:1 hexane: EtOAc, 30:1 hexane: EtOAc, and then 1:1 hexane: EtOAc until all product coming out.

¹H NMR of **14b** (500 MHz, Chloroform-*d*) δ 3.67 (s, 3H), 3.55 (m, 1H), 3.44 (s, 2H), 3.25 (s, 3H), 2.67 (dd, *J* = 15.0, 7.8 Hz, 1H), 2.52 (dd, *J* = 16.1, 4.3 Hz, 2H), 1.50 (m, 2H), 0.85 (t, *J* = 7.4 Hz, 3H).

¹³C NMR of **14b** (126 MHz, Chloroform-*d*) δ 201.69, 167.41, 77.97, 56.72, 52.08, 49.79, 46.86, 25.96, 8.90.

HRESIMS of **14b** *m/z* 211.09371 [M+Na]⁺ (211.09408 calculated for C₉H₁₆O₄Na).

Synthesis of **9aa**, **9ab**, **9ba** and **9bb** was adapted from the following reference⁵



Synthesis of **9aa**

95 mg **14a**, 6 mg [Ir-(S)-DTB-SpiroSAP] and 6 mg t-BuOK were dissolved in 2 ml anhydrous MeOH. The reaction was quickly relocated in the hydrogenation vessel and pressurized to 100 atm. After 2 days, monitored by NMR, the reaction was depressurized and the solvent was removed. 5 ml 5M NaOH solution was added to the residue and kept at 60 °C overnight. After that, the aqueous solution was washed with 10 ml EtOAc thrice and turned pH to 0. The aqueous solution was extracted by EtOAc 50 ml thrice and dried over Na₂SO₄. The organic layer was filtered through a CuSO₄ incorporated silica gel column. After that, the filtrate was co-evaporated with toluene to give **9aa** as a sticky yellow liquid without further separation. (70 mg, 77% yield)

¹H NMR of **9aa** (500 MHz, Chloroform-d) δ 4.24 (s, 1H), 3.44 (m, 1H), 3.34 (s, 3H), 2.52 (d, *J* = 6.4 Hz, 2H), 1.63 (m, 4H), 0.86 (t, *J* = 7.5 Hz, 3H).

¹³C NMR of **9aa** (126 MHz, Chloroform-*d*) δ 176.64, 81.98, 67.85, 55.90, 41.59, 39.12, 25.09, 8.44.

Synthesis of **9ab**

91 mg **14a**, 6 mg [Ir-(R)-DTB-SpiroSAP] and 6 mg t-BuOK were dissolved in 2 ml anhydrous MeOH. The reaction was quickly relocated in the hydrogenation vessel and pressurized to 100 atm. After 2 days, monitored by NMR, the reaction was depressurized and the solvent was removed. 5 ml 5M NaOH solution was added to the residue and kept at 60 °C overnight. After that, the aqueous solution was washed with 10 ml EtOAc thrice and turned pH to 0. The aqueous solution was extracted by EtOAc 50 ml thrice and dried over Na₂SO₄. The organic layer was filtered through a CuSO₄ incorporated silica gel column. After that, the filtrate was co-evaporated with toluene to give **9ab** as a sticky yellow liquid without further separation. (83 mg, 97% yield)

¹H NMR of **9ab** (500 MHz, Chloroform-*d*) δ 4.30 (m, 1H), 3.44 (m, 1H), 3.36 (s, 3H), 2.51 (d, *J* = 6.0 Hz, 2H), 1.61 (m, 4H), 0.88 (td, *J* = 7.5 Hz, 3H).

¹³C NMR of **9ab** (126 MHz, Chloroform-*d*) δ 176.53, 79.43, 65.29, 56.55, 41.52, 39.00, 25.47, 9.16.

Synthesis of **9ba**

41 mg **14b**, 2 mg [Ir-(S)-DTB-SpiroSAP] and 2 mg t-BuOK were dissolved in 1 ml anhydrous MeOH. The reaction was quickly relocated in the hydrogenation vessel and pressurized to 100 atm. After 2 days, monitored by NMR, the reaction was depressurized and the solvent was removed. 5 ml 5M NaOH solution was added to the residue and kept at 60 °C overnight. After that, the aqueous solution was washed with 5 ml EtOAc thrice and turned pH to 0. The aqueous solution was extracted by EtOAc 50 ml thrice and dried over Na₂SO₄. The organic layer was filtered through a CuSO₄ incorporated silica gel column. After that, the filtrate was co-evaporated with toluene to give **9ba** as a sticky yellow liquid without further separation. (32 mg, 83% yield)

¹H NMR of **9ba** (500 MHz, Chloroform-*d*) δ 4.32 (m, 1H), 3.46 (m, 1H), 3.37 (s, 3H), 2.53 (d, *J* = 6.1 Hz, 2H), 1.62 (m, 4H), 0.89 (t, *J* = 7.5 Hz, 3H).

¹³C NMR of **9ba** (126 MHz, Chloroform-*d*) δ 176.69, 79.59, 65.33, 56.63, 41.50, 38.78, 25.44, 9.23.

Synthesis of **9bb**

57 mg **14b**, 3 mg [Ir-(R)-DTB-SpiroSAP] and 3 mg t-BuOK were dissolved in 2 ml anhydrous MeOH. The reaction was quickly relocated in the hydrogenation vessel and pressurized to 100 atm. After 2 days, monitored by NMR, the reaction was depressurized and the solvent was removed. 5 ml 5M NaOH solution was added to the residue and kept at 60 °C overnight. After that, the aqueous solution was washed with 5 ml EtOAc thrice and turned pH to 0. The aqueous solution was extracted by EtOAc 50 ml thrice and dried over Na₂SO₄. The organic layer was filtered through a CuSO₄ incorporated silica gel column. After that, the filtrate was co-evaporated with toluene to give **9bb** as a sticky yellow liquid without further separation. (46 mg, 86% yield)

¹H NMR of **9bb** (500 MHz, Chloroform-*d*) δ 4.25 (m, 1H), 3.44 (m, 1H), 3.34 (s, 3H), 2.52 (d, *J* = 5.2 Hz, 2H), 1.62 (m, 4H), 0.86 (t, *J* = 7.5 Hz, 3H).

¹³C NMR of **9bb** (126 MHz, Chloroform-*d*) δ 176.68, 82.04, 67.89, 55.91, 41.60, 39.16, 25.10, 8.44.

Synthesis of **8aa**, **8ab**, **8ba**, **8bb** for LC/MS purpose adapted from following reference⁶

70 mg **9aa** was dissolved in 3 ml anhydrous THF. After that, 24 mg DMAP, 176 mg EDC-HCl, 250 mg NAC were added to the system. The slurry was kept stirring overnight and then quenched by 1 M HCl solution. The aqueous layer was extracted by EtOAc, and dried over Na₂SO₄. The organic solvent was passed through a CuSO₄-packed silica gel and removed under reduced pressure. The residue was subjected to LC-MS and HPLC-UV analysis.

83 mg **9ab** was dissolved in 3 ml anhydrous THF. After that, 28 mg DMAP, 207 mg EDC-HCl, 280 mg NAC were added to the system. The slurry was kept stirring overnight and then quenched by 1 M HCl solution. The aqueous layer was extracted by EtOAc, and dried over Na₂SO₄. The organic solvent was passed through a CuSO₄-packed silica gel and removed under reduced pressure. The residue was subjected to LC-MS and HPLC-UV analysis.

32 mg **9ba** was dissolved in 3 ml anhydrous THF. After that, 11 mg DMAP, 80 mg EDC-HCl, 110 mg NAC were added to the system. The slurry was kept stirring overnight and then quenched by 1 M HCl solution. The aqueous layer was extracted by EtOAc, and dried over Na₂SO₄. The organic solvent was passed through a CuSO₄-packed silica gel and removed under reduced pressure. The residue was subjected to LC-MS and HPLC-UV analysis.

46 mg **9bb** was dissolved in 3 ml anhydrous THF. After that, 16 mg DMAP, 115 mg EDC-HCl, 160 mg NAC were added to the system. The slurry was kept stirring overnight and then quenched by 1 M HCl solution. The aqueous layer was extracted by EtOAc, and dried over Na₂SO₄. The organic solvent was passed through a CuSO₄-packed silica gel and removed under reduced pressure. The residue was subjected to LC-MS and HPLC-UV analysis.

SUMMARY

In short, this work was proved as an initial achievement of general polyketide synthesis, though much of the work still remains to be optimized. The chemoenzymatic synthesis of two-stereocenter triketide building blocks was finished with overall yields of 2.0% of **9aa**, 1.3% of **9ab**, 1.7% of **9ba**, and 0.9% of **9bb**. Synthesis of the triketide products could be optimized in yield and stereochemistry, and also protecting group could be modified so that it would become easier for removal in the end. As many KRs are capable to establish two stereocenters during the reduction of α -substituted, β -ketoacyl substrates²⁰, the synthetic routine might be adapted to build libraries of three- or even four-stereocenter triketides, via methylmalonyl ethanethiol thioester in C-acylation reactions, for example. Further, other PKS enzymes like dehydratases and enoylreductases could be employed to modify the functionality of synthesized fragments. With some optimizations, another round of C-acylation and subsequent reduction would have chance to produce tetraketides at milligram levels. The above described stereoselective synthesis is ecofriendly, heavy-metal-free, chiral-auxiliary-free, and affordable. If it could be utilized in stereocomplex fragments construction, it would be an opportune to synthetic methodology and new medicine development in the near future.

ACKNOWLEDGEMENT

The authors thank the contribution of Alexis Cepeda, Mireya Luna, Melissa Hirsch, Kaan, Kumru, Jina Zhou. The authors also thank the National Institutes of Health (GM106112) and the Welch Foundation (F-1712). This work is also submitted to Chemical Communication of RSC with text modification.

Chapter 3: Seven-Enzymes Cascade Reaction Making Diketide^{43,1}

INTRODUCTION

Cascade reaction was always attractive because it allowed our lab to synthesize polyketides in one pot. Co-enzyme A was also an important biochemical source in our lab that it is a crucial precursor for many bioactive derivatives.

In previous works⁴⁴ (*R*)-3-hydroxybutyrate or enantiomer (*S*)-3-hydroxybutyrate had been generated involving enzymes from the polyhydroxyalkanoate pathway. In general, 2 molecules of acetyl-CoA were condensed by thiolase first to give acetoacetyl-CoA, which was then reduced by reductases to give different enantiomers. After that thioesterase would hydrolyze 3-hydroxybutyryl-CoA to provide corresponding 3-hydroxybutyrate. Different enzymes were tested in these works. For thiolases, they were BktB, Thl, and PhaA; for reductases they were Hbd and PhB; for thioesterases they were Ptb-Buk and TesB. Similarly, the reduction system was regenerated by GDH-NADPH system also utilized by our lab to produce other diketide building blocks²⁵.

Inspired by these works, we had various attempts to establish a mature methodology to achieve this goal: to utilize Co-A as an intermediate to make diketide in multi-enzyme cascade. (3*R*)-3-hydroxybutyryl-CoA was the first compound imagined in this project.

RESULTS AND DISCUSSIONS

Synthesis Design

The starting material was chosen as commercially available compound in-bulk acetic acid. Acetic acid could be grafted onto CoA, to form acetyl CoA using acetyl-CoA

¹ Parts of this chapter previously published as Luis E. Valencia, a Zhicheng Zhang, Alexis J. Cepeda and Adrian T. Keatinge-Clay, "Seven-enzyme in vitro cascade to (3*R*)-3-hydroxybutyryl-CoA," *Org. Biomol. Chem.*, **2019**, 17, 1375. See statement at end of chapter.

synthetase (ligase). The reason using CoA as the handle was because shorter handles like NAC didn't work on the enzyme. Longer handles, like pantetheine, were possibly better than NAC because the reduction on acetoacetyl-pantetheine could be detected on LC/MS. Thus, as the natural substrate CoA no doubt was the best candidate. Acetyl-CoA was then condensed by thiolase, like BktB, to generate acetoacetyl-CoA which was similar to Claisen condensation. However, the BktB reaction equilibrium was only 1.1×10^{-5} , totally disfavored in this reaction. In order to drive the reaction forward, other reactions should be coupled to drive equilibrium to the right side and render the reaction exergonic.⁴⁵ Thus, the acetoacetyl-CoA should be reduced by reductases as soon as possible to avoid accumulation in the system, which would be realized by GDH/NADPH regeneration system²⁵. The 3-hydroxybutyryl-CoA was then subjected to thiol-thiolester exchange to form 3-hydroxybutyryl-NAC again in order to facilitate characterizations on chiral UV-HPLC, because 3-hydroxybutyryl-CoA was difficult to separate on normal-phase chiral UV-HPLC due to its strong hydrophilicity (**Figure 3.1**).

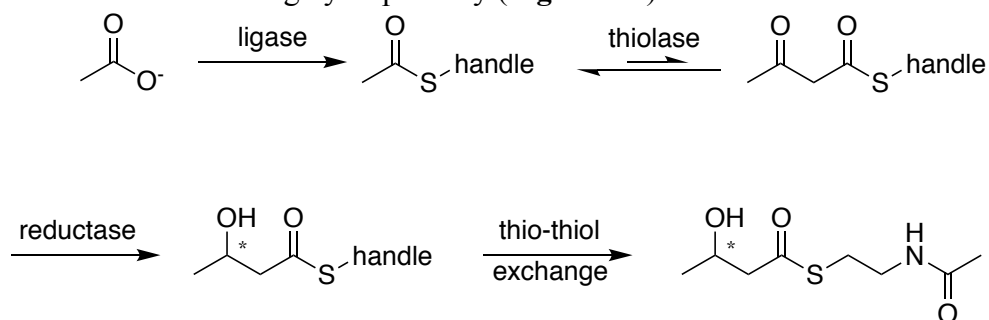


Figure 3.1. Proposed Synthesis Schedule for 3-hydroxybutyryl-NAC.

Synthesis

CoA **20** would first be made *in situ* by cascade reaction involving enzymes CoaA, CoaD and CoaE using pantetheine (reduced from pantethine **16**), DTT and ATP.⁴⁶ After that, CoA **20** was coupled with acetate to provide acetyl-CoA **21** by ACS. Subsequently BktB, PhaB, GDH, NADP⁺, and D-glucose were added together into the aqueous solution

buffer and monitored by LCMS until the reaction was done, giving desired product (3*R*)-3-hydroxybutyryl-CoA **23**. (3*R*)-3-hydroxybutyryl-CoA **23** could be subjected to thiol-thiolester exchange to give (3*R*)-3-hydroxybutyryl-NAC **24** for chiral HPLC analysis (Figure 3.2).

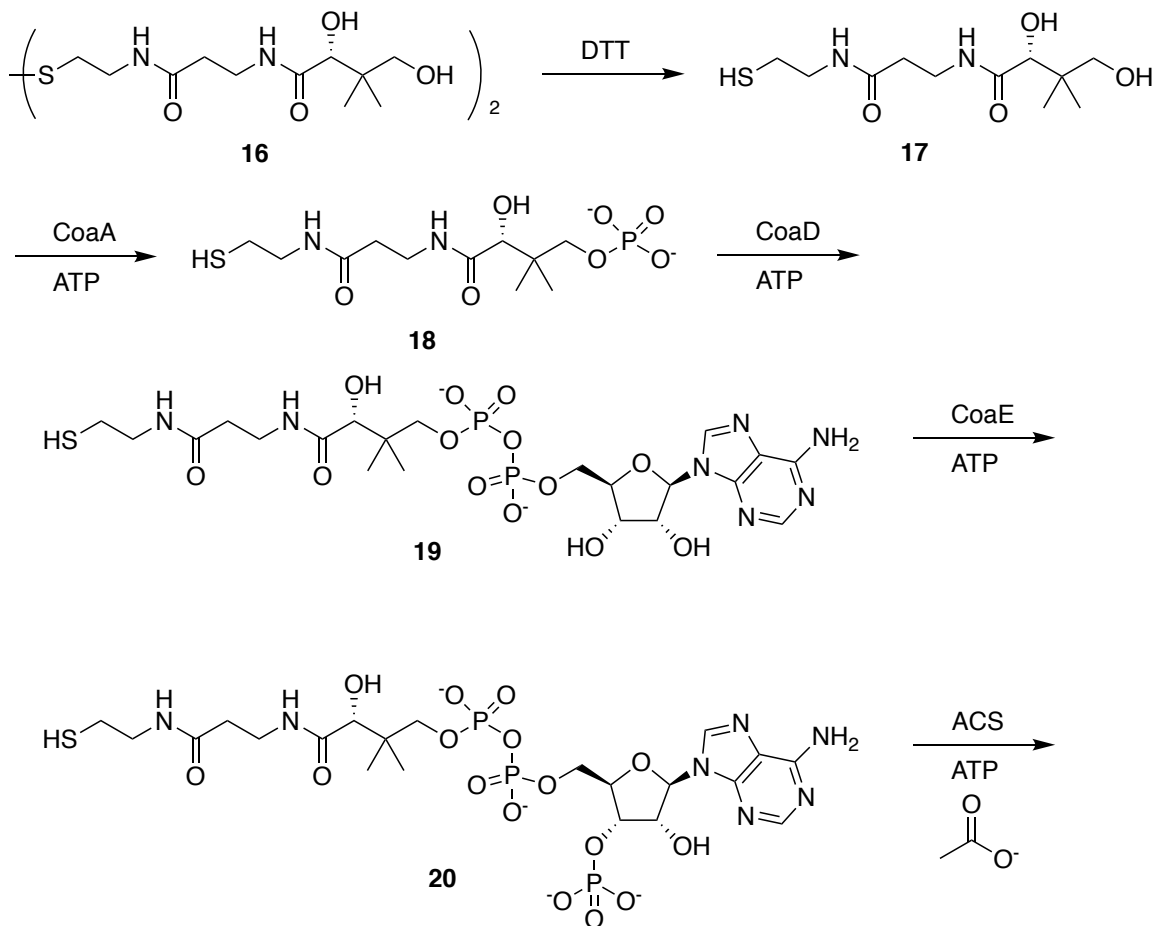


Figure 3.2A. Synthesis Schedule of CoA **20**. (to Figure 3.2B)

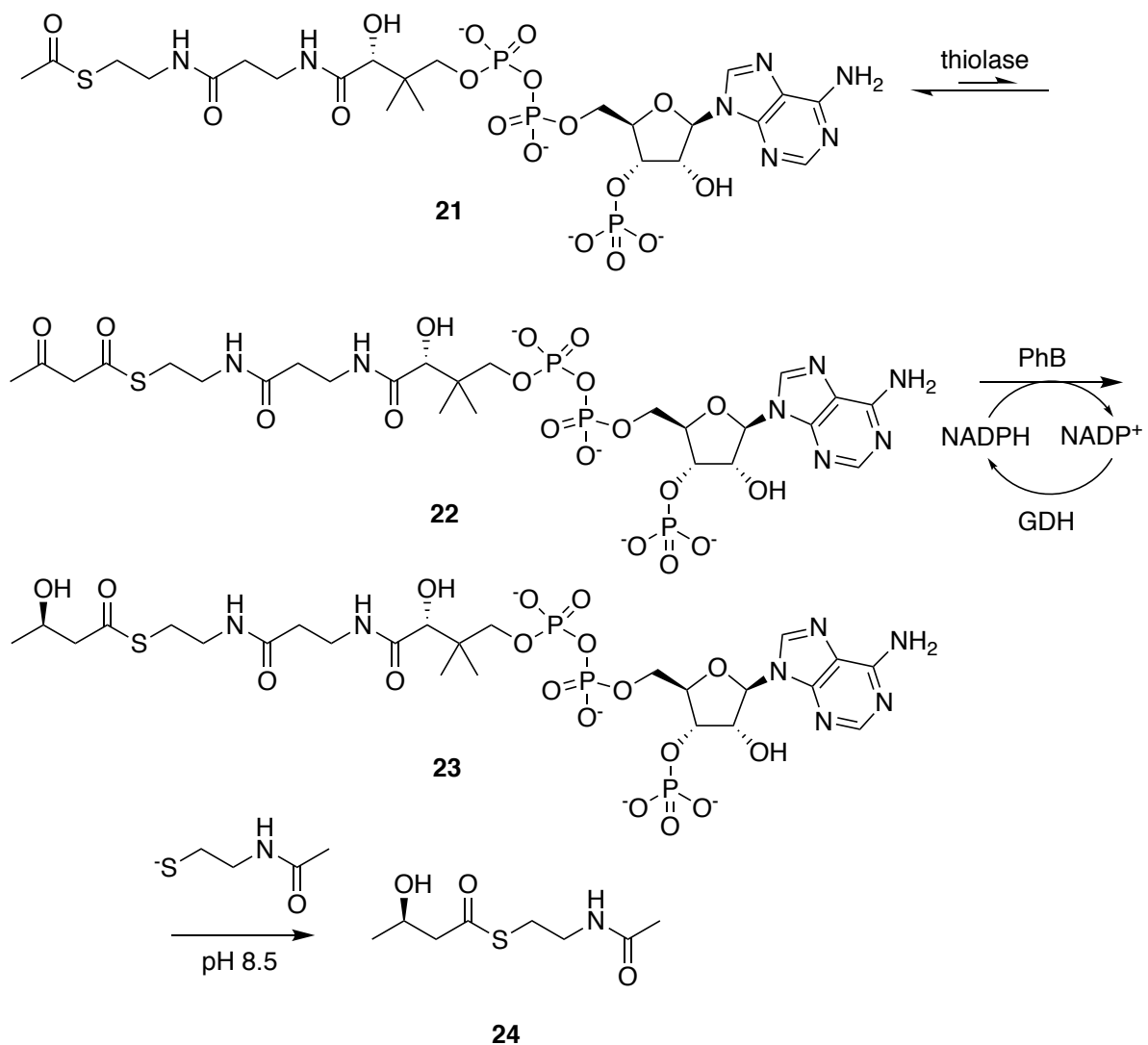


Figure 3.2B. Synthesis Schedule from CoA **20** to Final Product **23** and **24**.

Characterization

(3*R*)-3-hydroxybutyryl-CoA was strongly soluble in water thus it was sensitive to LCMS detection showing sharp [M-H]⁻ and [M-2H]²⁻ peaks on the graph. This was an easy method to demonstrate the existence of target species in order to monitor progress of the cascade reaction. Interestingly, other minor species, such as sodium adduct, could also be found on the graph with lower peak (**Figure 3.3**).

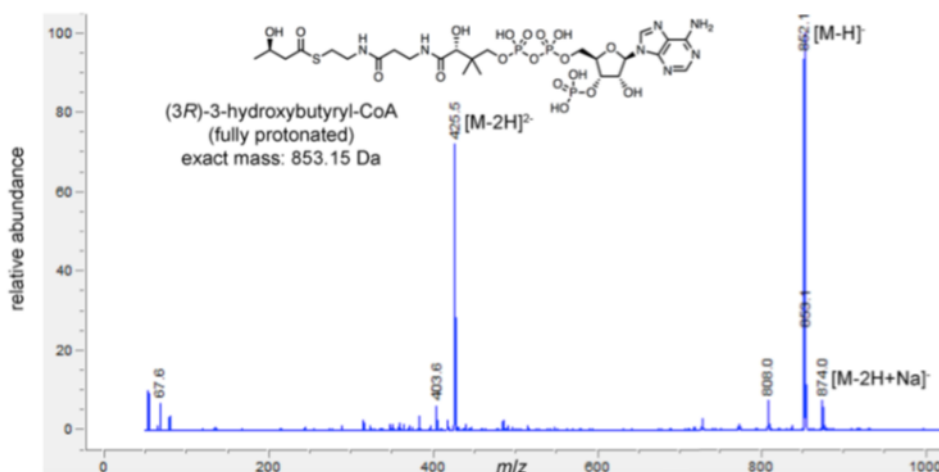


Figure 3.3. LC/MS Analysis of **23**.

To determine stereochemistry, (3*R*)-3-hydroxybutyryl-CoA **23** was then undergone thiol-thiolester exchange yielding (*R*)-3-hydroxybutyryl-SNAC **24** for chiral HPLC separation. Surprisingly but expected, the HPLC gave perfect result in comparison of synthesized chemical standard. It matched the retention time of authentic (*R*)-3-hydroxybutyryl-SNAC **24** and no obvious peak of (*S*)-3-hydroxybutyryl-SNAC **24** was detected, which meant the cascade reaction yielded high stereoisomer. Also, in order to prove the result, authentic chemical standards (*S*)-3-hydroxybutyryl-SNAC and (*R*)-3-hydroxybutyryl-SNAC were both made synthetically. After comparison on HPLC it turned out all the data were congruent. However, this method was failed to characterize product by ¹H NMR due to impurities in the product. The major byproduct was characterized as NAC dimer, which cannot be removed by regular silica chromatography because the polarity of NAC dimer resembles that of (*S*)-3-hydroxybutyryl-SNAC **24** (**Figure 3.4**).

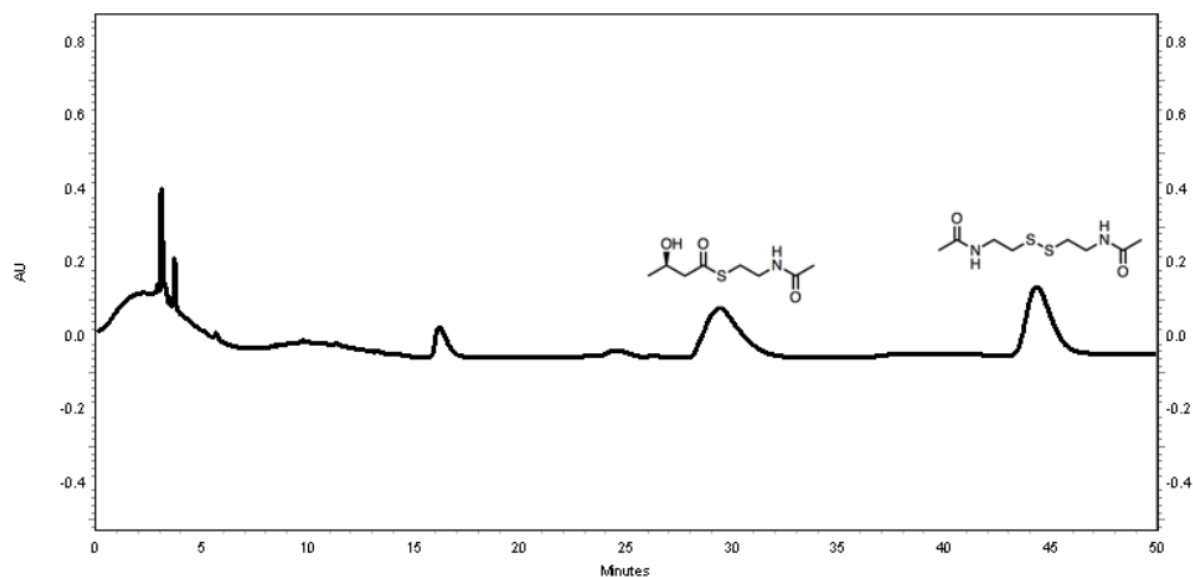


Figure 3.4. UV-HPLC Analysis of **24**, showing retention at 29.3 min, NAC dimer is on the right side.

Thus, inspired by peak-suppressing NMR technology, (3*R*)-3-hydroxybutyryl-CoA **23** was diluted without thiol-thiolester exchange and passed through Q-Sepharose ion exchange column. The column was then washed and eluted with 100mM HCl. The eluent containing (3*R*)-3-hydroxybutyryl-CoA was tested by H NMR and gave clear structure of (3*R*)-3-hydroxybutyryl-CoA **23** (See SI). In addition, P NMR was also taken to double-prove the result, that the 3 phosphorus peaks indicated the existence of 3 phosphoric residues in CoA (**Figure 3.5**).

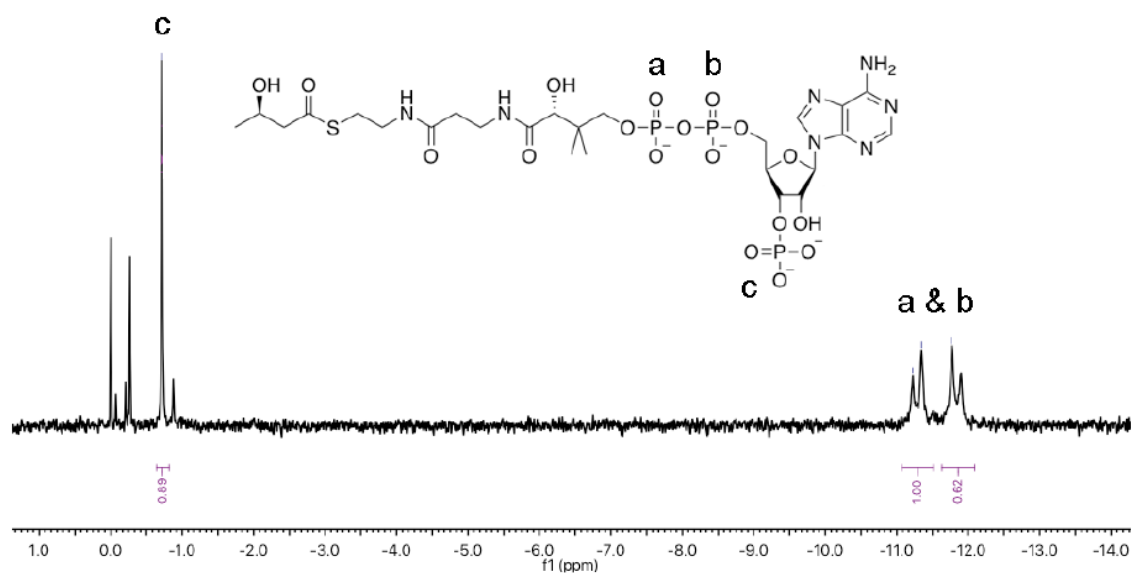


Figure 3.5. ^{31}P NMR Analysis of **23**, showing phosphorus in different chemical environment.

EXPERIMENTAL PROCEDURES

See publication in the appendix.

SUMMARY

In short, a successful attempt to generate chiral diketide building block (3*R*)-3-hydroxybutyryl-CoA was achieved via seven-enzyme reaction in one-pot. The reaction not only generated diketide but also valuable intermediate CoA derivatives as well without any traditional metal catalysts and high pressure.⁴⁷ Green chemistry, heavy metal free, high efficacy and convenient experimental procedure all render advantages for this cascade reaction. More optimization could be done at this point, such as immobilization of enzyme in order to reuse the material. Future study are also scheduled to explore more complex compounds⁴⁸ or more facile compounds⁴⁹ based this methodology.

ACKNOWLEDGEMENT

This work was published by RSC as *Org. Biomol. Chem.*, **2019**, *17*, 1375–1378, attached in the supporting information with the copyright belonging to RSC for thesis use. The second co-author worked for chemical standard synthesis, NMR characterization and chiral HPLC analysis. The second co-author also thanks first author Luis Valencia, and third author Alexis Cepeda. This work was supported by NIH (GM106112) and the Welch Foundation (F-1712). Other supports please see attached publication.

Chapter 4: Mechanism Study of Pyran Synthase Domain in *trans*-AT Assembly Line^{50,2}

INTRODUCTION

Trans-acyltransferase (*trans*-ATs) PKSs are a recently discovered PKS type which characterize those AT modules not embedded in the whole assembly line on the polypeptides. Traditional *cis*-ATs, however, are located within the assembly line. Functional modules in *cis*-AT PKSs are well studied whereas those, such as double bond isomerization, pyran formation, *O*-methylation, in *trans*-AT are not.⁵¹

Pyran synthases (PSs) catalyze the cyclization with 5/6-membered ring to form ethers in the polyketides made by *trans*-AT PKSs. They have similarities to dehydratases (DHs) but different by an Hx4P motif instead of Hx8P motif found in DH. PSs are widely discovered in different *trans*-AT PKS assembly lines like bryostatin (Bry), diaphorin (Dip), luminaolide (Lum), misakinolide (Mis), oocydin (Ooc), pederin (Ped), phormidolide (Phm), psymberin (Psy), sorangicin (Sor), spliceostatin (Fr9), thailanstatin (Tst), and tolytoxin (Tto). The thailanstatin and sorangicin assembly lines have two and three PSs. Except oocydin and phormidolide PSs, which generate 5-membered tetrahydrofuran fragment through an ϵ -hydroxyl group generated from monooxygenase in their biosynthetic routines, PSs usually catalyze 1,4-conjugate addition generating six-membered dihydropyran/tetrahydropyran rings through a ζ -hydroxyl group to C $_{\beta}$.⁵²

However, the mechanism of PS is not currently well studied. The *trans*-AT pathways suggested that β -carbon on a *trans*- α/β -unsaturated double bond was attacked by hydroxyl group via *oxa*-Michael addition.⁵¹ For nucleophile, some PSs utilize a D-

² Parts of this chapter previously published as Drew T. Wagner, Zhicheng Zhang, Roy A. Meoded, Alexis J. Cepeda, Jörn Piel, and Adrian T. Keatinge-Clay, "Structural and Functional Studies of a Pyran Synthase Domain from a *trans*-Acyltransferase Assembly Line," *ACS Chem. Biol.*, **2018**, *13*, 4, 975. See statement at end of chapter.

hydroxyl group as the nucleophile, whereas others utilize an L-hydroxyl group as the nucleophile. For double bond addition, Some PSs catalyze *oxa*-Michael addition to the *re* face, while others catalyze *oxa*-Michael addition to the *si* face. Previous studies from the misakinolide and pederin assembly lines (MisPS16 and PedPS9) showed cyclization activity on the natural substrate analogue, ζ -hydroxyacyl N-acetylcysteamine (NAC) thioester substrates preferred more *anti* products than *syn* products. The study of PedPS9 PS showed that the L- ζ -hydroxy substrate was slightly favored over the D- ζ -hydroxy substrate, when in both cases the β -carbon atom on the double bond was attacked at its *si* face (**Figure 4.1**).⁵³

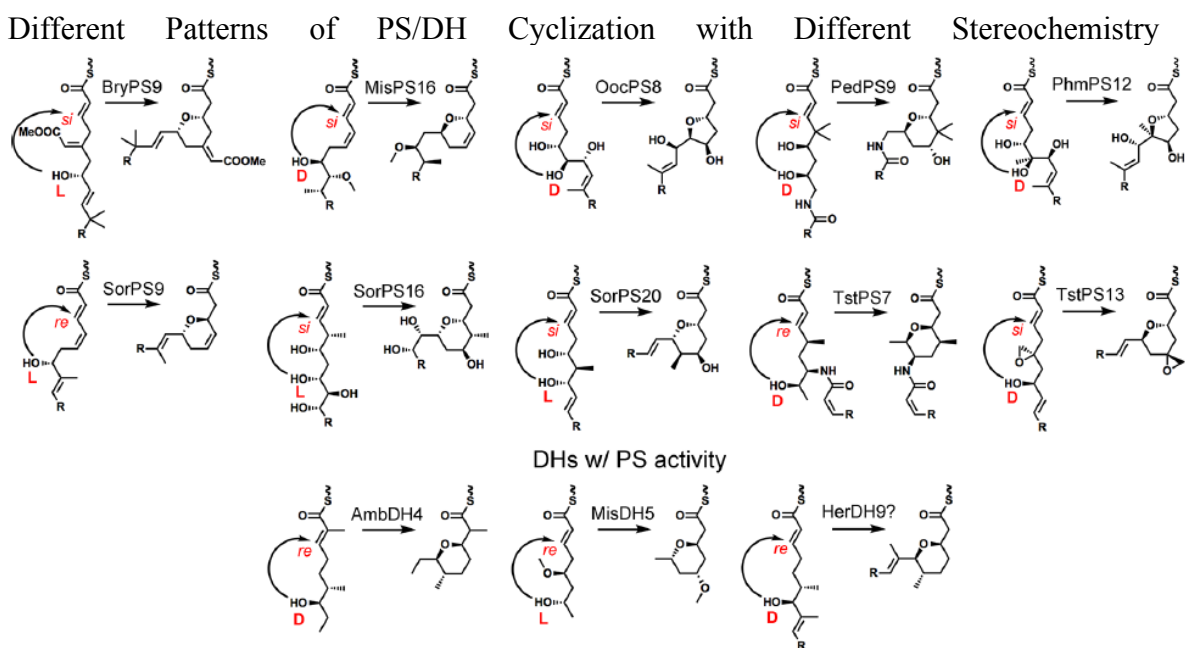


Figure 4.1. Different Patterns of PS/DH Cyclization with Different Stereochemistry.⁵⁰

Herein, a pyran synthase SorPS9 from the *Sorangium cellulosum* trans-AT assembly line, which produced sorangicin antibiotics,⁵⁴ was reported by our lab with 1.55 Å resolution structure. Different synthetic chemical analogues, the trans- α/β -unsaturated ζ -hydroxyacyl NAC thioester substrates, were tested on wild type and mutated SorPS9s. The

mechanism study confirmed that active site of SorPS9 contains a histidine and an asparagine residues equivalent to the catalytic histidine and aspartate of DHs.

RESULTS AND DISCUSSIONS

Structural Study of PS

See publication in the appendix.

Synthesis of Chemical Analogues

Since the natural substrate was complex, the synthesis was simplified to resemble natural substrate with NAC-mimics **31** and **37**. For the scenario of non-substituted pyran, the synthesis started with commercially available compound **26**. Ester **26** was carefully reduced to colorless aldehyde **27** by DIBAL-H DCM solution at low temperature under argon with moderate yield 40.5 %.⁵⁵ Aldehyde **27** was directly used for the next step without separation because aldehyde **27** was perishable to oxygen. Using Doebner-Knoevenagel condensation and decarboxylation,⁵⁶ Aldehyde **27** was easily transformed into both starting material and product for PS enzymatic reaction acyclic acid **28** and cyclized acid **29** via 2 consecutive steps with the ratio nearly 1:1 in one pot. Fore sure although oil bath was originally intended for decarboxylation, there was cyclized acid **29** observed. This implied even without the help of PS, acyclic acid **28** would undergo cyclization to form more thermodynamically stable compound acid **29** when temperature was raised. The transformation was accelerated at room temperature by PS. After that, by simple EDH-HCl coupling with NAC handle, natural substrate analogues **30** and **31** were obtained with 44.4 % and 4.7 % yields respectively as yellowish sticky oils. The low coupling yield of acyclic acid **29** was attributed to the active hydroxyl proton on the acid. For the scenario of methyl-substituted pyran, the reaction protocol was the same with no

huge difference. The synthesis started with commercially available compound **32**. Ester **32** was carefully reduced to colorless aldehyde **33** with all possible stereoisomers with low yield 21.4 %⁵⁵ and then aldehyde **33** was directly for use as well. Using the same Doebner-Knoevenagel condensation and decarboxylation,⁵⁶ Aldehyde **33** was transformed into both starting material and product for PS enzymatic reaction racemic acyclic acid **34** and cyclized acid **35** with 27.5 % and 15.0 % yields respectively. The yield of compound **35** was lower probably due to increased steric hindrance on methyl group. Also synthesized cyclized acid **35** was almost in *syn* configuration according to a previous report,⁵⁷ which was opposite to enzymatic pyran configuration. After that, by simple EDH-HCl coupling with NAC handle, natural substrate analogues **36** and **37** were obtained with 51.0 % and 31.0 % yields respectively as yellowish sticky oils as well (**Figure 4.2**).

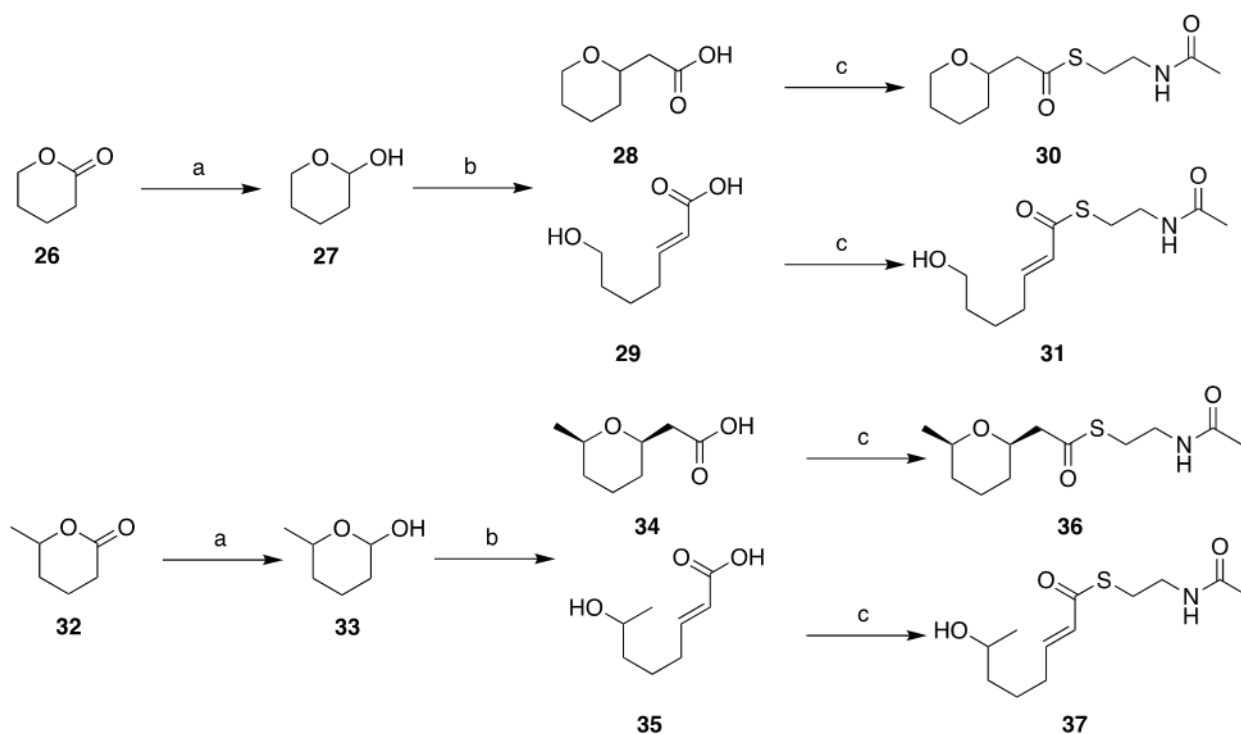


Figure 4.2. Synthesis of Chemical Analogues **30**, **31**, **36**, **37**.

Conditions: a) DIBAL-H (1.2 eq.), DCM, -78°C, 2h, 40.5% **27**/21.4 % **33**. b) malonic acid (1.0 eq.), pyridine (cat.), piperidine (cat.), r.t., overnight, then oil bath 105 °C for 4 h, 27.2 % **28**/25.7 % **29**/27.5 % **34**/17.0 % **35**. c) EDC-HCl (2.0 eq.), DCM, *N*-acetylcysteamine (NAC) (1.2 mmol), DMAP (cat.), r.t., 4h, 44.4 % **30**/4.7 % **31**/51.0 % **36**/31.0 % **37**.

Enzymatic Reactions

In order to test the enzyme activity, wild type SorPS9 was incubated with substrate mimic **31** overnight at 22 °C. Liquid chromatography/mass spectrometry (LC/MS) analysis reflected the disappearance of **31** and new peaks not observed in negative control respectively. Consistent with pyran formation, the characteristic UV absorbance of the new peak shifted from 265 nm (trans- α/β -unsaturated thioester substrate) to 230 nm. Then methyl-substituted **37** was subjected to SorPS9 giving the similar result. LC/MS analysis showed the disappearance of **37a** and **37b** and two roughly equal new peaks with the same mass of the substrates. This demonstrated that SorPS9 generated products from both D-

and L- ζ -hydroxy substrates. In addition, when SorPS9 was incubated with cyclized pyran products (**30** and **36**), no starting material (**31** and **37**) was detected. This implied the reaction equilibrium heavily favors pyran formation. Also, Other mutated SorPS9, H33A, N186H, N186A, and N186D, were generated and incubated with SorPS9 to determine the active site of SorPS9. For the H33A mutant, no discernible activity was detected. This indicated the histidine residue was catalytic. For the N186H mutant, activity was significantly retained. For the N186A and N186D mutants, the activities were reduced to minimal and none, respectively (**Figure 4.3**).

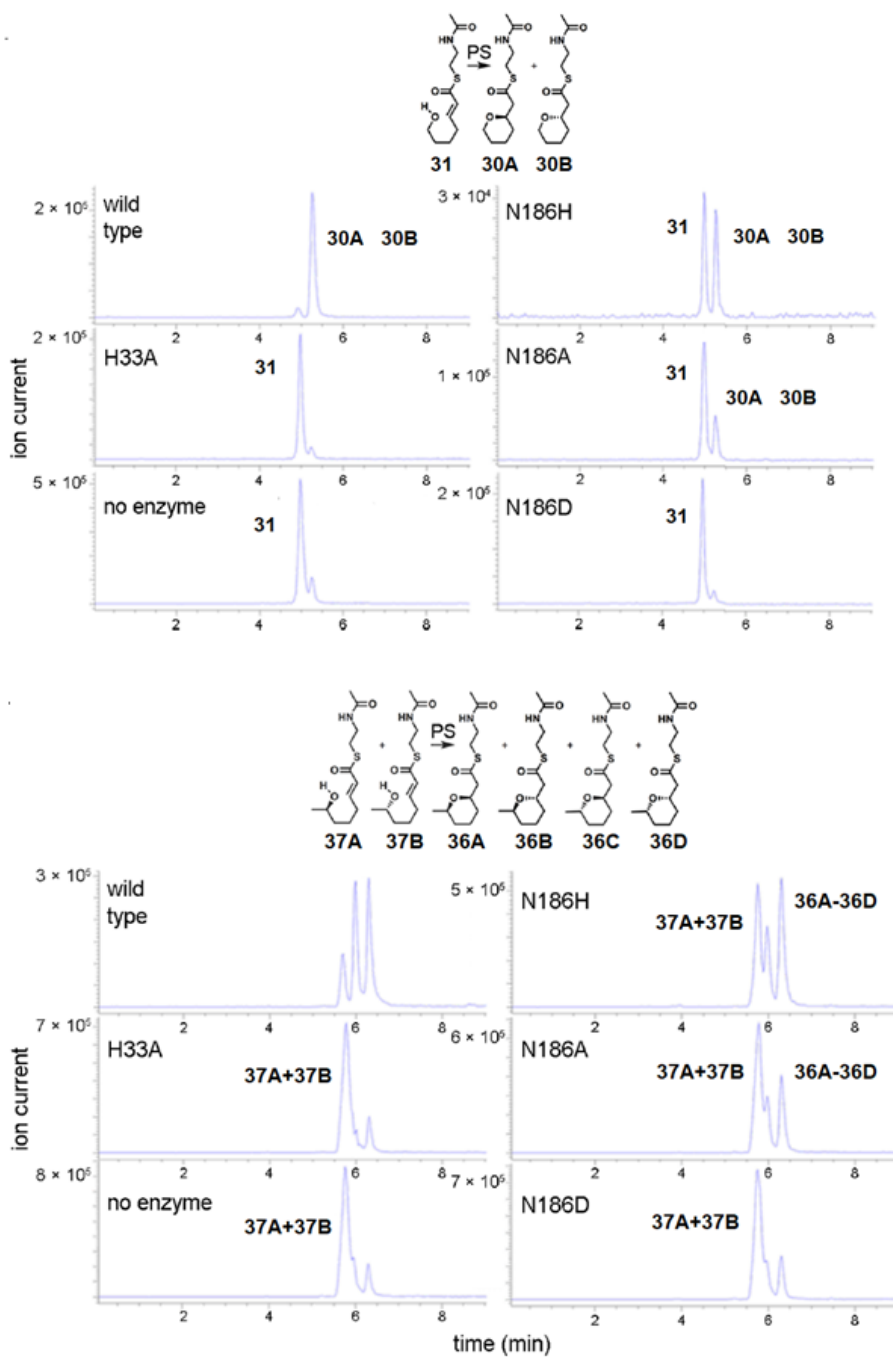


Figure 4.3. Activity Assays of SorPS9 and Point Mutants. LC/MS analysis of incubations with **31/37** revealed wild-type SorPS9 generated **30/36**, while the H33A mutant was inactive. In both cases, the N186H and N186A mutants showed some activity, but no activity was observed from the N186D mutant. Traces show extracted ion current at m/z 268/282 respectively.⁵⁰

Brief Mechanism of PS

Thus, it turned out H33 and N186 were crucial residues catalyzing the ring formation in SorPS9. The proposed mechanism involved the H33, N186 and a molecule of water created by A39 in an oxyanion hole. First, the water molecule and N186 form hydrogen bond to stabilize the new entered substrate. Second, the ζ -hydroxyl attacked β -*trans*-double bond to generate the oxyanion intermediate. After that, H33 functioned as a proton acceptor to remove the proton from the pyran oxygen and then transferred it finally to enolate oxygen. The cyclized pyran product left the active site. Since σ bond was stronger than π bond, the pyran formation was actually irreversible. Regarding the stereochemistry, SorPS9 catalyzed addition at C_β on the *re* face whereas most PSs catalyzed addition on the *si* face. However, attacking on the *si* face was possible if the thioester adopted s-cis conformation (**Figure 4.4**). Therefore, the preferred conformation of a substrate in the PS active site would tell whether to adopt the s-cis or s-trans geometry and whether the *si* or *re* face of C_β would be attacked.

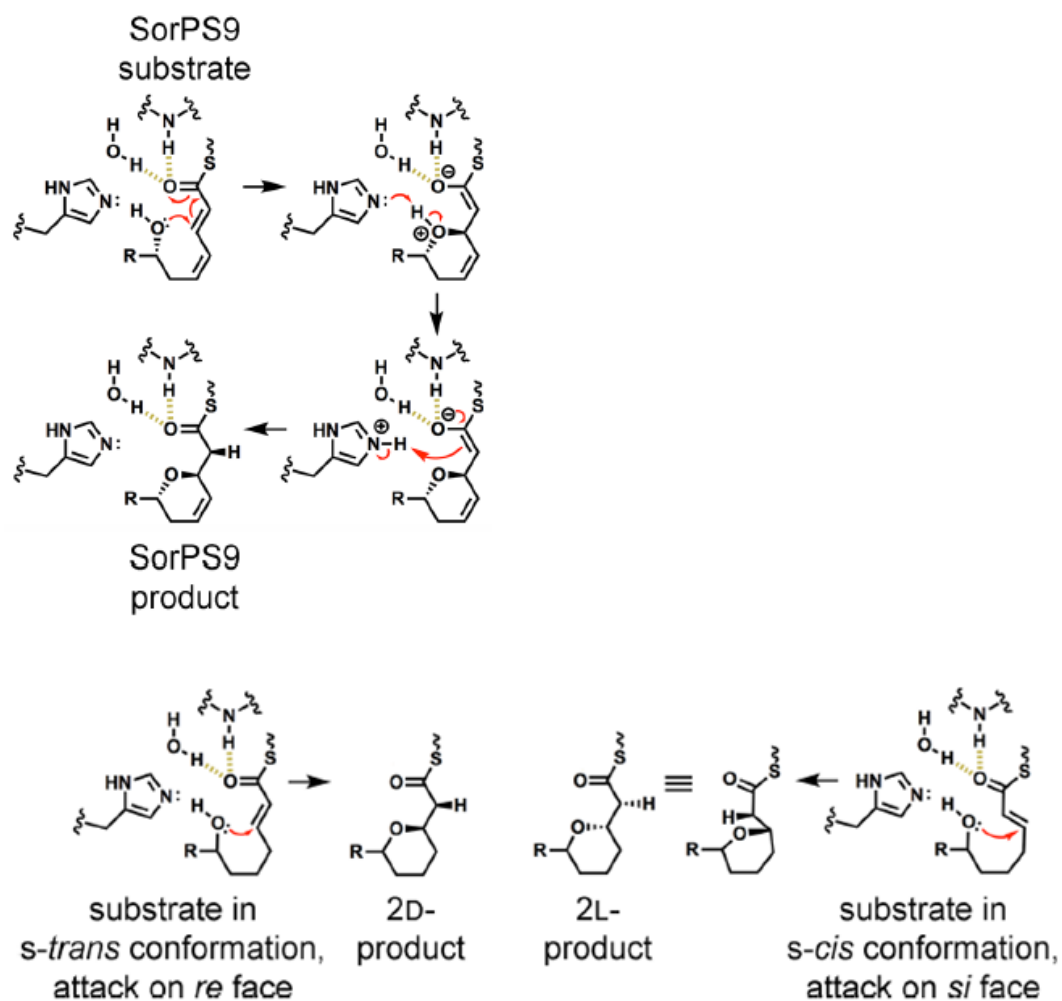


Figure 4.4. Proposed Mechanism of PS Active Site and Conformation of *Oxa*-Michael Addition. For the Attacking on the *re* Face, Thioester Carbonyl and C α adopted *s-trans* conformation.

EXPERIMENTAL PROCEDURES

See publication in the appendix.

SUMMARY

In short, the structure and mechanism of SorPS9 from *trans*-AT assembly lines were studied. Different simplified chemical analogues were synthesized to test the enzyme activity. Mutagenesis was performed to successfully locate the residues charging the substrate cyclization. As the result, the active site of SorPS9 included a histidine residue mediating proton transfer, and the asparagine residue helping create the oxyanion hole through a water molecule. It turned out SorPS9 is capable to generate chiral pyran ring which could be utilized as an efficient biocatalyst. With the development of research, more mysteries will be revealed in *trans*-AT assembly lines so that they could be employed and engineered as biocatalyst to provide unusual reactions or even help generate new valuable medicines in the future.

ACKNOWLEDGEMENT

This work was published by ACS as *ACS Chem. Biol.* **2018**, *13*, 975–983, attached in the supporting information with the copyright belonging to ACS for thesis use. The second co-author worked for chemical standard synthesis, NMR characterization and partial LC/MS analysis. The second co-author also thanks first author Drew Wagner, and other co-authors. This work was supported by NIH (GM106112) and the Welch Foundation (F-1712). Other supports please see attached publication.

Chapter 5: Structural and Mechanism Study of gem-Dimethylating Methyltransferase from a *trans*-AT Assembly Line⁵⁸

BRIEF INTRODUCTION

The methyl substituents in polyketides made by *trans*-acyltransferase assembly lines are usually deprived from S-adenosylmethionine (SAM)-dependent methyltransferase (MT) domains. The MT from polyketide disorazol assembly lines DisMT3 was revealed with 1.75-Å-resolution crystal structure in this work. Mutagenesis on β -ketoacyl chains to an acyl carrier protein handle (ACP) and N-acetylcysteamine handle were conducted and tested on the activities. This provided the mechanism of MT active site residues. An alanine replacement with a phenylalanine at an obvious gatekeeping position (A326F) led in more monomethylation than demethylation (**Figure 5.1**).

³ Parts of this chapter previously published as Jessica L. Meinke, M. Rachel Mehaffey, Drew T. Wagner, Ningze Sun, Zhicheng Zhang, Jennifer S. Brodbelt, and Adrian T. Keatinge-Clay, "Structural and Functional Studies of a gem-Dimethylating Methyltransferase from a *trans*-Acyltransferase Assembly Line," *ACS Chem. Biol.*, **2018**, *13*, 12, 3306. See statement at end of chapter.

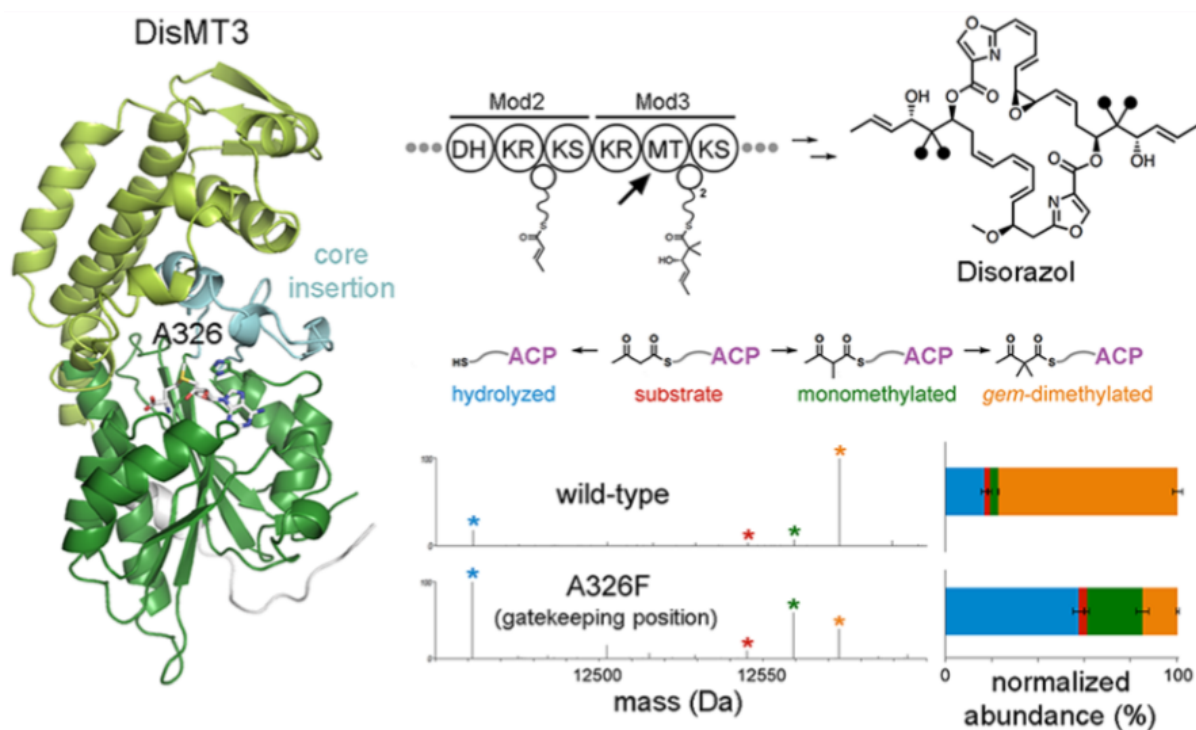


Figure 5.1. The Model of DisMT3 and Mutagenesis Study on LC/MS.⁵⁸

My work included synthesis of monomethylated and dimethylated analogues α -methyl- β -ketopentanoyl-SNAC and α -dimethyl- β -ketopentanoyl-SNAC as chemical standards for Wild-type DisMT3 enzyme activity test. The result turned out, wild-type DisMT3 did not yield any gem-dimethylated product but did only generate some monomethylated product (**Figure 5.2**).

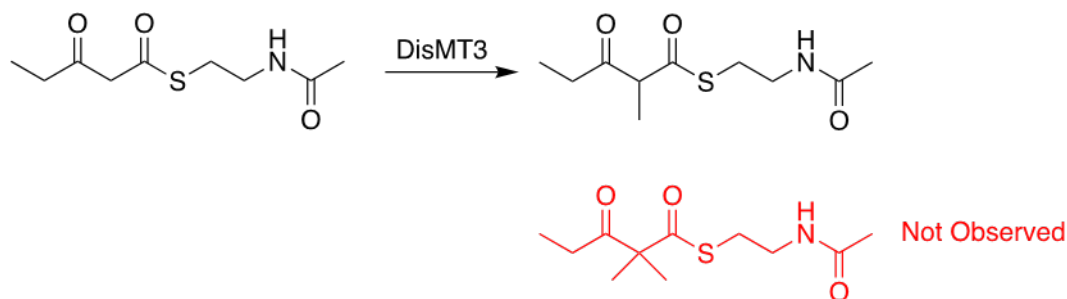


Figure 5.2. Reaction of DisMT3 with Ketopentanoyl-SNAC. The Product Structure of α -methyl- β -ketopentanoyl-SNAC and α -dimethyl- β -ketopentanoyl-SNAC.

Also, only the Y170F point mutant provided traceable levels of the monomethylated product. This suggested that the interaction between the MT and ACP domains might be important to transfer both methyl groups. The DisMT3 and NAC mimics didn't provide sufficient binding energy to forward the second methylation. In addition, the N285A, E314A, and E314Q mutants suffered more activity loss in scenario of the SNAC-bound substrate than that in the ACP-bound substrate. Maybe small molecules were more dependent on active site residue interaction. This result helped to interpret how the MT catalyzed the two methyl groups addition.

ACKNOWLEDGEMENT

This work was published by ACS as *ACS Chem. Biol.* **2018**, *13*, 3306–3314., attached in the supporting information with the copyright belonging to ACS for thesis use. The co-author worked for chemical standard synthesis, NMR characterization and partial LC/MS analysis. The co-author also thanks all the other authors for finishing the major work in this project. This work was supported by NIH (GM121714 / GM106112) and the Welch Foundation (F-1155 / F-1712). Other supports please see attached publication.

Chapter 6: Structural Study of Four-Helix Bundle Docking Domain in *trans*-Acyltransferase Modular Polyketide Synthases⁵⁹

BRIEF INTRODUCTION

In PKS assembly lines, domain-domain connection involves both covalent connection and non-covalent connection. In the non-covalent connection situation, docking domain plays an important role to interconnect those PKS domains in the correct order. Recently, new discovery has been made in *trans*-acyltransferase polyketide synthases. These 25-residue, two helix, pseudosymmetric docking domains are found in the C-termini and N-termini of many polypeptides. The motifs connect domains between and with PKS modules. A 1.72 Å-resolution structure of the N-terminal portion of the MlnE (macrolactin synthase polypeptide) had been revealed as an uncomplexed and preorganized N-terminal docking motif (**Figure 6.1**).

⁴ Parts of this chapter previously published as Jia Zeng, Drew T. Wagner, Zhicheng Zhang, Luisa Moretto, Janci D. Addison, and Adrian T. Keatinge-Clay, "Portability and Structure of the Four-Helix Bundle Docking Domains of *trans*-Acyltransferase Modular Polyketide Synthases," *ACS Chem. Biol.*, **2016**, *11*, 9, 2466. See statement at end of chapter.

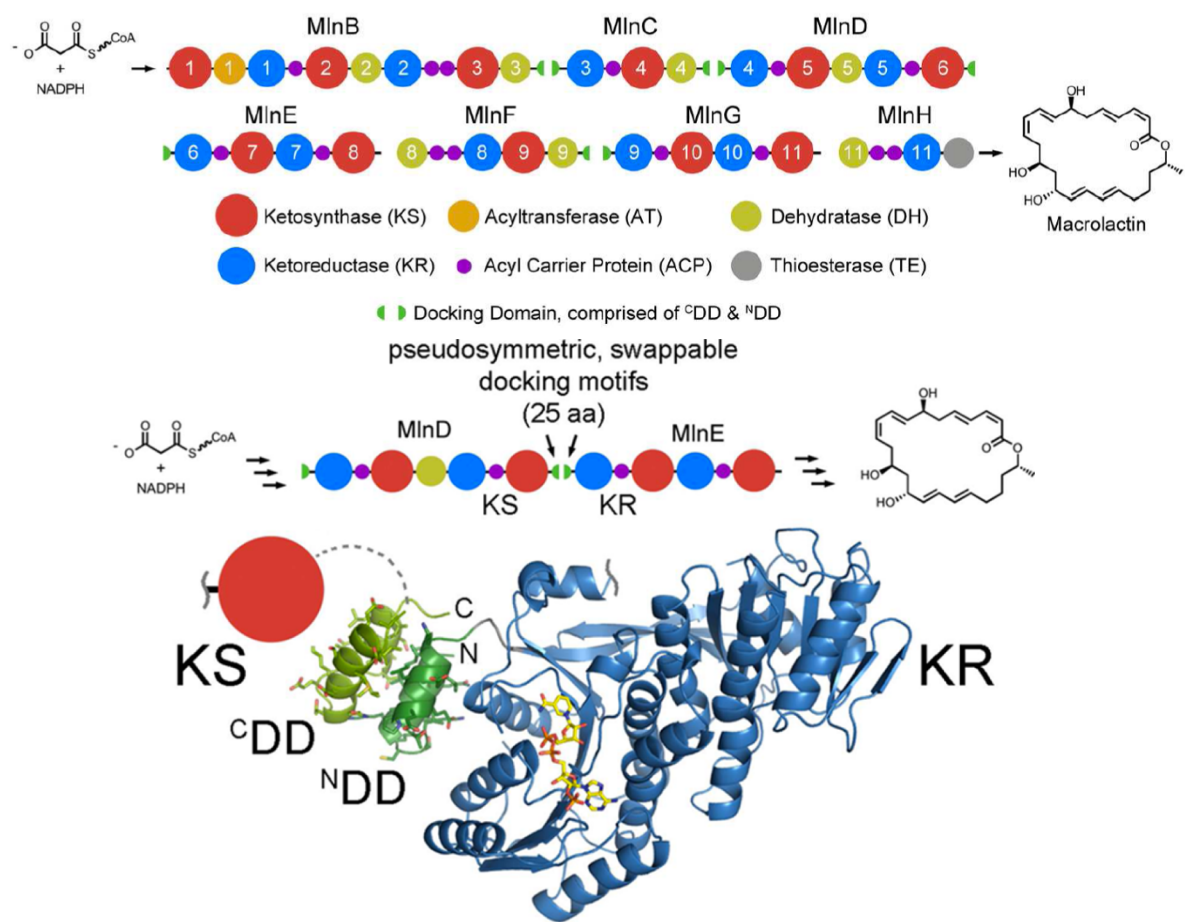


Figure 6.1. Mln Synthesis Assembly Line and The Four-Helix Docking Motifs between KS in MlnD and KR in MlnE.⁵⁹

My work included preparing those PKS modules with modified docking domains. By targeted domain swapping, different chimera protein complexes with compatible ^CDD and ^NDD have been created to demonstrate the portability of docking motifs (**Figure 6.2**).

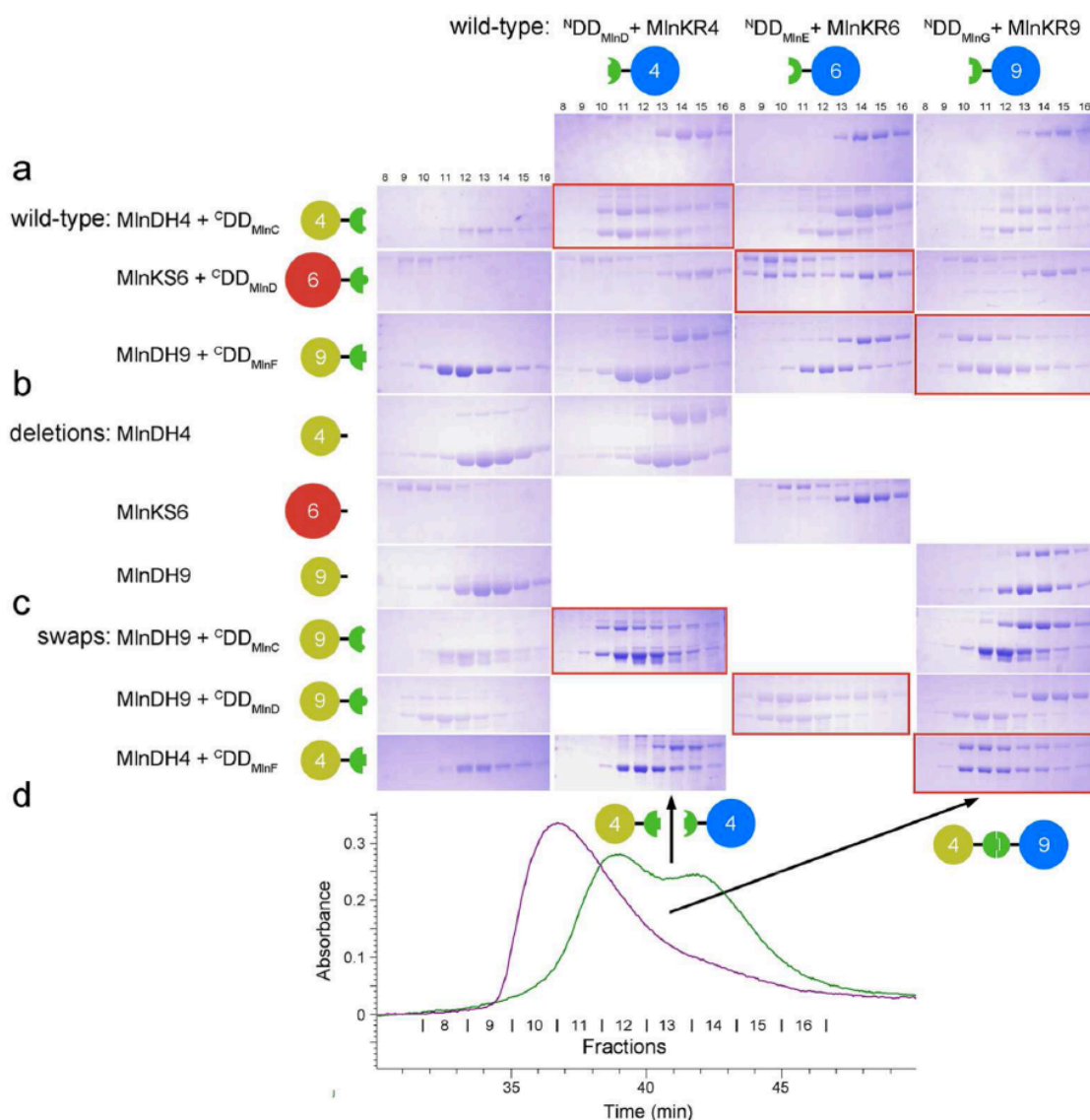


Figure 6.2. Polypeptide Association Mediated by DD Motifs. Each stained SDS/PAGE gel shows fractions 8–16 from size-exclusion chromatography. (A) Each pair of constructs containing cognate DD motifs apparently formed complexes. Each pair of constructs containing non-cognate DD motifs did not show complex formation. (B) The removal of CDDs resulted in no complex formation, indicating that they are necessary in mediating an association with a polypeptide containing a cognate NDD. (C) When CDDs were swapped between constructs, they were sufficient to mediate the association with a polypeptide containing a cognate NDD. Gels showing complex formation are boxed in red. (D) Representative size exclusion chromatograms showing constructs not possessing matching docking motifs migrating as if they had been run individually as well as constructs possessing matching docking motifs migrating more quickly.⁵⁹

ACKNOWLEDGEMENT

This work was published by ACS as *ACS Chem. Biol.* **2016**, *11*, 2466–2474, attached in the supporting information with the copyright belonging to ACS for thesis use. The third co-author worked for enzyme preparation and dproduction. The co-author also thanks first author Jia Zeng, and fourth author Louis Moretto and fifth author Janci Addison. This work was supported by NIH (GM106112) and the Welch Foundation (F-1712). Other supports please see attached publication.

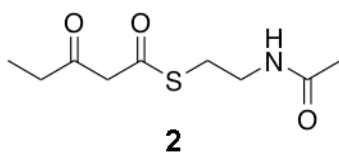
Conclusion and Future Directions

Polyketide synthases are shining and attracting more and more researchers to delve into this area. In Chapter 2, we demonstrated a total synthesis of triketide building blocks with the help from ketoreductases. In Chapter 3, we successfully utilize different enzymes to synthesize a useful polyketide with great stereochemistry in one-pot. In Chapter 4, we synthesize chemical analogues to test the activities of wild type pyran synthase and its mutants to determine the active site residues. In Chapter 5, we attempted to assay the methylation activity of both natural products and analogues to explore the mechanism of methyltransferase. In Chapter 6, we elucidated the structural of a docking motif located in a *trans*-acyltransferase assembly line and conducted docking domain swapping to create new protein complex.

However, we are not satisfied with our current situation. Our laboratory is looking forward to employ more enzymes from PKS assembly line to create more valuable chiral compounds potential for pharmaceutical industry. Also, we would be gratefully to update our technology to explore more mysteries in the structural and functional study of PKS assembly line.

Appendix

All the characterization in included before are here.



S-(2-acetamidoethyl) 3-oxopentanethioate

Chemical Formula: C₉H₁₅NO₃S

PROTON.01
zz6604-packed

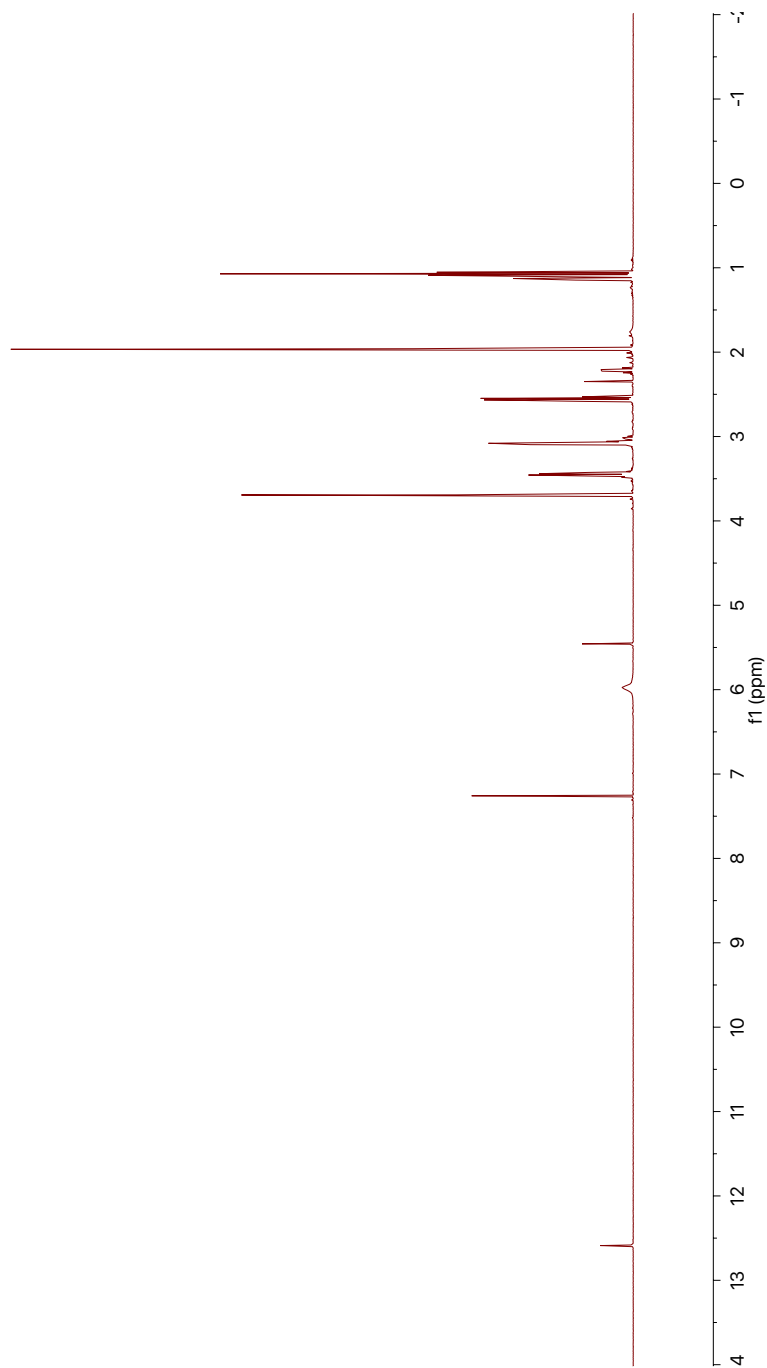


Figure S2-1. ^1H NMR

CARBON_01
zzc0147

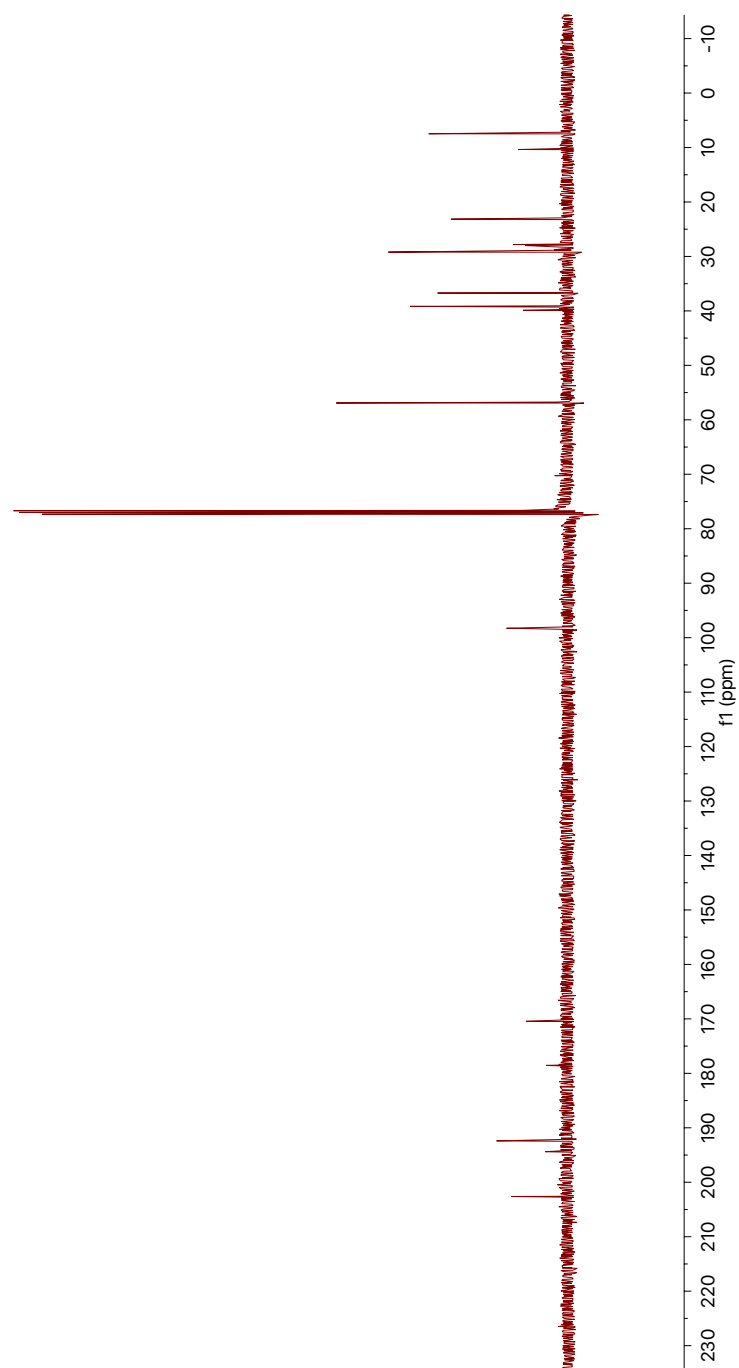
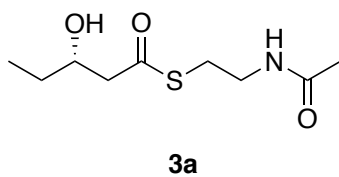


Figure S2-2. ^{13}C NMR



S-(2-acetamidoethyl) (*S*)-3-hydroxypentanethioate

Chemical Formula: C₉H₁₇NO₃S

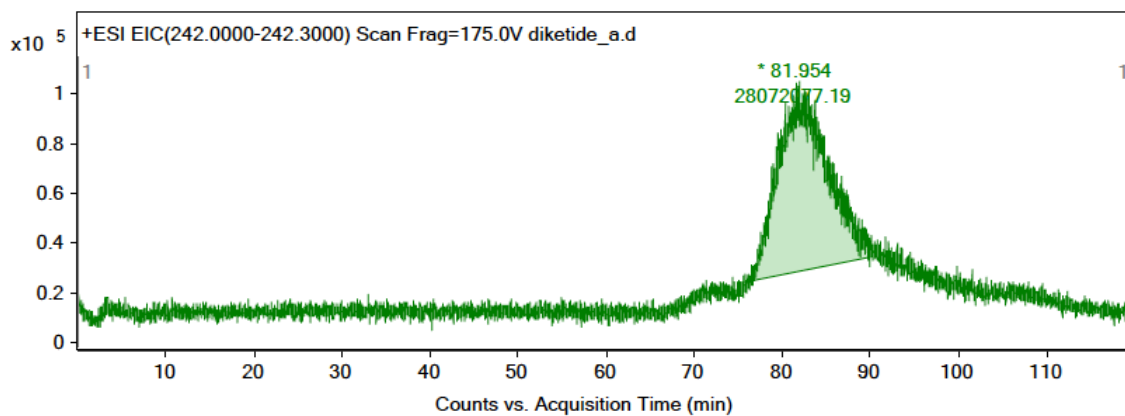


Figure S3A-1. Extracted-Ion Chromatogram of LC/MS

PROTON_01
zzc0155

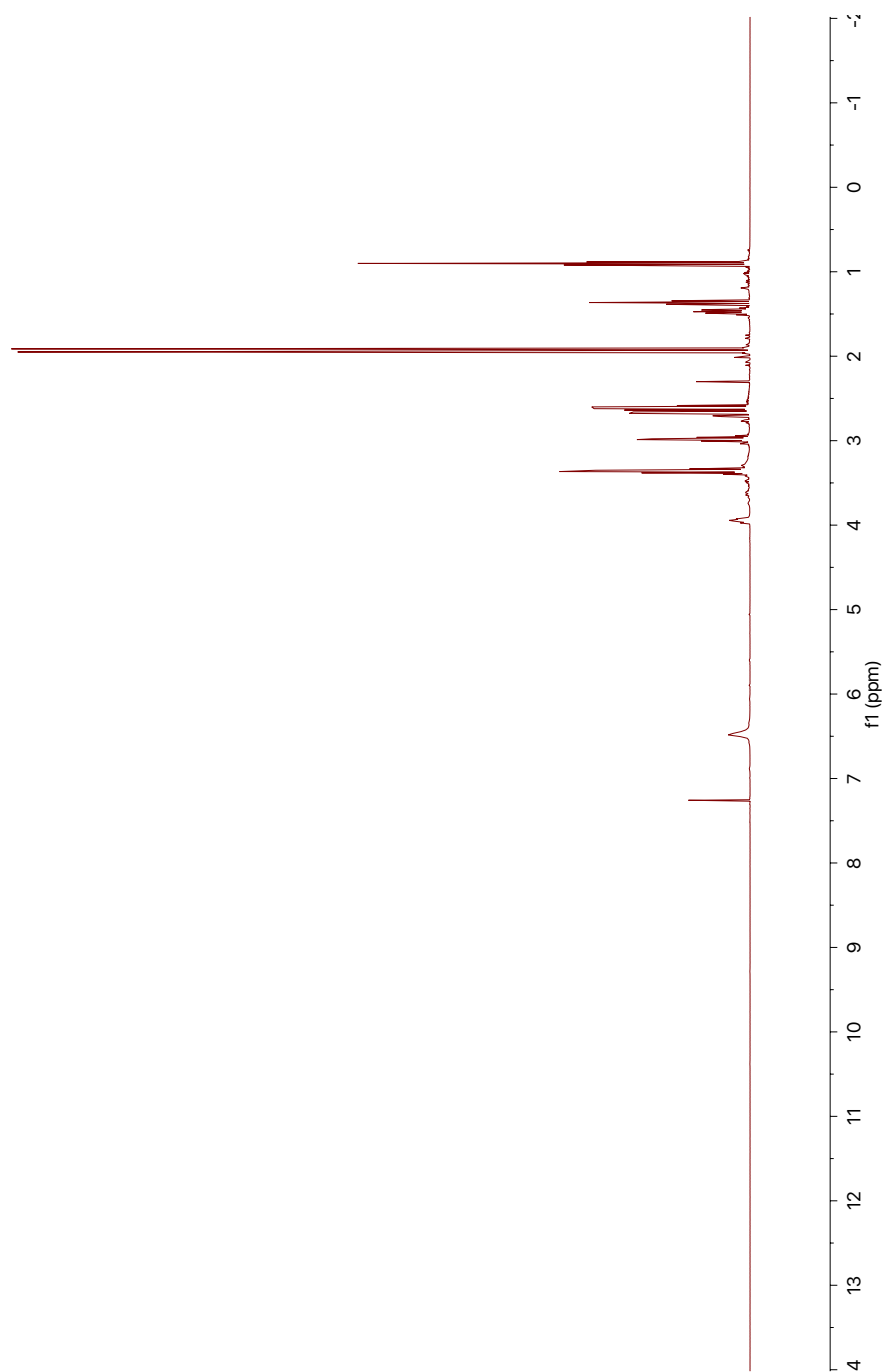
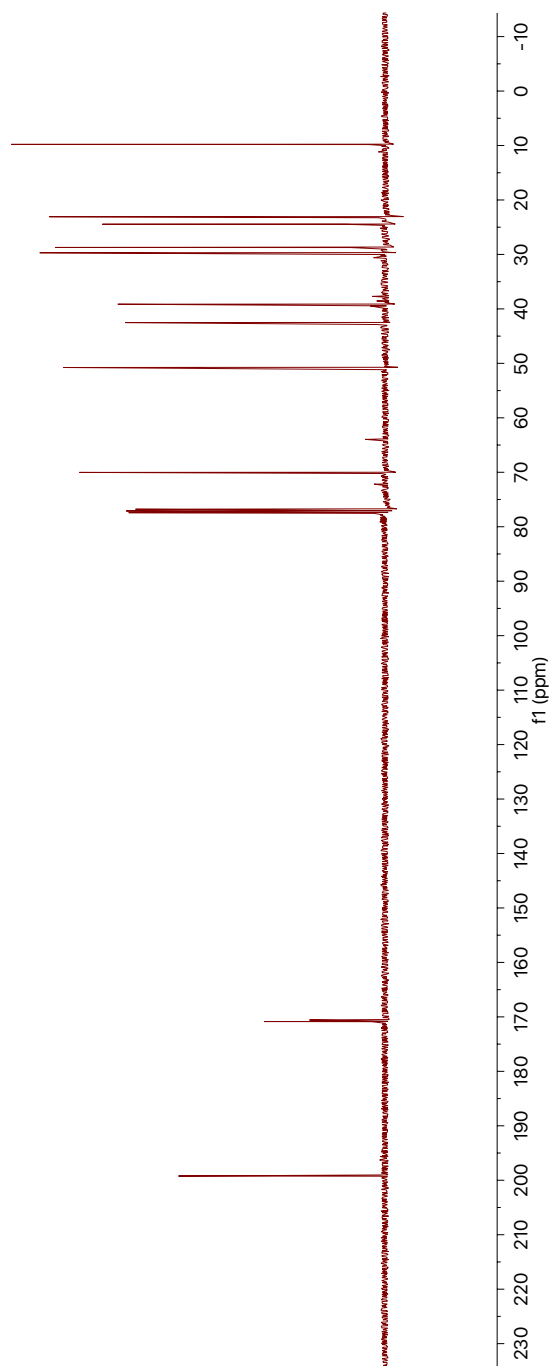
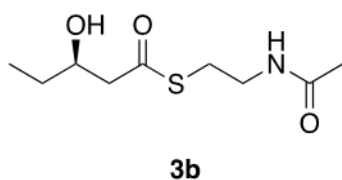


Figure S3A-2. ^1H NMR

CARBON_01
zzc0155

Figure S3A-3. ^{13}C NMR





S-(2-acetamidoethyl) (*R*)-3-hydroxypentanethioate

Chemical Formula: C₉H₁₇NO₃S

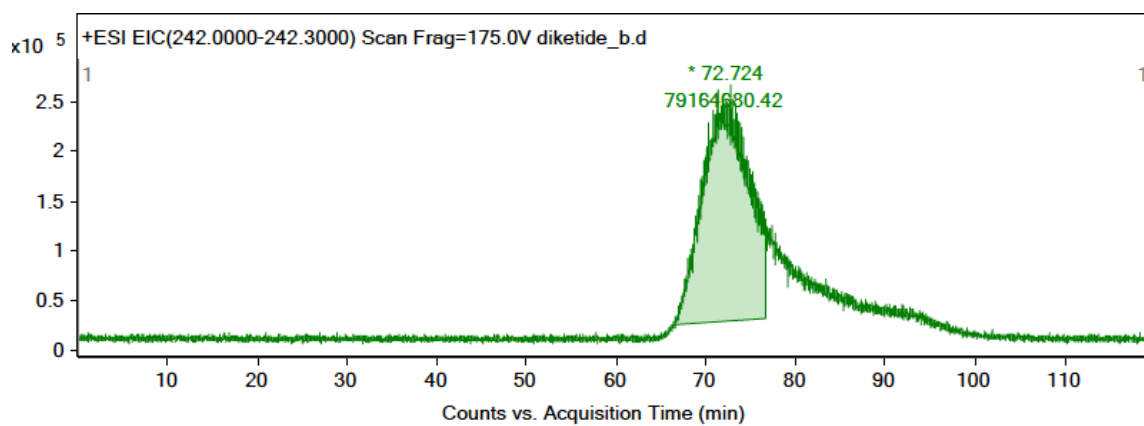


Figure S3B-1. Extracted-Ion Chromatogram of LC/MS

PROTON_01
zzc0150

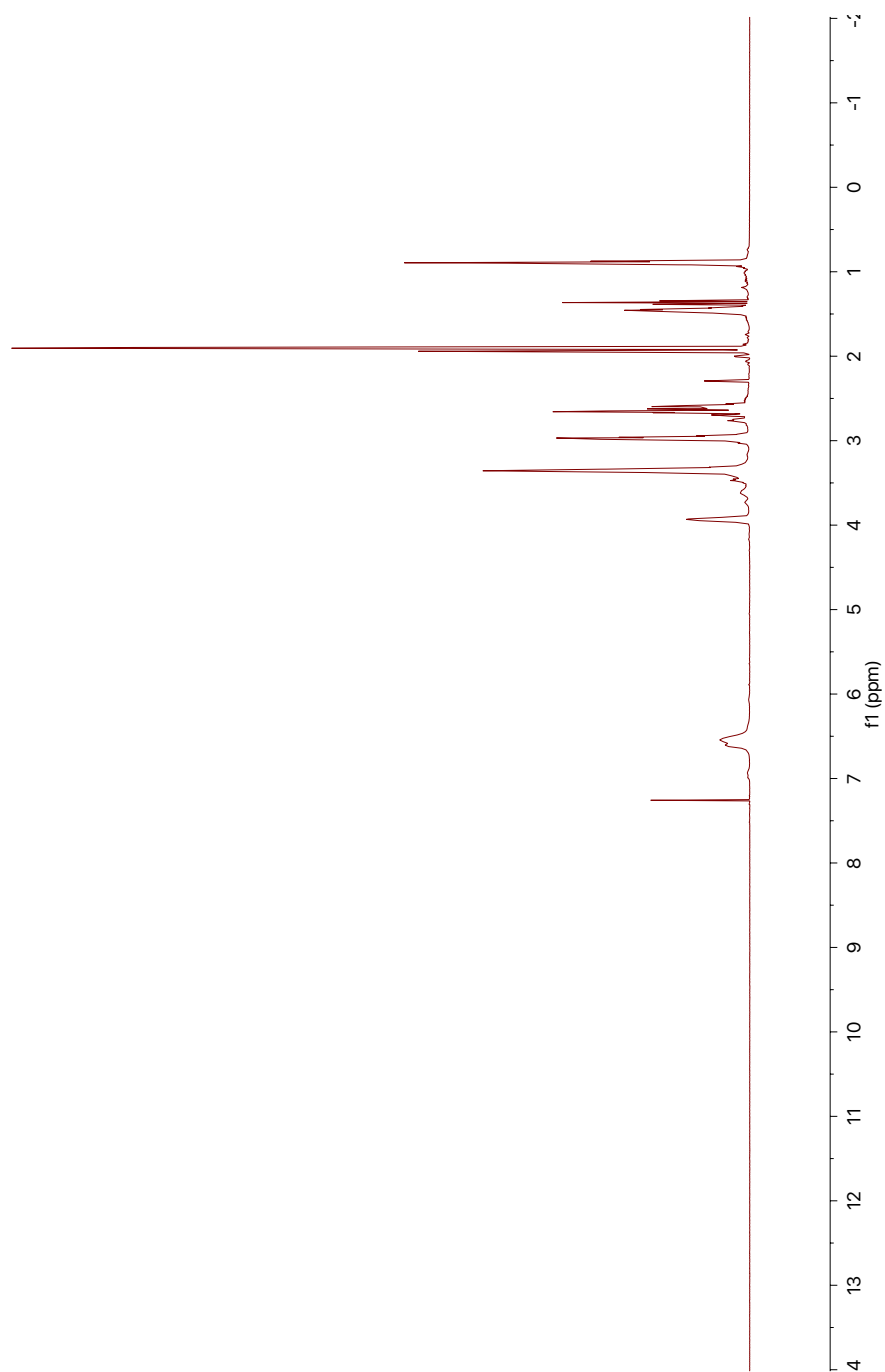


Figure S3B-2. ^1H NMR

CARBON_01
zzc0150

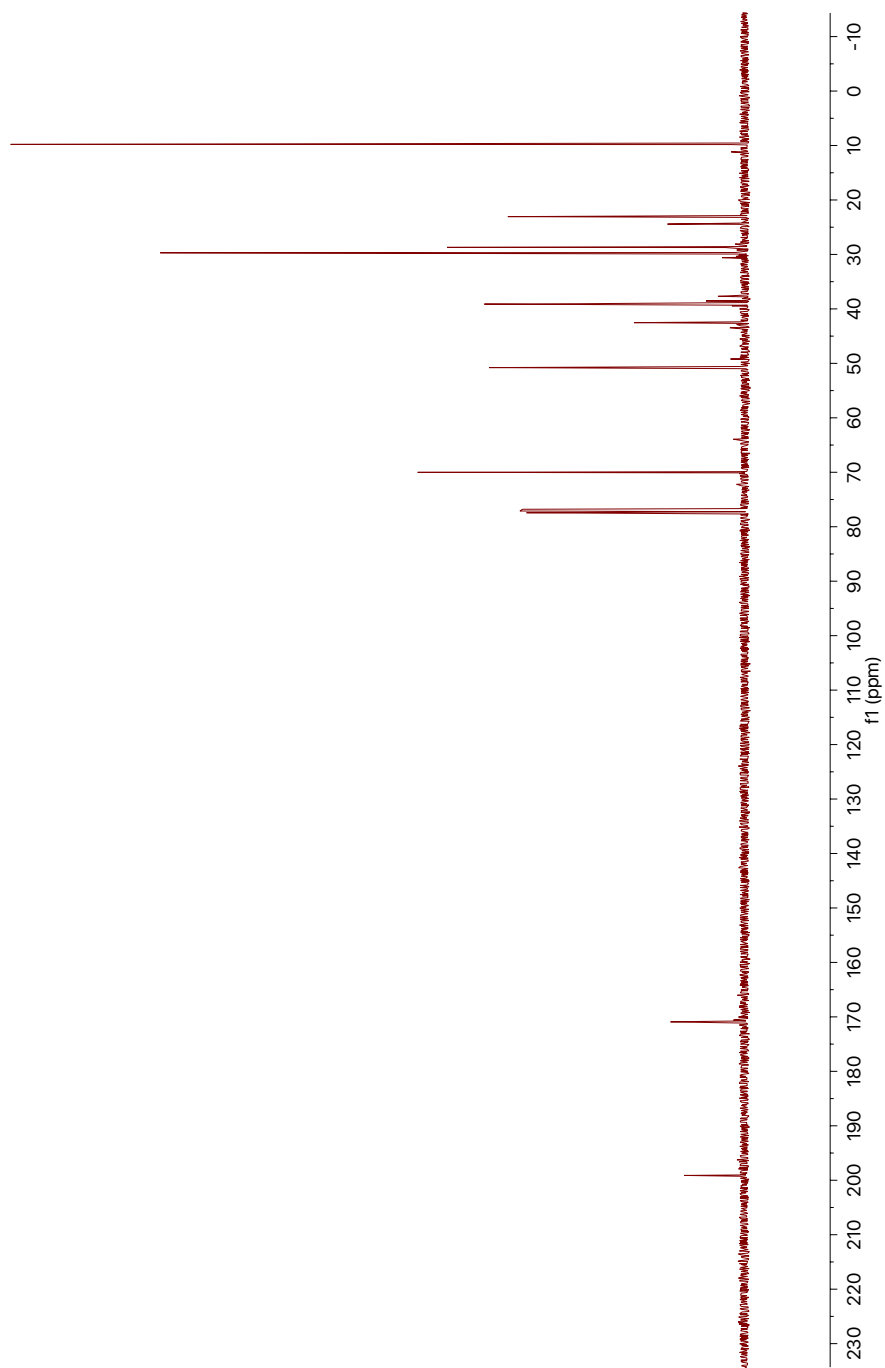
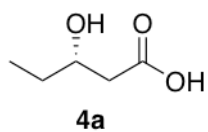


Figure S3B-3. ^{13}C NMR

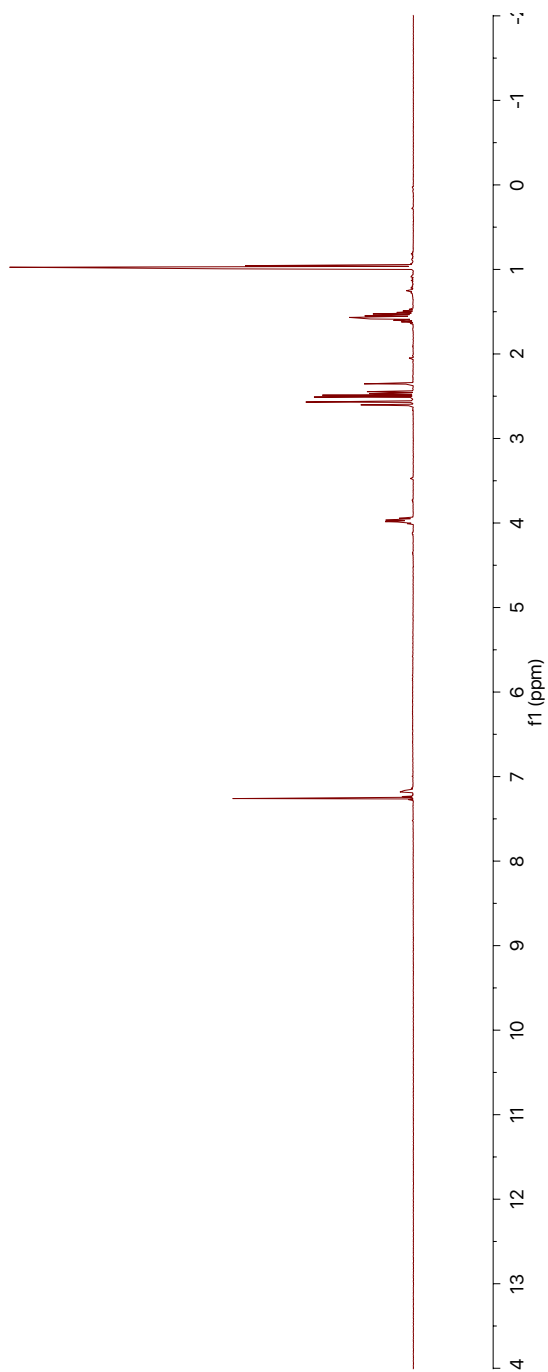


(*S*)-3-hydroxypentanoic acid

Chemical Formula: C₅H₁₀O₃

PROTON_01
zzc0285

Figure S4A-1. ^1H NMR



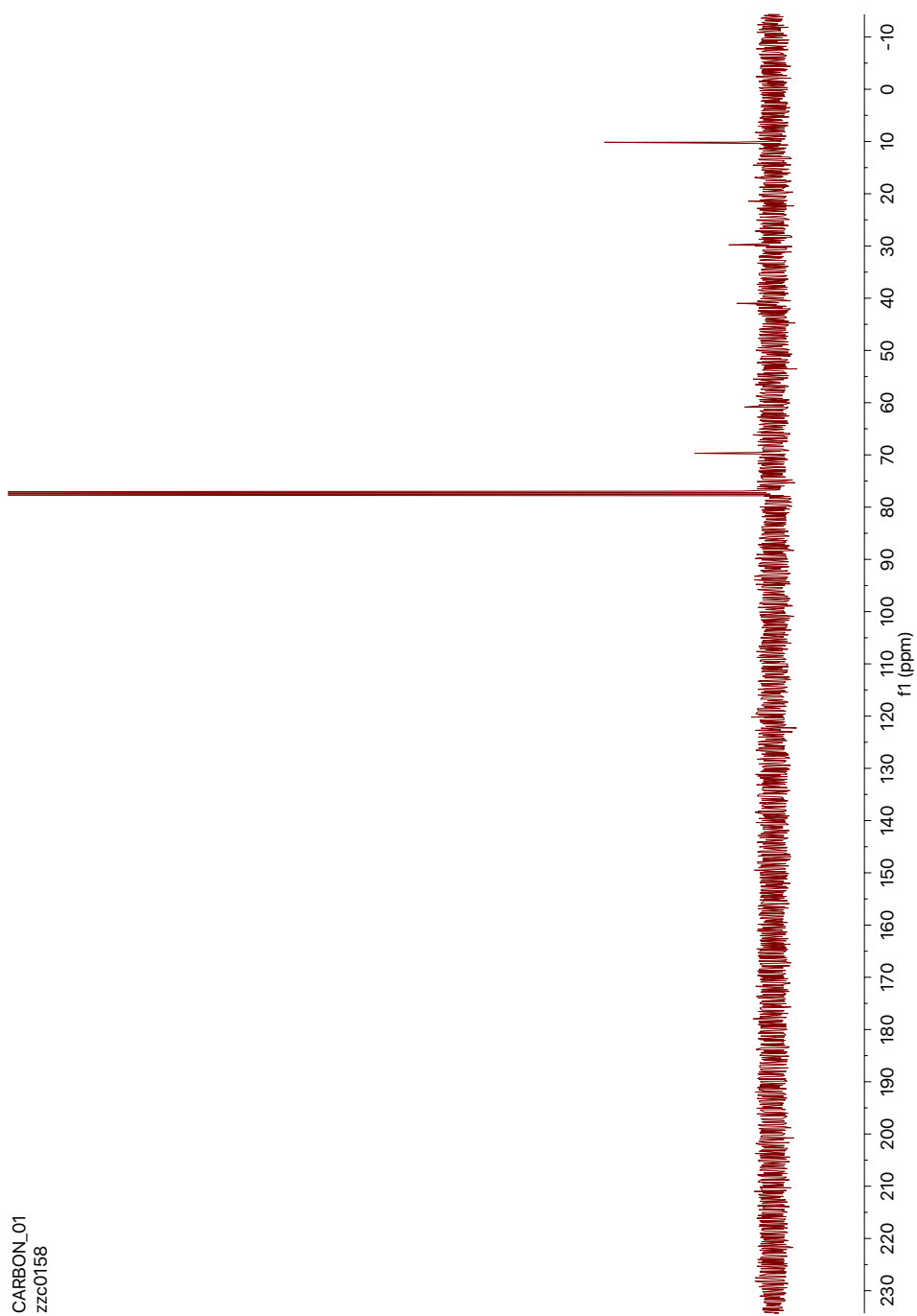
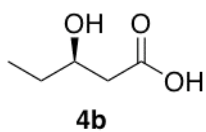


Figure S4A-2. ^{13}C NMR

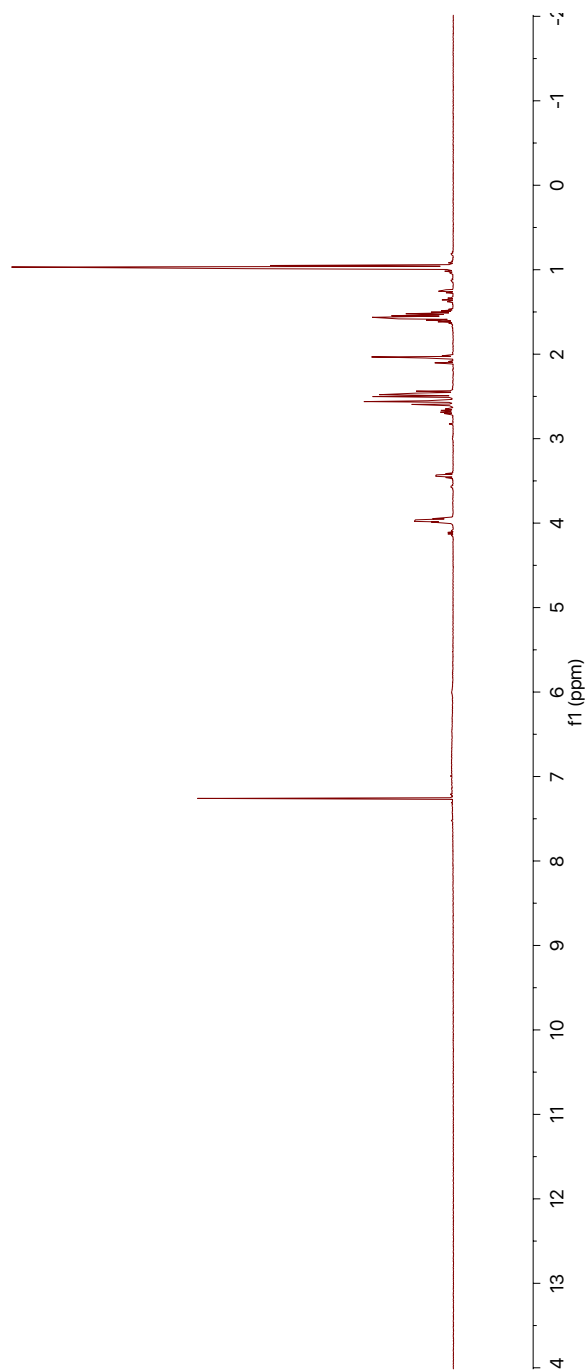


(*R*)-3-hydroxypentanoic acid

Chemical Formula: C₅H₁₀O₃

PROTON_01
zzc3hydroxy/pentioicacid

Figure S4B-1. ^1H NMR



CARBON_01
zzccarbonacid

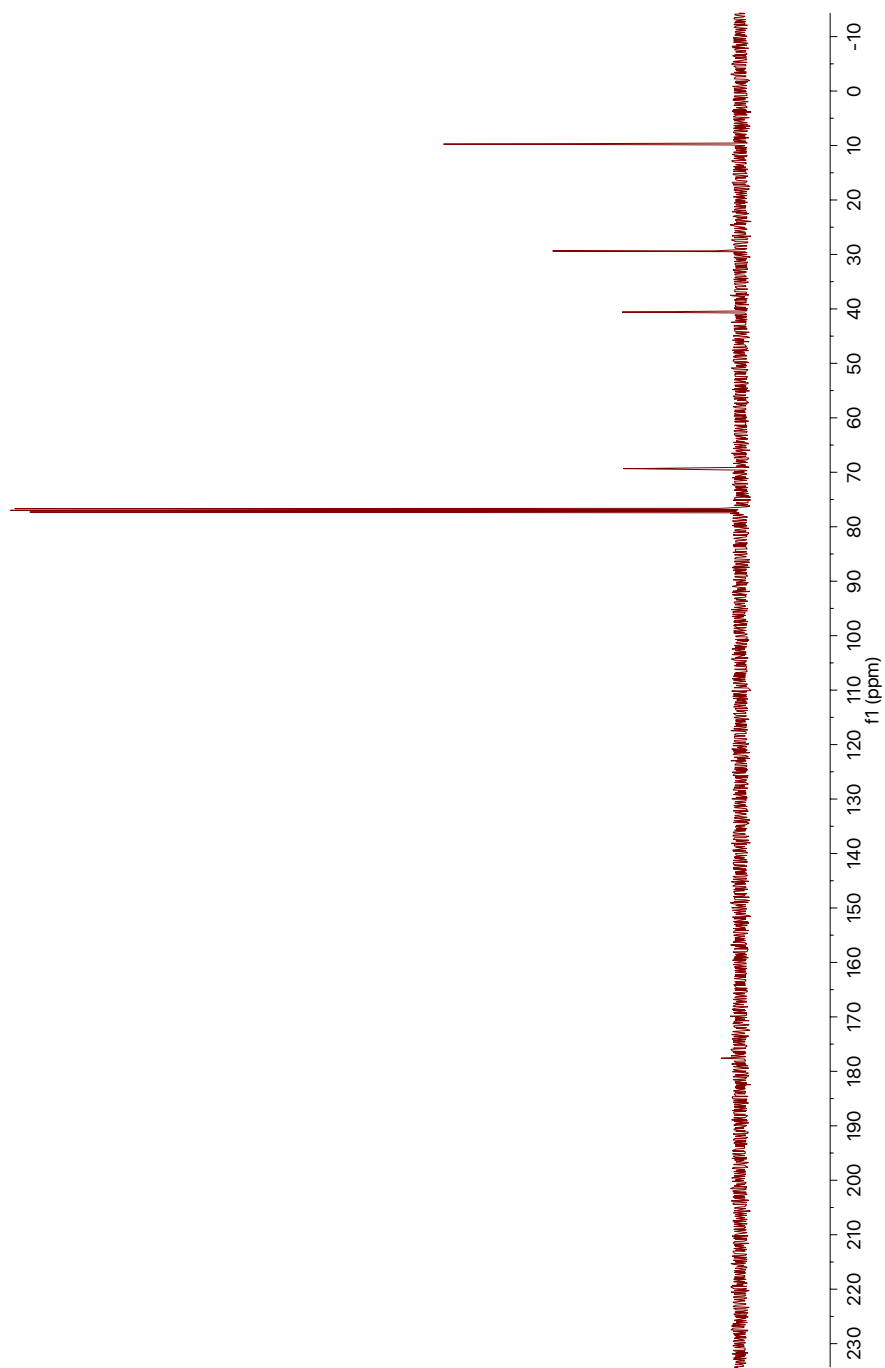
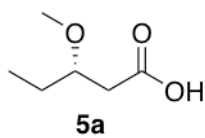


Figure S4B-2. ^{13}C NMR



(*S*)-3-methoxypentanoic acid

Chemical Formula: C₆H₁₂O₃

PROTON_01
zzc0286

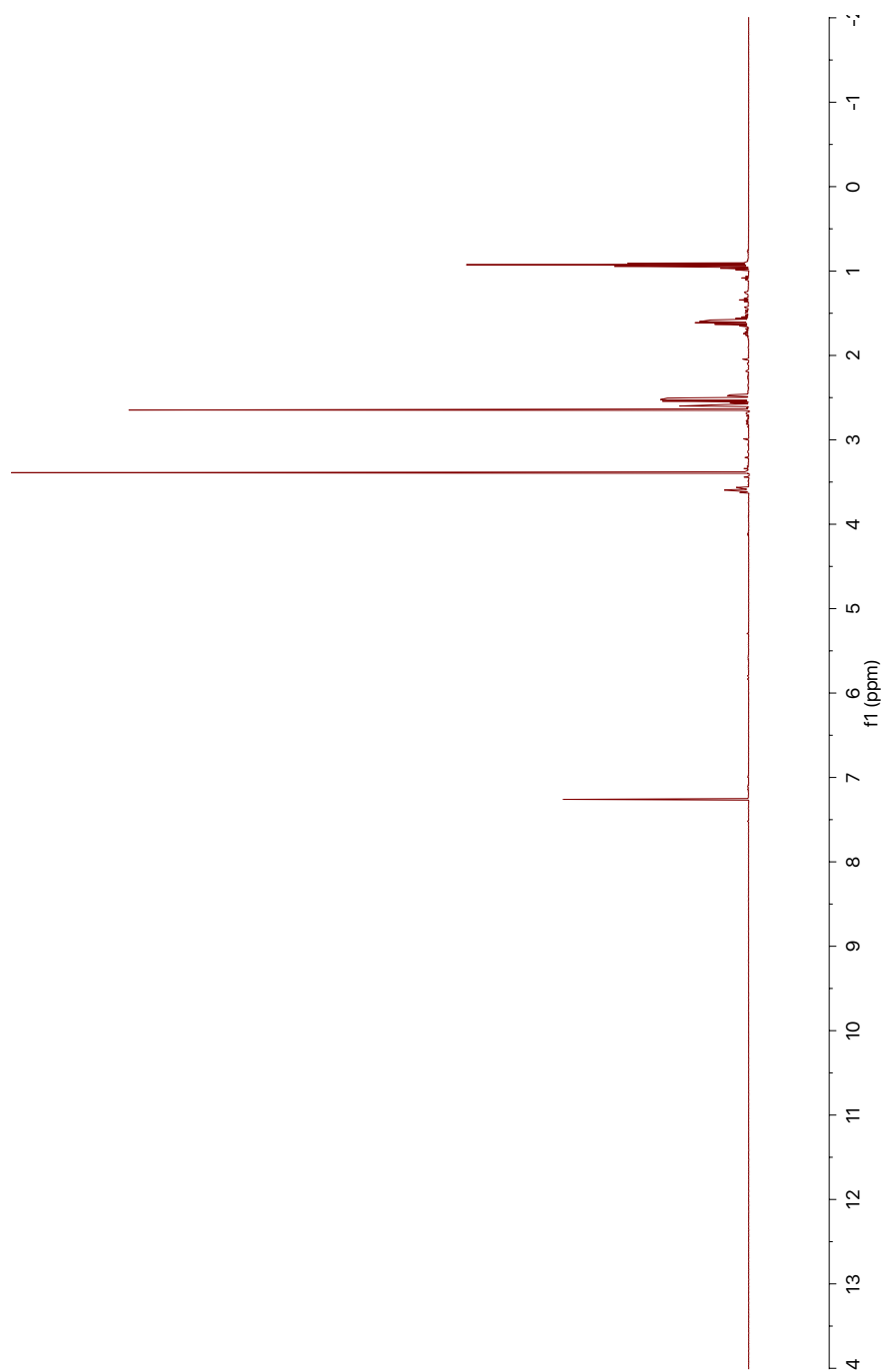
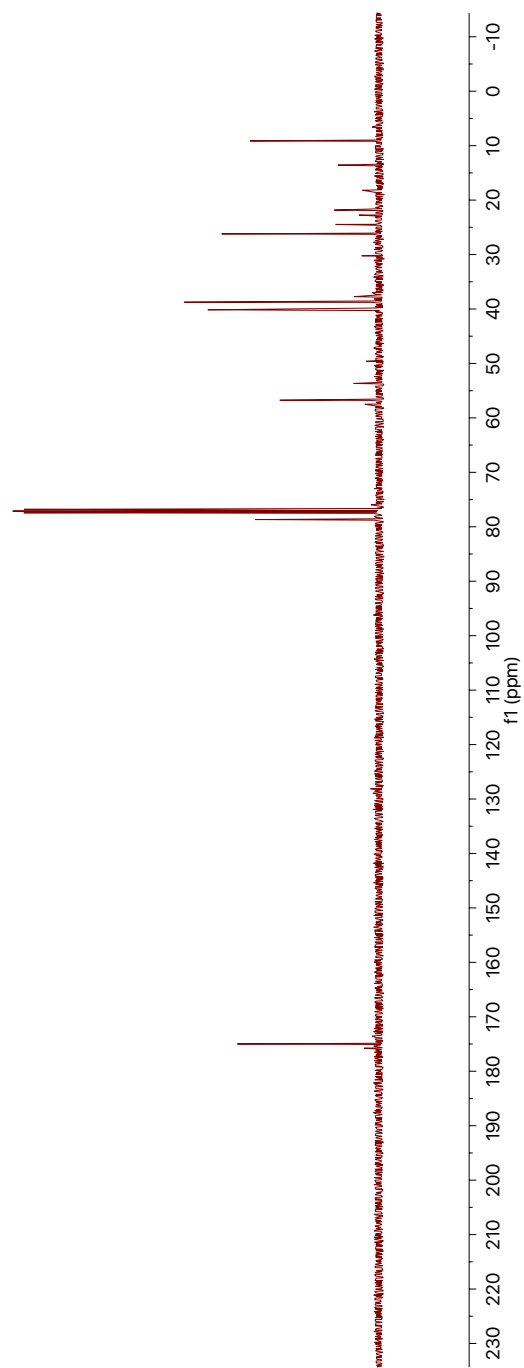
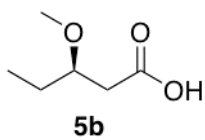


Figure S5A-1. ^1H NMR

CARBON_01
zzcmethoxy/pentanoicacida

Figure S5A-2. ^{13}C NMR





(*R*)-3-methoxypentanoic acid

Chemical Formula: C₆H₁₂O₃

PROTON_01
alexis_dmsd_remove

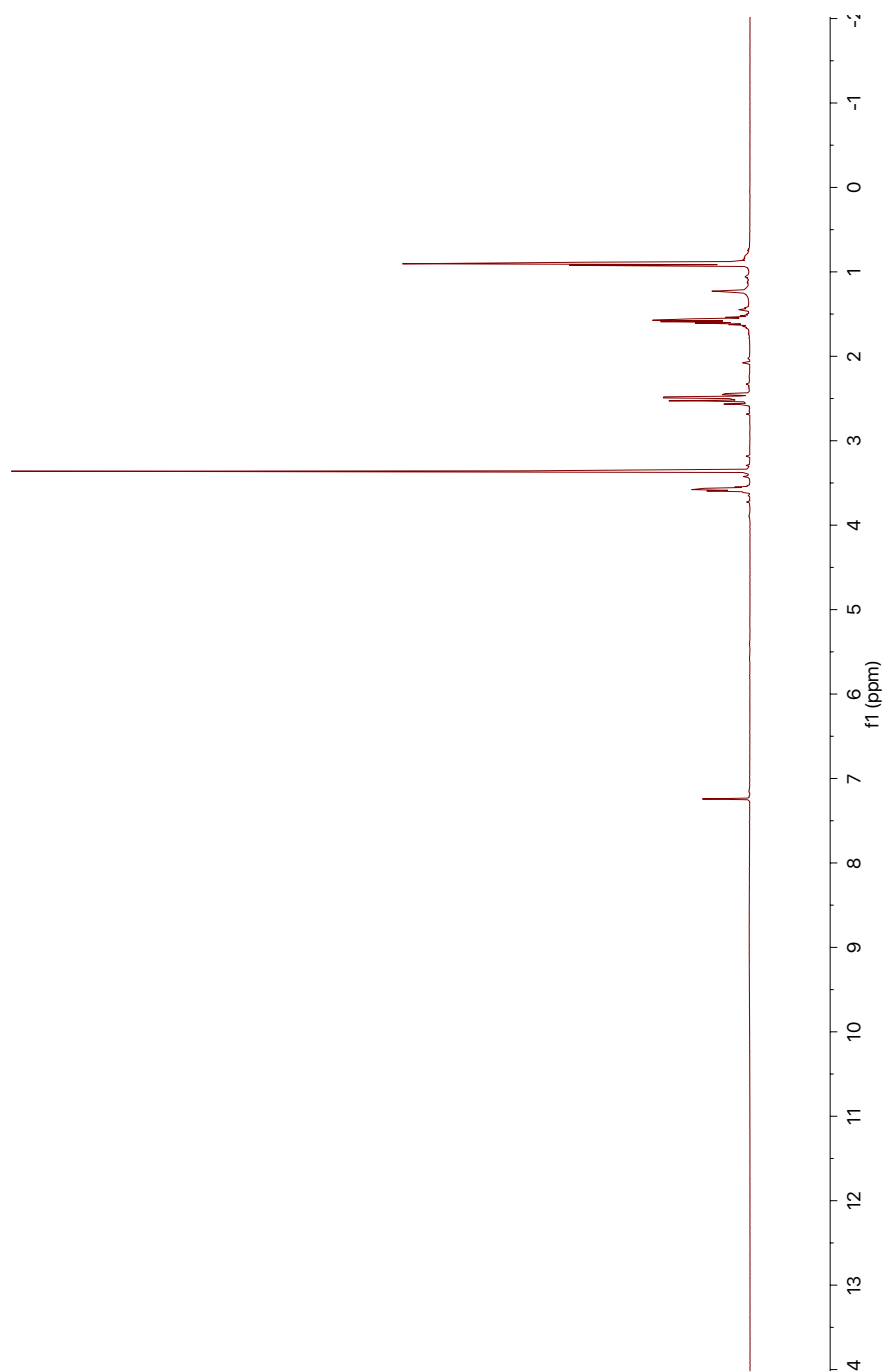
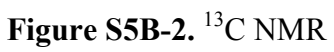
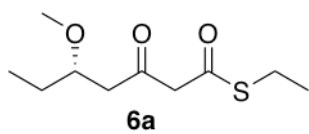


Figure S5B-1. ^1H NMR

CARBON_01



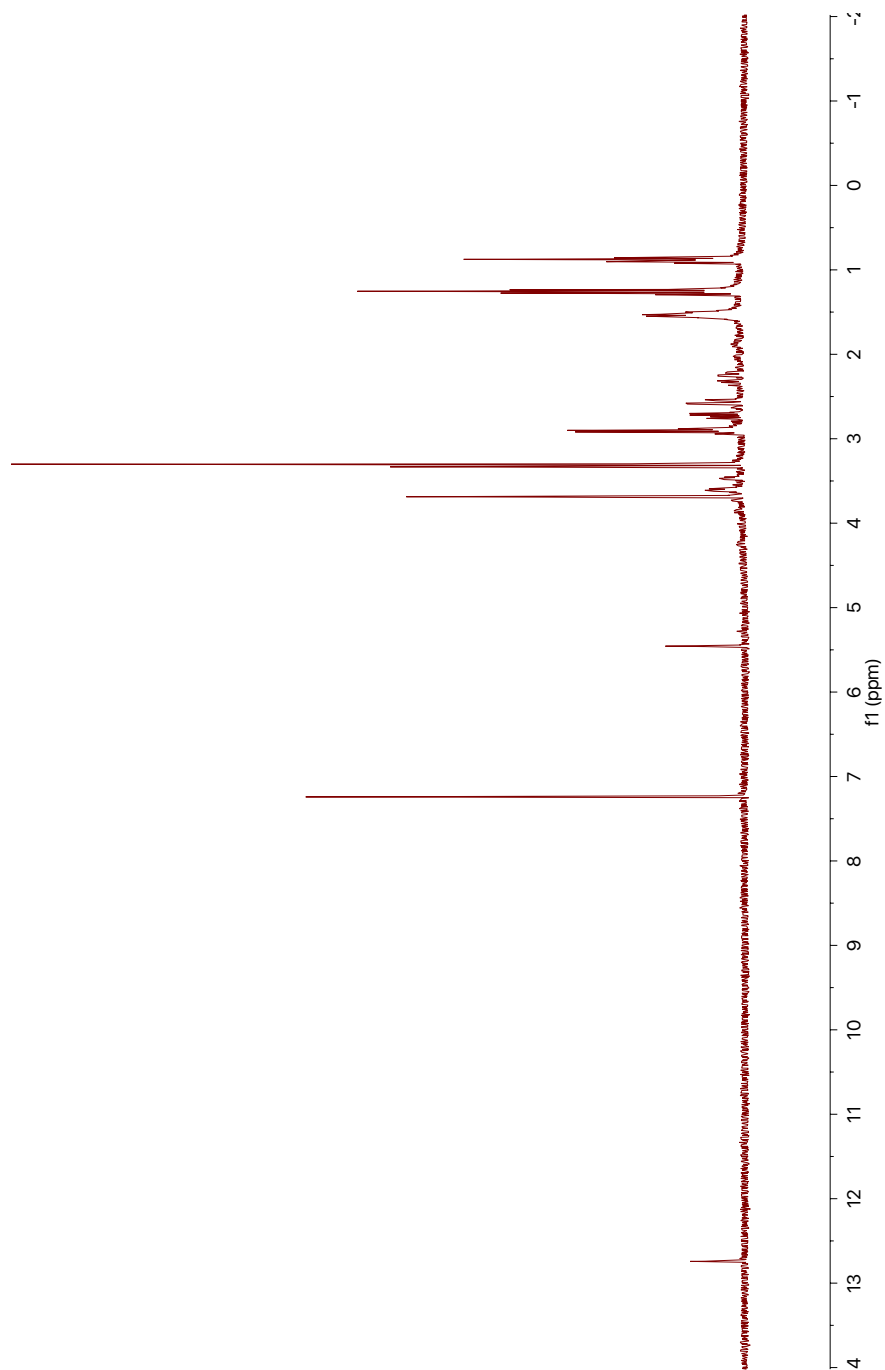


S-ethyl (*S*)-5-methoxy-3-oxoheptanethioate

Chemical Formula: C₁₀H₁₈O₃S

PROTON_01
zzc0287

Figure S6A-1. ^1H NMR



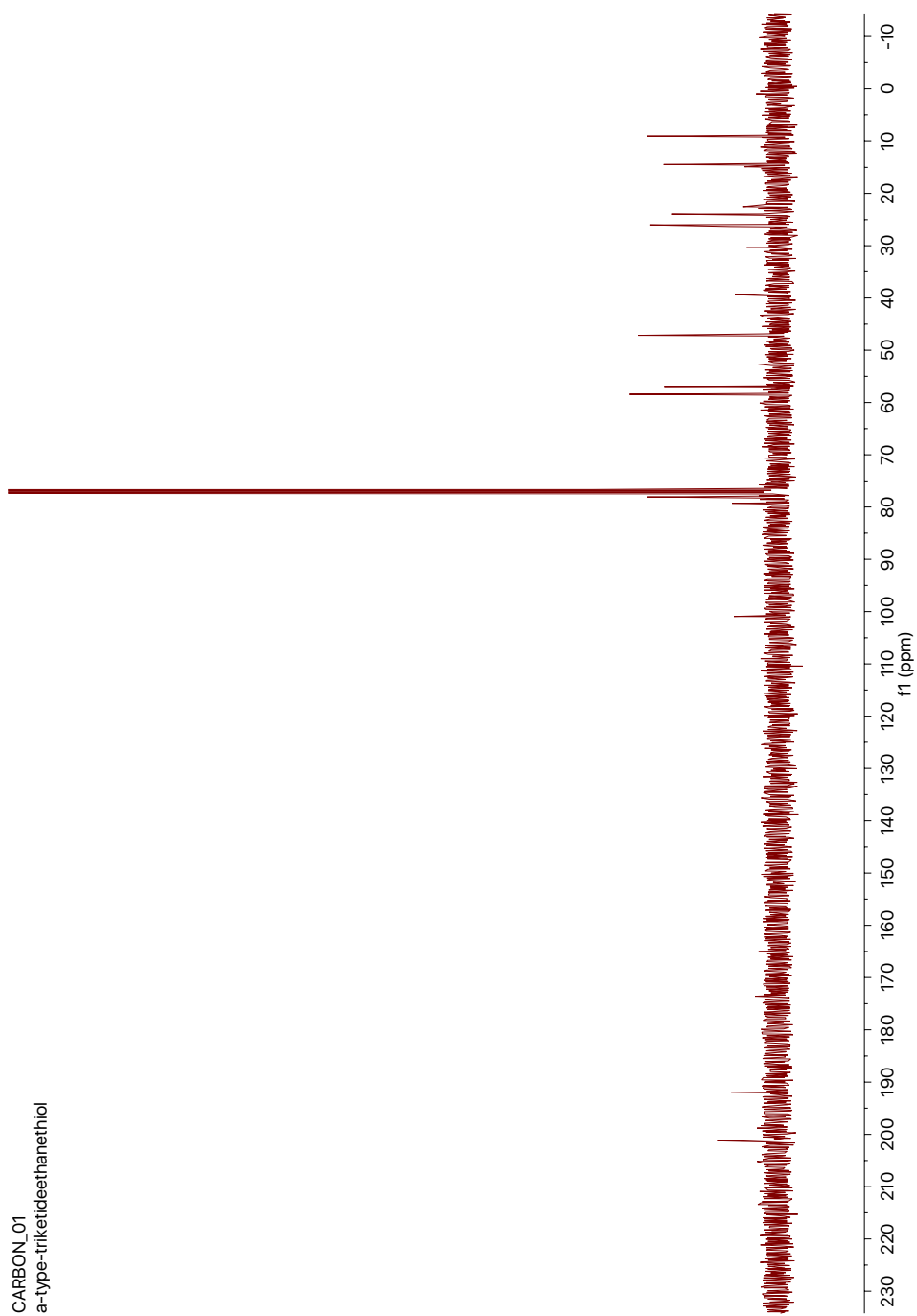


Figure S6A-2. ^{13}C NMR

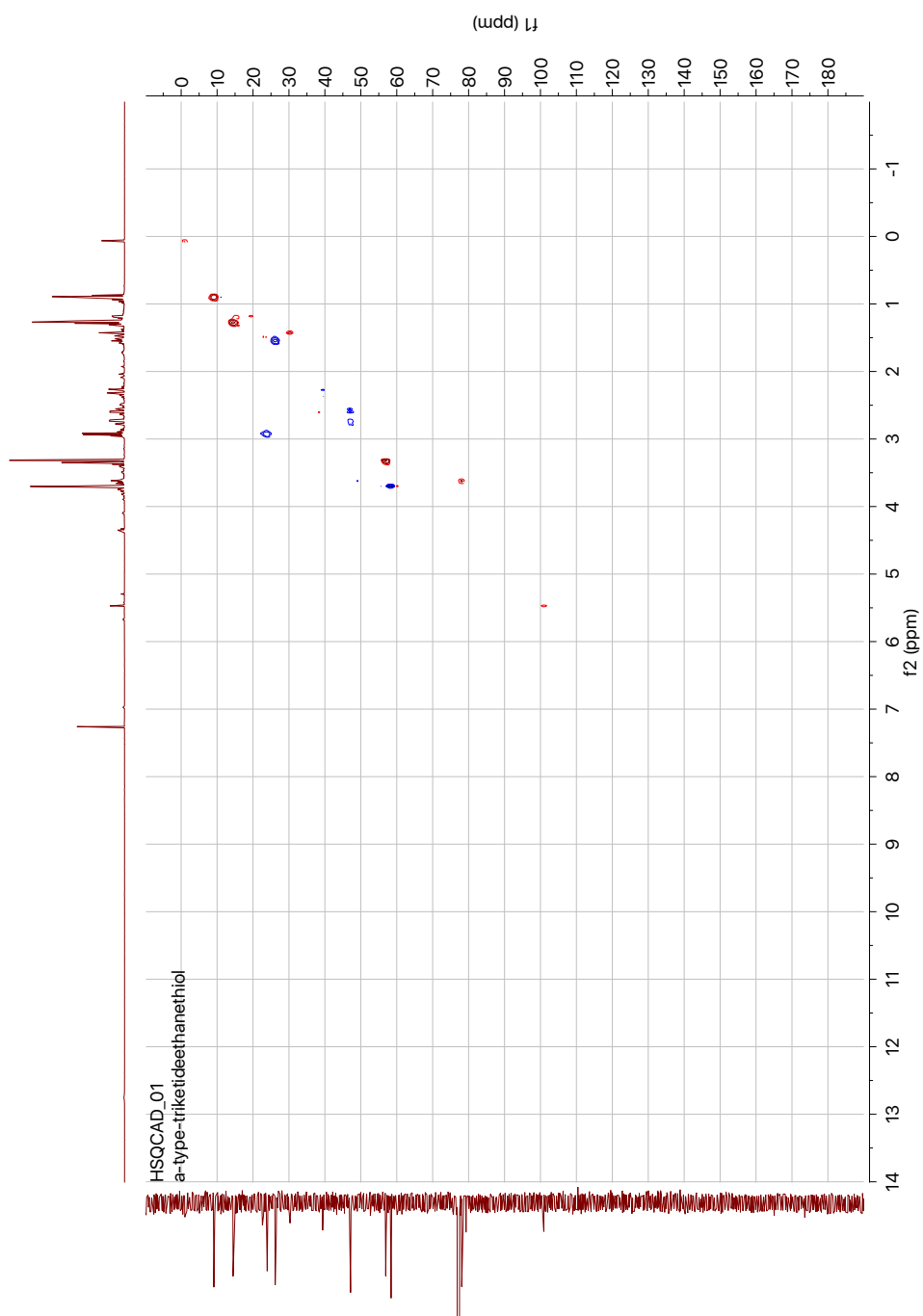
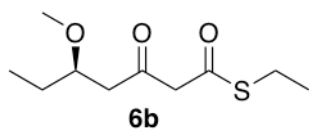


Figure S6A-3. ^1H - ^{13}C HSQC



S-ethyl (*R*)-5-methoxy-3-oxoheptanethioate

Chemical Formula: C₁₀H₁₈O₃S

PROTON_01
zzc0274

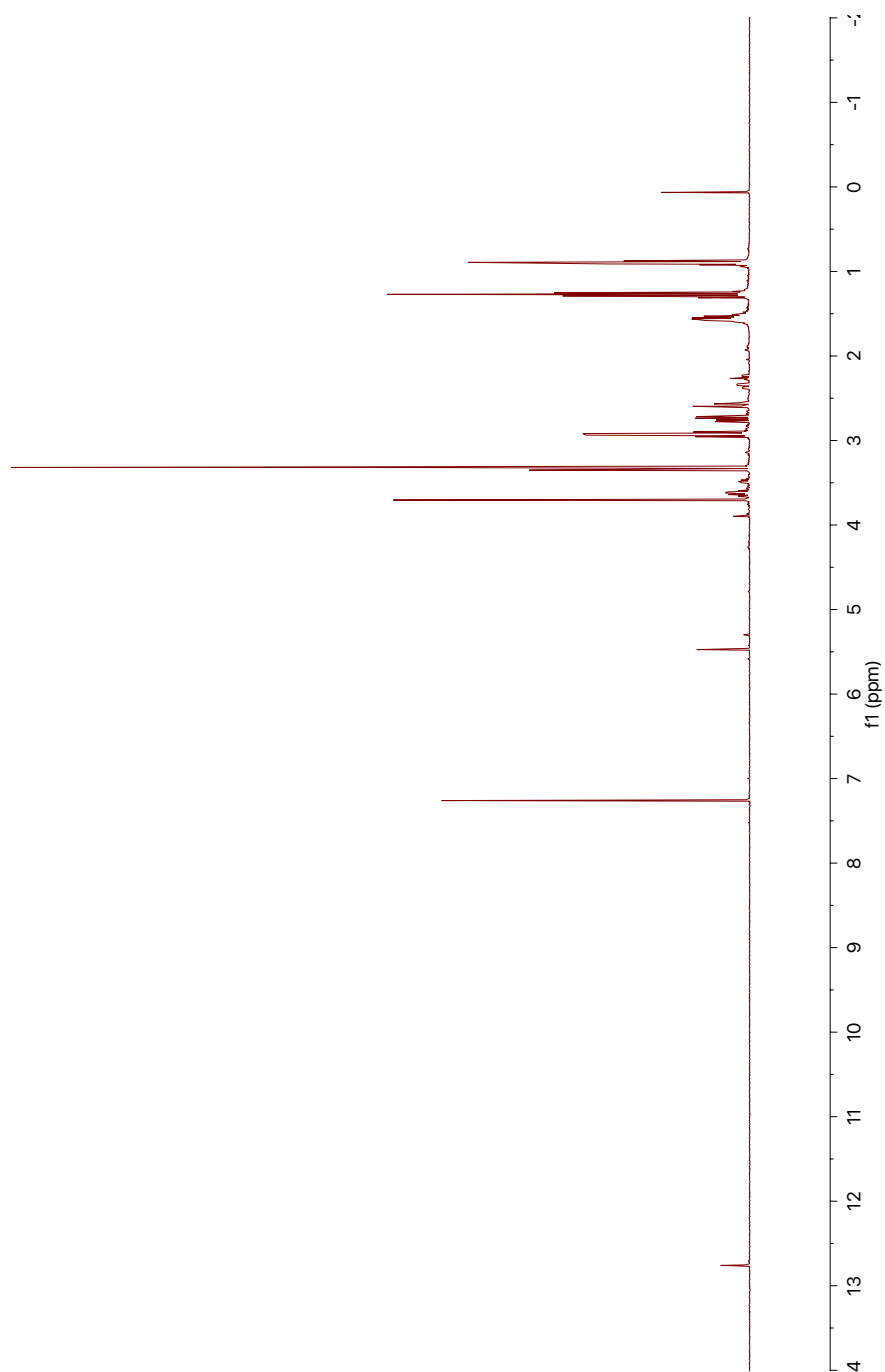


Figure S6B-1. ^1H NMR

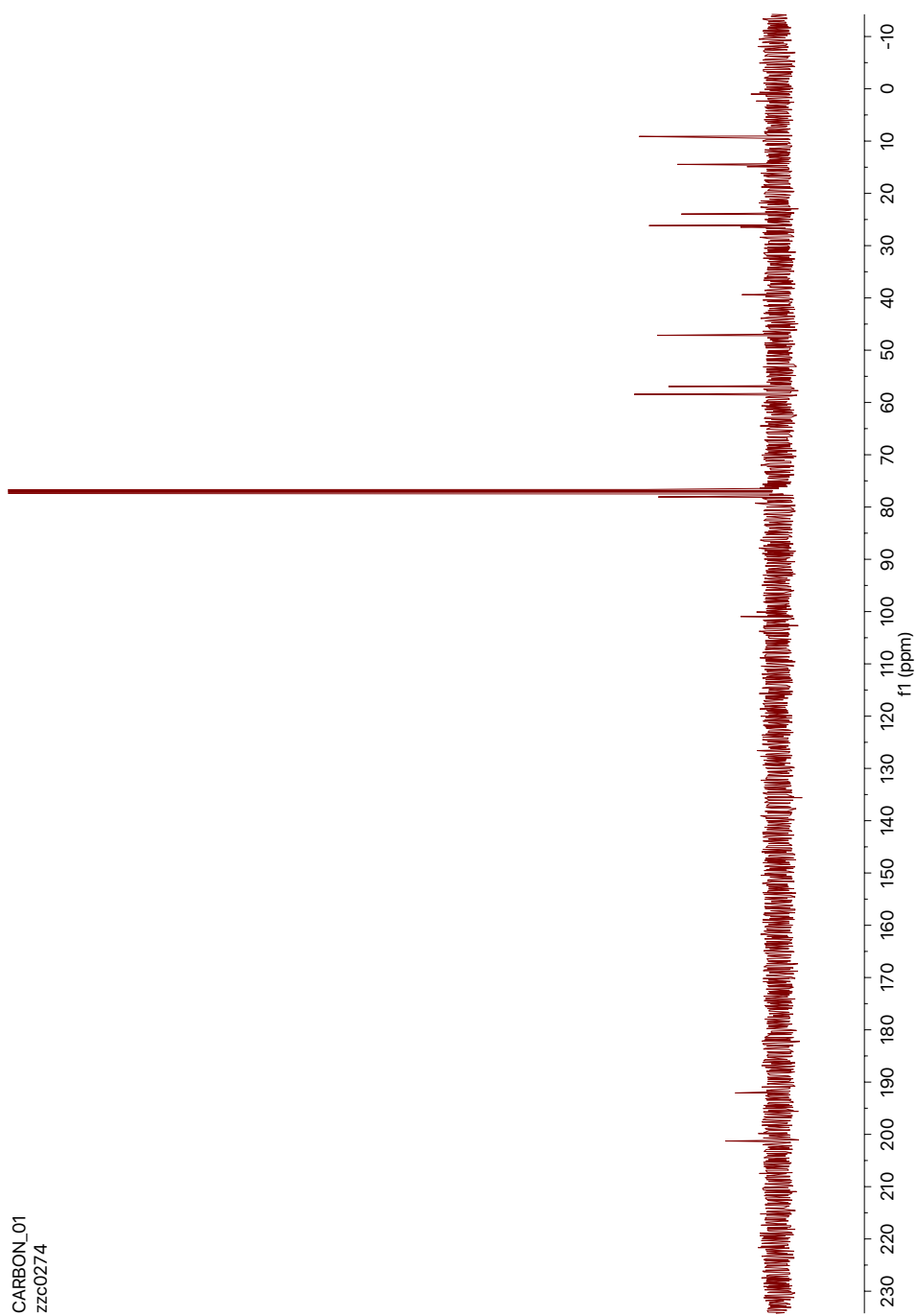


Figure S6B-2. ^{13}C NMR

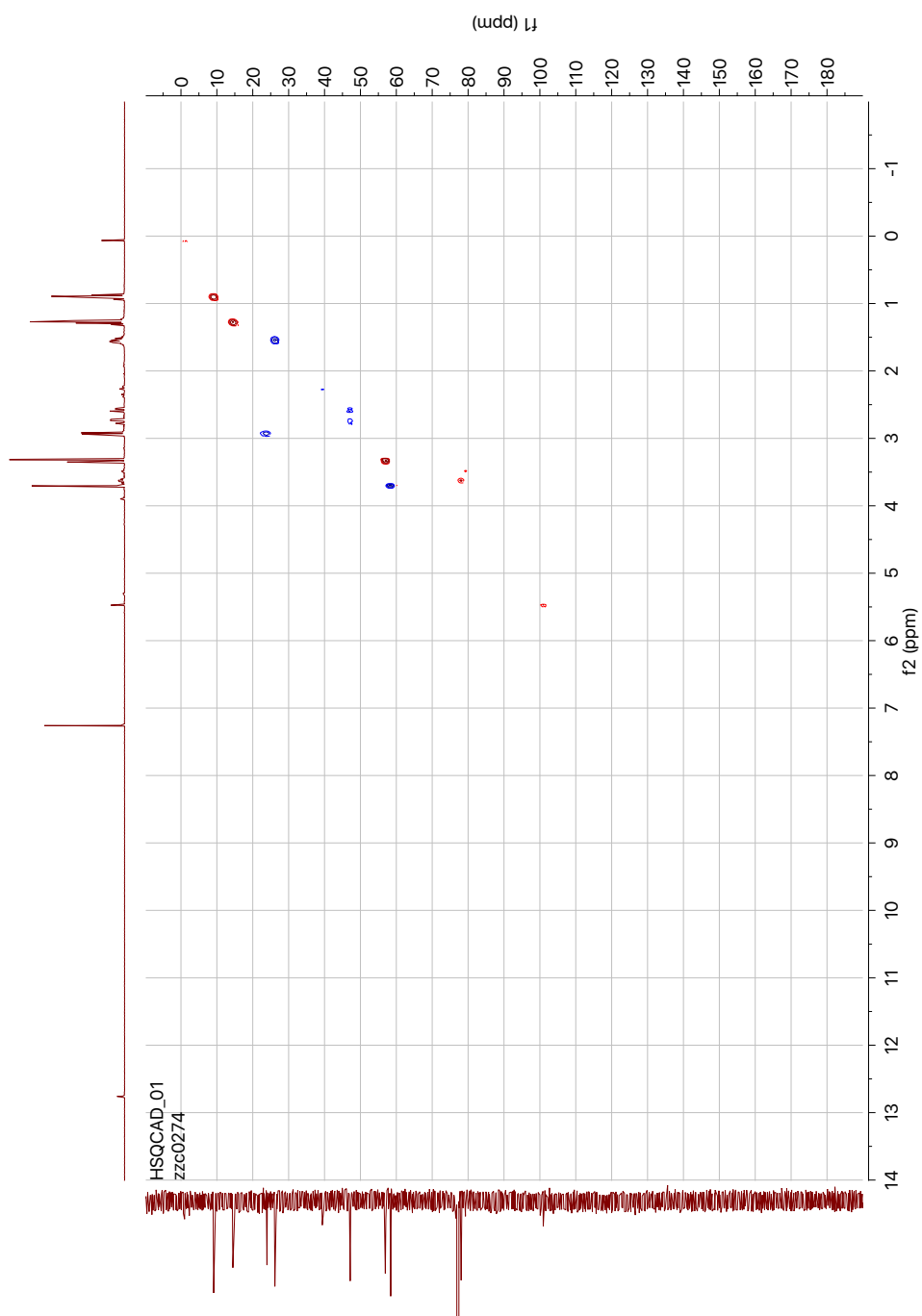
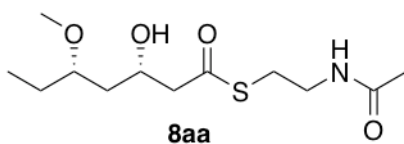


Figure S6B-3. ^1H - ^{13}C HSQC



S-(2-acetamidoethyl) (3*S*,5*S*)-3-hydroxy-5-methoxyheptanethioate (enzyme)

Chemical Formula: C₁₂H₂₃NO₄S

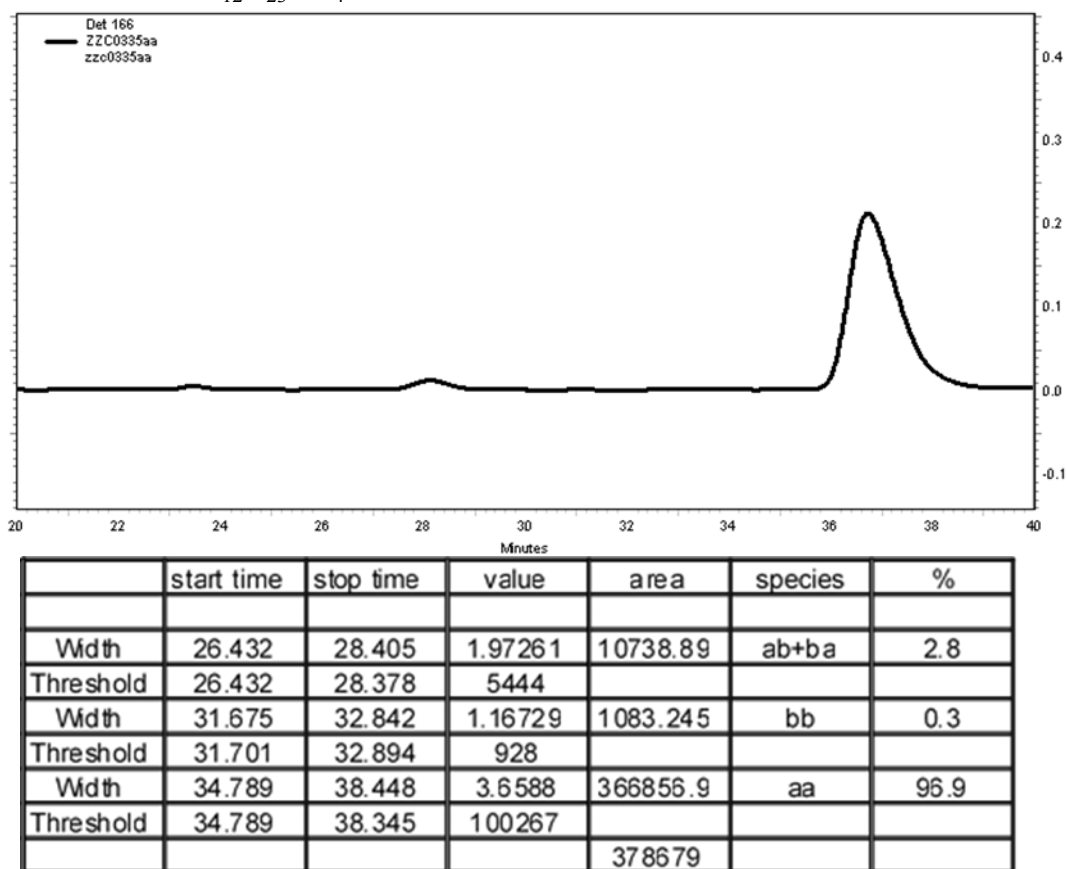
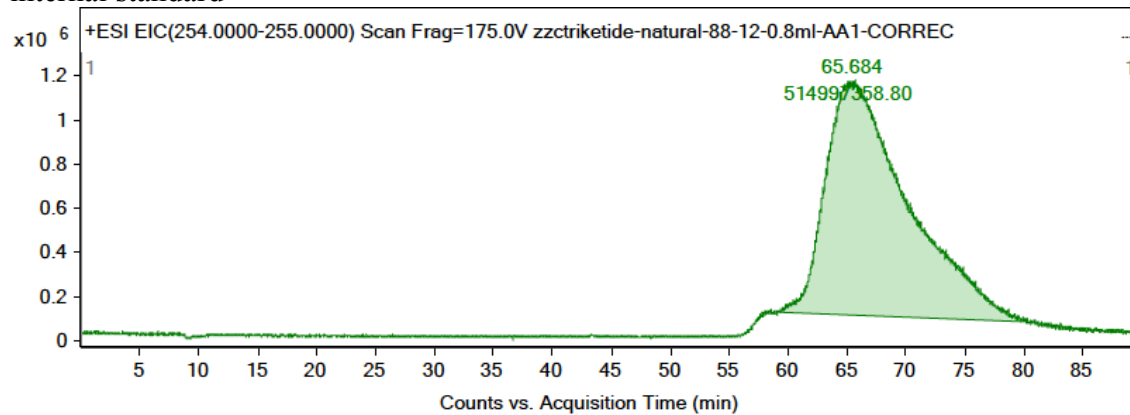
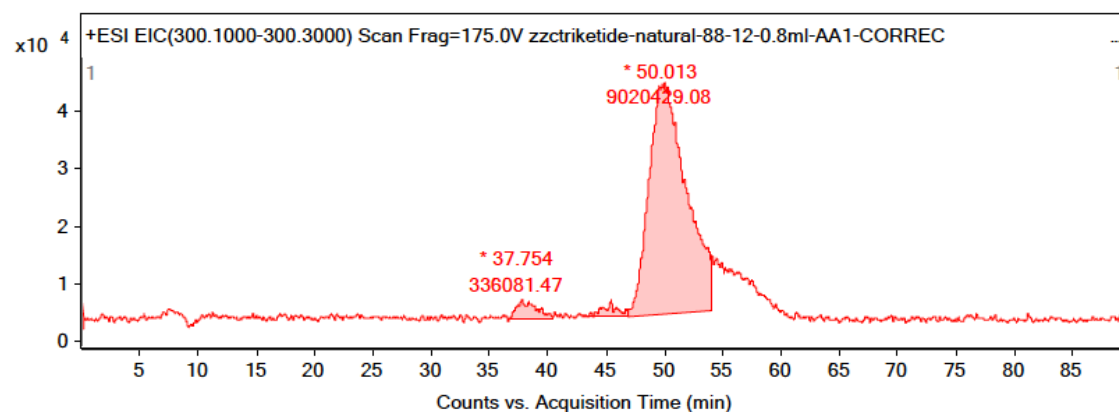


Figure S8AA-E1. HPLC Retention time: 36.8 min

internal standard



smoothed target species extract



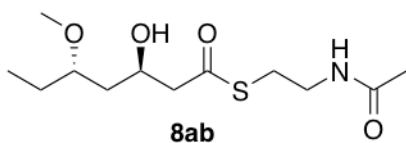
Integration Peak List

Peak	Start	RT	End	Height	Area	Area %
1	36.511	37.754	40.388	3160.59	336081.47	3.73
2	43.171	45.407	46.915	2971.19	229395.42	2.54
3	46.931	50.013	53.972	40420.11	9020429.08	100

area%	species	%
3.73	ba	3.5
2.54	ab	2.4
100	aa+bb	94.1
106.27		

Conclusion on HPLC and LCMS: 90% **8aa**

Figure S8AA-E2. LC/MS Retention time: 50.013 min



S-(2-acetamidoethyl) (3*R*,5*S*)-3-hydroxy-5-methoxyheptanethioate (enzyme)

Chemical Formula: C₁₂H₂₃NO₄S

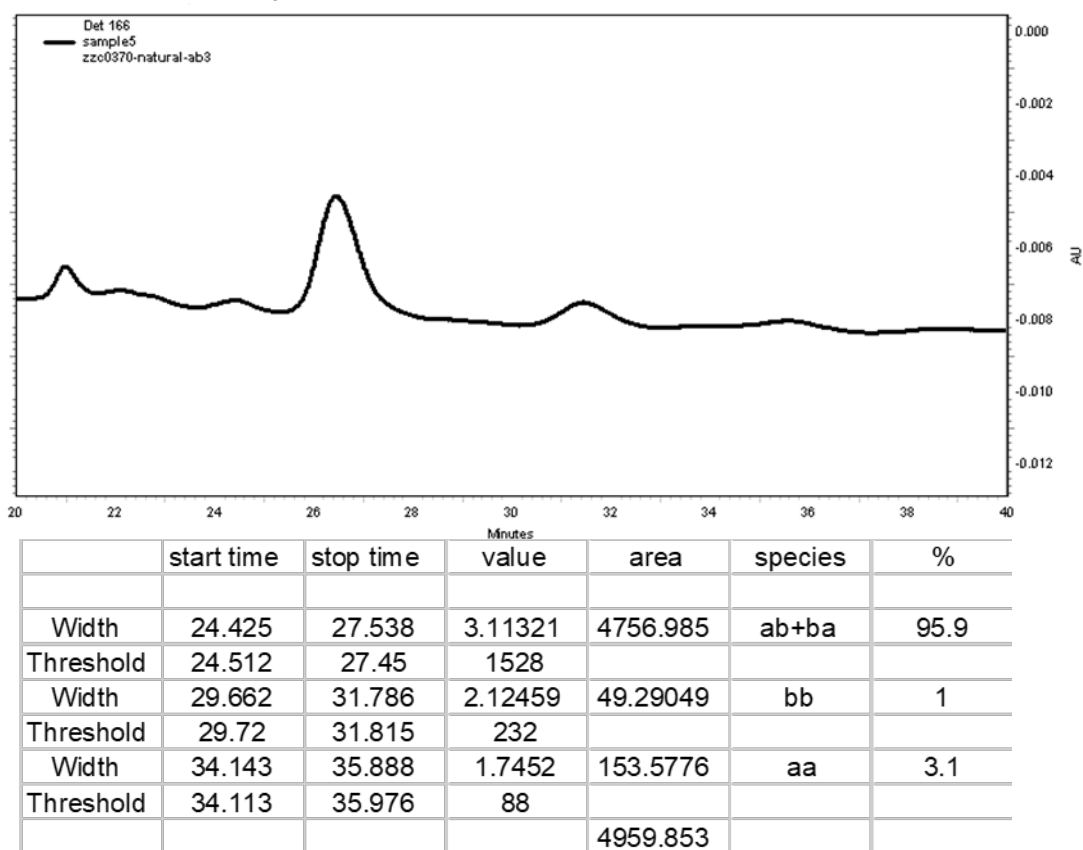
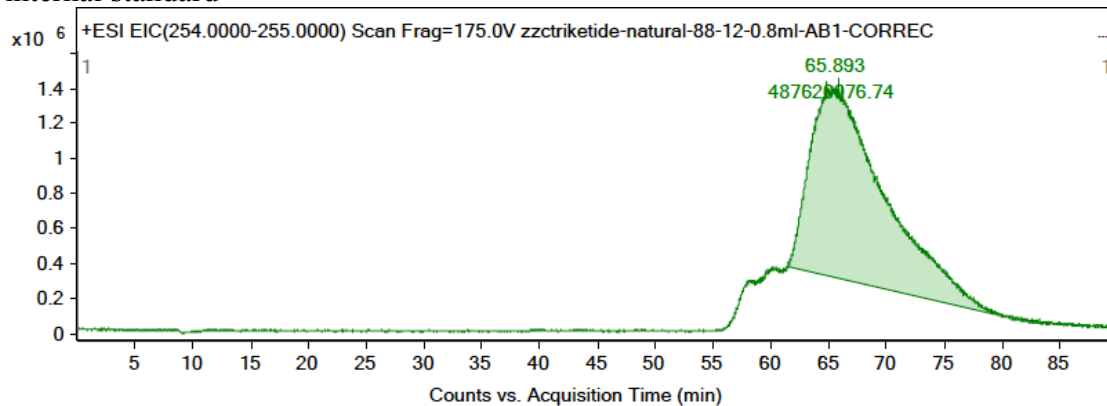
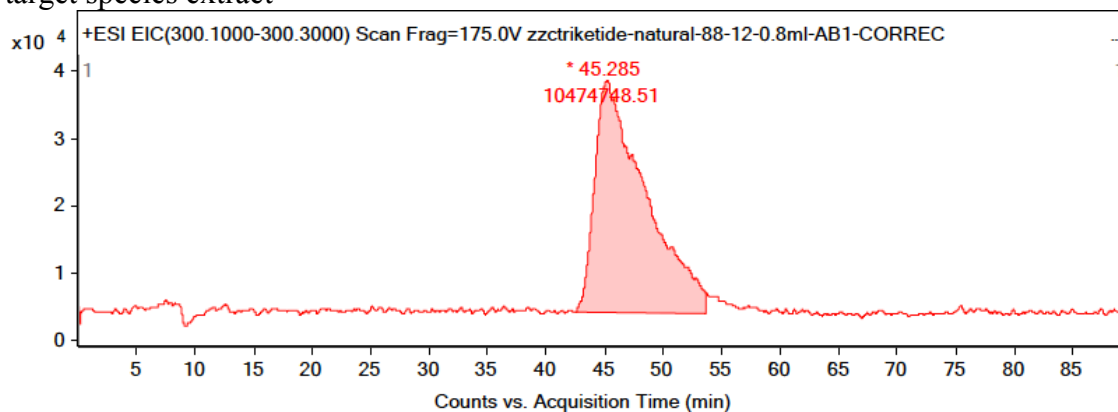


Figure S8AB-E1. HPLC Retention time: 26.4 min

internal standard



target species extract



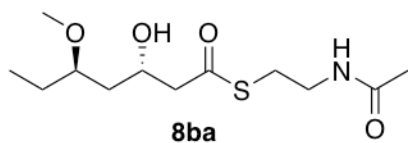
Integration Peak List

Peak	Start	RT	End	Height	Area	Area %
1	42.502	45.285	53.701	34649.73	10474748.51	100

area%	species	%
0	ba	~0
100	ab	100
0	aa+bb	~0
100		

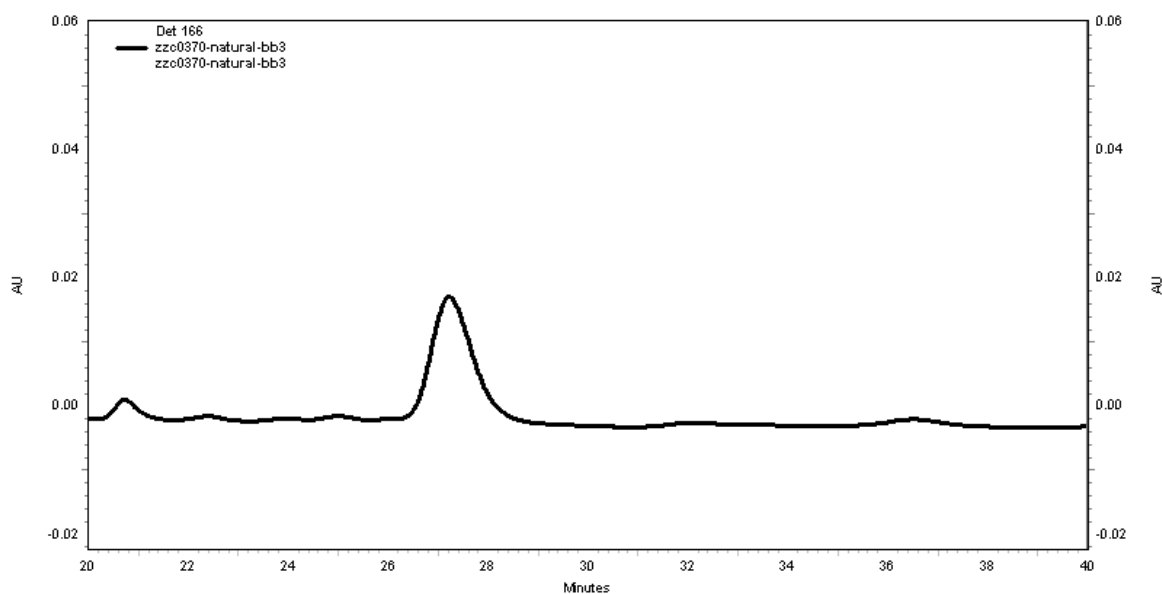
Conclusion on HPLC and LCMS: 96% **8ab**

Figure S8AB-E2. LC/MS Retention time: 45.285 min



S-(2-acetamidoethyl) (3*S*,5*R*)-3-hydroxy-5-methoxyheptanethioate (enzyme)

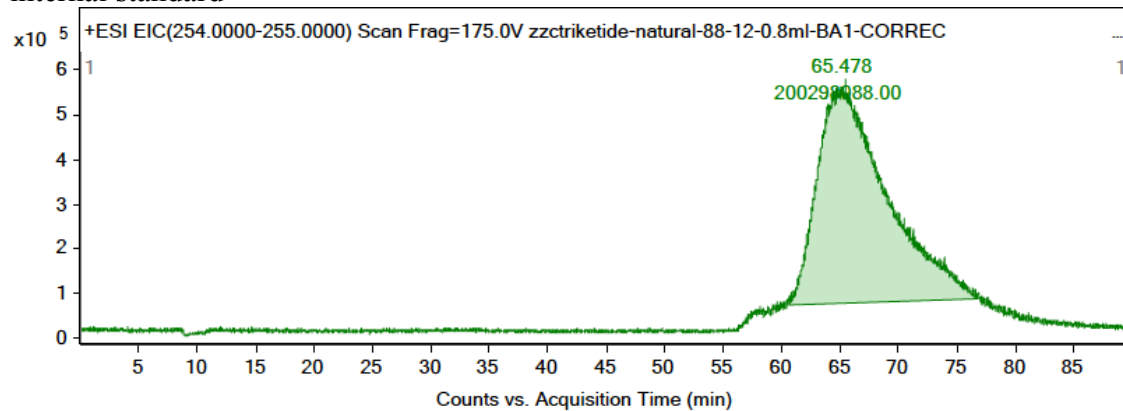
Chemical Formula: C₁₂H₂₃NO₄S



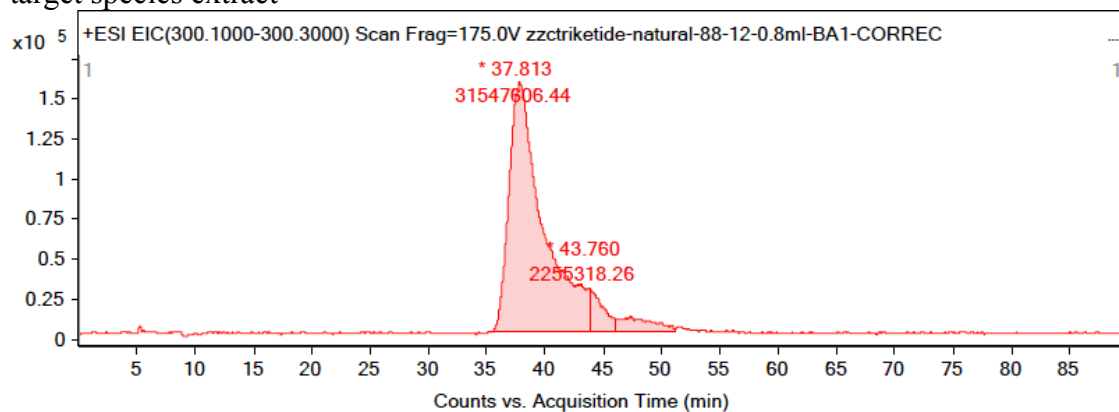
	start time	stop time	value	area	species	%
Width	26.211	29.085	2.87447	26189.3	ab+ba	94.8
Threshold	26.171	29.006	9111			
Width	31.37	33.969	2.59908	610.7838	bb	2.2
Threshold	31.37	34.01	235			
Width	35.348	37.829	2.48148	813.9254	aa	3
Threshold	35.506	37.947	328			
				27614.01		

Figure S8BA-E1. HPLC Retention time: 27.0 min

internal standard



target species extract



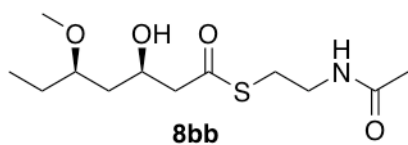
Integration Peak List

Peak	Start	RT	End	Height	Area	Area %
1	35.245	37.813	43.76	155964.06	31547606.44	100
2	43.76	43.76	46.112	26296.48	2255318.26	7.15
3	46.112	47.355	51.082	9125.59	1834958.8	5.82

area%	species	%
100	ba	88.6
7.15	ab	6.3
5.82	aa+bb	5.1
112.97		

Conclusion on HPLC and LCMS: 89% **8ba**

Figure S8AB-E2. LC/MS Retention time: 37.813 min



S-(2-acetamidoethyl) (3*S*,5*S*)-3-hydroxy-5-methoxyheptanethioate (enzyme)

Chemical Formula: C₁₂H₂₃NO₄S

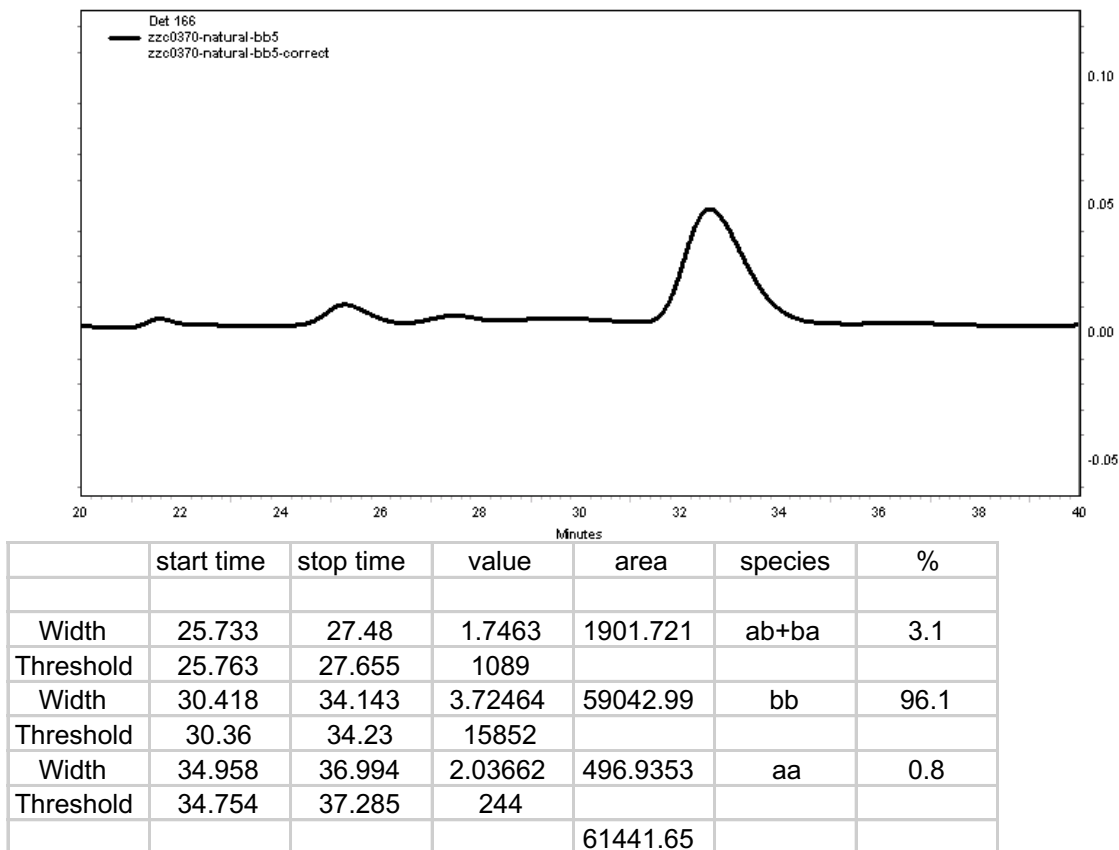
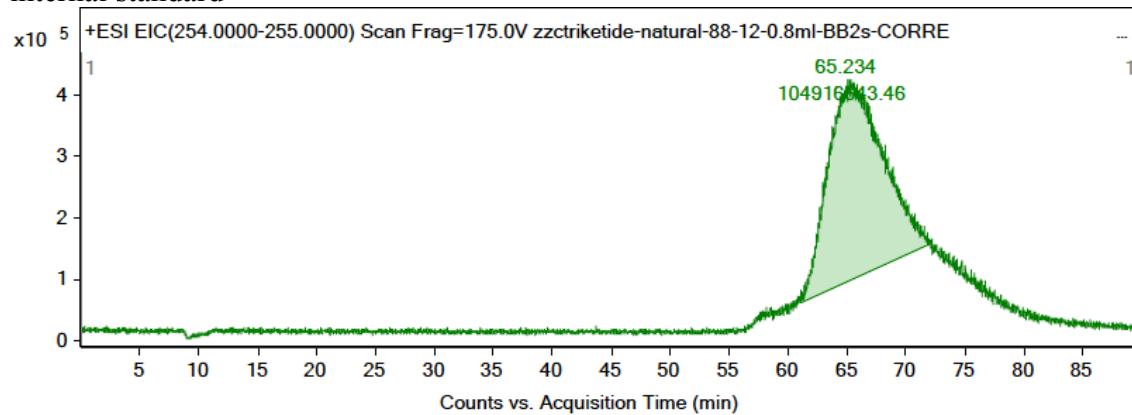
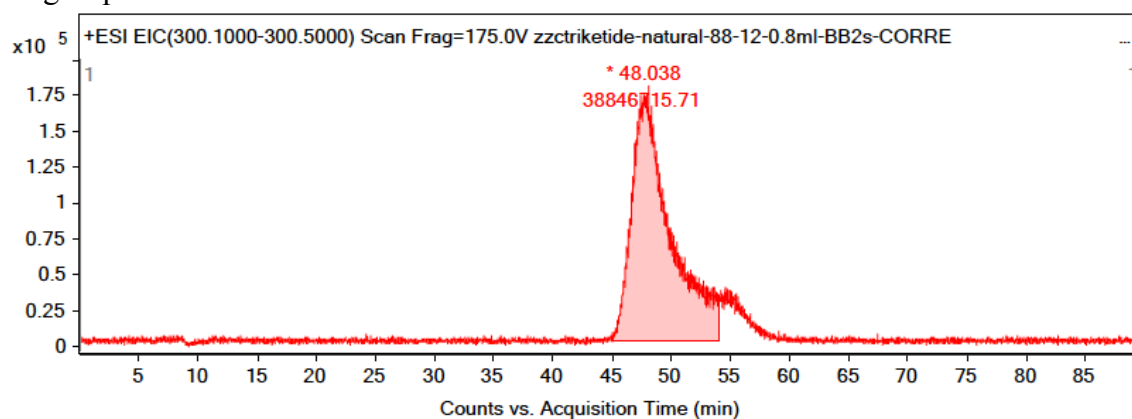


Figure S8BB-E1. HPLC Retention time: 32.4 min

internal standard



target species extrac



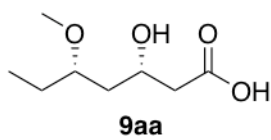
Integration Peak List

Peak	Start	RT	End	Height	Area	Area %
1	44.99	48.038	54.051	178233.67	38846715.71	100

area%	species	%
0	ba	0
0	ab	0
100	aa+bb	100
100		

Conclusion on HPLC and LCMS: 96% **8bb**

Figure S8BB-E2. LC/MS Retention time: 48.038 min



(3*S*,5*S*)-3-hydroxy-5-methoxyheptanoic acid (enzyme)

Chemical Formula: C₈H₁₆O₄

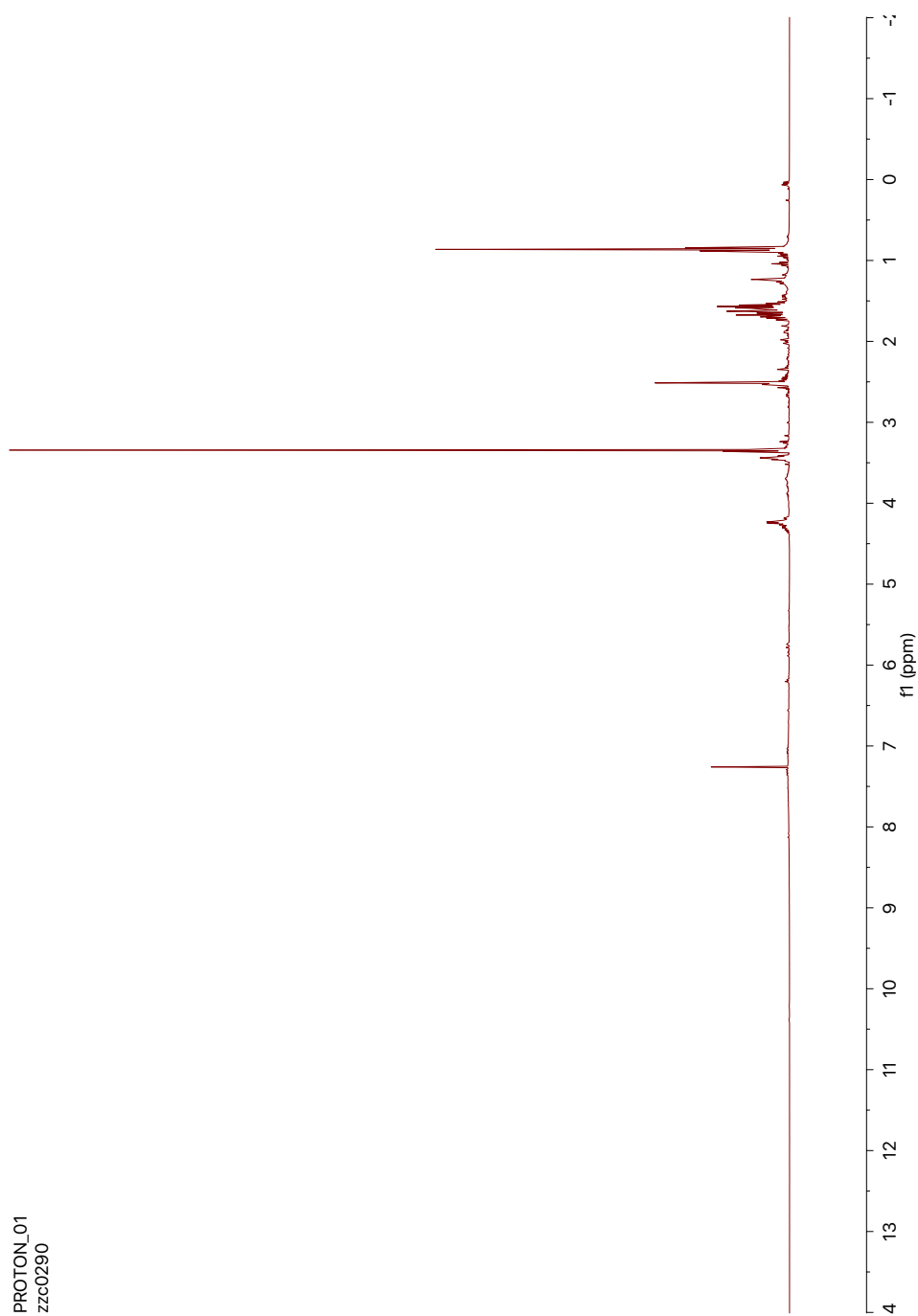
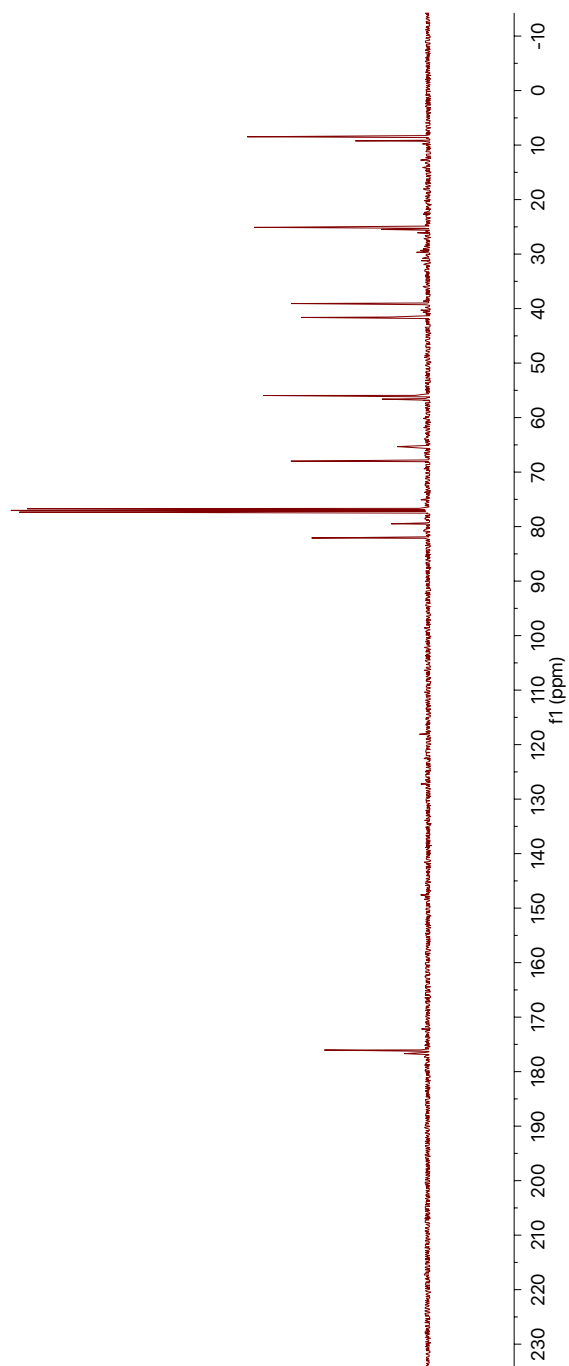


Figure S9AA-E1. ^1H NMR

CARBON_01
zzc0290

Figure S9AA-E2. ^{13}C NMR



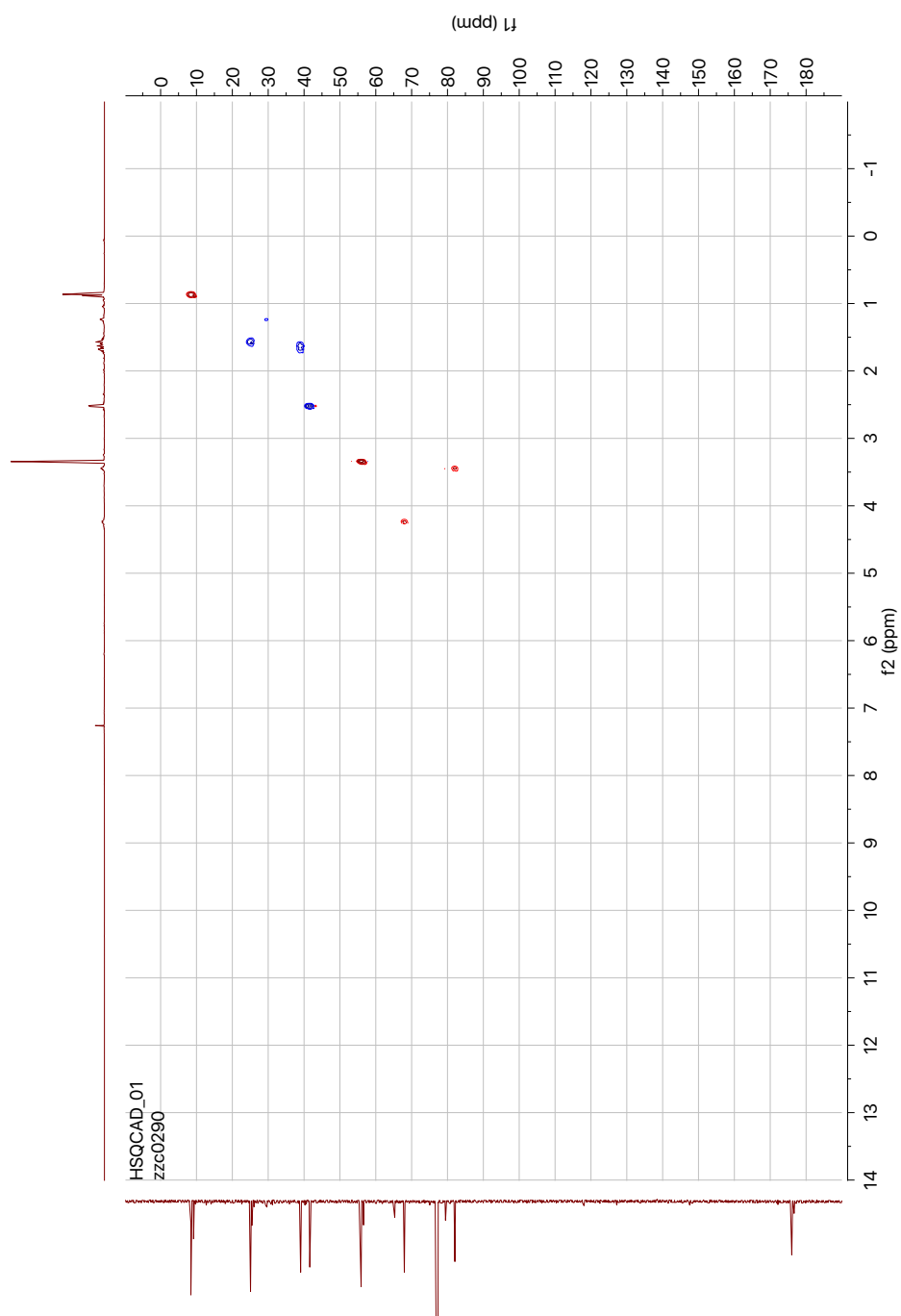
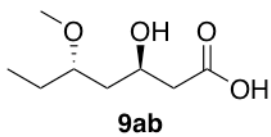


Figure S9AA-E3. ^1H - ^{13}C HSQC



(3*R*,5*S*)-3-hydroxy-5-methoxyheptanoic acid (enzyme)

Chemical Formula: C₈H₁₆O₄

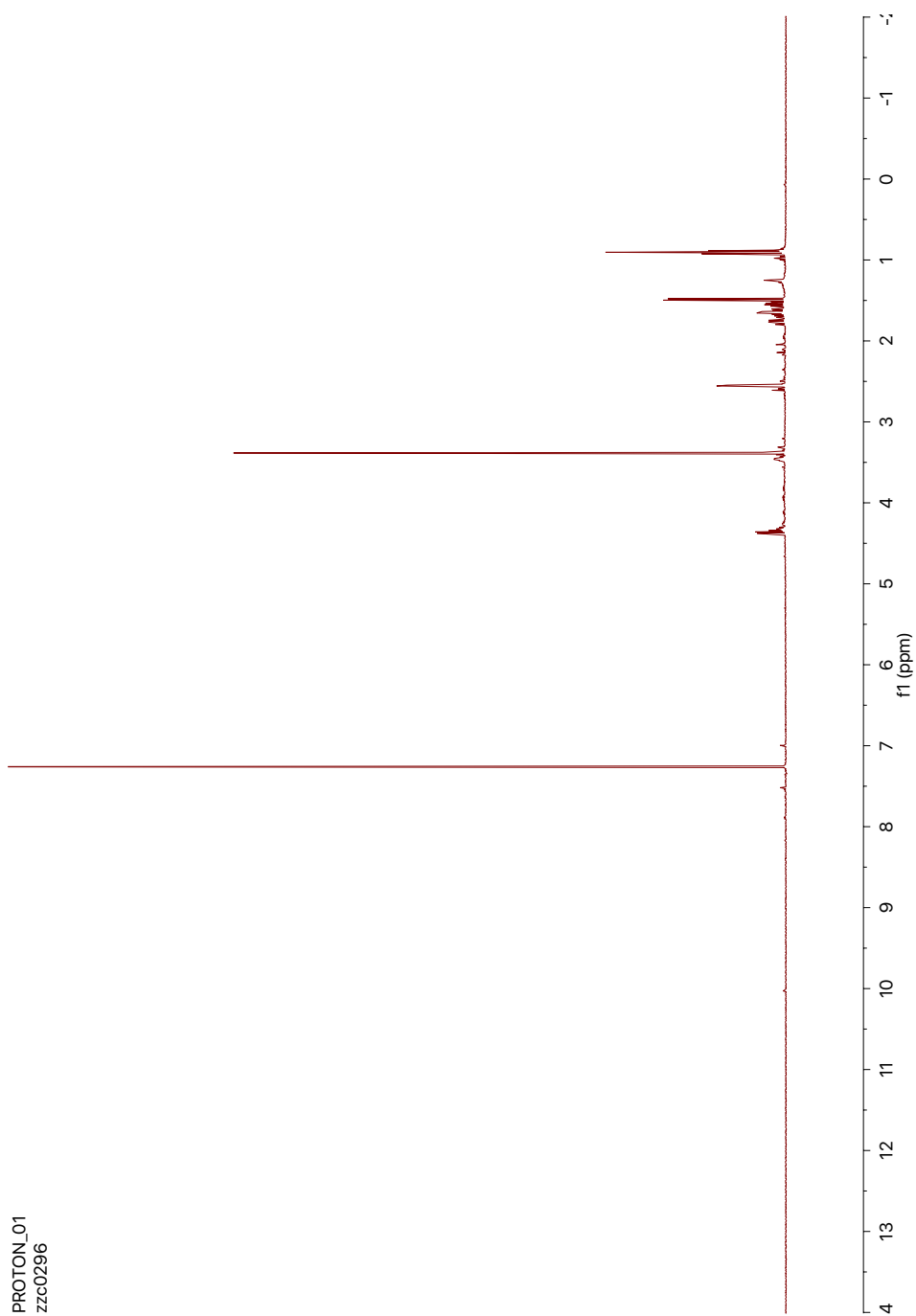


Figure S9AB-E1. ^1H NMR

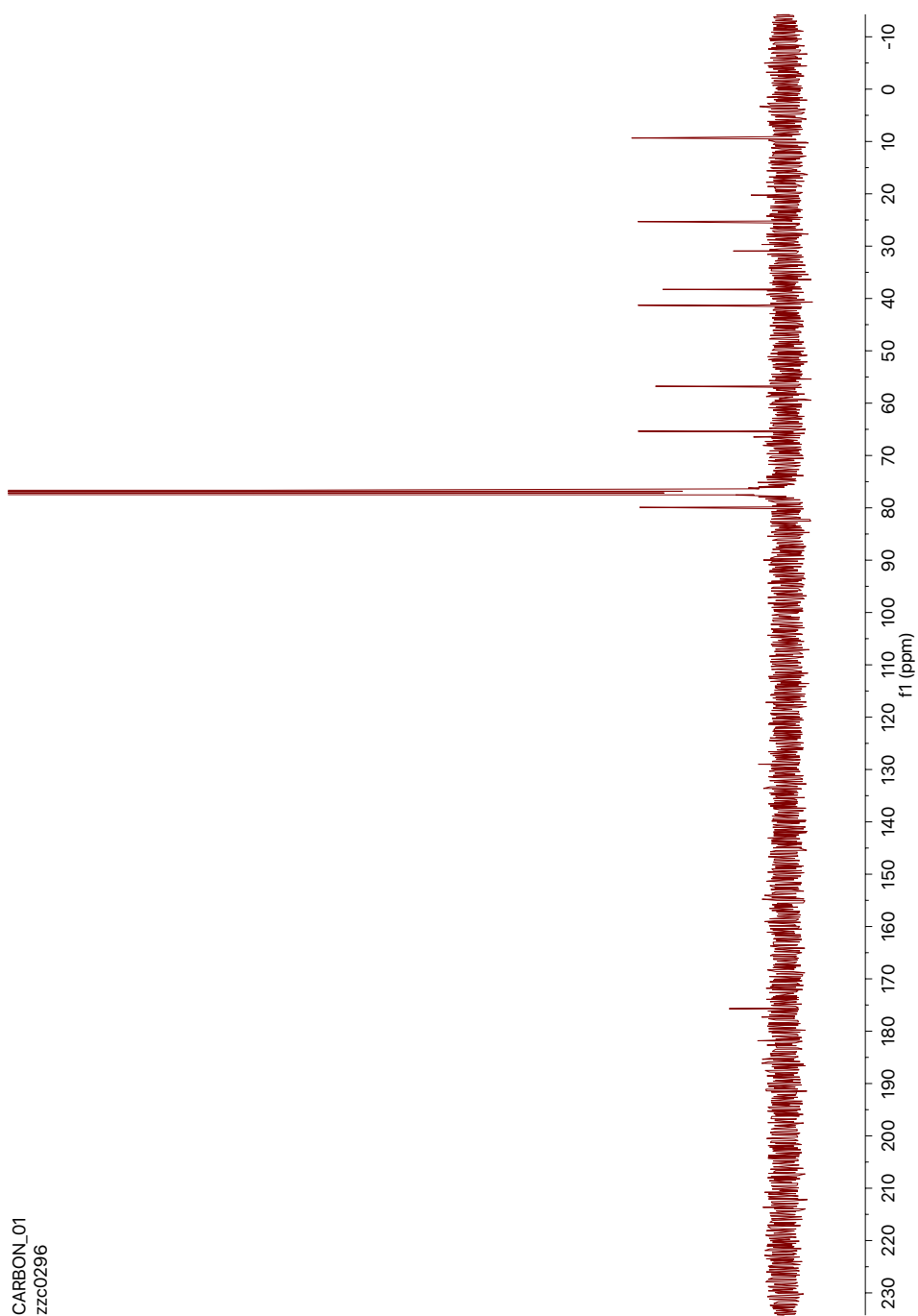


Figure S9AB-E2. ^{13}C NMR

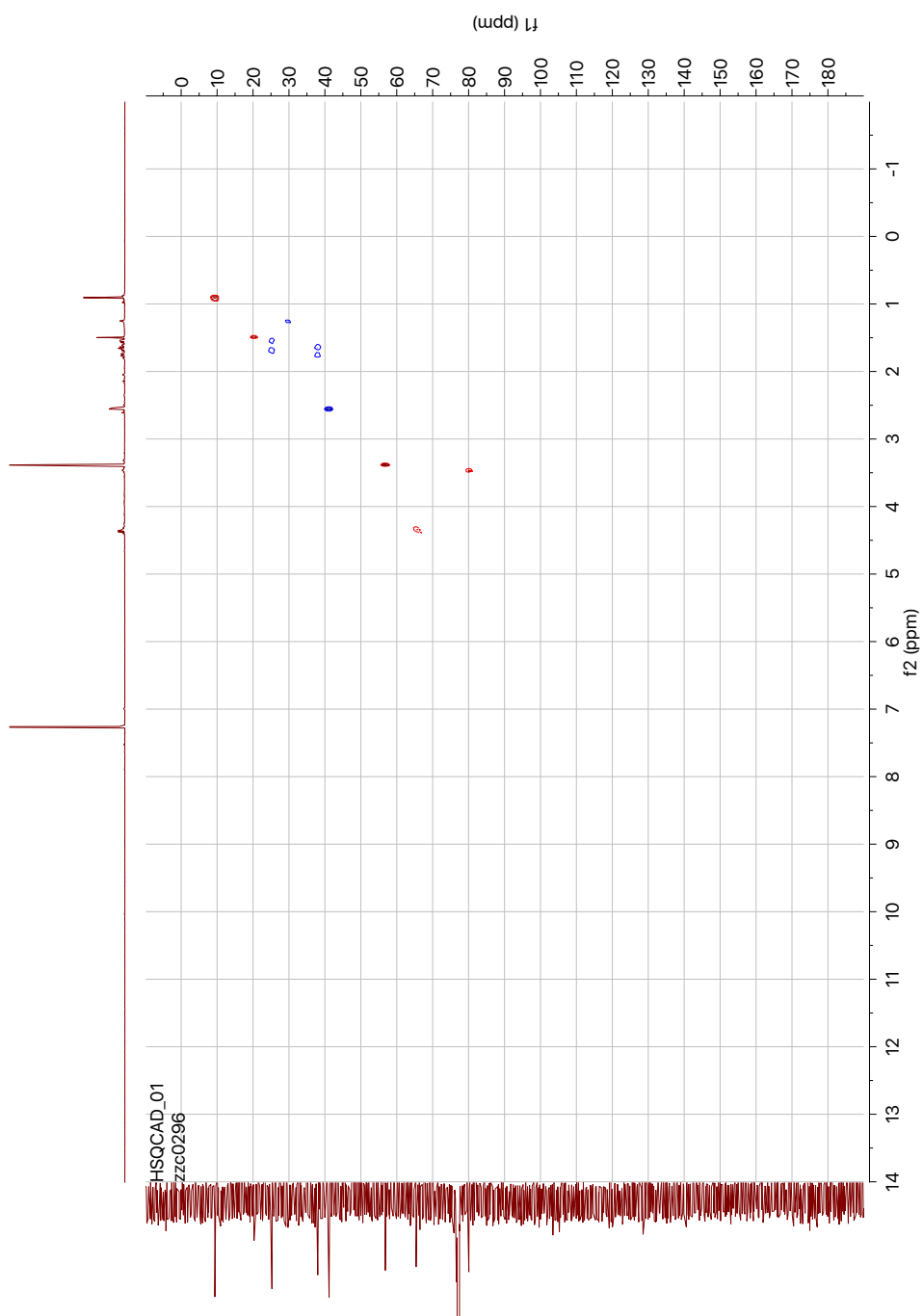
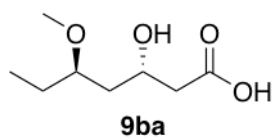


Figure S9AB-E3. ^1H - ^{13}C HSQC



(3*S*,5*R*)-3-hydroxy-5-methoxyheptanoic acid (enzyme)

Chemical Formula: C₈H₁₆O₄

PROTON_01
zzc0290.tyl_myc

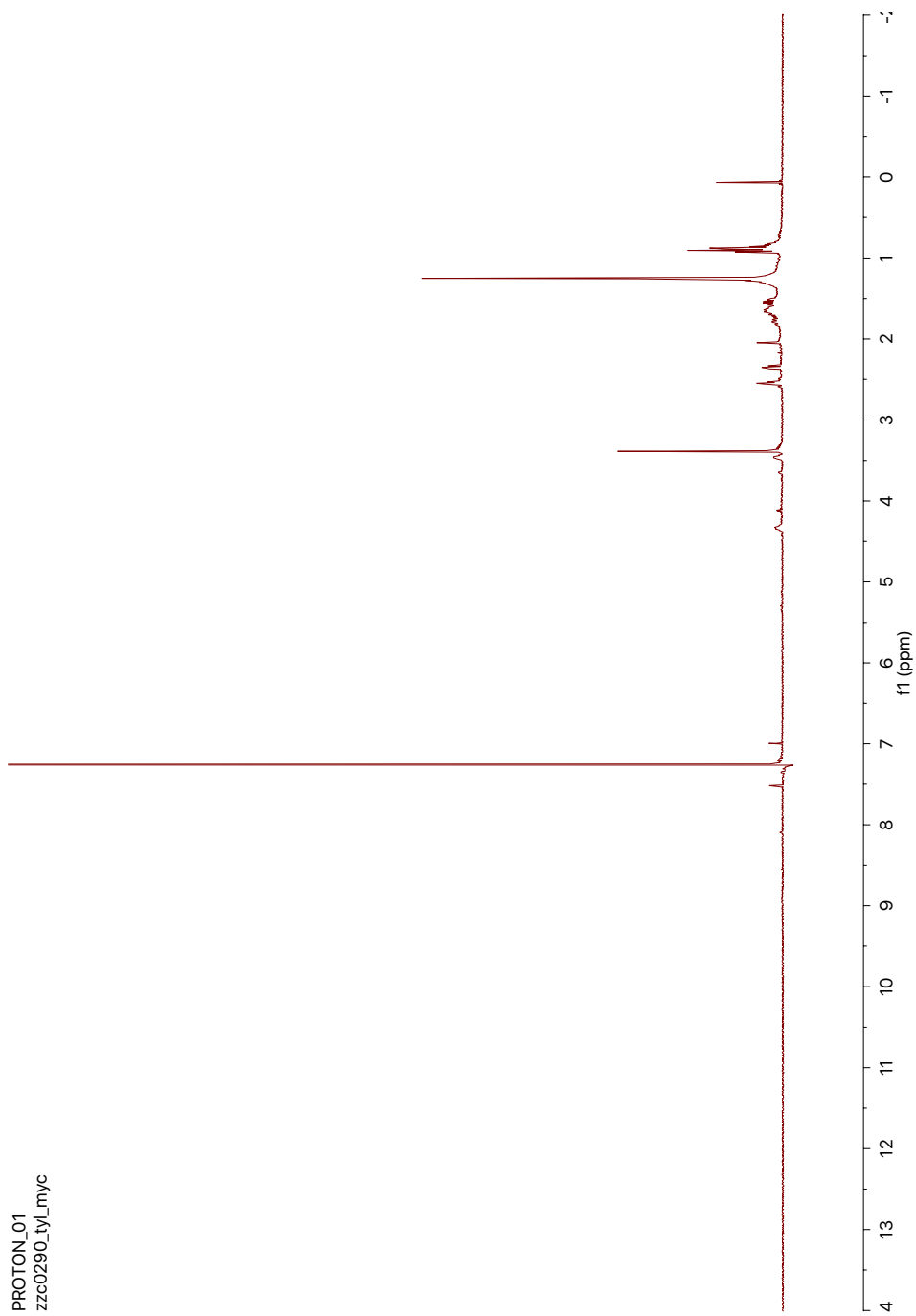


Figure S9BA-E1. ^1H NMR

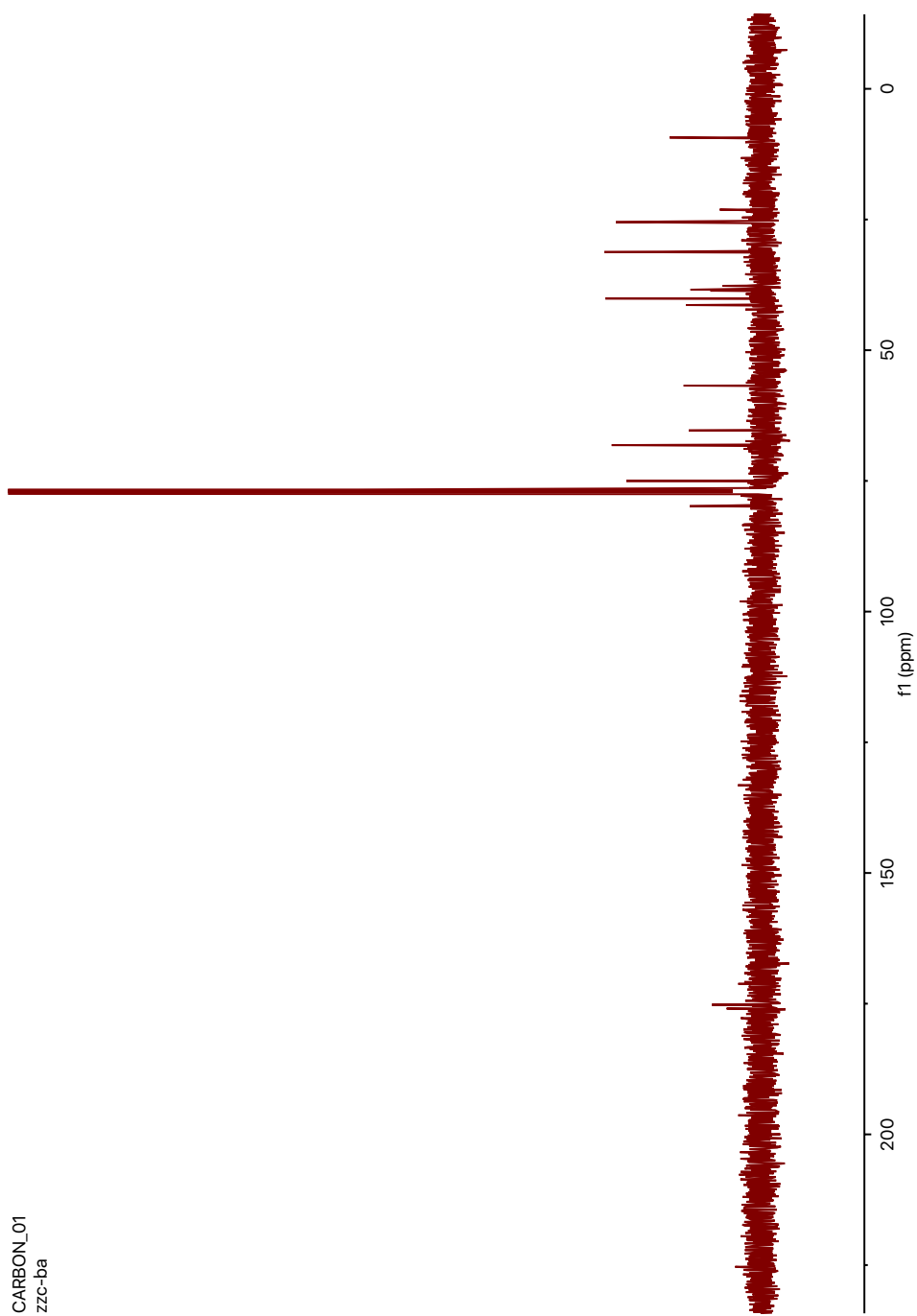


Figure S9BA-E2. ^{13}C NMR

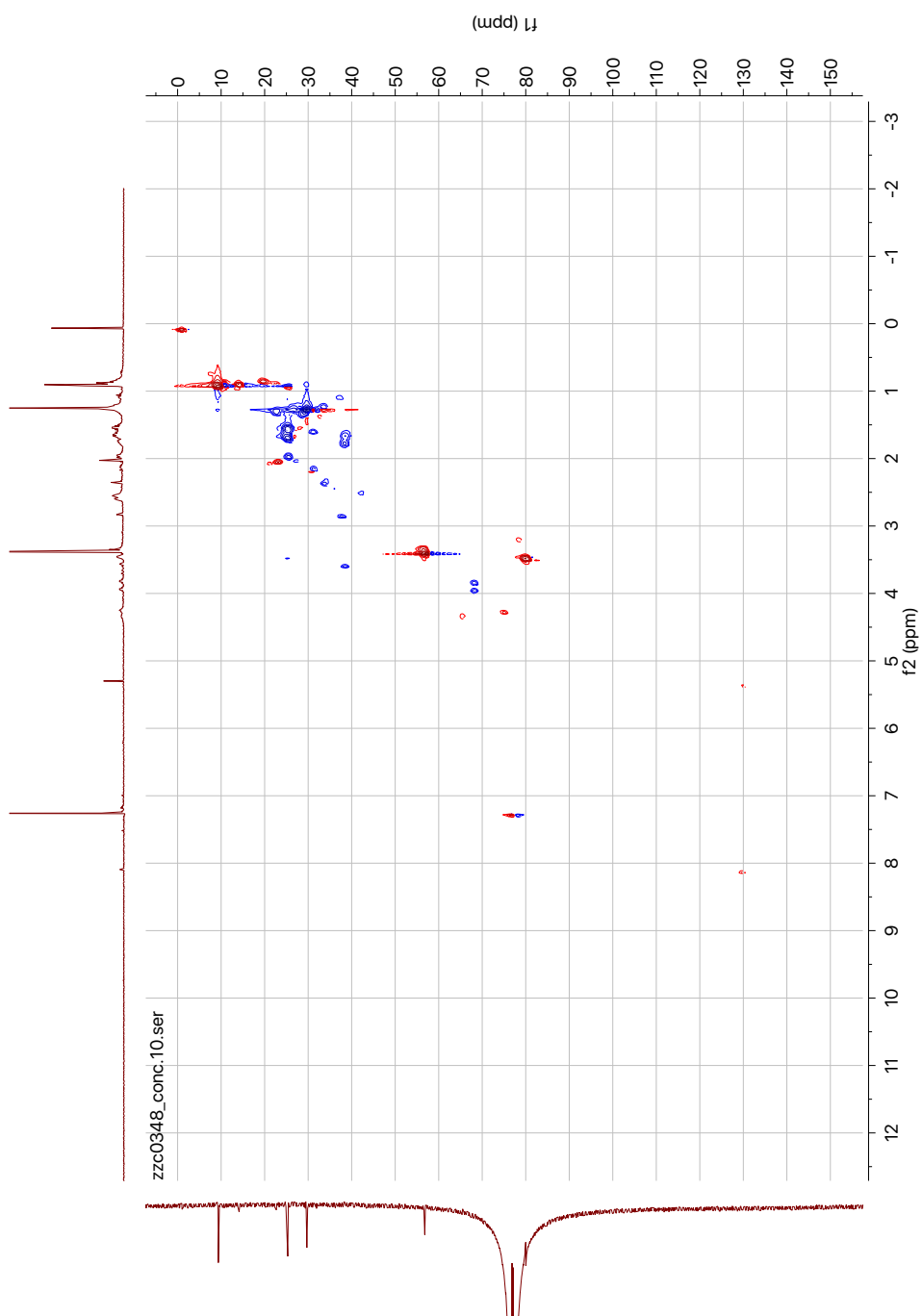
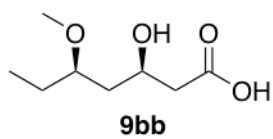


Figure S9BA-E3. ^1H - ^{13}C HSQC



(3*R*,5*R*)-3-hydroxy-5-methoxyheptanoic acid (enzyme)

Chemical Formula: C₈H₁₆O₄

PROTON_01
zzc0308A

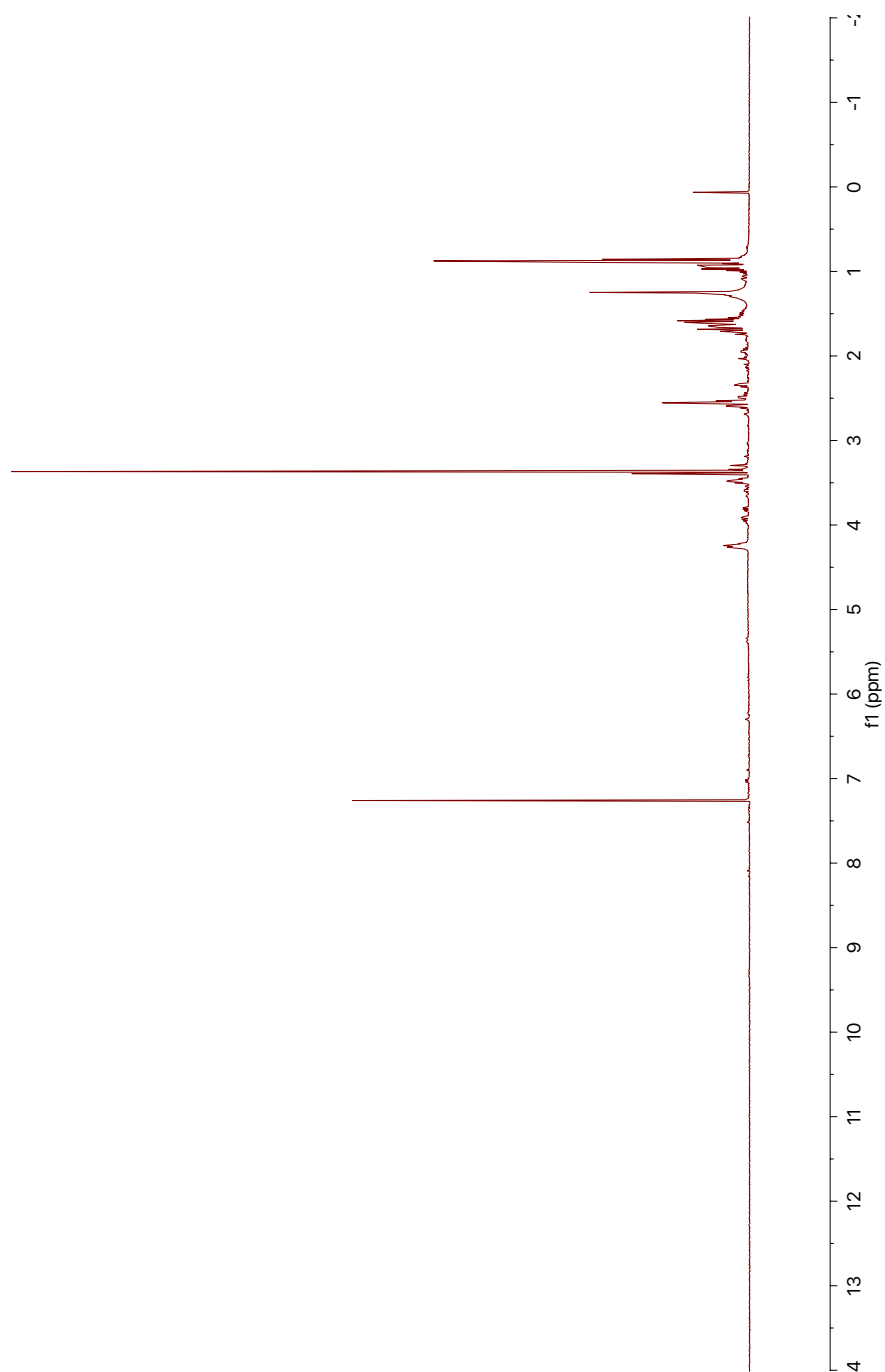


Figure S9BB-E1. ^1H NMR

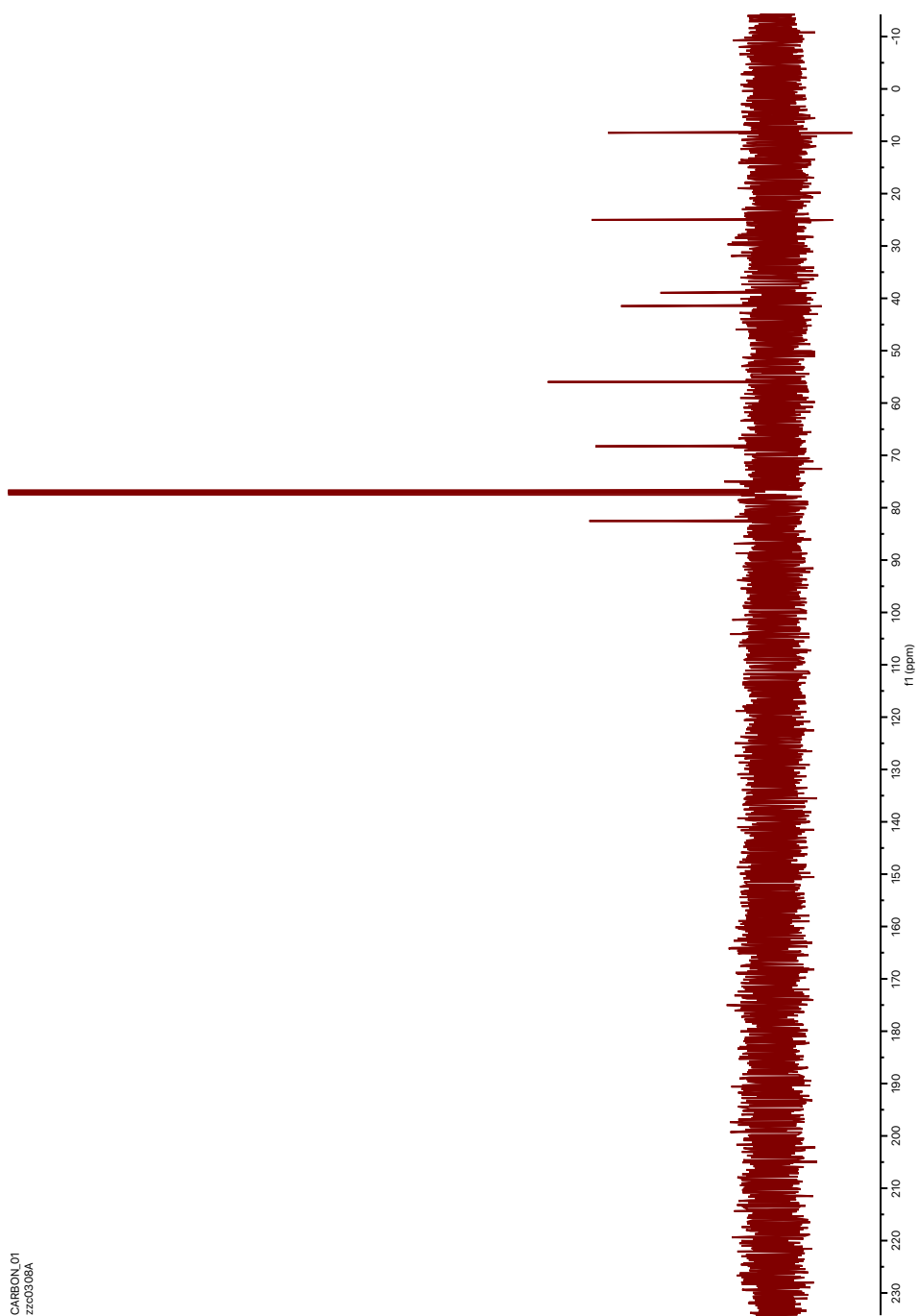


Figure S9BB-E2. ^{13}C NMR

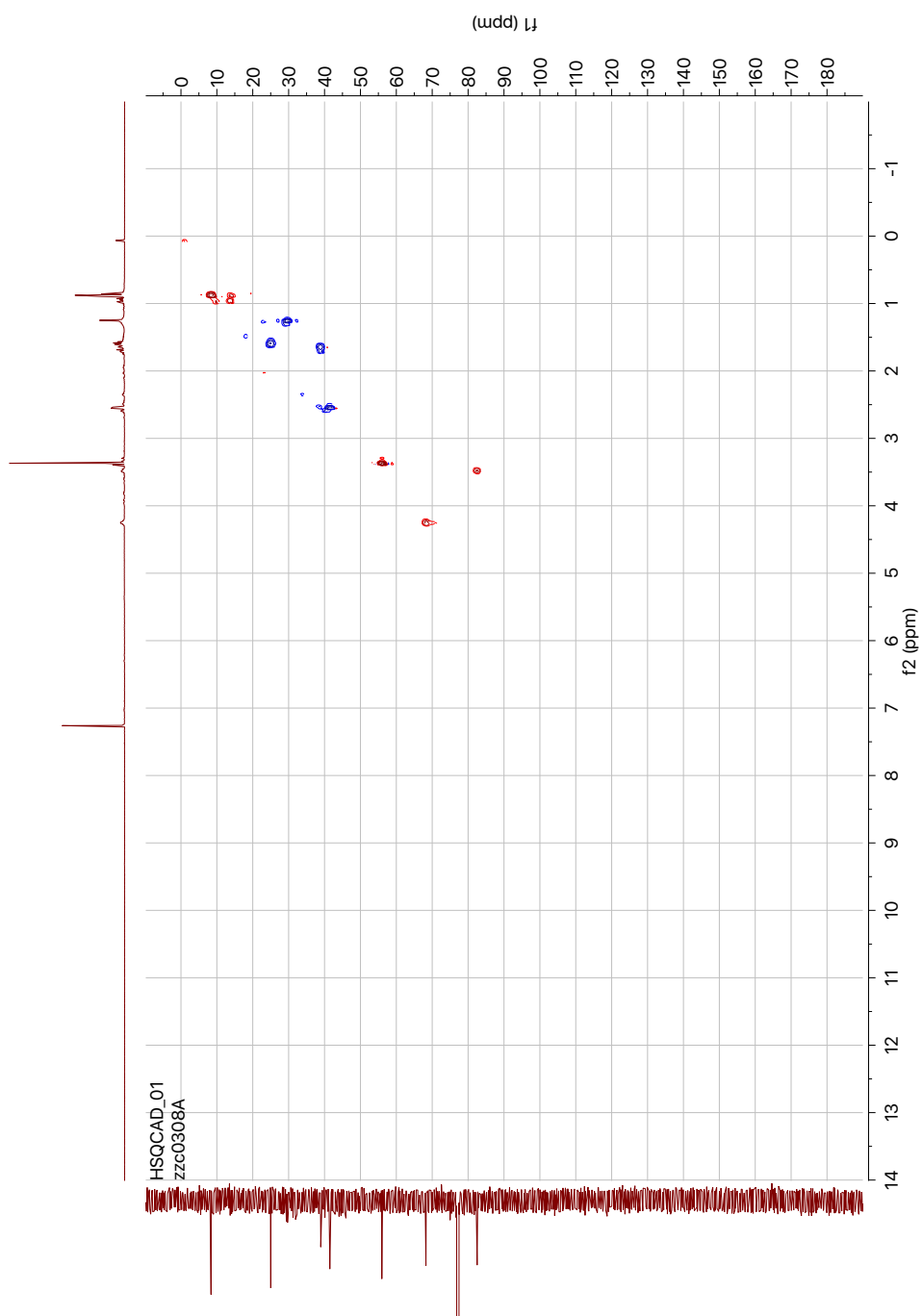


Figure S9BB-E3. ^1H - ^{13}C HSQC

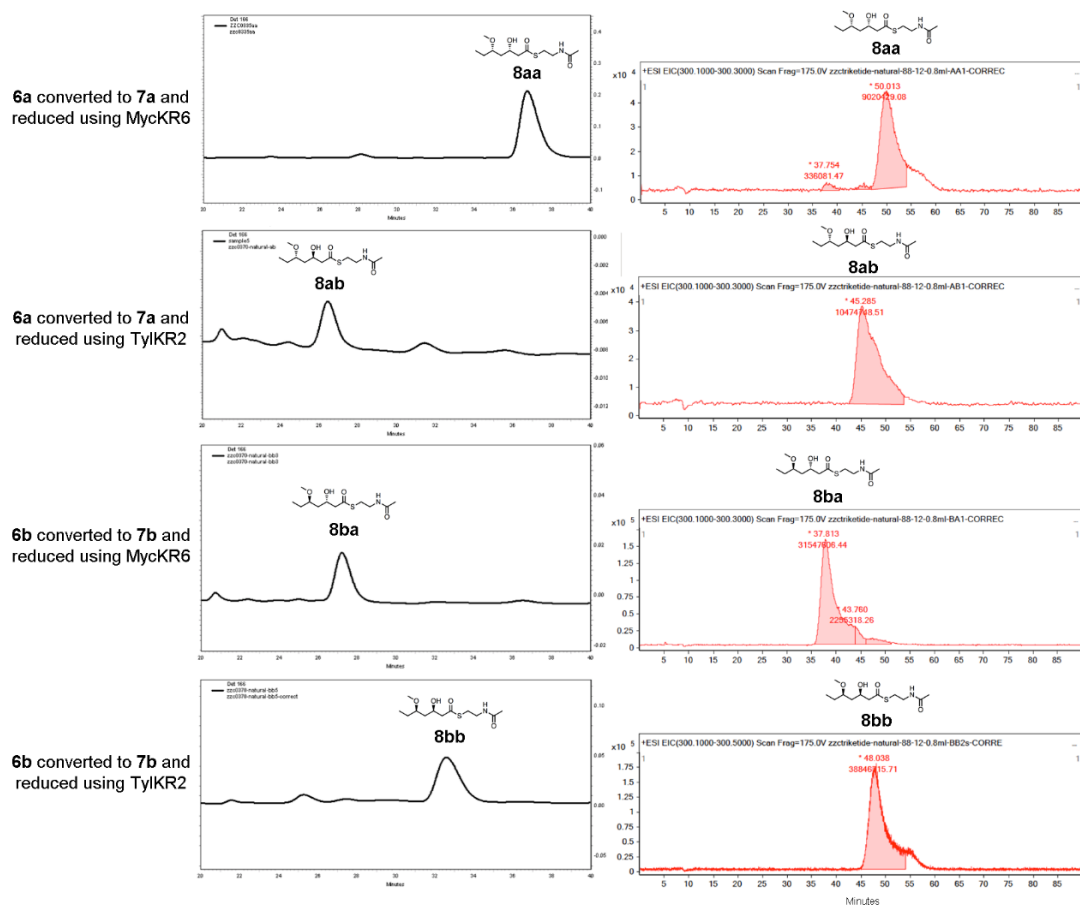
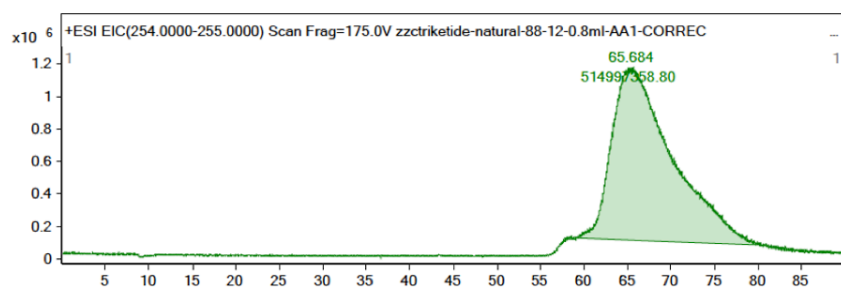
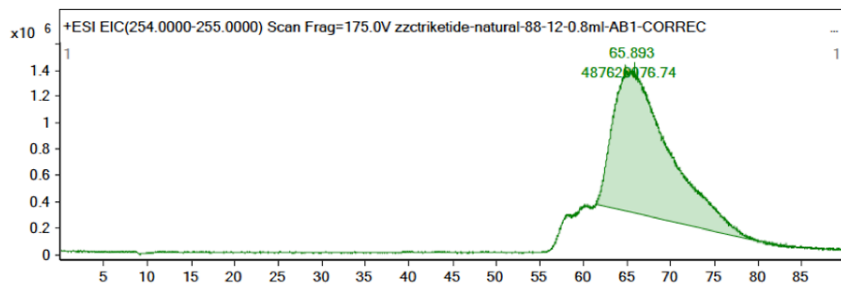


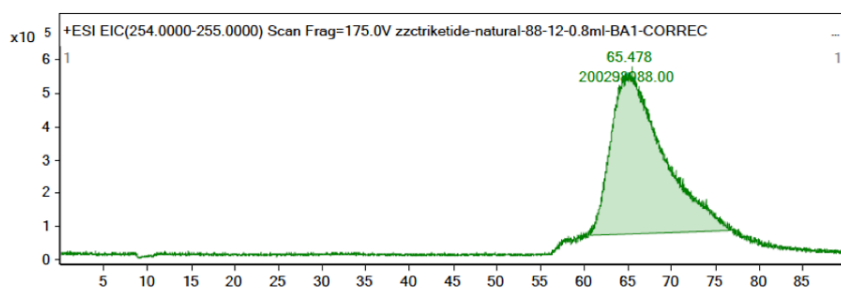
Figure S0-1. Normal phase HPLC-UV and Reverse phase LC/MS analysis of actual enzymatic reaction of triketide



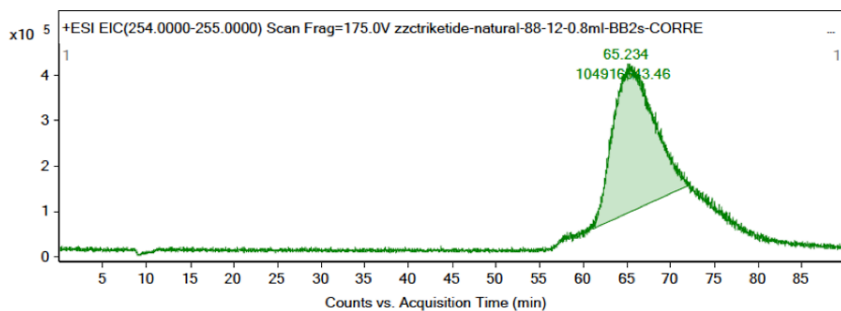
analysis of **8aa** product
using KR catalyst



analysis of **8ab** product
using KR catalyst

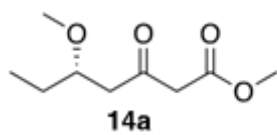


analysis of **8ba** product
using KR catalyst



analysis of **8bb** product
using KR catalyst

Figure S0-2. Normal phase HPLC-UV and Reverse phase LC/MS analysis for internal chemical standards **11**.



methyl (*S*)-5-methoxy-3-oxoheptanoate

Chemical Formula: C₉H₁₆O₄

zxc0400.10.fid

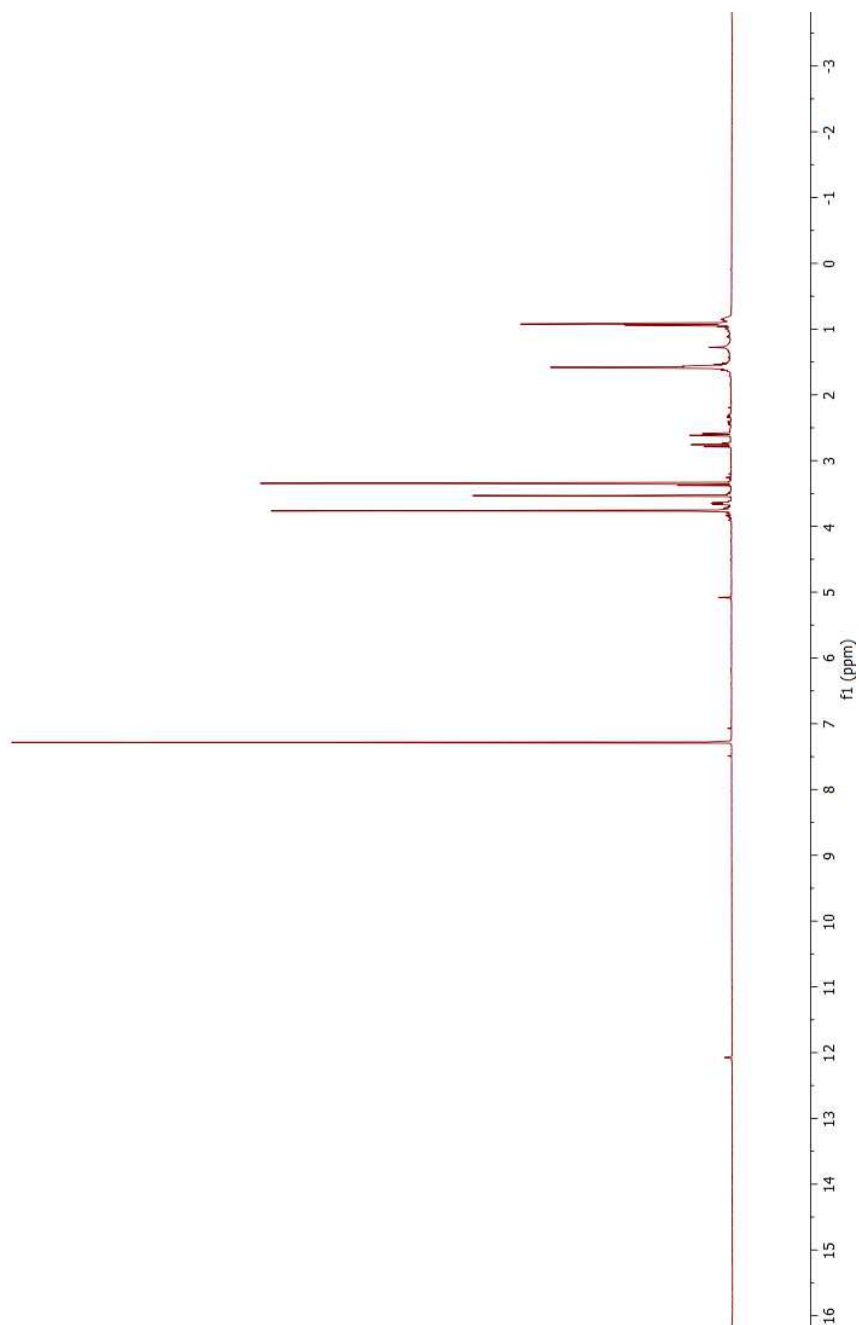


Figure S14A-1. ^1H NMR

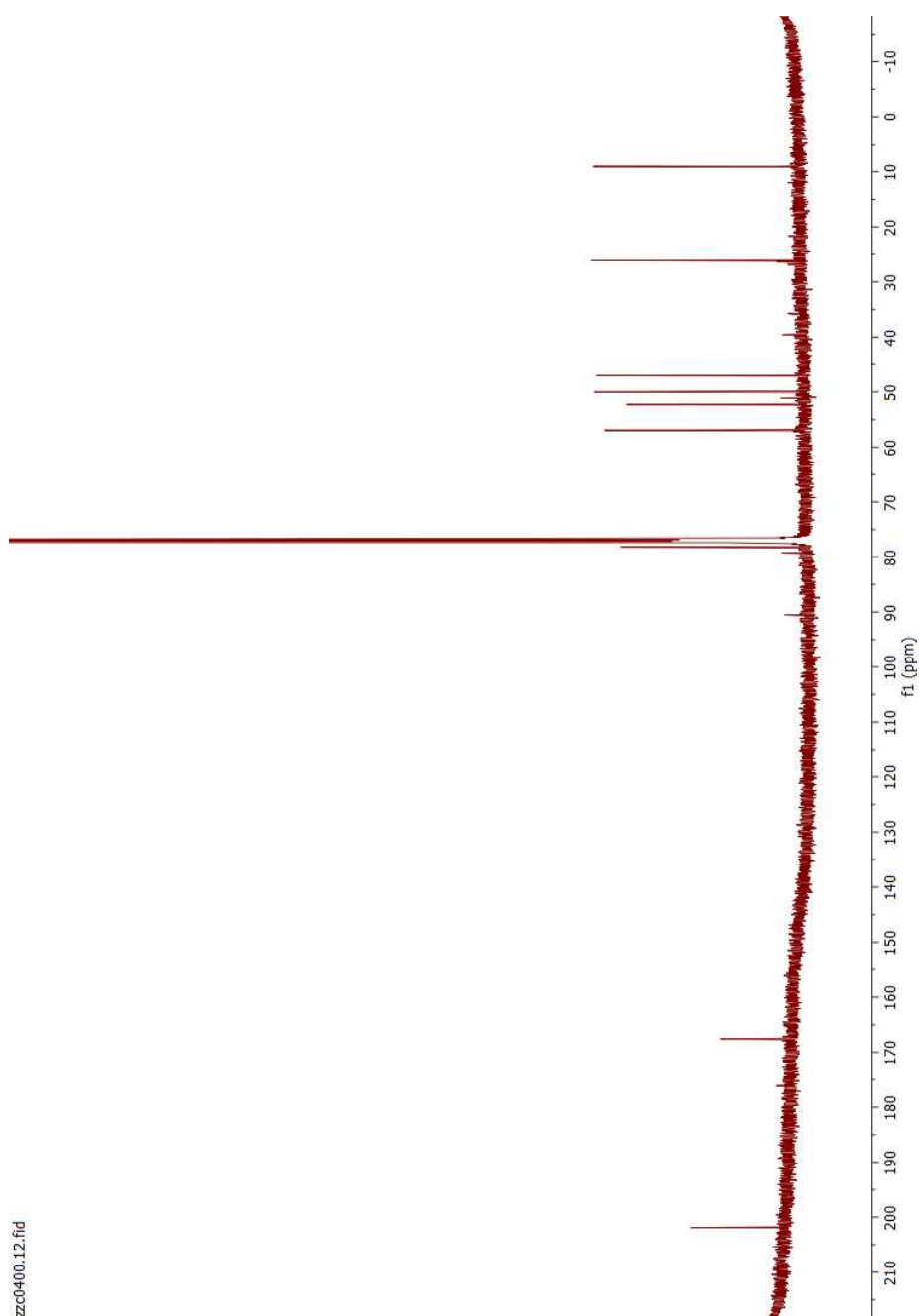


Figure S14A-2. ^{13}C NMR

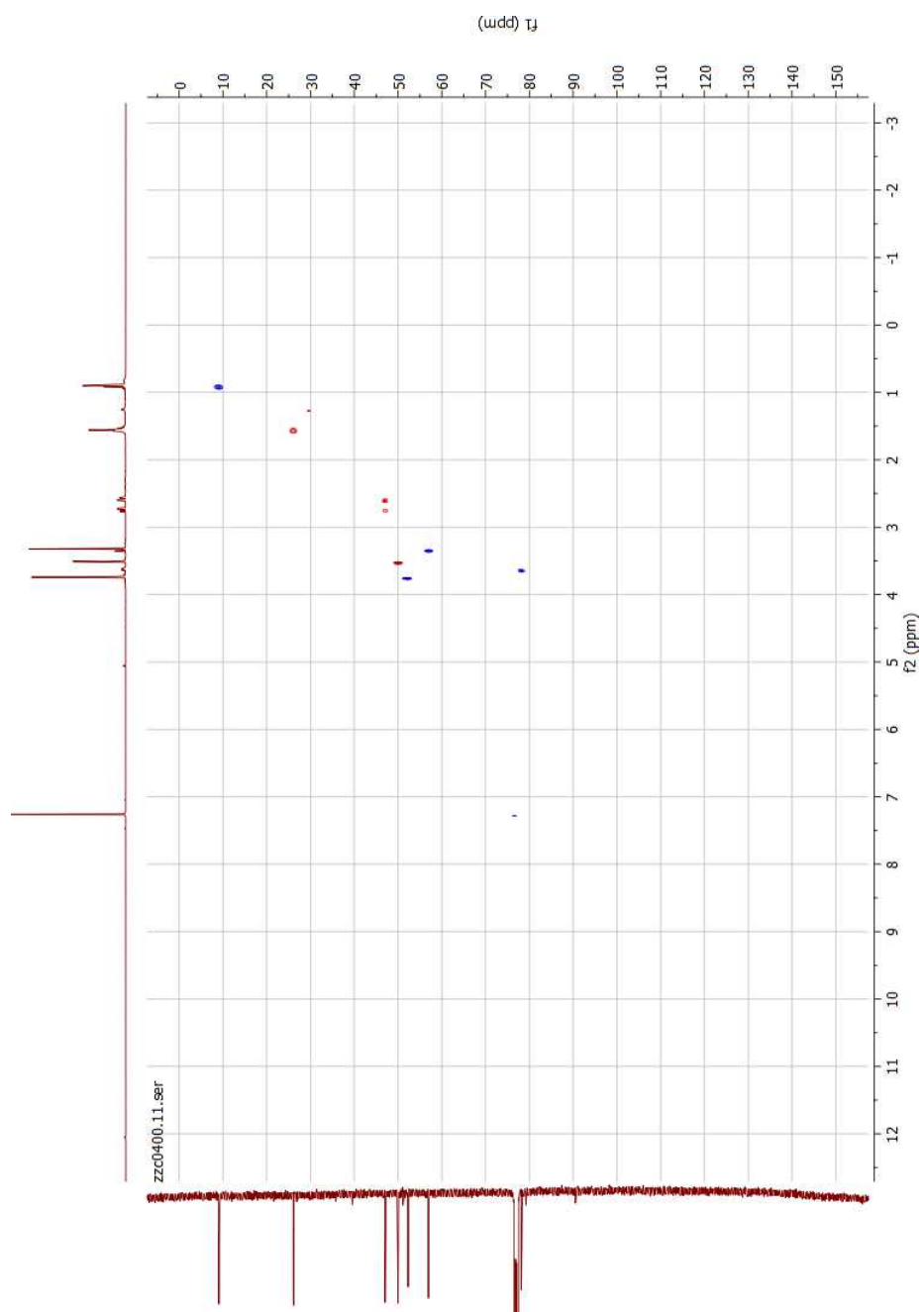
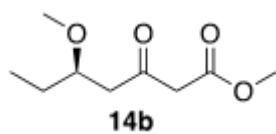


Figure S14A-3. ^1H - ^{13}C HSQC



methyl (*R*)-5-methoxy-3-oxoheptanoate

Chemical Formula: C₉H₁₆O₄

zzc0413.10.fid

zco0413.13.fid

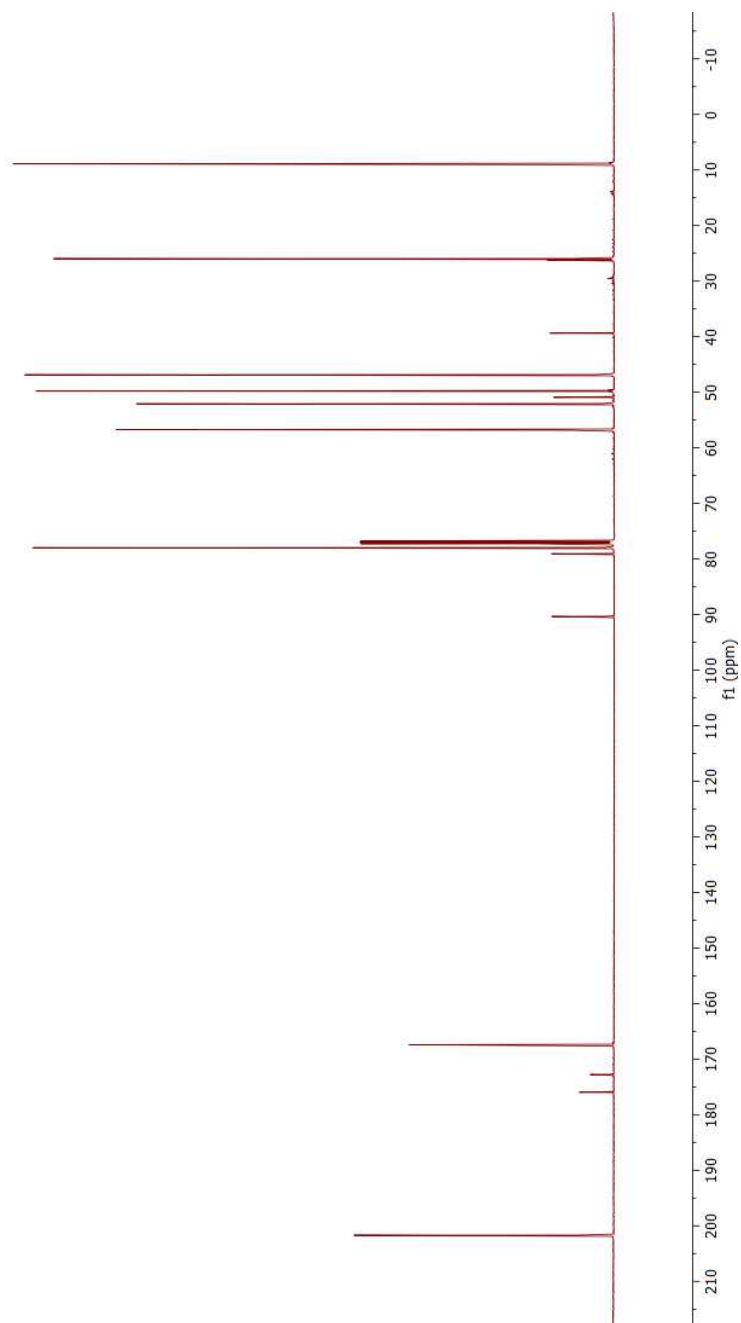


Figure S14B-2. ^{13}C NMR

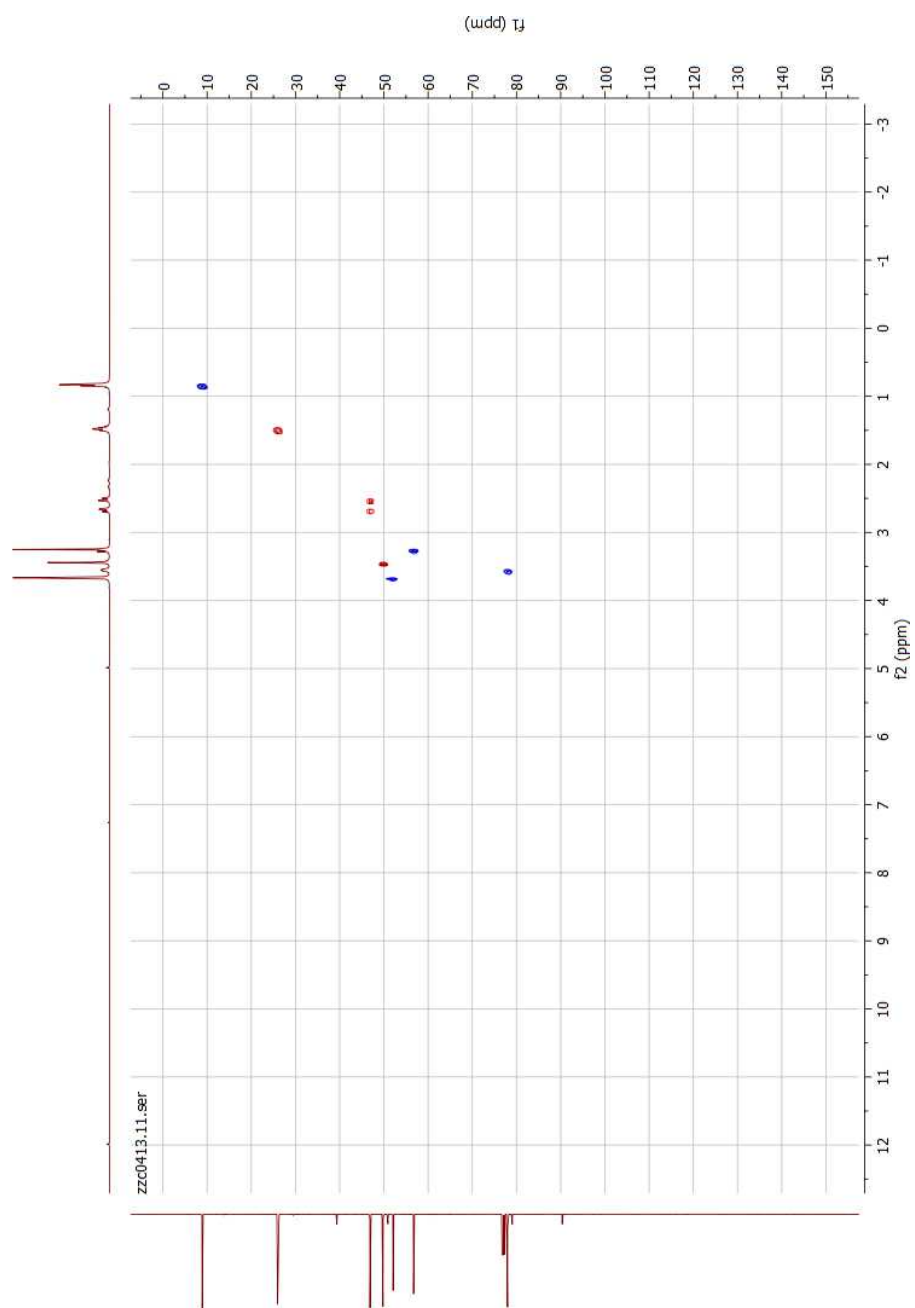
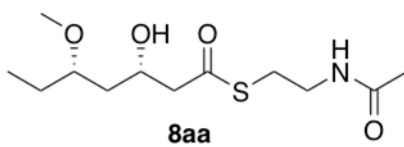


Figure S14B-3. ^1H - ^{13}C HSQC



S-(2-acetamidoethyl) (3*S*,5*S*)-3-hydroxy-5-methoxyheptanethioate (chemical)

Chemical Formula: C₁₂H₂₃NO₄S

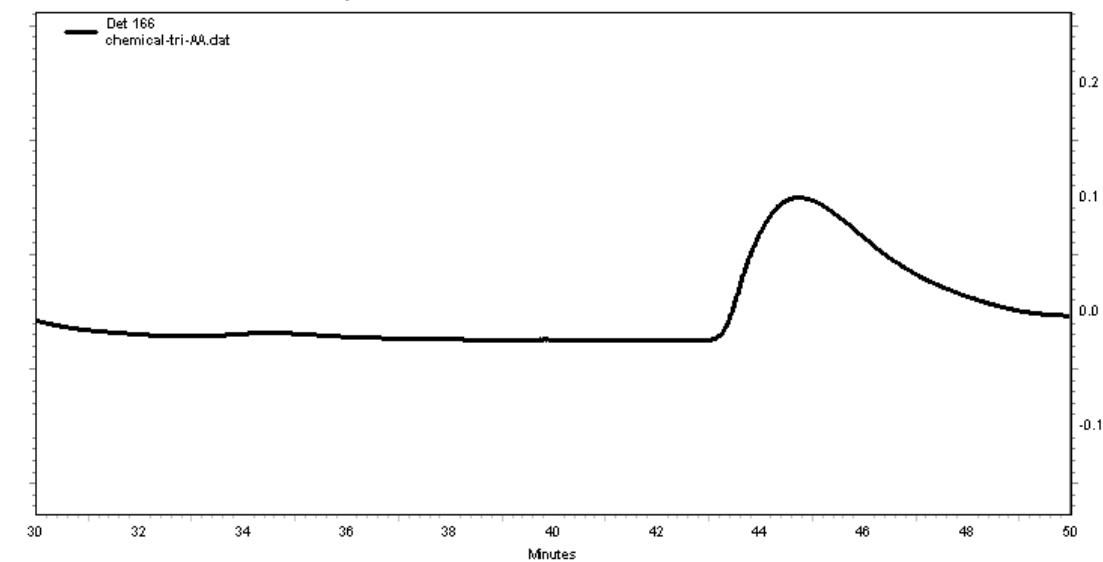
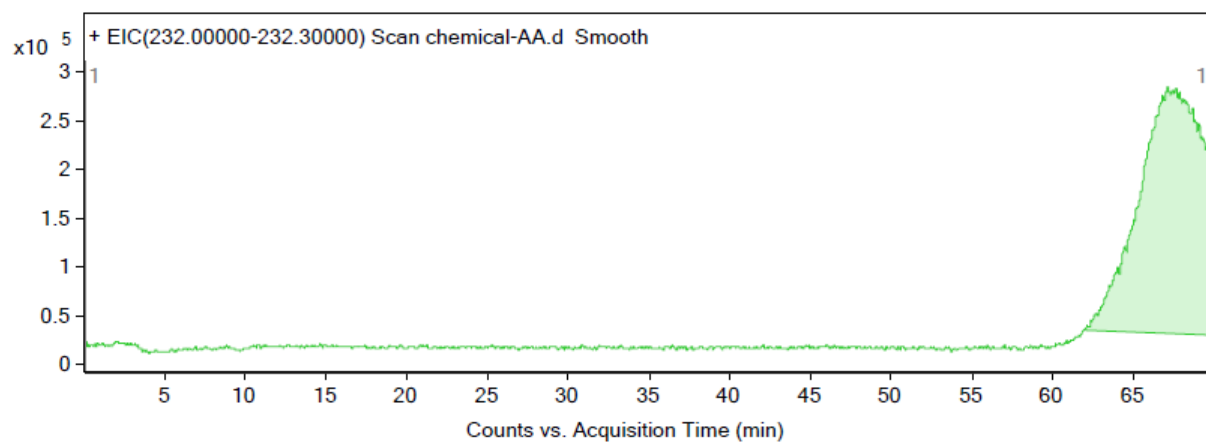


Figure S8AA-C1. HPLC Retention time: 44.8 min

internal standard



target species

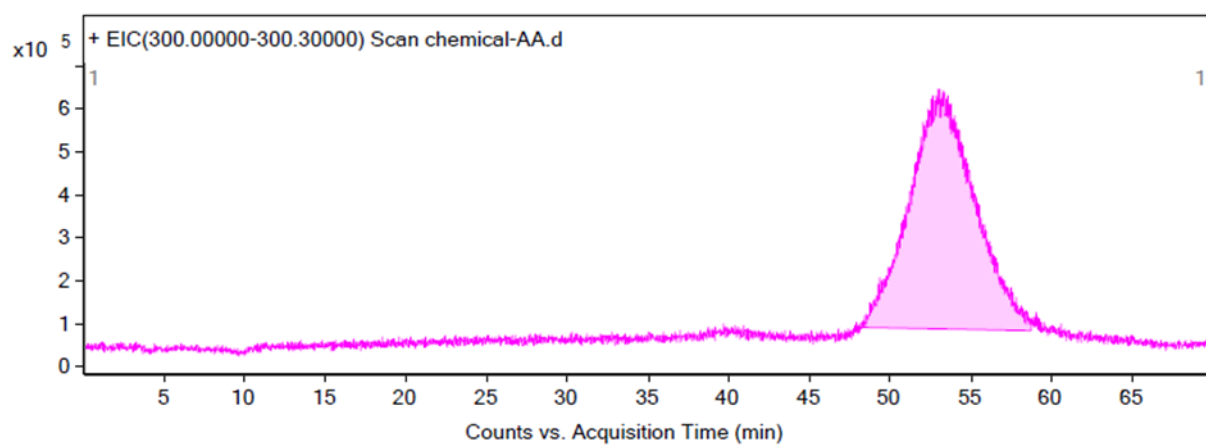
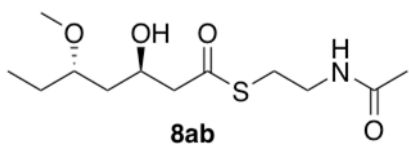


Figure S8AA-C2. LC/MS Retention time: 53.012 min/target, 67.159 min/standard



S-(2-acetamidoethyl) (3*R*,5*S*)-3-hydroxy-5-methoxyheptanethioate (chemical)

Chemical Formula: C₁₂H₂₃NO₄S

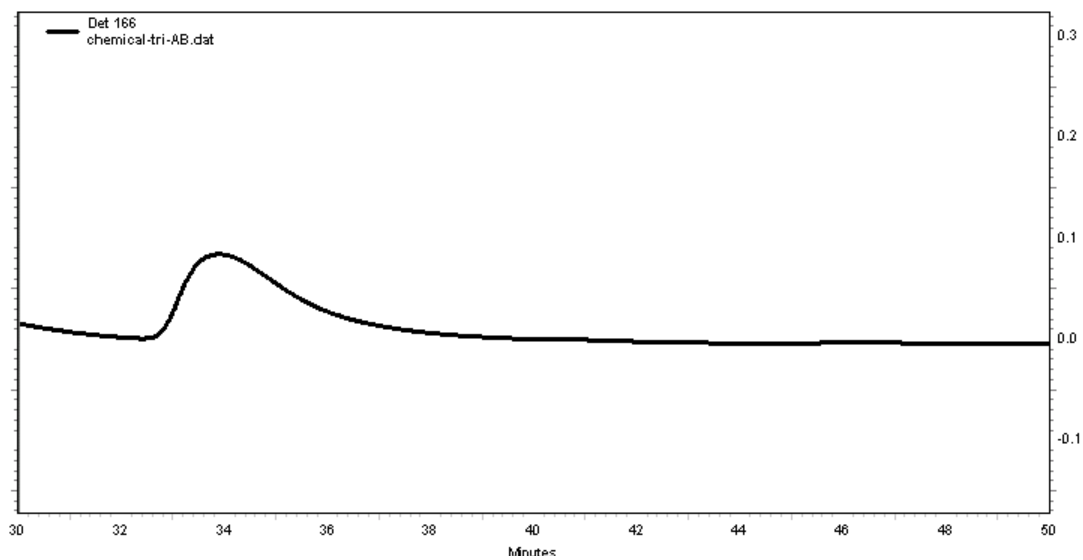
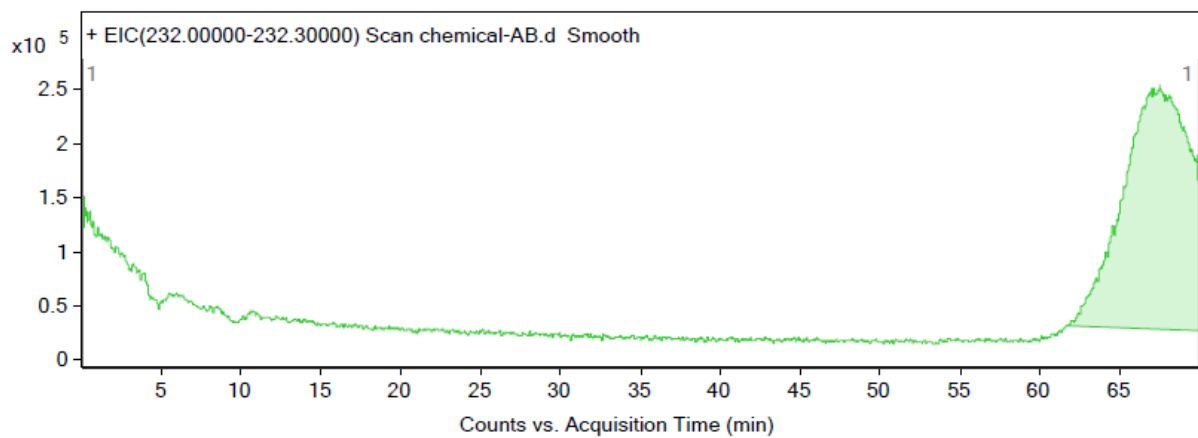


Figure S8AB-C1. HPLC Retention time: 34.0 min

internal standard



target species

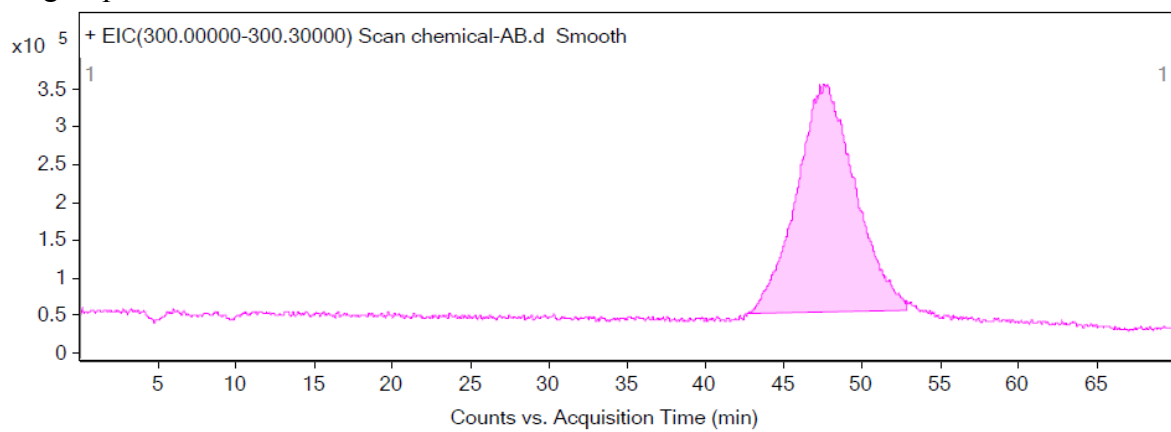
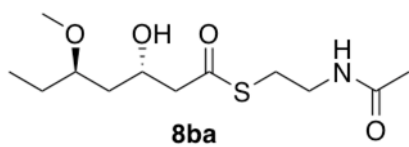


Figure S8AB-C2. LC/MS Retention time: 47.806 min/target, 67.52 min/standard



S-(2-acetamidoethyl) (3*S*,5*R*)-3-hydroxy-5-methoxyheptanethioate (chemical)

Chemical Formula: C₁₂H₂₃NO₄S

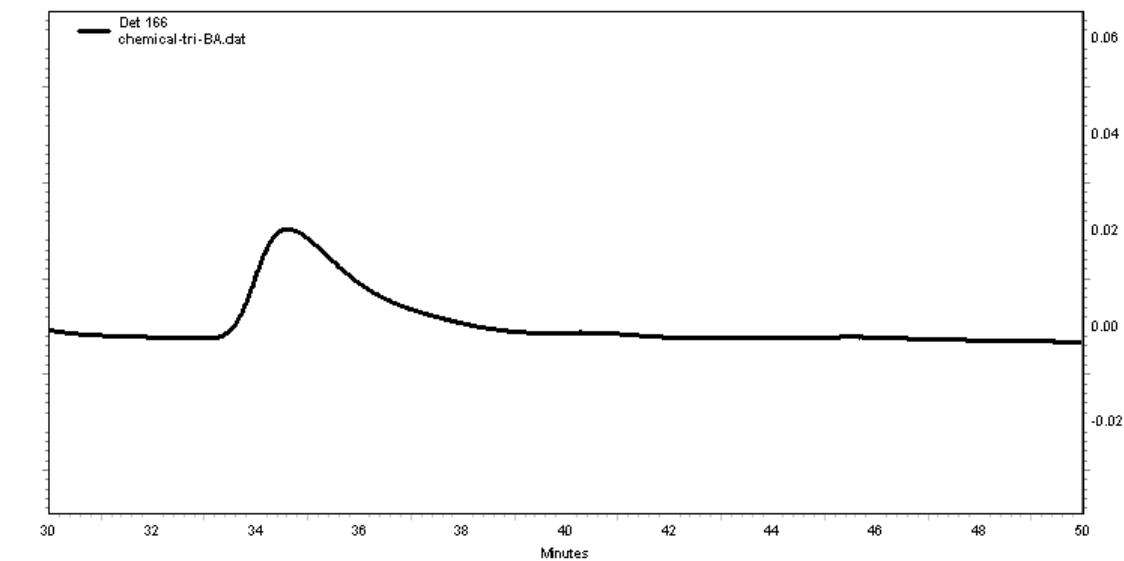
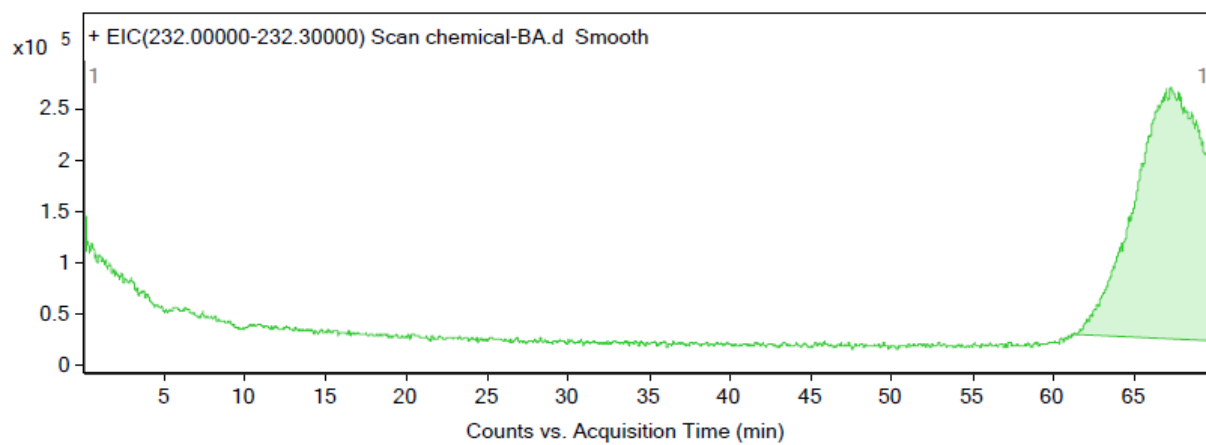


Figure S8BA-C1. HPLC Retention time: 34.6 min

internal standard



target species

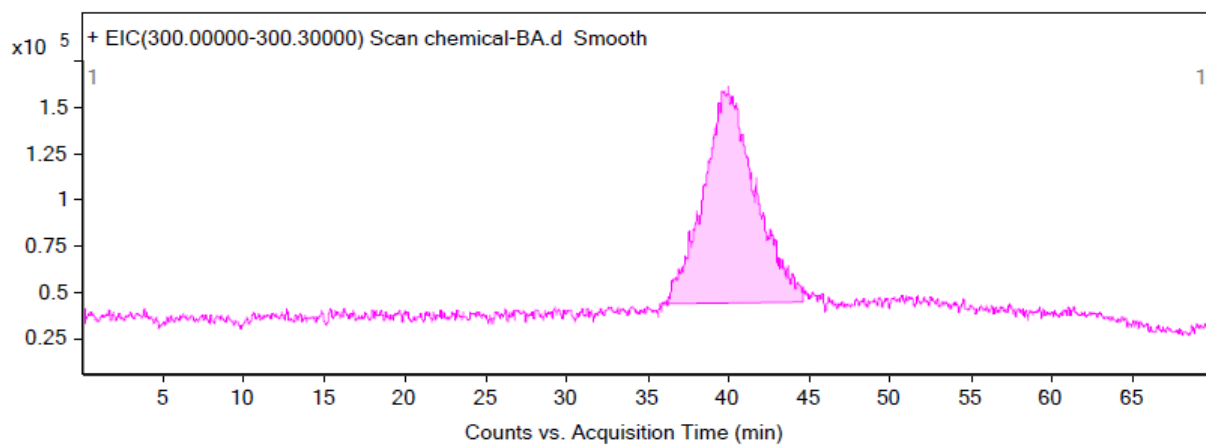
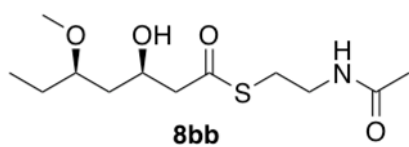


Figure S8BA-C2. LC/MS Retention time: 39.968 min/target, 67.26 min/standard



S-(2-acetamidoethyl) (3*R*,5*R*)-3-hydroxy-5-methoxyheptanethioate (chemical)

Chemical Formula: C₁₂H₂₃NO₄S

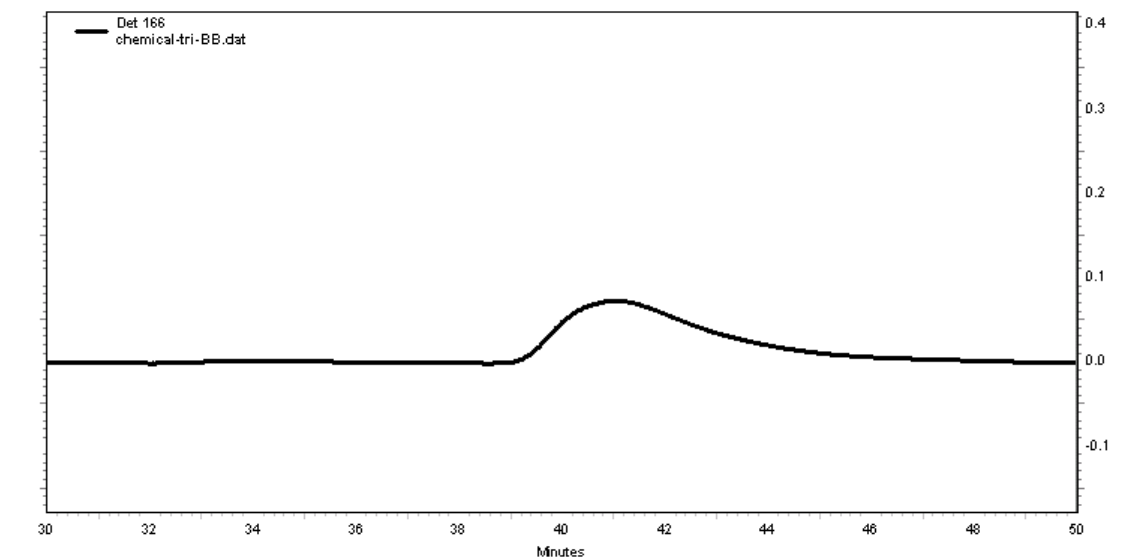
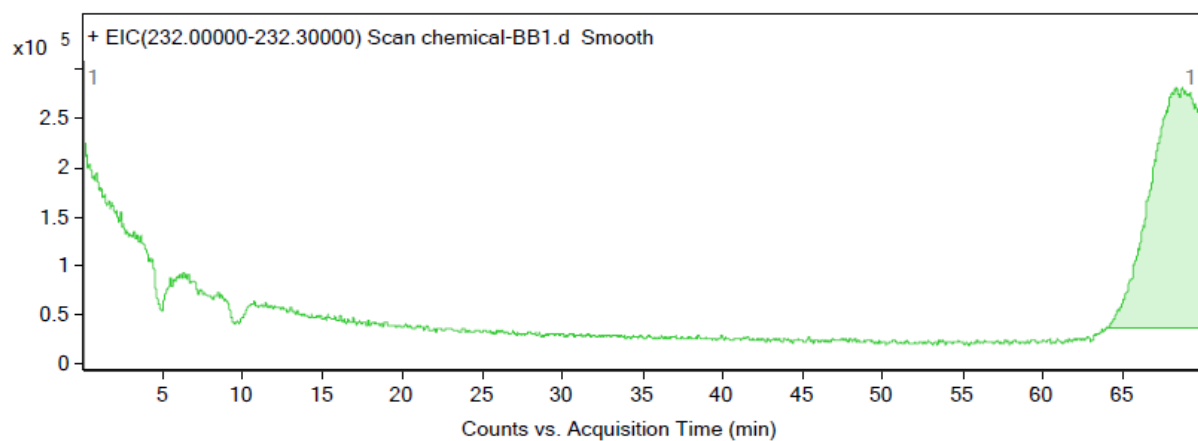


Figure S8BB-C1. HPLC Retention time: 41.2 min

internal standard



target species

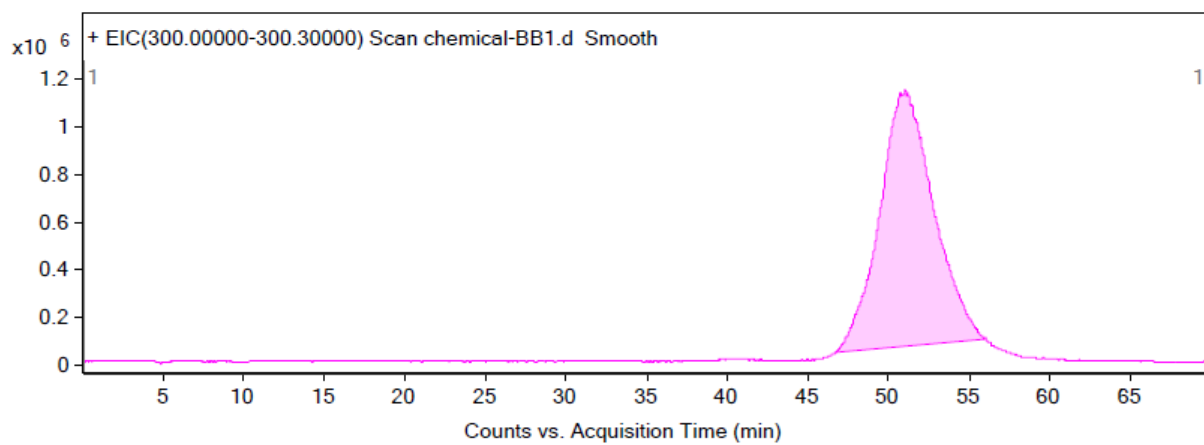
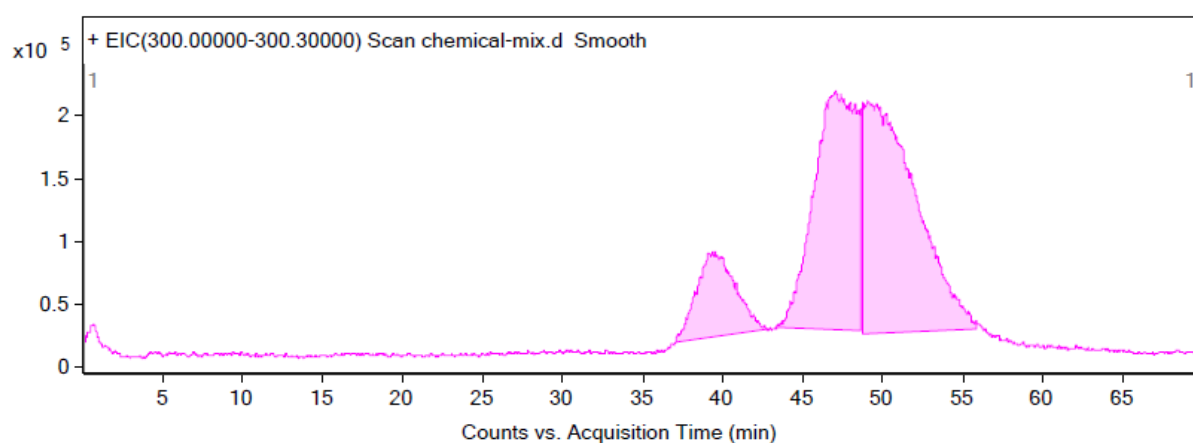


Figure S8BB-C2. LC/MS Retention time: 51.029 min/target, 68.77 min/standard

	Enzymatic	Synthesis
8aa	-15.7 min	-14.1 min
8ab	-20.6 min	-19.7 min
8ba	-27.7 min	-27.3 min
8bb	-17.2 min	-17.7 min

Table S1. LCMS Corrected Retention Time (In comparison to Internal Standard **11**)

1



2

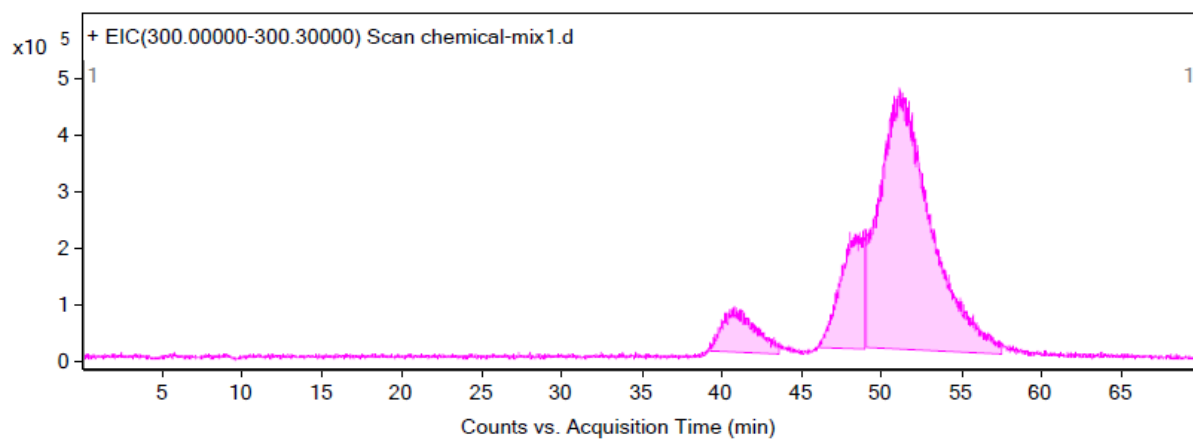


Figure S0-3. All Four Isomers Mixture: **8ba**, **8ab**, **8aa/8bb** on LC/MS

	Enzymatic	Synthesis
8aa	10.4 min	10.8 min
8ab	0.0 min	0.0 min
8ba	0.6 min	0.6 min
8bb	6.0 min	5.6 min

Table S2. HPLC Corrected Retention Time (In comparison to **8ab**)

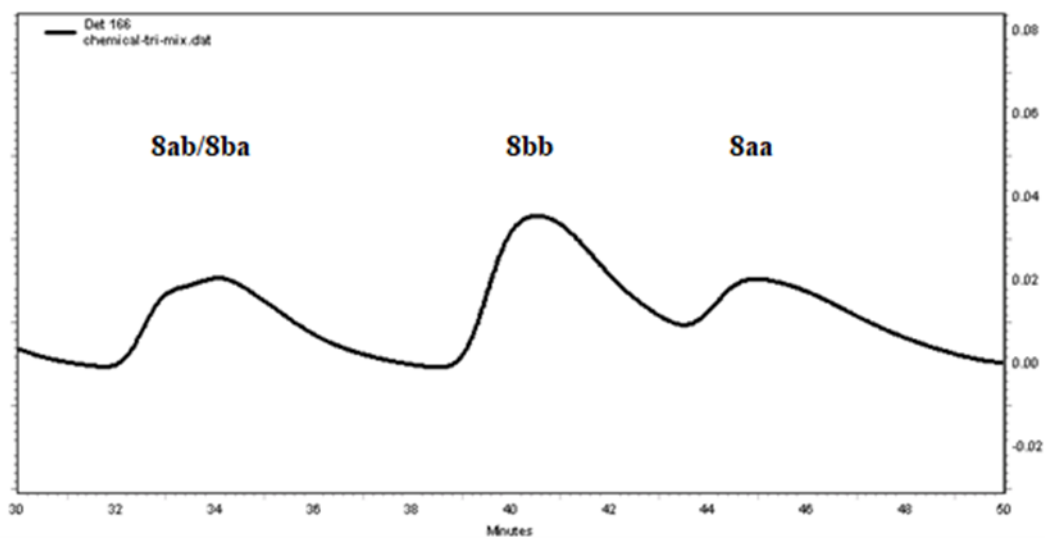
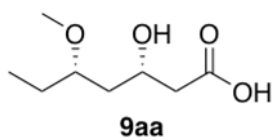


Figure S0-4. All Four Isomers Mixture: **8ab/8ba**, **8bb**, **8aa** on LC/MS



(3*S*,5*S*)-3-hydroxy-5-methoxyheptanoic acid

Chemical Formula: C₈H₁₆O₄

zco0414a_10.fid

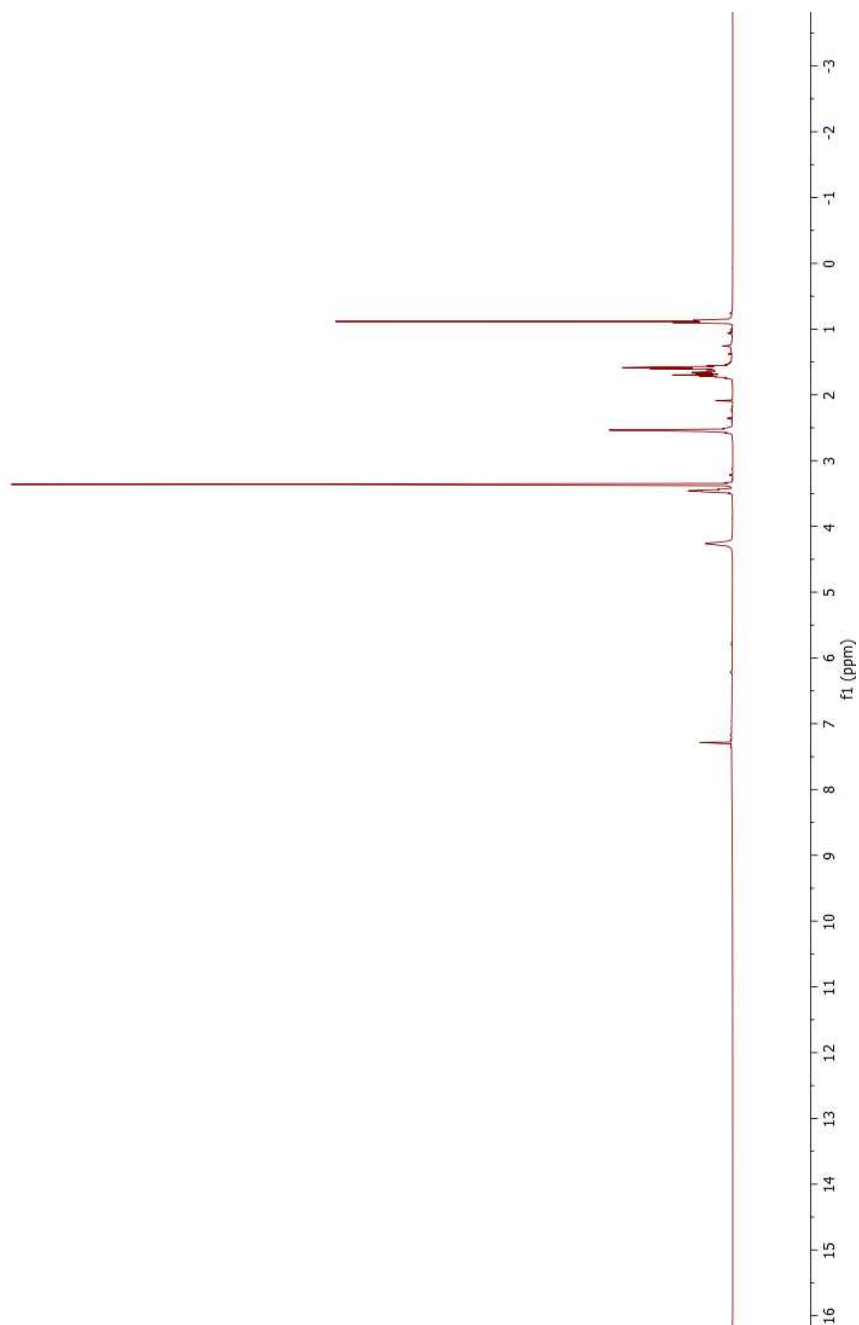


Figure S9AA-1. ^1H NMR

zco0414A.13.fid

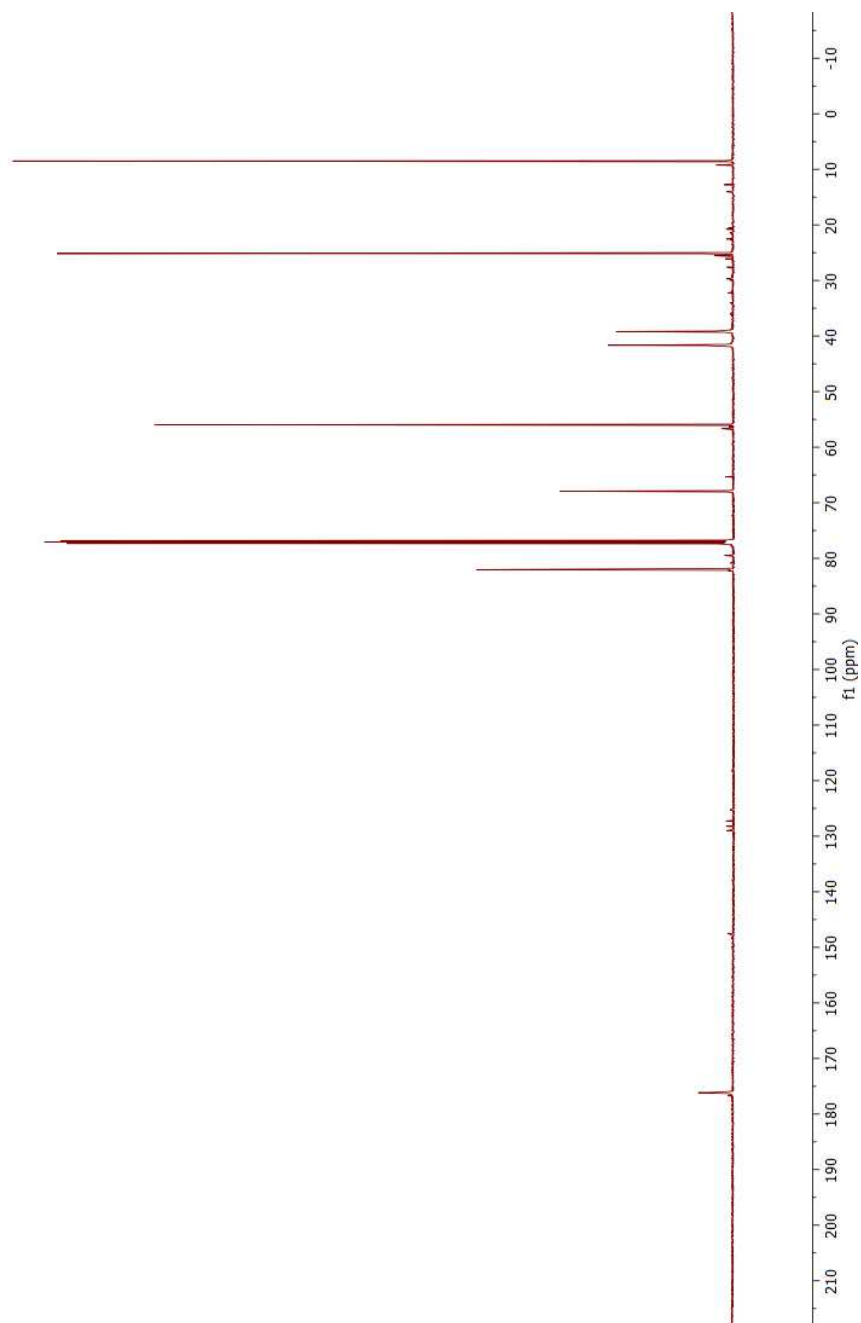


Figure S9AA-2. ^{13}C NMR

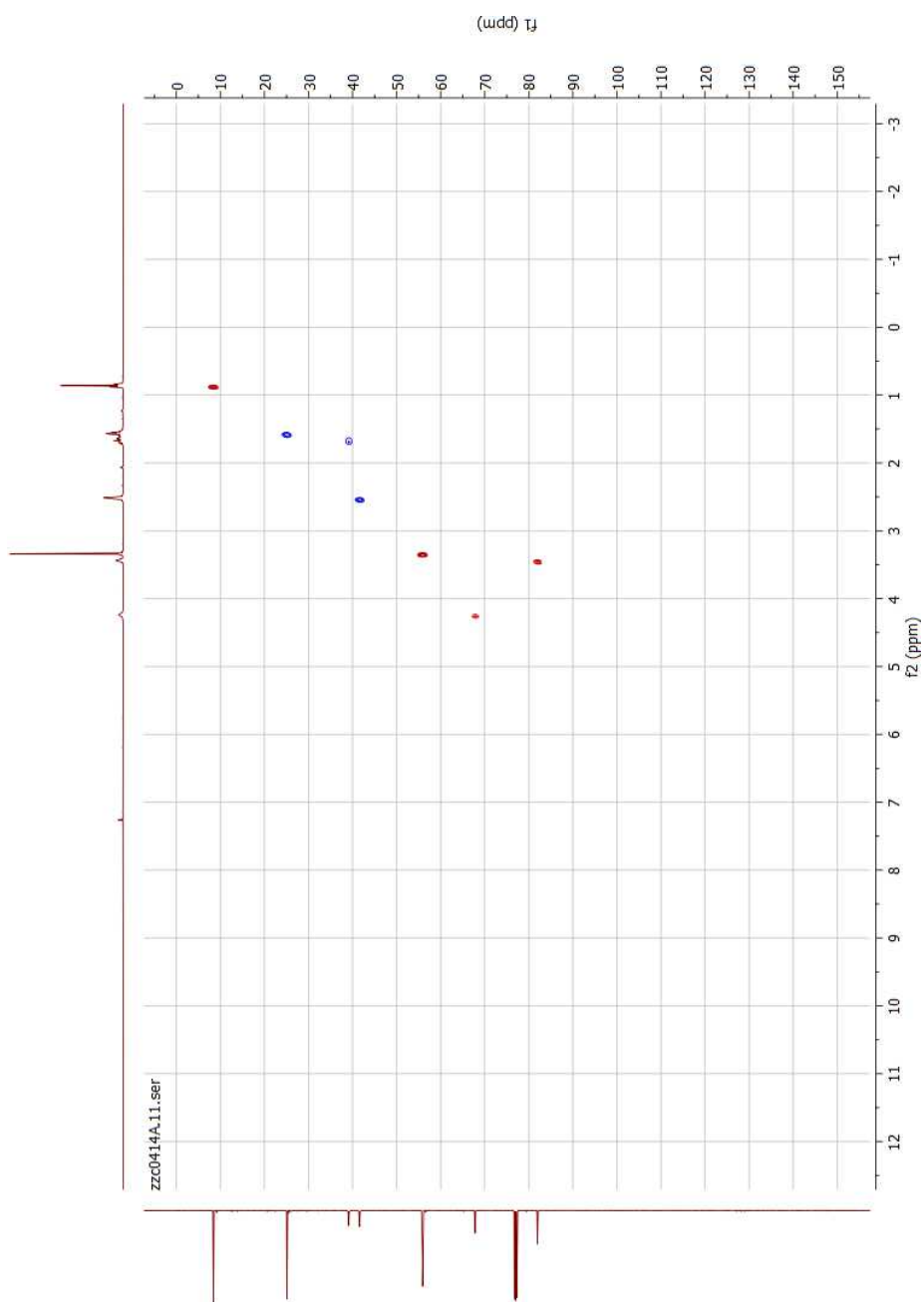


Figure S9AA-3. ^1H - ^{13}C HSQC

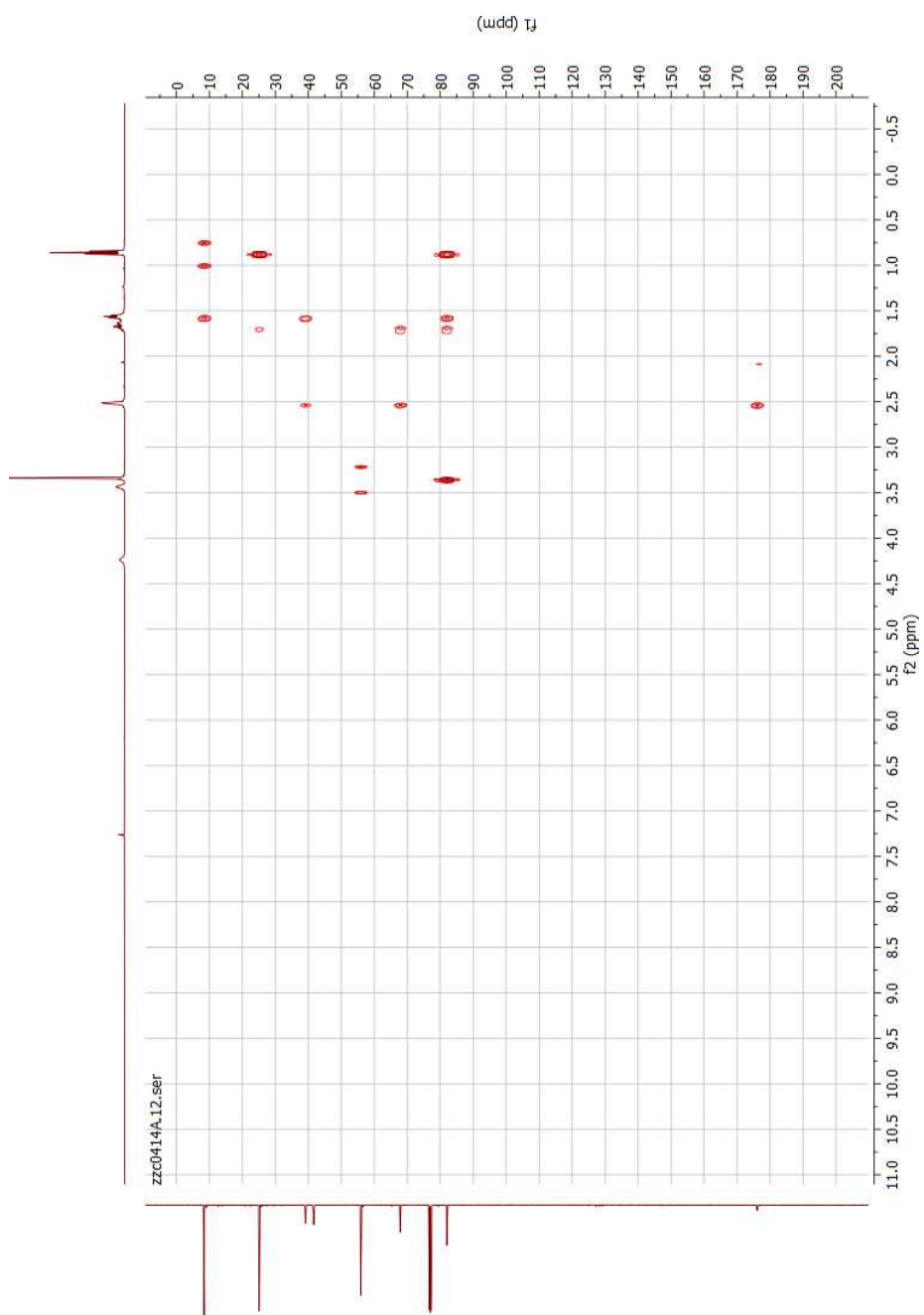
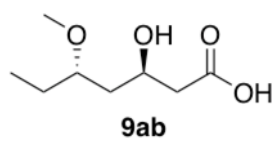


Figure S9AA-4. ^1H - ^{13}C HMBC



(3*R*,5*S*)-3-hydroxy-5-methoxyheptanoic acid

Chemical Formula: C₈H₁₆O₄

zco04148-10.fid

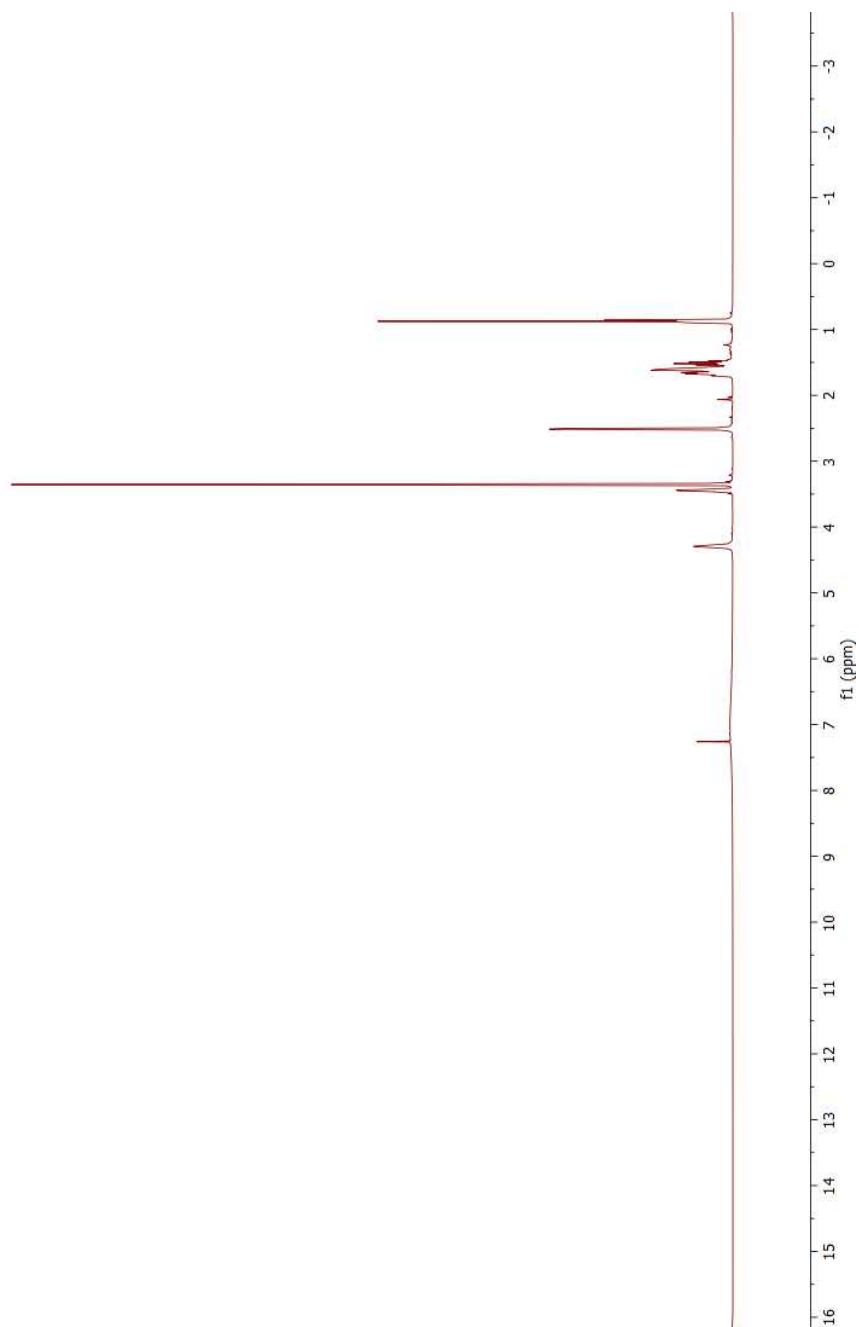


Figure S9AB-1. ^1H NMR

zco04148.13.fid

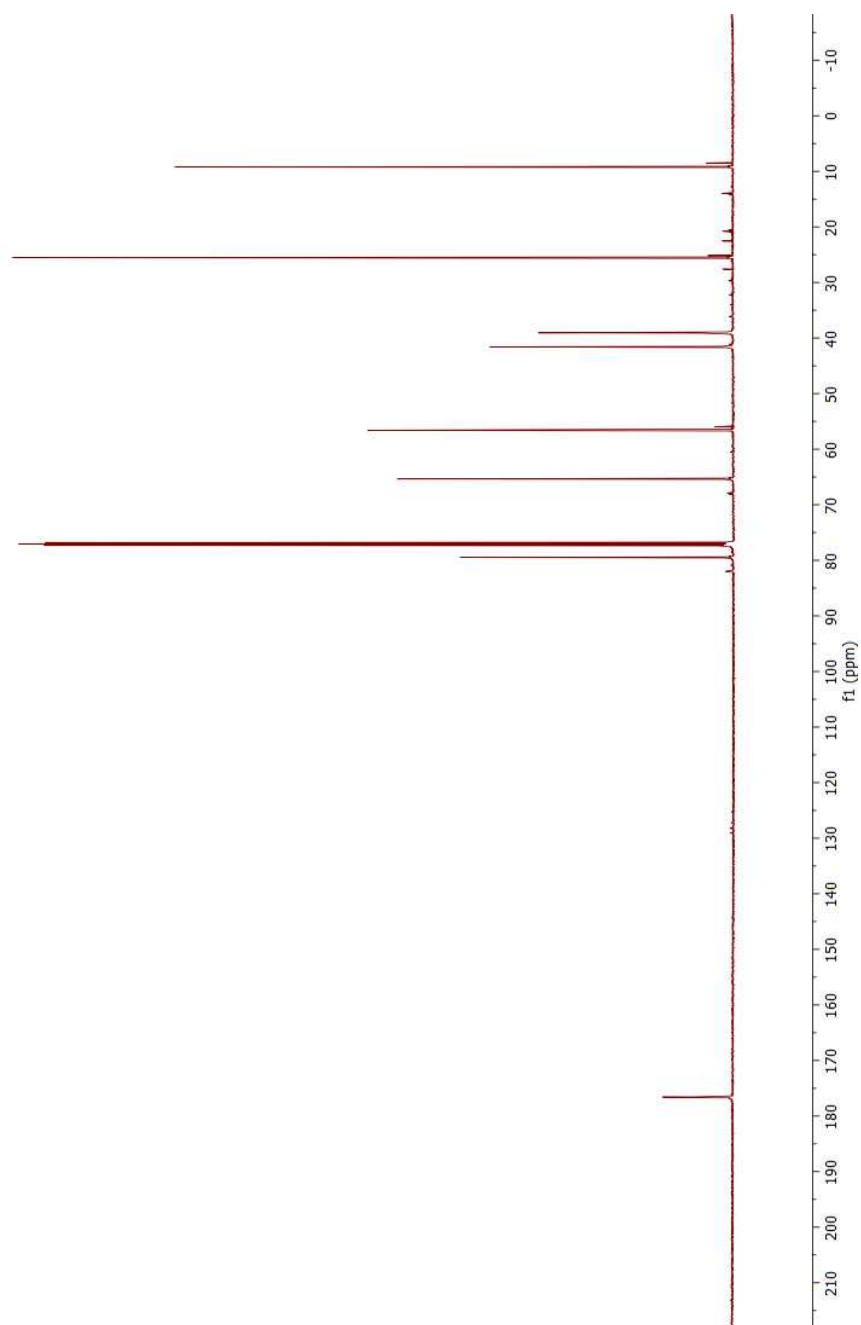


Figure S9AB-2. ^{13}C NMR

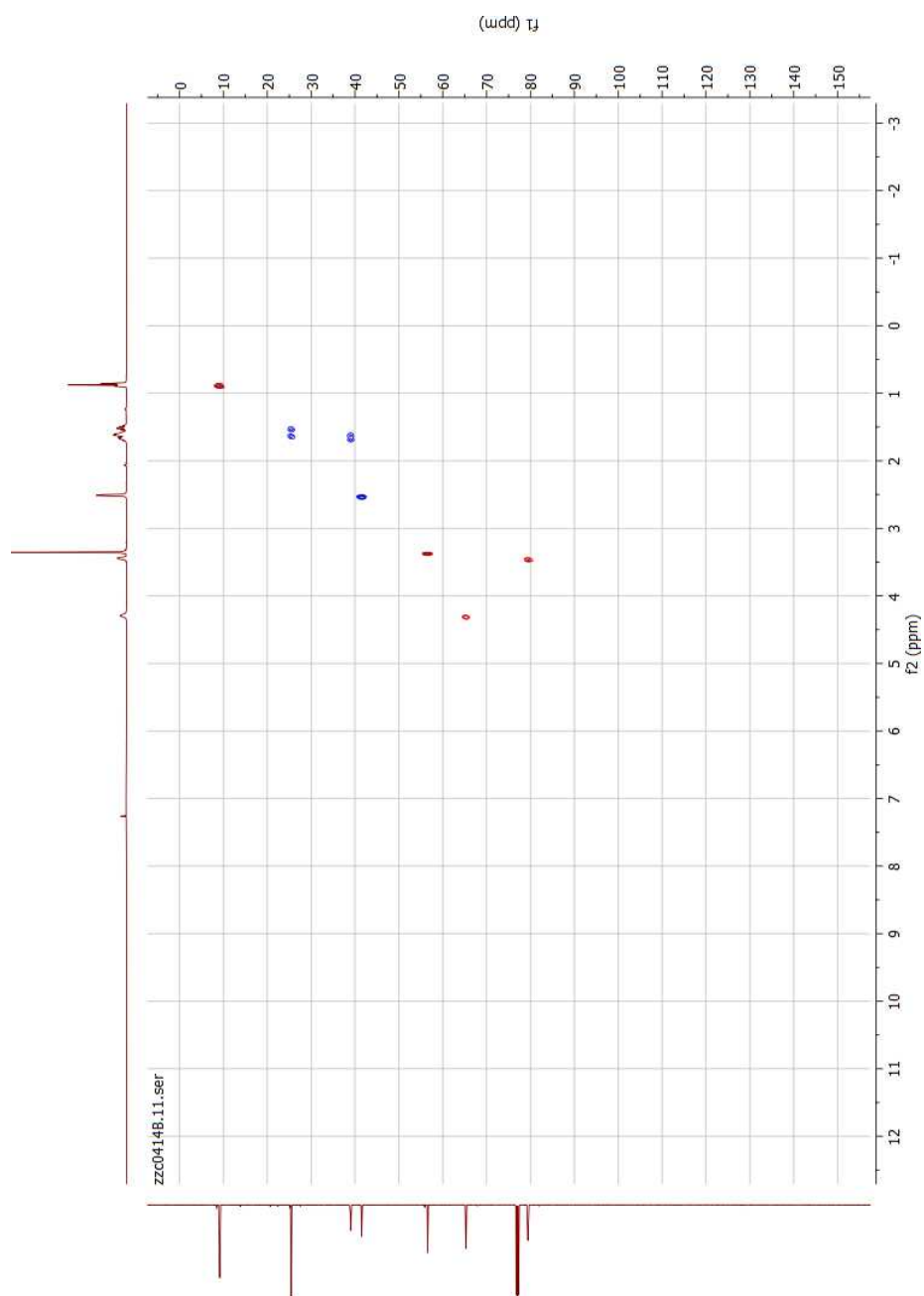


Figure S9AB-3. ^1H - ^{13}C HSQC

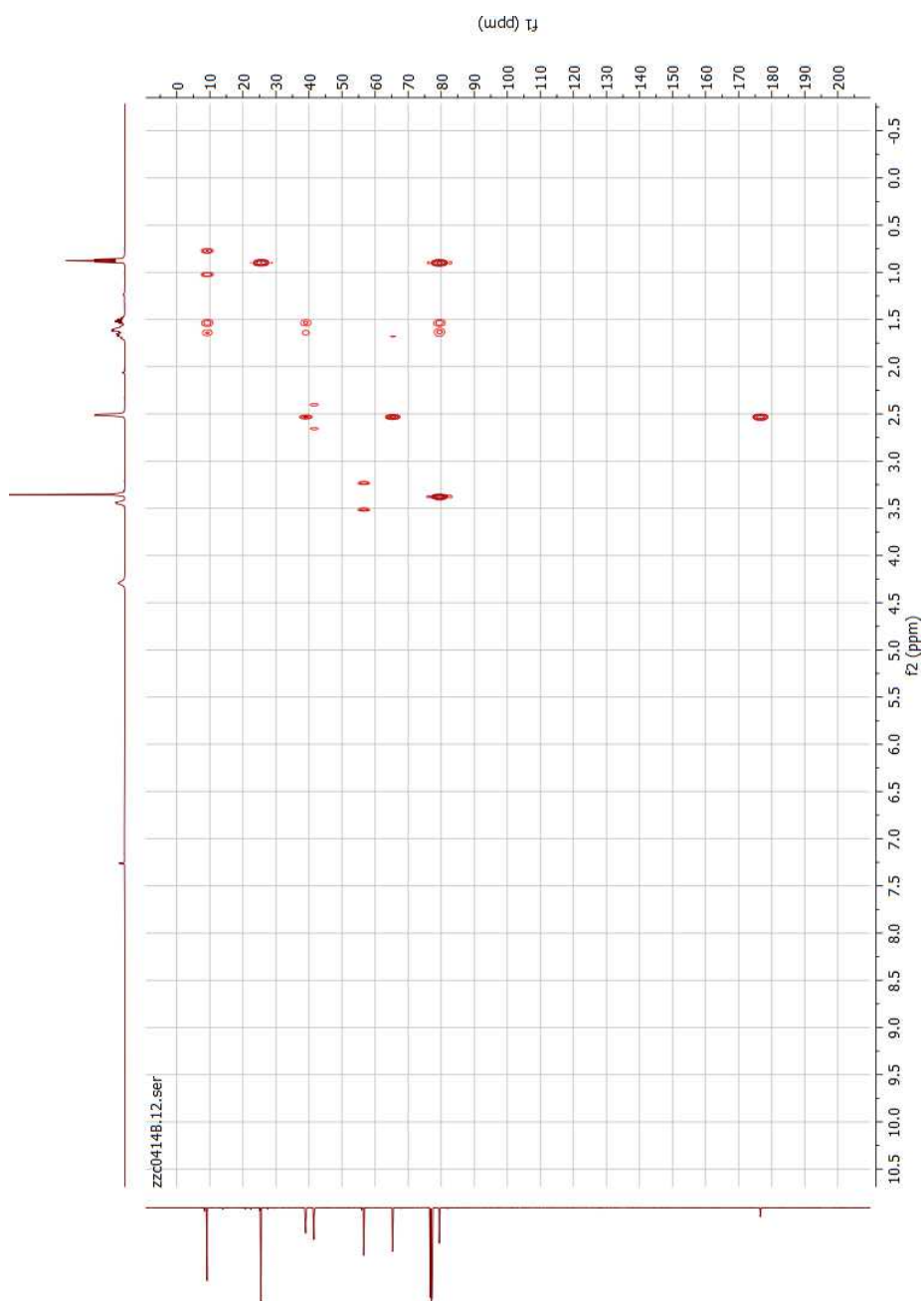
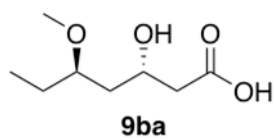


Figure S9AB-4. ^1H - ^{13}C HMBC



(3*S*,5*R*)-3-hydroxy-5-methoxyheptanoic acid

Chemical Formula: C₈H₁₆O₄

zxc04108-10.fid

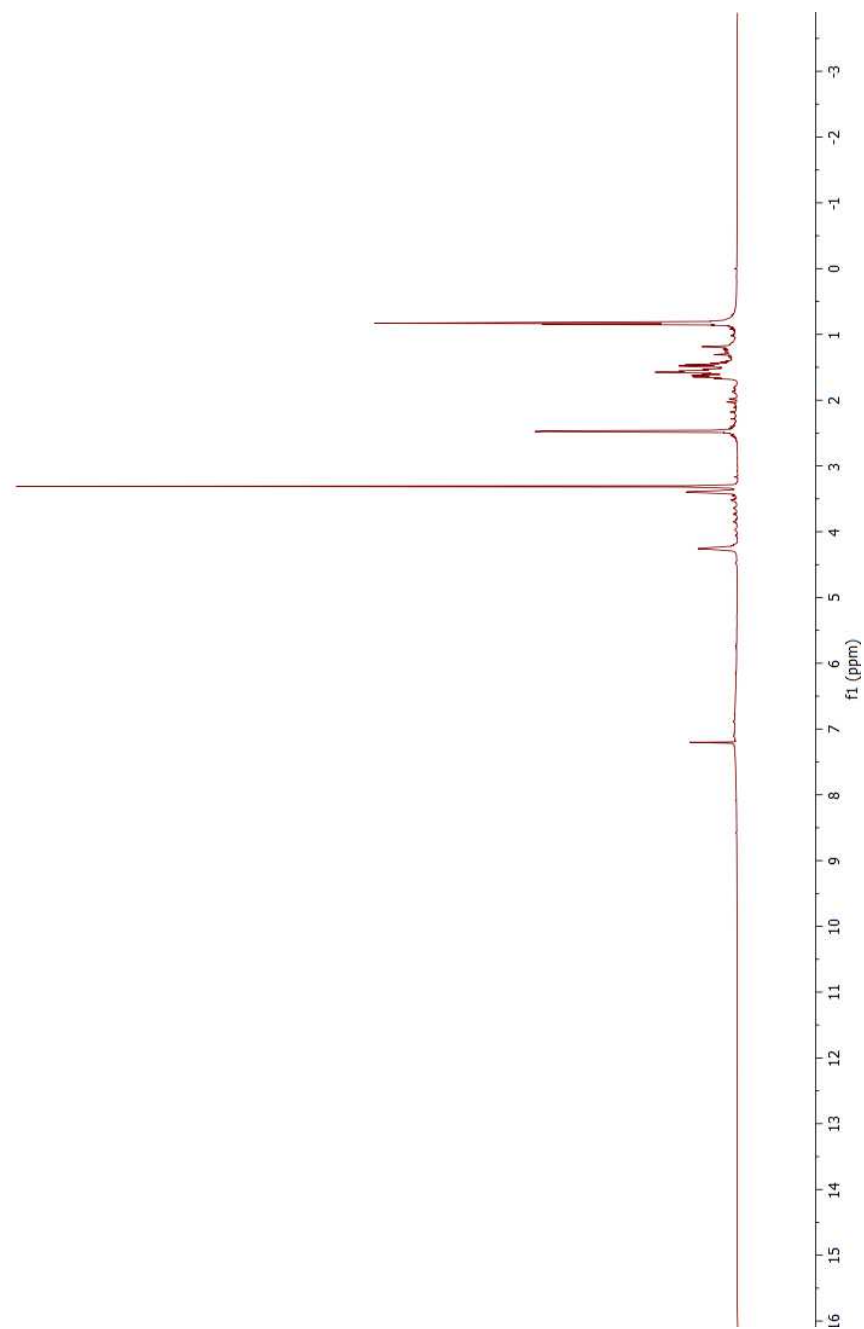


Figure S9BA-1. ^1H NMR

zxc04108.13.fid

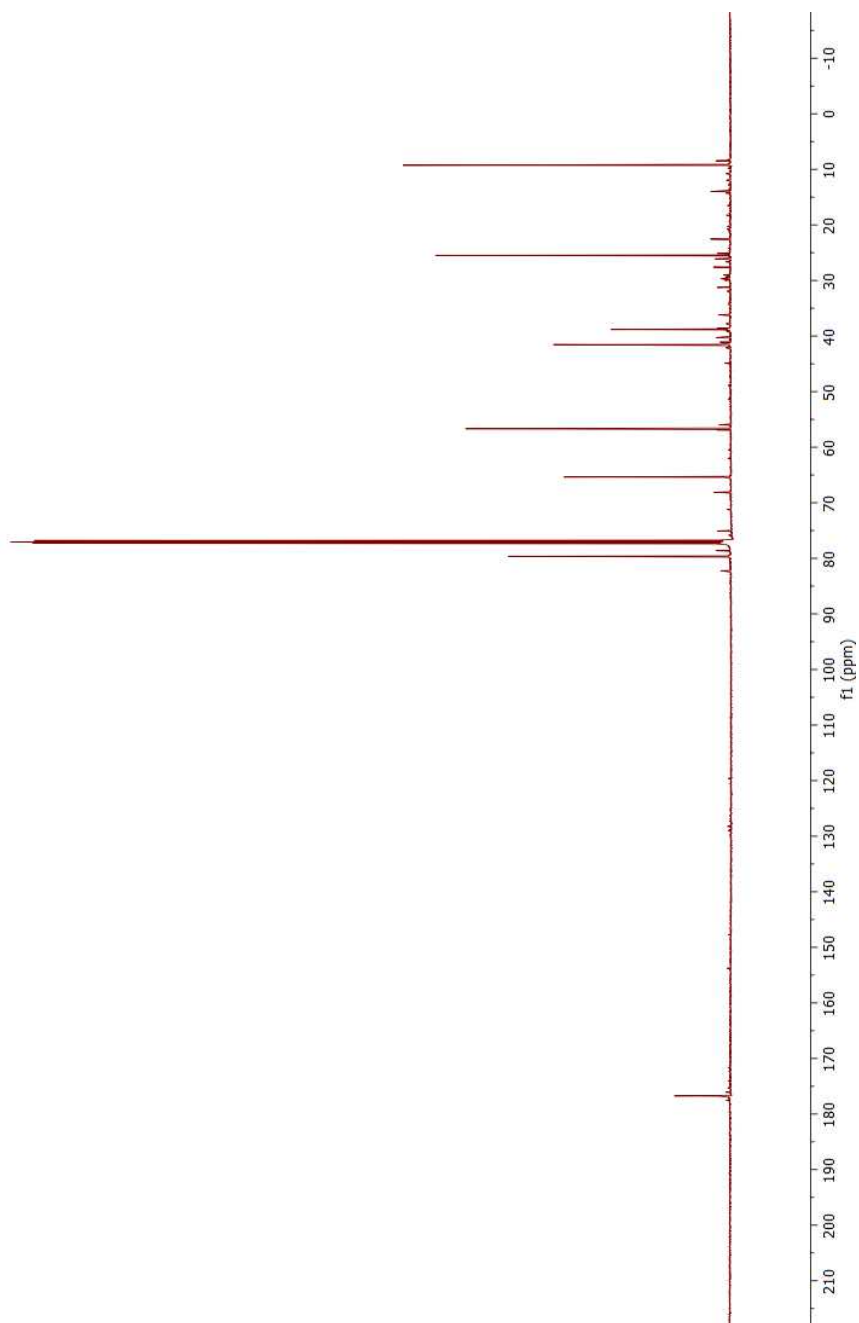


Figure S9BA-2. ^{13}C NMR

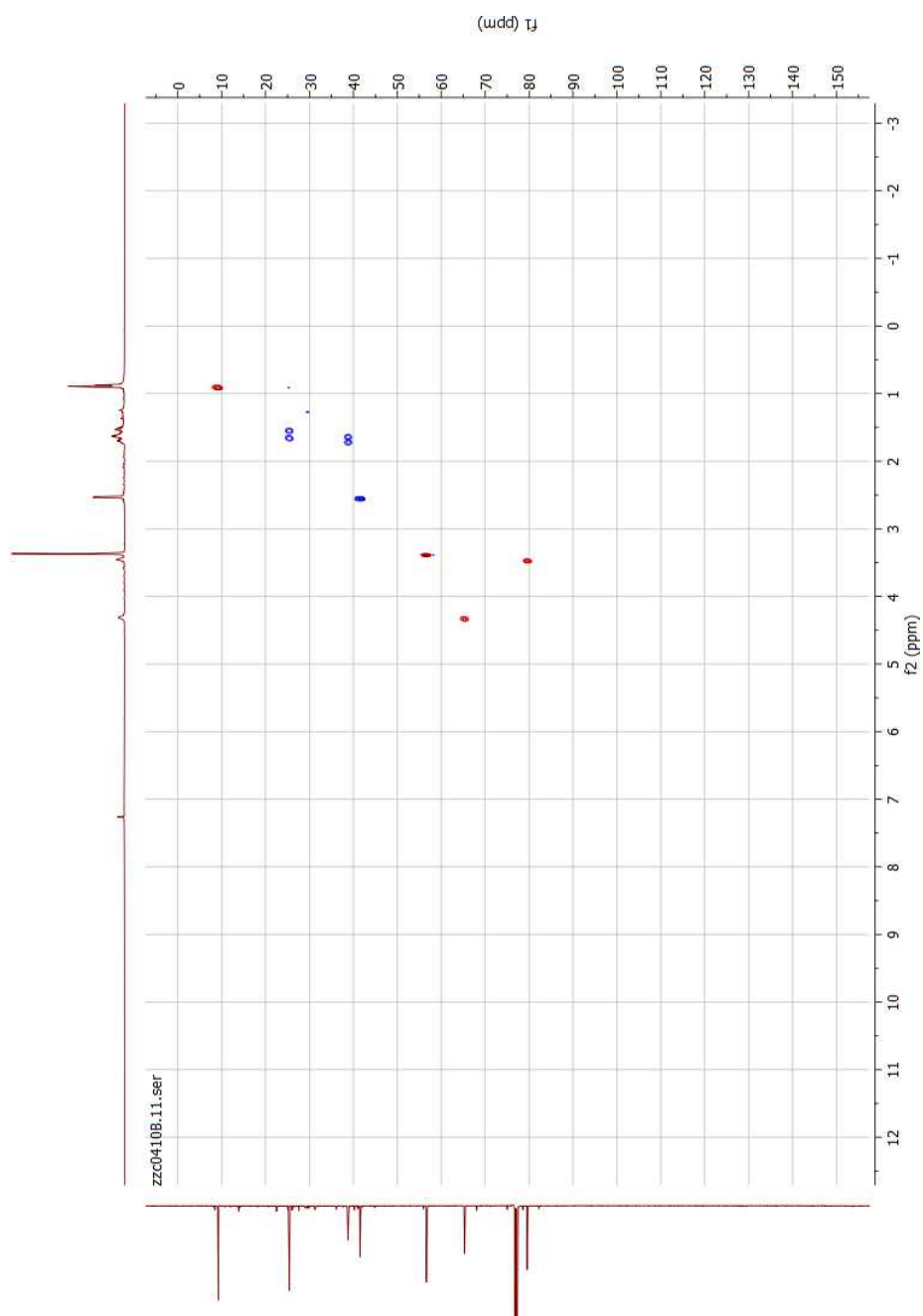


Figure S9BA-3. ^1H - ^{13}C HSQC

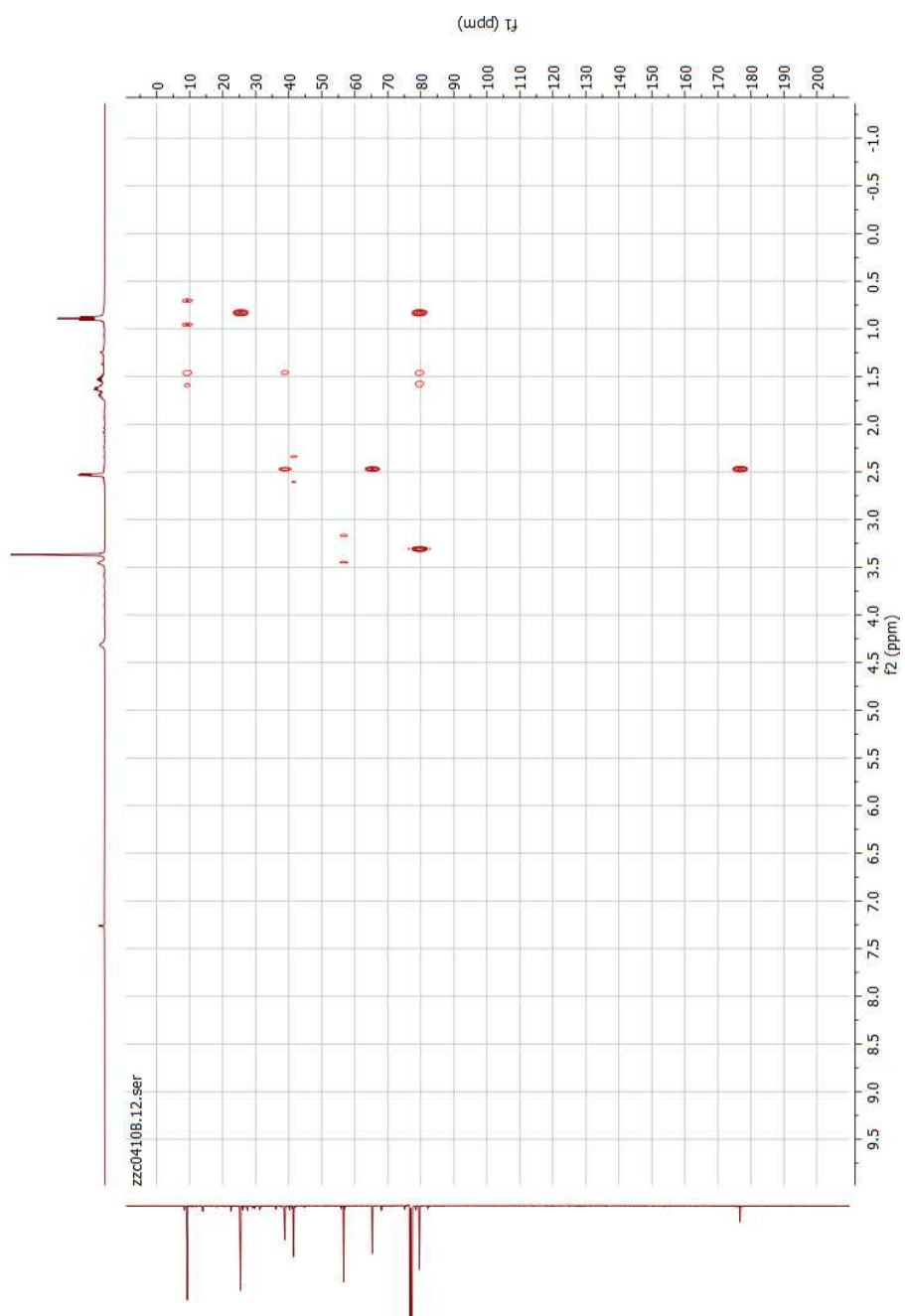
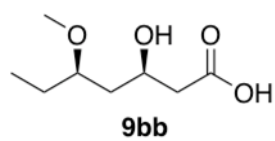


Figure S9BA-4. ^1H - ^{13}C HMBC



(3*R*,5*R*)-3-hydroxy-5-methoxyheptanoic acid

Chemical Formula: C₈H₁₆O₄

zco04118-10.fid

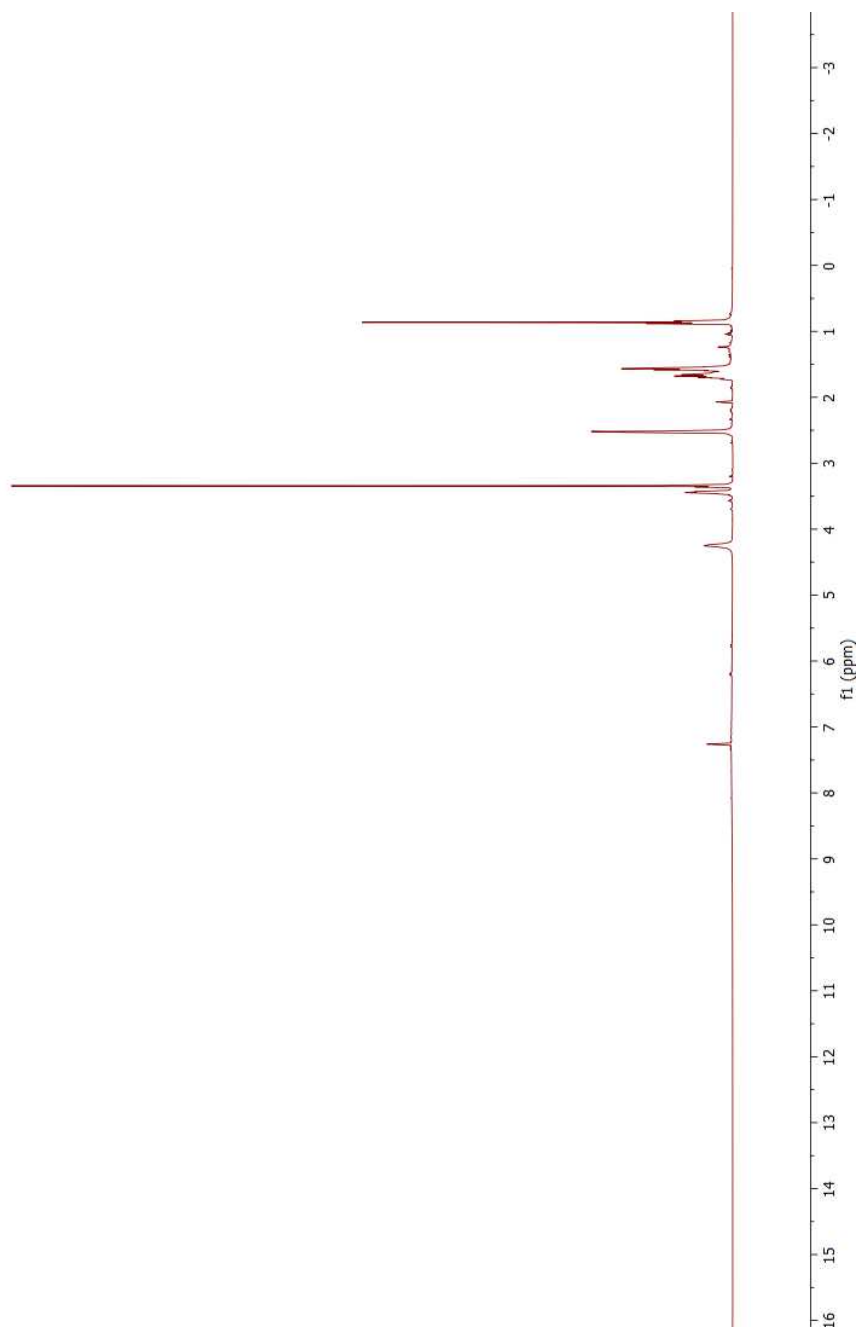


Figure S9BB-1. ^1H NMR

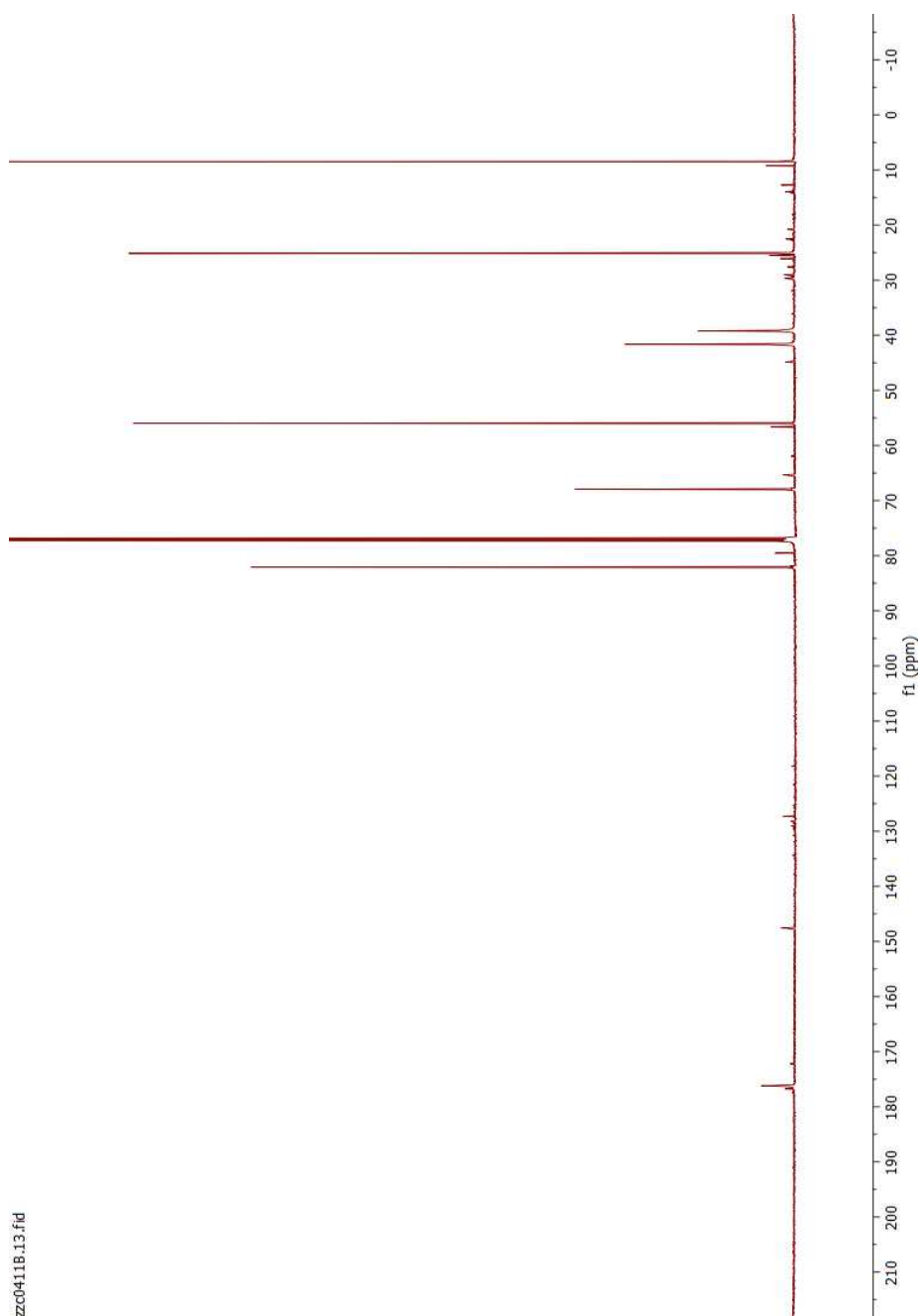


Figure S9BB-2. ^{13}C NMR

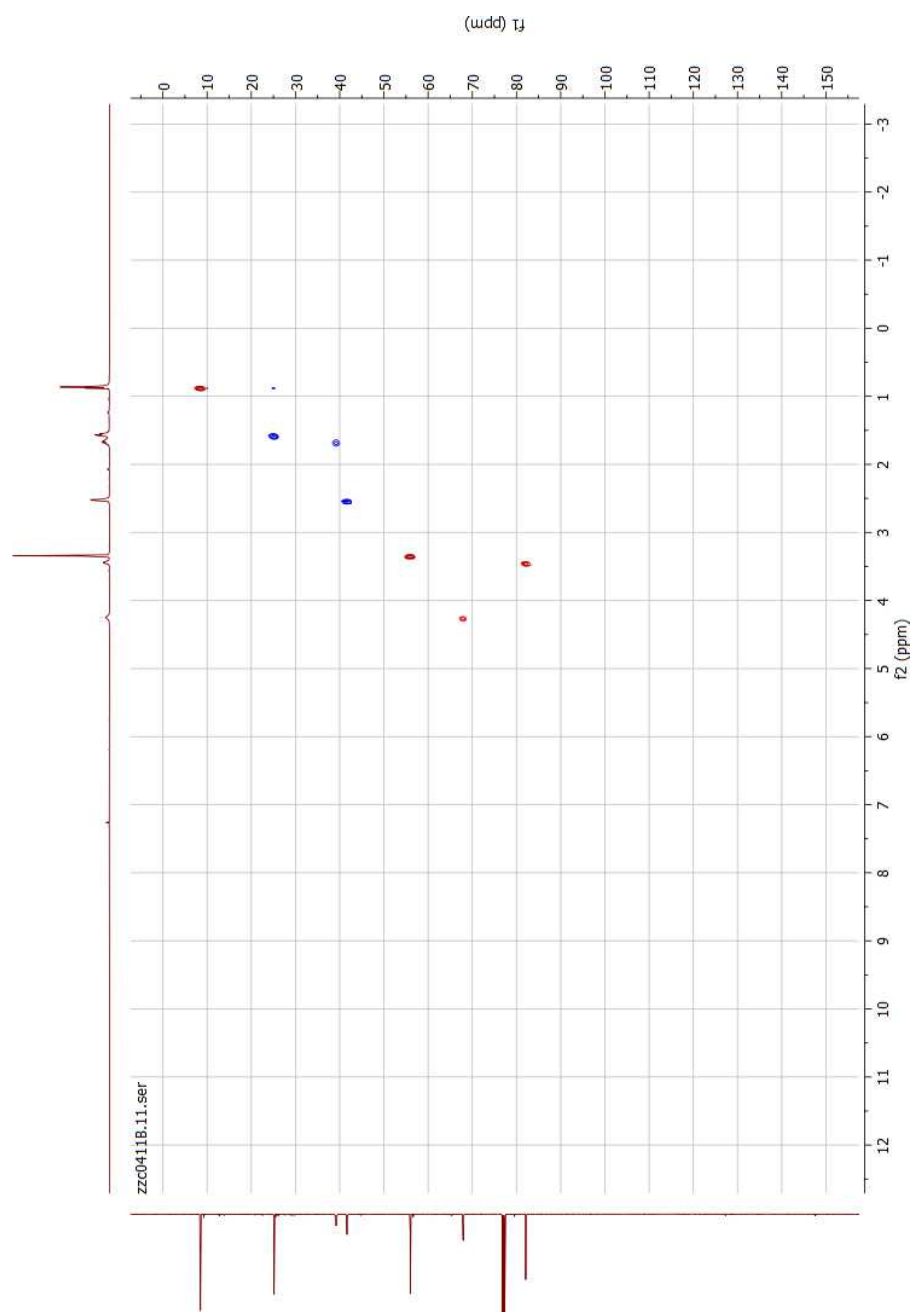


Figure S9BB-3. ^1H - ^{13}C HSQC

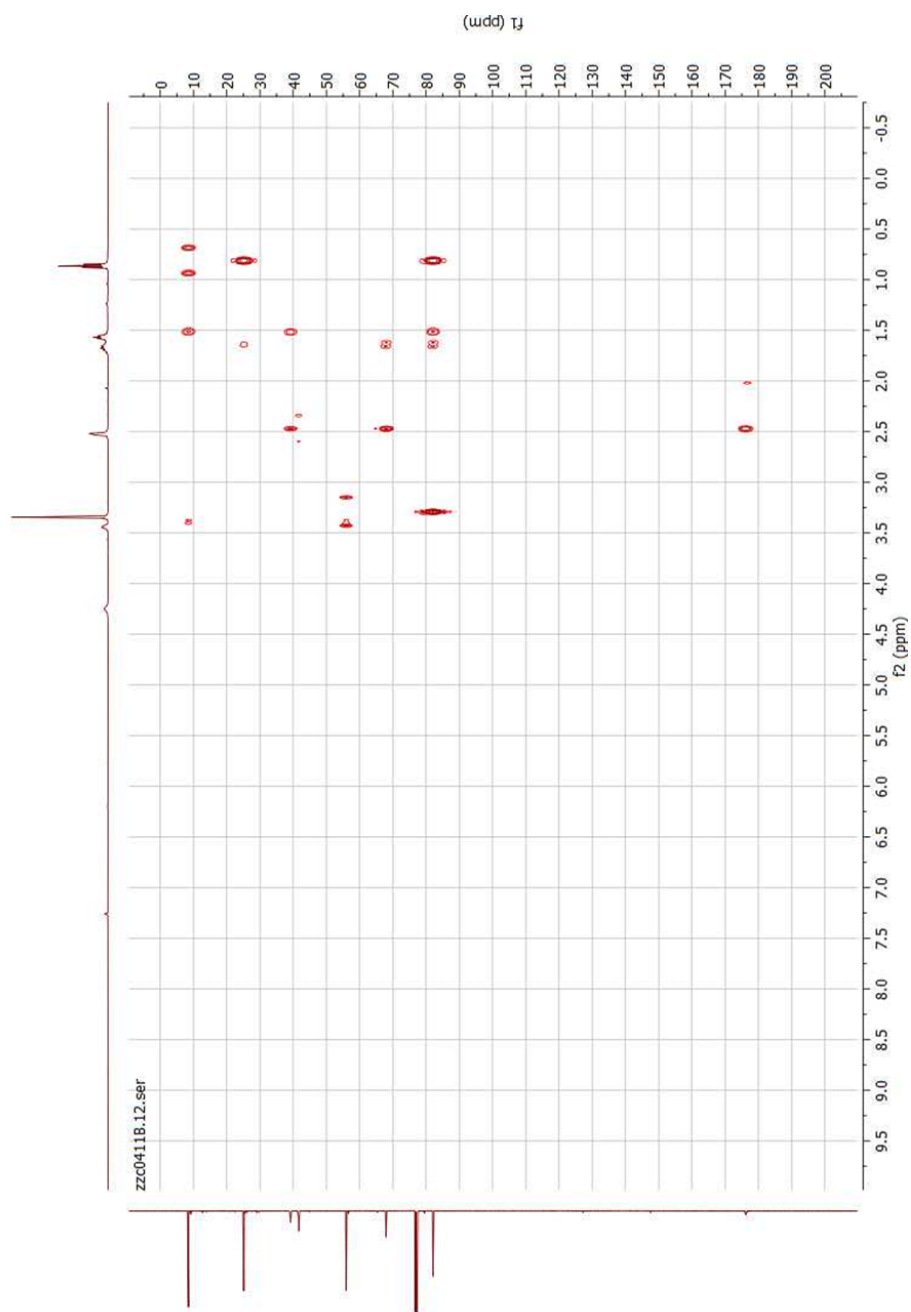


Figure S9BB-4. ^1H - ^{13}C HMBC

Appendix B

Publication List

Seven-enzyme in vitro cascade to (3R)-3-hydroxybutyryl-CoA

Org. Biomol. Chem., **2019**, *17*, 1375.

Structural and Functional Studies of a gem-Dimethylating Methyltransferase from a trans-Acyltransferase Assembly Line.

ACS Chem. Biol., **2018**, *13*, 12, 3306.

Structural and Functional Studies of a Pyran Synthase Domain from a trans-Acyltransferase Assembly Line.

ACS Chem. Biol., **2018**, *13*, 4, 975.

Portability and Structure of the Four-Helix Bundle Docking Domains of trans-Acyltransferase Modular Polyketide Synthases.

ACS Chem. Biol., **2016**, *11*, 9, 2466.

A Highly Practical Approach to Chiral Homoallylic—Homopropargylic Amines via Aza-Barbier Reaction.

ChemInform **2016**, 47(36).

A Highly Practical Approach to Chiral Homoallylic-homopropargylic Amines via aza-Barbier Reaction.

Tet. Lett. **2016**, *57*, 2147.

A highly Efficient Access to Enantiopure Tetrahydropyridines: dual-organocatalyst-promoted Asymmetric Cascade Reaction.

Chem. Commun. **2013**, 49, 4024.

References

- (1) (a) Editorial. *Nat. Chem. Biol.* **2007**, *3*, 351. (b) Newman, D. J.; Cragg, G. M.; Snader, K. M. *J. Nat. Prod.* **2003**, *66*, 1022.
- (2) (a) Newman, D. J.; Cragg, G. M. *J. Nat. Prod.* **2016**, *79*, 629. (b) Pascolutti, M.; Quinn, R. J. *Drug Discovery Today* **2014**, *19*, 215.
- (3) (a) Harvey, A. L. *Drug Discovery Today* **2008**, *13*, 894. (b) Harvey, A. L.; Edrada-Ebel, R.; Quinn, R. J. *Nature Reviews Drug Discovery* **2015**, *14*, 111. (c) Gautam, A.; Pan, X. *Drug Discovery Today* **2016**, *21*, 379.
- (4) Hirata, Y.; Uemura, D. *Pure Appl. Chem.* **1986**, *58*, 701.
- (5) Bai, R. L.; Paull, K. D.; Herald, C. L.; Malspeis, L.; Pettit G. R.; Hamel, E. *J. Biol. Chem.* **1991**, *266*, 15882.
- (6) Towle, M. J.; Salvato, K. A.; Budrow, J.; Wels, B. F.; Kuznetsov, G.; Aalfs, K. K.; Welsh, S.; Zheng, W.; Seletsky, B. M.; Palme, M. H.; Habgood, G. J.; Singer, L. A.; Dipietro, L. V.; Wang, Y.; Chen, J. J.; Quincy, D. A.; Davis, A.; Yoshimatsu, K.; Kishi, Y.; Yu, M. J.; Littlefield, B. A. *Cancer Res.* **2001**, *61*, 1013.
- (7) <http://www.fda.gov/NewsEvents/Newsroom/PressAnnouncements/ucm233863.htm>
- (8) Leoford, H. *Nature* **2010**, *468*, 608.
- (9) Hirata, Y.; Uemura, D. *Pure Appl. Chem.* **1986**, *58*, 701.
- (10) Weissman, K. J.; Leadley, P. F. *Nat. Rev. Microbiol.* **2005**, *12*, 925.
- (11) Li, J.; Vederas, J. *Science* **2009**, *325*, 161.
- (12) (a) Vederas, J. C. *Biosynthesis : polyketides and vitamins*, Springer, Berlin, 2000, p. 52. (b) Woodward, R. B.; Au-Yeung, B. W.; Balaram, P.; Browne, L.; Ward, D. E.; Card,

- P. J.; Chen, C. H. *J. Am. Chem. Soc.* **1981**, *103*, 3210. (c) Woodward, R. B.; Au-Yeung, B. W.; Balaram, P.; Browne, L.; Ward, D. E.; Card, P. J.; Chen, C. H. *J. Am. Chem. Soc.* **1981**, *103*, 3213. (d) Woodward, R. B.; Au-Yeung, B. W.; Balaram, P.; Browne, L.; Ward, D. E.; Card, P. J.; Chen, C. H. *J. Am. Chem. Soc.* **1981**, *103*, 3215.
- (13) Woodward, R.B. *Perspectives in Organic Chemistry*, Wiley-Interscience, New York, 1956, p. 160.
- (14) (a) Aicher, T. D.; Buszek, K. R.; Fang, F. G.; Forsyth, C. J.; Jung, S. H.; Kishi, Y.; Matelich, M. C.; Scola, P. M.; Spero, D. M.; Yoon, S. K. *J. Am. Chem. Soc.* **1992**, *114*, 3162. (b) Yamamoto, A.; Ueda, A.; Brémond, P.; Tiseni, P. S.; Kishi, Y. *J. Am. Chem. Soc.* **2012**, *134*, 893. (c) Ueda, A.; Yamamoto, A.; Kato, D.; Kishi, Y. *J. Am. Chem. Soc.* **2014**, *136*, 5171.
- (15) Hanessian, S. *J. Chem. Educ.* **1985**, *62*, 190.
- (16) (a) Hannessian, S. *Pure Appl. Chem.* **1993**, *65*, 1189. (b) Santaniello, E.; Ferraboschi, P.; Grisenti, P.; Manzocchi, A. *Chem. Rev.* **1992**, *92*, 1071.
- (17) Hilterhaus, L.; Liese, A. *Adv. Biochem. Engin./Biotechnol.* **2007**, *105*, 133.
- (18) For selected examples for application of chiral building blocks, see: (a) Altmann, K. H.; Gaugaz, F. Z.; Schiess, R. *Mol. Divers.* **2011**, *15*, 383. (b) Schaus, S.E.; Brånalt, J.; Jacobsen, E. N. *J. Org. Chem.* **1998**, *63*, 4876. (c) Mehta, G.; Islam, K. *Tetrahedron Letters* **2004**, *45*, 7683. (d) Tachiharaa, T.; Kitahara, T. *Tetrahedron* **2003**, *59*, 1773.
- (19) Khosla, C.; Gokhale, R. S.; Jacobsen, J. R.; Cane, D. E. *Annual Review of Biochemistry* **1999**, *68*, 219.
- (20) Keatinge-Clay, A. T. *Nat. Prod. Rep.* **2012**, *29*, 1050.

- (21) Hertweck, C. *Angew. Chem. Int. Ed.* **2009**, *26*, 4688.
- (22) Leadley, P. F. *Nature* **2014**, *510*, 512.
- (23) Jenke-Kodama, H.; Sandmann, A.; Müller, R.; Dittmann, E. *Molecular Biology and Evolution* **2005**, *22*, 2027.
- (24) Zheng, J.; Gay, D. C.; Demeler, B.; White M. A.; Keatinge-Clay, A. T. *Nat. Chem. Biol.* **2012**, *8*, 615.
- (25) Piasecki, S. K.; Taylor, C. A.; Detelich, J. F.; Liu, J.; Zheng, J.; Komsoukianants A.; Siegel, D. R.; Keatinge-Clay, A. T. *Chem. Biol.* **2011**, *18*, 1331.
- (26) Hughes, A. J.; Detelich J. F.; Keatinge-Clay, A. T. *Med. Chem. Commun.* **2012**, *3*, 956.
- (27) Harper, A. D.; Bailey, C. B.; Edwards, A. D.; Detelich, J. F.; Keatinge-Clay, A. T. *Chembiochem.* **2012**, *13*, 2200.
- (28) Hughes, A. J.; Keatinge-Clay, A. *Chem. Biol.* **2011**, *18*, 165.
- (29) Keatinge-Clay, A. T. *Chem. Biol.* **2007**, *14*, 898.
- (30) Caffrey, P. *ChemBioChem.* **2003**, *4*, 654.
- (31) Pan, Y.; Tan, C. *Synthesis.* **2011**, *13*, 2044.
- (32) Ramírez-Fernández, J.; Botubol, J. M.; Bustillo, A. J.; Aleu, J.; Collado I. G.; Hernández-Galán, R. *Nat. Prod. Commun.* **2011**, *6*, 443.
- (33) Brooks, D.; Lu, L.; Masamune, S. *Angew. Chem. Int. Ed.* **1979**, *18*, 72.
- (34) Noyori, R. *Angew. Chem. Int. Ed.* **2002**, *41*, 2008.
- (35) (a) Gridnev, I. D.; Imamoto, T. *Acc. Chem. Res.* **2004**, *379*, 633. (b) Church, T. L.; Andersson, P. G. *Coordination Chemistry Reviews* **2008**, *252*, 513. (c) Enthaler, S.;

- Junge, K.; Beller, M. *Angew. Chem. Int. Ed.* **2008**, *47*, 3317.
- (36) Bao, D.; Wu, H.; Liu, C.; Xie, J.; Zhou, Q. *Angew. Chem. Int. Ed.* **2015**, *54*, 8791.
- (37) (a) Che, W.; Li, Y.; Liu, J.; Zhu, S.; Xie, J.; Zhou, Q. *Organic Letters* **2019**, *21* (7), 2369-2373. (b) Che, W.; Wen, D.; Zhu, S.; Zhou, Q. *Helv.Chim.Acta* **2019**, *102*, e19000.
- (38) Oikawa, Y.; Sugano, K.; Yonemitsu, O. *J Org Chem* **1978**, *43*, 2087.
- (39) Bailey, C. B.; Pasman, M. E.; Keatinge-Clay, A. T. *Chem Commun* **2016**, *52*, 792.
- (40) Page, P. C. B.; Chan, Y. H.; Heaney, H.; McGrath, M. J.; Moreno, E. *Synlett* **2004**, 2606.
- (41) Hoffmann, R.W.; Weidmann, U. *Chem. Ber.* **1985**, *118*, 3980.
- (42) Tang, M.; He, H.; Zhang, F.; Tang, G. *ACS Catal.* **2013**, *3*, 3, 444.
- (43) Valencia, L. E.; Zhang, z.; Cepeda, A. J.; Keatinge-Clay, A. T. *Org. Biomol. Chem.*, **2019**, *17*, 1375.
- (44) (a) H. C. Tseng, C. H. Martin, D. R. Nielsen and K. L. J. Prather *Appl. Environ. Microbiol.*, **2009**, *75*, 3137. (b) S. H. Lee, S. J. Park, S. Y. Lee and S. H. Hong, *Appl. Microbiol. Biotechnol.*, **2008**, *79*, 633. (c) S. H. Lee and O. J. Park, *Appl. Microbiol. Biotechnol.*, **2009**, *84*, 817.
- (45) (a) Masamune, S.; Walsh, C. T.; Sinskey, A. J.; Peoples, O. P. *Pure Appl. Chem.*, **1989**, *61*, 303–312. (b) Lan, E. I.; Liao, J. C. *Proc. Natl. Acad. Sci. U. S. A.*, **2012**, *109*, 6018.
- (46) van Wyk, M.; Strauss, E. *Chem. Commun.*, **2007**, 398.
- (47) Noyori, R.; Ohkuma, T.; Kitamura, M.; Takaya, H.; Sayo, N.; Kumobayashi, H.; Akutagawa, S. *J. Am. Chem. Soc.*, **1987**, *109*, 5856.

- (48) Killenberg, P. G.; Dukes D. F., *J Lipid Res* **1976**, *17*, 451.
- (49) Vergnolle, O.; Hahn, F.; Baerga-Ortiz, A.; Leadlay, P. F.; Andexer, J. N., *Chembiochem* **2011**, *12*, 1011.
- (50) Wagner, D.T.; Zhang, Z.; Meoded, R. A.; Cepeda, A. J.; Piel, J.; Keatinge-Clay, A. *ACS Chem. Biol.* **2018**, *13*, 975.
- (51) (a) Piel, J. *Nat. Prod. Rep.* **2010**, *27*, 996.
- (b) Helfrich, E. J., and Piel, J. *Nat. Prod. Rep.* **2016**, *33*, 231.
- (52) (a) Matilla, M. A., Stockmann, H., Leeper, F. J., and Salmond, G. P. *A. J. Biol. Chem.* **2012**, *287*, 39125.
- (b) Bertin, M. J., Vulpanovici, A., Monroe, E. A., Korobeynikov, A., Sherman, D. H., Gerwick, L., and Gerwick, W. H. *ChemBioChem* **2016**, *17*, 164.
- (53) (a) Poplau, P., Frank, S., Morinaka, B. I., and Piel, J. *Angew. Chem., Int. Ed.* **2013**, *52*, 13215. (b) Ueoka, R., Uria, A. R., Reiter, S., Mori, T., Karbaum, P., Peters, E. E., Helfrich, E. J., Morinaka, B. I., Gugger, M., Takeyama, H., Matsunaga, S., and Piel, J. *Nat. Chem. Biol.* **2015**, *11*, 705.
- (54) (a) Keatinge-Clay, A. T. *Angew. Chem., Int. Ed.* **2017**, *56*, 4658.
- (b) Zhang, L., Hashimoto, T., Qin, B., Hashimoto, J., Kozono, I., Kawahara, T., Okada, M., Awakawa, T., Ito, T., Asakawa, Y., Ueki, M., Takahashi, S., Osada, H., Wakimoto, T., Ikeda, H., Shin-Ya, K.; Abe, I. *Angew. Chem., Int. Ed.* **2017**, *56*, 1740. (c) Irschik, H., Jansen, R., Gerth, K., Hofle, G.; Reichenbach, H. *J. Antibiot.* **1987**, *40*, 7. (d) Irschik, H., Kopp, M., Weissman, K. J., Buntin, K., Piel, J., Muller, R. *ChemBio-Chem* **2010**, *11*, 1840.

- (55) Chen, S. H.; Hong, B. C.; Su, C. F.; Sarshar, S., *Tetrahedron Lett* **2005**, *46*, 8899.
- (56) Kennedy, J.; Mccorkindale, N. J.; Raphael, R. A., *J. Chem. Soc.* **1961**, 3813.
- (57) Mohapatra, D. K.; Maity, S.; Banoth, S.; Gonnade, R. G.; Yadav, J. S., *Tetrahedron Lett.* **2016**, *57*, 53.
- (58) Meinke, J. L.; Mehaffey, M.R.; Wagner, D. T.; Sun, N.; Zhang, Z.; Brodbelt, J. S.; Keatinge-Clay, A. T. *ACS Chem. Biol.* **2018**, *13*, 3306.
- (59) Zeng, J.; Wagner, D. T.; Zhang, Z.; Moretto, L.; Addison, J. D.; Keatinge-Clay, A. T. *ACS Chem. Biol.* **2016**, *11*, 2466.

Vita

Zhicheng Zhang, (Alexandre) était né à Shanghai, Chine., 7^{er} septembre 1990. Il a passé son enfance à Avenue Haig/Huashan Road, près Zicawei. Il a étudié à Université Fudan pour chimie organique de 2009 et obtenu licence en sciences à 2013. Après cela, il a déménagé aux États-Unis pour poursuivre ses études à UT Austin sous la supervision de Dr Keatinge-Clay.

Courriel permanent : gundelfingen1945@gmail.com

Cette dissertation était tapée par Zhicheng Zhang.